FLOWER ABSCISSION AND FRUIT SET ON TABLE GRAPES (*Vitis vinifera* L.): UNRAVELING PHYSIOLOGICAL AND MOLECULAR MECHANISMS

SARA NOBRE GONÇALVES DOMINGOS

ORIENTADORA: Doutora Cristina Maria Moniz Simões Oliveira

COORIENTADOR: Doutor Luís Filipe Sanches Goulão

TESE APRESENTADA PARA OBTENÇÃO DO GRAU DE DOUTOR EM ENGENHARIA AGRONÓMICA

Presidente: Doutora Maria Helena Mendes da Costa Ferreira Correia de Oliveira, Professora Associada do Instituto Superior de Agronomia, Universidade de Lisboa.

Vogais: Doutor Hernâni Varanda Gerós, Professor Associado com Agregação da Escola de Ciências da Universidade do Minho;

Doutora Sara Barros Queiroz Amâncio, Professora Associada com Agregação do Instituto Superior de Agronomia da Universidade de Lisboa;

Doutora Cristina Maria Moniz Simões de Oliveira, Professora Associada com Agregação do Instituto Superior de Agronomia da Universidade de Lisboa;

Doutor João Manuel Mota Barroso, Professor Associado da Escola de Ciências e Tecnologia da Universidade de Évora;

Doutora Ana Margarida da Costa Macedo Fortes, Investigadora Auxiliar da Faculdade de Ciências da Universidade de Lisboa.

Fundação para a Ciência e Tecnologia
2016

Agradecimentos

Este espaço é dedicado às inúmeras contribuições que permitiram a realização deste trabalho, a todos um muito obrigado com o mais profundo reconhecimento.

Aos meus orientadores Professora Cristina Oliveira e Doutor Luís Goulão, pela oportunidade que me deram para a realização do doutoramento, pelo apoio e orientação do trabalho ao longo destes anos, pela amizade, por me inspirarem e desafiarem a fazer sempre melhor.

Ao Doutor Pietro Scafidi e ao Professor Rosario Di Lorenzo, da Universidade de Palermo, pelas ideias que contribuíram para melhorar este trabalho, pelo convite para realizar parte dele na Sicíla, pelo apoio e carinho com que me receberam.

A toda a equipa da Herdade Vale da Rosa, especialmente ao Doutor António Silvestre, pelo apoio a este projecto, pela disponibilidade e amizade que tiveram para comigo ao longo destes anos.

À Joana Fino e ao Professor Octávio Paulo, da Faculdade de Ciências, pelas análises bioinformáticas indispensáveis para a realização do trabalho e pelo apoio e sugestões que permitiram melhorá-lo.

Aos Doutores José Cochico e Eduardo Leitão, do IICT, pelo apoio nos procedimentos e determinações fisiológicas e bioquímicas, bem como pela leitura e crítica de partes do trabalho.

Às Doutoras Cláudia Sanchez e Carmen Serrano, do INIAV, e Doutor Robert Larcher, da Fondazione Edmund Mach em Itália, pelo apoio nas determinações bioquímicas.

A todos os colegas, principalmente Vânia Cardoso, Hugo Nóbrega, Isabela Soares, Ana Raposo e Carlos Correira pela ajuda preciosa nos ensaios e determinações, pela amizade, pelas sugestões e pelo espírito de equipa ao longo de todo o trabalho.

À minha família, especialmente à minha mãe, ao meu pai, ao Jorge, à minha irmã e aos meus avós, a quem devo o que sou hoje, por todo o amor e apoio incondicional, pela constante ajuda e incentivo ao longo do todo o percurso académico.

Ao Vasco, pela ajuda e o amor dedicados, por estar ao meu lado todos dias, por me transmitir calma e fazer rir nos momentos de maior nervosismo.

A realização de todo este trabalho só foi possível através do financiamento da bolsa individual de doutoramento (SFRH/BD/69076/2010) e do projecto VitiShade: PTDC/AGR-GPL/116923/2010 pela Fundação para a Ciência e Tecnologia, e do projecto ProDeR Medida 4.1 - Cooperação para a Inovação: PROdUVA 23921/2/3/4.

Abstract

Despite the importance of grapevine (*Vitis vinifera* L.) as one of the most cultivated species, the molecular events occurring during the critical period of fruit set, are far from elucidated. Aiming at providing a new insight on flower-to-fruit transition and flower abscission regulation, transcriptomic (RNA-Seq) and metabolomic analyzes were performed in the inflorescences and vine physiological alterations were investigated. Regarding flower-to-fruit transition regulation the results showed involvement of nutrient transport regulation and alterations on carbohydrates, secondary and hormone metabolism. In particular, induction of indole-3-acetic acid accumulation and activation of ethylene and sugar signaling were hypothesized to induce bioactive gibberellins biosynthesis, stimulating cell division within inflorescences. Assays with gibberellic acid (GAc) spraying and reduction of light interception during bloom allowed to promote flower abscission and suggested that growth regulator application and C-starvation resulted in distinct effects on inflorescence metabolism. GAc response involved stimulation of photosynthetic and respiratory machinery, nucleotide biosynthesis and carbon metabolism. Conversely, shading repressed photosynthesis, induced carbon/nitrogen imbalance and comprehensive alterations on hormone-related pathways, resulting in repression of cell division and induction of senescence. Candidates as common pathways leading to abscission were putrescine catabolism regulation, auxin biosynthesis induction, gibberellin biosynthesis repression and ROS signaling/detoxification although often through changes on specific transcripts and metabolites levels. Aiming at optimizing thinning methods, mandatory on table grapes production for guarantee bunch quality, GAc spray and shading during bloom were tested in seedless and seeded cultivars growing under field and greenhouse conditions. 'Thompson Seedless' showed to be sensitive to both thinning methods resulting in increased flower drop and reduced bunch compactness, but only GAc spray enhanced berry quality. Both treatments induced flower abscission in 'Black Magic' growing in late cycle on greenhouse production system, whereas during early cycle, only shade enhanced flower drop, bunch aspect and berry quality, resulting in an effective thinning method.

Key-words: abscission, fruit set, grapevine, gibberellic acid, shade

Resumo

Apesar da importância da videira (*Vitis vinifera* L.) como umas uma das espécies mais cultivadas, os mecanismos moleculares que ocorrem durante o período do vingamento, continuam por esclarecer. Análises do transcritoma (RNA-Seq) e metaboloma das inflorescências e das alterações fisiológicas da videira permitiram clarificar alguns mecanismos de regulação da transição de flor para bago e abscisão de flores. Relativamente ao vingamento, foram observadas alterações na regulação do transporte de nutrientes, no metabolismo secundário, dos hidratos de carbono e hormonal. A acumulação de ácido indol-3-acético e activação das vias de sinalização dos açúcares e do etileno podem induzir a síntese de giberelinas, estimulando a divisão celular. As análises realizadas após a pulverização com ácido giberélico (GAc) e redução da radiação incidente durante a floração, promovendo a queda de flores, sugeriram que estes dois estímulos provocam efeitos opostos no metabolismo das inflorescências. A resposta ao GAc envolveu um reforço do metabolismo energético e indução da biossíntese de nucleótidos. Pelo contrário, a sombra inibiu a fotossíntese, induziu a um desequilíbrio C/N e uma alteração global do metabolismo hormonal. As vias metabólicas comuns conduzindo à abscisão foram o catabolismo da putrescina, indução da biossíntese de auxinas, repressão da biossíntese de giberelinas e activação de mecanismos antioxidantes, por transcritos e metabolitos específicos. Para optimizar métodos de monda indispensáveis na produção de uva de mesa, a aplicação de GAc e do sombreamento durante a floração foram testados em diferentes cultivares. A 'Thompson Seedless' mostrou ser sensível a ambos os métodos em condições de campo, no entanto apenas a aplicação de GAc melhorou a qualidade dos bagos. Os dois tratamentos induziram a queda de flores na 'Black Magic' durante o ciclo de produção tardio em estufa, enquanto que no ciclo precoce apenas o sombreamento melhorou a qualidade dos cachos e bagos, sendo efectivo como método de monda.

Palavras-chave: abscisão, ácido giberélico, sombreamento, videira, vingamento.

Resumo alargado

Abscisão de flores e vingamento em uva de mesa (*Vitis vinifera* L.): estudo dos mecanismos fisiológicos e moleculares

Na videira (*Vitis vinifera* L.), o vingamento e a abscisão de flores ocorrem simultaneamente, após a queda das caliptras, determinando o número final de bagos, o seu calibre e a productividade. Apesar da importância da espécie cultivada, os mechanismos moleculares que regulam estes processos na videira foram pouco estudados. Este trabalho pretendeu caracterizar as alterações fisiológicas, metabólicas e transcritómicas que ocorrem durante a fase de transição de flor para bago e durante a indução de abscisão das flores, recorrendo a técnicas de transcritómica (RNA-Seq com a tecnologia Illumina) e metabolómica (plataforma que conjuga UHLC/MS/MS2 e GC/MS) em larga escala, integradas com análises cromatográficas de metabolitos específicos, determinações das trocas gasosas e teor de clorofila nas folhas e medição do crescimento vegetativo, ao longo do tempo. Estas técnicas foram aplicadas nas análises realizadas com a cultivar apirénica Thompson Seedless em condições de campo e com a cultivar com semente Black Magic em condições controladas em estufa, à excepção do RNA-Seq na Black Magic.

Foram analisadas inflorescências da 'Thompson Seedless' recolhidas a 3, 5 e 7 dias após 100% da queda das caliptras. Os nossos resultados mostraram que o processo de vingamento requer a indução da divisão celular, inibição da transcrição de genes relacionados com a senescência e com a regulação do transporte molecular, assim como das vias metabólicas relacionados com o metabolismo secundário. Foram também verificadas alterações no metabolismo dos hidratos de carbono, açúcares de sinalização e no metabolismo hormonal nas inflorescências, durante esta fase de transformação dos carpelos em bagos. Relativamente ao balanço hormonal, a repressão de genes involvidos na inactivação do ácido indol-3-acético (IAA) e de factores de transcrição MADS-box associados a auxinas, e o aumento da transcrição de um gene que codifica a giberelina 20 oxidase 2 (GA20ox2), sugerem o aumento da concentração de IAA e giberelinas no início do vingamento. A acumulação de transcritos que codificam um factor de transcrição da família AP2/ERF e uma citocinina desidrogenase, sugeriram também a activação da via de sinalização do etileno e a degradação de citocininas.

Contudo, o excessivo vingamento é um dos principais problemas apresentado pelas cultivares utilizadas na produção de uva de mesa, principalmente nas cultivares apirénicas, sendo necessária a aplicação de técnicas de monda de flores e de bagos. Elucidar o modo de acção de dois agentes indutores de abscisão de flores, identificando especificidades e pontos de comunicação entre diferentes vias que conduzem à abcisão, é um dos objectivos deste trabalho. Após a aplicação de dois tratamentos, em paralelo durante a floração, nomeadamente a

pulverização com uma solução de ácido giberélico (GAc) e a redução da luz incidente através da utilização de redes de sombra, recolhemos e analisámos as inflorescências enriquecidas com dois estímulos diferentes (alteração do balanço hormonal e redução de fotoassimilados) que levam ao aumento de queda de flores.

No caso da 'Thompson Seedless', os tratamentos consistiram na aplicação de GAc (10ppm+12.5ppm+12.5ppm) a 20%, 50% e 100% de queda das caliptras, e na intercepção total da radiação desde 50% da queda das caliptras durante 14 dias. As inflorescências analisadas foram recolhidas a 5, 7 e 10 dias após 100% da queda das caliptras. Nas videiras em vaso da cultivar Black Magic, durante o curto ciclo de produção tardio que decorre durante o verão, ambos os tratamentos foram impostos a 50% da queda das caliptras: GAc foi aplicado na concentração de 15ppm e a sombra correspondente a 90% de redução da radiação indicente durante 12 dias. As inflorescências analisadas foram recolhidas a 1, 3 e 4 dias após a data de imposição.

Os nossos resultados mostraram que a aplicação de GAc e a sombra levam à queda de flores com base em diferentes impactos no metabolismo celular. A aplicação de GAc induziu a acumulação de metabolitos e transcritos relacionados com um reforço do aparelho fotossíntetico e respiratório, assim como indução do metabolismo dos hidratos de carbono e dos nucleótidos. Por outro lado, a sombra reprimiu a fotossíntese e o metabolismo dos hidratos de carbono e provocou um desequilíbrio C/N levando à repressão da divisão celular e senescência. A sombra induziu também efeitos abrangentes nas vias relacionadas com o metabolismo e sinalização das hormonas e a sinalização dos açúcares. As vias metabólicas partilhadas durante a resposta aos dois tratamentos indutores de abscisão floral foram a regulação do catabolismo da putrescina, a indução da biossíntese de auxinas, a repressão da biossíntese de giberelinas e a activação de mecanismos antioxidantes, frequentemente revelada pela participação de transcritos e metabolitos específicos de cada tratamento.

As principais diferenças entre as duas cultivares foram observadas ao nivel do impacto da sombra no crescimento vegetativo, teor de clorofila e nas alterações promovidas nas vias metabólicas relacionadas com o metabolismo secundário.

A aplicação de métodos de monda é essencial na produção de uva de mesa, para promover a redução da compacidade dos cachos, o crescimento e desenvolvimento da cor dos bagos, uniformizar o estado de maturação e reduzir a suscetibilidade a podridões do cacho. A aplicação de GAc durante a floração é a técnica mais utilizada a nível mundial, no entanto a sua eficácia depende, entre outros fatores, das condições climáticas, sendo frequentemente reduzida. A exigência global pela mínima utilização de produtos químicos, levou também a que a aplicação deste regulador de crescimento não seja homologada em vários países. Surge assim a

necessidade de procurar técnicas de monda alternativas e a hipótese de estudar o sombreamento artificial como técnica de monda em uva de mesa.

Para comparar os efeitos dos dois métodos em diferentes cultivares, realizámos ensaios durante dois anos consecutivos na Sugraone, Thompson Seedless e Crimson Seedless em pleno campo, e durante dois ciclos produtivos, precoce e tardio, na Black Magic em estufa.

A solução de GAc foi aplicada nas concentrações recomendadas para cada cultivar e a redução da luz incidente variou entre 90 a 100%. Durante a floração foram medidas as trocas gasosas ao nível das folhas, o crescimento vegetativo e a percentagem de queda de flores. À colheita, foram analisados o peso e compacidade dos cachos, peso, diâmetro, teor de sólidos solúveis, acidez total e firmeza dos bagos e cor e teor de polifenóis na película. A aplicação de GAc levou à redução da compacidade dos cachos e melhoria da qualidade dos bagos na 'Thompson Seedless', e não apresentou resultados consistentes na 'Sugraone' e na 'Crimson Seedless'. No segundo ano de ensaios, a aplicação de GAc conduziu a um decréscimo da concentração de malvidina-3-O-glucósido na película dos bagos de ‘Crimson Seedless’, comparando com o controlo não tratado e com o tratamento sombra. A redução de 90% da radiação incidente na 'Sugraone' e 100% da radiação incidente na 'Thompson Seedless' e 'Crimson Seedless', imposta a 50% de queda das caliptras (estado fenológico 65 da escala BBCH), durante 18 dias em média, levou à redução da compacidade dos cachos à colheita. A Thompson Seedless mostrou ser a cultivar apirénica mais sensível à monda de flores provavelmente devido ao maior vigor vegetativo. Na cultivar Black Magic produzida em estufa, ambos os tratamentos levaram ao aumento da percentagem de queda de flores durante o ciclo de produção tardio, enquanto no ciclo precoce apenas a sombra induziu a queda de flores e melhorou a qualidade dos cachos e dos bagos, revelando-se um método de monda eficiente. A resposta às técnicas de monda mostrou ser dependente do genótipo/ambiente.

Table of contents

Abbreviations

ABA	Abscisic acid
ACC	1-Aminocyclopropane-1-carboxylic acid
AMP	Adenosine 5'-monophosphate
Aux/IAA	Auxin/indole-3-acetic acid transcription factor
ARF	Auxin response factor
AZ	Abscission zone
BR	Brassinosteroid
CIRAS	Infrared gas analyzer
CK	Cytokinin
CW	Cell wall
d	Days after 100% cap fall
DAB	Days after bloom (50% cap fall)
DAD	Diode array detector
DEG	Differential expressed genes
E	Transpiration rate
ERF	Ethylene response factor
FDR	False discovery rates
FPKM	Fragments per kilobase of exon per million fragments mapped
FS	Fruit set stage
GA	Gibberellin
GAc	Gibberellic acid
GAox	Gibberellin oxidase
GC	Gas chromatography/mass spectrometry
GID	Gibberellin-insensitive dwarf
GO	Gene Ontology
g_s	Stomatal conductance
HPLC	high performance liquid chromatography
IAA	Indole-3-acetic acid
IAMT	Indole-3-acetate-O-methyltransferase
IDA	Inflorescence deficient in abscission
JA	Jasmonic acid
KEGG	Kyoto Encyclopedia Of Genes And Genomes
KOG	euKaryotic Orthologous Groups
MAPK	Mitogen activated protein kinase
NAA	1-Naphthaleneacetic acid
NCBI	National Center for Biotechnology Information
PA	Polyamine
PAR	Photosynthetic active radiation
PCC	Pearson correlation coefficient
PCD	Programmed cell death
PCoA	Principal coordinate analysis
PCR	Polymerase chain reaction
PMN	Plant Metabolic Network
P_n	Net photosynthetic rate
q-rtPCR	Quantitative reverse transcription polymerase chain reaction
RFO	Raffinose family oligosaccharides

RI	Refractive index detector
RNA-Seq	High throughput RNA sequencing
ROS	Reactive oxygen species
RuBisCO	Ribulose-1,5-bisphosphate carboxylase-oxygenase
SA	Salicylic acid
SSC	Soluble solids content
SAH	S-adenosylhomocysteine
SAM	S-adenosylmethionine
se	Standard error
TA	Titratable acidity
TCA	Tricarboxylic acid
UHLC/MS/MS2	Ultrahigh performance liquid chromatography/tandem mass spectrometry

Figure list

Table list

Chapter 1

General introduction

1. General introduction

1.1 Introduction

1.1.1 Importance of grapevine and berry quality

Grapevine (*Vitis vinifera* L.) is a widely cultivated and economically important fruit crop and grapes are the third most produced fruit in the world fruit, after banana and apple, with a world production of 77 millions of tons in 2013 (http://faostat3.fao.org/). Grapes can be used as fresh fruit, dried raisins and for wine and distillates making. According to the International Organization of Vine and Wine (OIV), 30% of the total grapes produced in the world are table grapes for fresh market, in which the aspect, the size of bunches and the berries, the uniform color, taste and texture typical of each cultivar are important features valued by consumers.

Due to its economic importance and making use of the published genome sequence (Jaillon et al., 2007; Velasco et al., 2007), grapevine stands as a woody fruit crop model that can be used to study the flower abscission and fruit set processes. It has a diploid genome with a haploid chromosome number of 19. The version of the grapevine genome available at Genoscope (http://www.genoscope.cns.fr/spip/), with 12X coverage, contains an estimated size of 500Mbp and *ca*. 26500 annotated genes.

1.1.2 Flowering, fruit set and berry development

The flowering of grapevine spreads over two seasons. The first one is dedicated to the initiation of inflorescence primordia, whereas during the second one inflorescence emergence, flower and then berry development occurs (Vasconcelos et al., 2009). The inflorescences appear after leaf expansion stage, and flowers are progressively separated by floral peduncle elongation. Anthesis begins at stage 60 of BBCH scale and continues for about one week (Lorenz et al., 1994), full bloom is reached when 50% of flower caps have fallen (stage 65) and ends when 100% of caps have fallen (stage 69). Self-pollination is the most frequent, which can occur before or after cap fall, depending on cultivar (Meneghetti et al., 2006). The stage 71 marks the onset of berry development from the fertilized ovules, called fruit set. Stamens then degenerate and the young berries are visible (Lebon et al., 2008).

Grapevine berries are non-climacteric fleshy fruits disposed in clusters and undergo a double sigmoid pattern of growth, which is divided into three distinct phases (Coombe, 1992; Pratt, 1971). The first phase involves rapid growth and cell division and the number of cells is established in the developing fruit in the first two weeks after flowering, followed by a subsequent sigmoid increase in berry size over approximately 60 days due to cell expansion. The second is characterized as a lag phase and the last phase begins with veraison and is

characterized by the initiation of color development, berry softening and the continuing of berry growth. In some seedless cultivars, development of embryo and endosperm is arrested at various stages, resulting in stenospermocarpic berries. In other seedless cultivars fertilization does not occur and their berries are parthenocarpic (Pratt, 1971; Varoquaux et al., 2000).

Most of the research in grapevine have been focused on later stages of berry development in wine cultivars (Cramer et al., 2014; Deluc et al., 2007; Grimplet et al., 2007; Sweetman et al., 2012; Venturini et al., 2013; Zenoni et al., 2010). The few studies targeting flower-to-fruit transition stage demonstrated that carbohydrates availability and hormone-related pathways, mainly auxin, gibberellin and polyamines metabolism, are involved in onset of berry development in grapevine (Aziz, 2003; Dauelsberg et al., 2011; Giacomelli et al., 2013; Lebon et al., 2008; Perez et al., 2000). During the fruit set, berries increase their size several times and nearly final cell number per berry is established (Ojeda et al., 1999). Therefore, the success of this developmental stage, which is highly sensitive to biotic and abiotic stresses (Vasconcelos et al., 2009; Zinn et al., 2010), is critical to determine berry number, their final size and yield potential.

1.1.3 Thinning methods in table grapes

Fruit set is often excessive on table grape production, limiting potential berry growth and resulting in compacted bunches, small berries, inadequate color development of berries and in a greater susceptibility to bunch rot. Thus thinning berries is an important cultural practice in table grape production to maximize the quality and value of the production (Di Lorenzo et al., 2011). Excluding exclusively labor-demanding manual thinning, the most common thinning practice is chemical thinning with gibberellic acid spray (GAc) spray during bloom followed by hand adjustments when necessary. However, the success of GAc treatment depends on the environmental conditions (Dokoozlian, 1998; Reynolds and Savigny, 2004; Reynolds et al., 2006), its use is not authorized in organic production, and in some countries, in integrated crop management system. Due to the inconsistent results and restrictions, to find an alternative thinning method is needed. Previous works reported by Byers et al. (1990, 1991), Schneider (1978) and by ourselves (Zibordi et al., 2009), in apple (*Malus* x *domestica*), showed that thinning via shading has similar effects on fruit drop compared to chemical thinners. According to these authors shading in a specific period, when the stored carbohydrates reached a minimum, leads to a deficit in the carbon reserves and will increase the competition between vegetative and reproductive organs and promote flower abortion and abscission. In grapes, it was verified that carbon shortage caused by defoliation and by shade conditions during bloom reduced berry set and the final number of berries per bunch (Ferree et al., 2001; Lohitnavy et al., 2010; Roubelakis and Kliewer, 1976).

1.1.4 Flower abscission regulation

During the first two weeks after anthesis also natural flower abscission takes place (Bessis and Fournioux, 1992). Abscission is a separation process that enables vegetative and reproductive organs to be shed in response to developmental, hormonal and environmental cues. The current accepted model of abscission (Estornell et al., 2013; Patterson, 2001) defines four major stages in the abscission pathway: differentiation of the abscission zone (AZ), acquisition by the AZ cells of competence to react to abscission signals (regulation phase), activation of the abscission process within the AZ and organ detachment (execution phase), and differentiation of a protective layer on the plant's side surface (Fig.1.1). The formation of AZ, composed by specialized cells, involves transcription factors belonging to different gene families (Lashbrook and Cai, 2008; Nakano et al., 2014). AZ cells, which are maintained in a state of apparent lack of differentiation throughout organ development, can respond to abscission signals that may be triggered by stress situations or development cues and are mediated by hormones. The acquisition of sensitivity to ethylene by the AZ cells has been associated with an altered expression of auxin-regulated genes as a result of auxin depletion (Basu et al., 2013; Meir et al., 2010). In addition, signals derived from energy deprivation may participate together with hormones in the abscission signaling pathway (Baena-González and Sheen, 2008). The natural reduction of fruit set is called the physiological drop which enables the plant to drop off the weaker sinks regulating the fruit load with its ability in producing the metabolic energy required to attain the final development of reproductive and vegetative structures (Bonghi et al 2000). Aiming to clarify abscission mechanisms and answer the question how chemical/environmental stimuli enhance abscission, recent works have been published regarding fruit abscission as a response to growth regulators application and to light reduction in fruit crops as tomato (*Solanum lycopersicum*) (Meir et al., 2010; Nakano et al., 2013; Wang et al., 2013) and apple (Botton et al., 2011; Eccher et al., 2015; Ferrero et al., 2015; Zhu et al., 2011). However, the exact mechanisms of each stage of abscission model, the differences between organ and species and in response to different abscission inducing signals are far from elucidated.

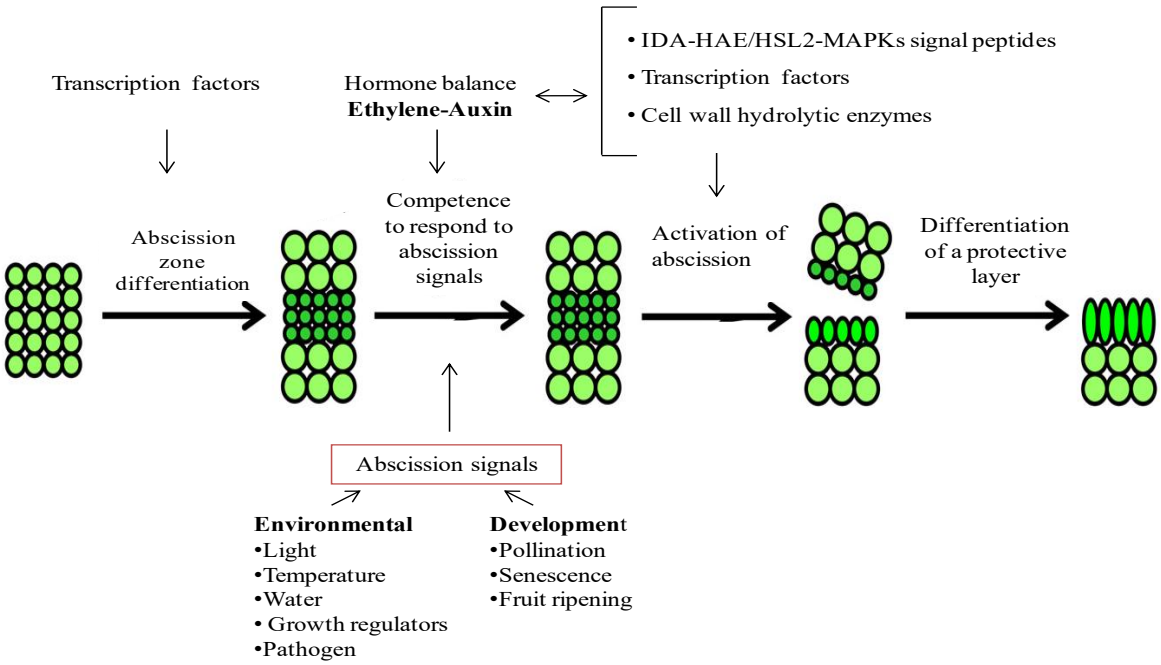

Figure 1.1. The four-phase model to describe the abscission process and putative regulators implicated in the development, regulation and activation of the abscission zone (AZs) (adapted from Estornell et al., 2013; Tripathi et al., 2008).

1.1.5 Large-scale omics data

The development of high-throughput sequencing methods provides powerful tolls to accurately quantifying transcriptomes with relatively reduced time and cost per-reaction (Wang et al., 2009). RNA-Seq can reveal novel information for an organism without having prior information and also can add more informative results to the current data on genome-known organisms. The produced data allied with the development of bioinformatic tools have shown the transcriptome magnitude and complexity, and can be used for many applications, ranging from gene expression profiling, *de novo* assembly to mining for single nucleotide polymorphisms (SNPs) and for alternative splicing, among others (Jazayeri et al., 2015). RNA-Seq is a quantitative method that allows accessing RNA expression levels more accurately than microarrays, allowing determine the absolute quantity of every molecule in a cell population, and directly compare results between experiments (Wang et al., 2009). Gene expression levels are closely correlated with q-rtPCR and RNA spike-in controls (Marioni et al., 2008).

Altered gene expression is ultimately reflected in changes on the primary and secondary metabolites. In turn, the metabolome captures the functional or physiological state of the cell and can influence gene expression and protein stability (Tugizimana et al., 2013). Global metabolic-profiling technology is an excellent tool for analyzing metabolism due to its ability to

assess a relatively large number of compounds, without any pre-selection, in a single or a small number of analyses, combining GC/MS and LC/MS platforms (Evans et al, 2009; Lombardo et al., 2011).

The large-scale analysis promote new possibilities for understanding complex biological processes in a wider scale and can be applied to field trials, connecting genotype and environment, which in agriculture is influenced by multi-stress conditions (Alexandersson et al., 2014). These techniques were already used with success in grapevine (Hochberg et al., 2013 and Zamboni et al., 2010 (for metabolomics); Perazzolli et al., 2013; Sweetman et al., 2012; Venturini et al., 2013 and Zenoni et al., 2010 (for RNA-Seq).

1.2 Objectives and thesis outline

The aim of the research described here of was to determine the transcriptomic, metabolomic and physiological changes occurring during the complex processes of fruit set and flower abscission in table grapevines, which have a profound impact on the later stages of berry development. Using GAc application and reduction of light interception in parallel allowed to produce sample sets with predictable floweret destiny ‘to abscise or not to abscise’, triggered by different cues (chemical and low light), which were analyzed by integrated cutting-edge metabolomics and RNA-Seq transcriptomics coupled with targeted chromatography in time-course assays. In addition, the imposition of GAc spray or shading was tested in different cultivars and vines growing in greenhouse and field conditions, aiming to determine its effectiveness as thinning methods.

To accomplish the above mentioned aims, we intend to fulfill the following specific research objectives:

i) To ascertain the main pathways involved in fruit set in stenospermocarpic table grapes specifically targeting the early phase of this development stage.

ii) To provide a first insight for understanding the changes occurring in vine inflorescences and canopy that explain flower abscission on 'Black Magic' vines triggered by GAc spraying and shade. Assays were conducted in different climatic conditions occurring during early and later production cycles in a greenhouse production system, enabling to test for the first time shading as an alternative thinning method in table grapes.

iii) To identify specificities and communication within pathways leading to flower abscission triggered by different cues (GAc and C-starvation) in 'Thompson Seedless' grapevine growing in the field conditions.

iv) To investigate the potential of light reduction using shading nets and GAc application during bloom in stenospermocarpic table grape cultivars, namely Sugraone, Thompson Seedless and Crimson Seedless, as thinning methods, to reduce fruit set, improve bunch compactness and berries quality.

For these purposes four research topics were chosen and developed in each chapter, where a detailed introduction on each topic can be found, according to the thesis organization described in Fig 1.2.

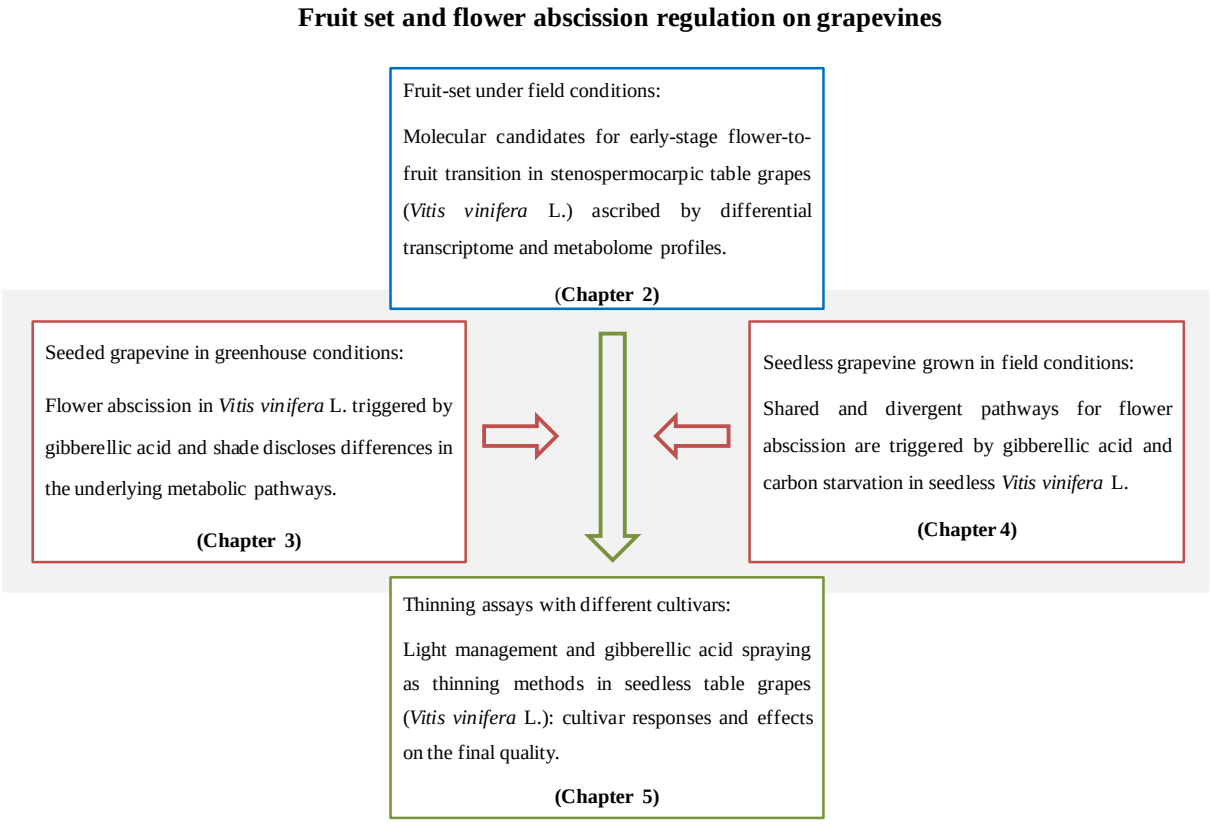

Figure 1.2. Diagram of thesis organization. Advancing in knowledge about fruit set regulation and flower abscission mechanism triggered by different stimuli has the final scope of improving control of crop load in table grape production.

1.3 References

Alexandersson E, Jacobson D, Vivier MA, Weckwerth W and Andreasson E. 2014. Field-omics-understanding large-scale molecular data from field crops. *Front. Plant Sci.* 5: 286.

Aziz A. 2003. Spermidine and related metabolic inhibitors modulate sugar and amino acid levels in *Vitis vinifera* L.: possible relationships with initial fruitlet abscission. *J. Exp. Bot.* 54: 355–363.

Baena-González E and Sheen J. 2008. Convergent energy and stress signaling. *Trends Plant Sci.* 13: 474–482.

Basu MM, González-Carranza ZH, Azam-Ali S, Tang S, Shahid AA and Roberts JA. 2013. The manipulation of auxin in the abscission zone cells of Arabidopsis flowers reveals that indoleacetic acid signaling is a prerequisite for organ shedding. *Plant Physiol.* 162: 96–106.

Bessis R and Fournioux JC. 1992. Abscission zone and berry drop in grapevine. *Vitis*. 31: 9–21.

Bonghi C, Tonutti P and Ramina A. 2000. Biochemical and molecular aspects of fruitlet abscission. *Plant Growth Regul*. 31: 35–42.

Botton A, Eccher G, Forcato C, Ferrarini A, Begheldo M, Zermiani M, Moscatello S, et al. 2011. Signaling pathways mediating the induction of apple fruitlet abscission. *Plant Physiol.* 155: 185–208.

Byers R, Barden J and Carbaugh D. 1990. Thinning of spur Delicious apples by shade, terbacil, carbaryl, and ethephon. *J. Amer. Soc. Hort. Sci.* 15:9–13.

Byers R, Carbaugh D, C. P and Wolf T. 1991. The influence of low light on apple fruit abscission. *J. Hort. Sci. Biotech*. 115: 9-13

Coombe BG. 1992. Research on Development and Ripening of the Grape Berry. *Am. J. Enol. Vitic.* 43: 101–110.

Cramer GR, Ghan R, Schlauch KA, Tillett RL, Heymann H, Ferrarini A, Delledonne M, et al. 2014. Transcriptomic analysis of the late stages of grapevine (*Vitis vinifera* cv. *Cabernet Sauvignon*) berry ripening reveals significant induction of ethylene signaling and flavor pathways in the skin. *BMC Plant Biol.* 14: 370.

Dauelsberg P, Matus JT, Poupin MJ, Leiva-Ampuero A, Godoy F, Vega A and Arce-Johnson P. 2011. Effect of pollination and fertilization on the expression of genes related to floral transition, hormone synthesis and berry development in grapevine. *J. Plant Physiol.* 168: 1667–1674.

Deluc LG, Grimplet J, Wheatley MD, Tillett RL, Quilici DR, Osborne C, Schooley DA, et al. 2007. Transcriptomic and metabolite analyses of *Cabernet Sauvignon* grape berry development. *BMC Genomics*. 8: 429.

Di Lorenzo R, Gambino C and Scafidi P. 2011. Summer Pruning in Table Grape. *Adv. Hortic. Sci.* 25: 143–150.

Dokoozlian NK. 1998. Use of plant growth regulators in table grape production in California. in Dokoozlian, N.K. (Ed.),*Proc.Univ. Calif. Table Grape Prod. Course. 30:* 200–210.

Eccher G, Begheldo M, Boschetti A, Ruperti B and Botton A. 2015. Roles of ethylene production and ethylene-receptor expression in regulating apple fruitlet abscission. *Plant Physiol.*15.00358

Estornell LH, Agustí J, Merelo P, Talón M and Tadeo FR. 2013. Elucidating mechanisms underlying organ abscission. *Plant Sci.* 199–200: 48–60.

Evans A, DeHaven C and Barrett T. 2009. Integrated, nontargeted ultrahigh performance liquid chromatography/electrospray ionization tandem mass spectrometry platform for the identification and relative. *Anal. Chem.* 16: 6656–6667.

Ferree DC, McArtney SJ and Scurlock DM. 2001. Influence of Irradiance and Period of Exposure on Fruit Set of French-American Hybrid Grapes. *J. Am. Soc. Hortic. Sci.* 126: 283–290.

Ferrero S, Carretero-Paulet L, Mendes MA, Botton A, Eccher G, Masiero S and Colombo L. 2015. Transcriptomic signatures in seeds of apple (*Malus domestica* L. Borkh) during fruitlet abscission. *PLoS One*. 10: e0120503.

Giacomelli L, Rota-Stabelli O, Masuero D, Acheampong AK, Moretto M, Caputi L, Vrhovsek U, et al. 2013. Gibberellin metabolism in *Vitis vinifera* L. during bloom and fruit-set: functional characterization and evolution of grapevine gibberellin oxidases. *J. Exp. Bot.* 64: 4403–4419.

Grimplet J, Deluc LG, Tillett RL, Wheatley MD, Schlauch KA, Cramer GR and Cushman JC. 2007. Tissue-specific mRNA expression profiling in grape berry tissues. *BMC Genomics*. 8: 187.

Hochberg U, Degu A, Toubiana D, Gendler T, Nikoloski Z, Rachmilevitch S and Fait A. 2013. Metabolite profiling and network analysis reveal coordinated changes in grapevine water stress response. *BMC Plant Biol.* 13: 184.

Jazayeri SM, Melgarejo-Muñoz LM and Romero HM. 2014. Rna-seq: a glance at technologies and methodologies. *Acta Biol. Colomb*. 20: 23–35.

Jaillon O, Aury J-M, Noel B, Policriti A, Clepet C, Casagrande A, Choisne N, et al. 2007. The grapevine genome sequence suggests ancestral hexaploidization in major angiosperm phyla. *Nature*. 449: 463–467.

Lashbrook CC and Cai S. 2008. Cell wall remodeling in Arabidopsis stamen abscission zones: Temporal aspects of control inferred from transcriptional profiling. *Plant Signal Behav*. 3: 733–736.

Lebon G, Wojnarowiez G, Holzapfel B, Fontaine F, Vaillant-Gaveau N and Clément C. 2008. Sugars and flowering in the grapevine (*Vitis vinifera* L.). *J. Exp. Bot.* 59: 2565–2578.

Lohitnavy N, Bastina S and Collins C. 2010. Early leaf removal increases flower abscission in *Vitis vinifera* 'Semillon'. *Vitis*. 49: 51–53

Lombardo VA, Osorio S, Borsani J, Lauxmann MA, Bustamante CA, Budde CO, Andreo CS, et al. 2011. Metabolic profiling during peach fruit development and ripening reveals the metabolic networks that underpin each developmental stage. *Plant Physiol.* 157: 1696–1710.

Lorenz D, Eichhorn K, Bleiholder H, Klose R, Meier U and Weber E. 1994. Phänologische Entwicklungsstadien der Rebe (*Vitis vinifera* L. ssp. *vinifera*). Codierung und Beschreibung nach der erweiterten BBCH-Skala. *Vitic. Enol. Sci.* 49: 66-70

Marioni JC, Mason CE, Mane SM, Stephens M and Gilad Y. 2008. RNA-seq: an assessment of technical reproducibility and comparison with gene expression arrays. *Genome Res.* 18: 1509–1517.

Meir S, Philosoph-Hadas S, Sundaresan S, Selvaraj KSV, Burd S, Ophir R, Kochanek B, et al. 2010. Microarray analysis of the abscission-related transcriptome in the tomato flower abscission zone in response to auxin depletion. *Plant Physiol.* 154: 1929–1956.

Meneghetti S, Gardiman M and Calo A. 2006. Flower biology of grapevine. A review. *Adv. Hortic. Sci.* 20: 317-325

Nakano T, Fujisawa M, Shima Y and Ito Y. 2013. Expression profiling of tomato pre-abscission pedicels provides insights into abscission zone properties including competence to respond to abscission signals. *BMC Plant Biol.* 13: 40.

Nakano T, Fujisawa M, Shima Y and Ito Y. 2014. The AP2/ERF transcription factor SlERF52 functions in flower pedicel abscission in tomato. *J. Exp. Bot.* 65: 3111–3119.

Ojeda H, Deloire A, Carbonneau A, Ageorges A and Romieu C. 1999,July30. Berry development of grapevines: Relations between the growth of berries and their DNA content indicate cell multiplication and enlargement. *Vitis.* 38: 145-150.

Patterson SE. 2001. Cutting Loose. Abscission and Dehiscence in Arabidopsis. *Plant Physiol.* 126: 494–500.

Perazzolli M, Moretto M, Fontana P, Ferrarini A, Velasco R, Moser C, Delledonne M, et al. 2012. Downy mildew resistance induced by Trichoderma harzianum T39 in susceptible grapevines partially mimics transcriptional changes of resistant genotypes. *BMC Genomics.* 13: 660.

Perez FJ, Viani C and Retamales J. 2000. Bioactive Gibberellins in Seeded and Seedless Grapes: Identification and Changes in Content During Berry Development. *Am. J. Enol. Vitic.* 51: 315–318.

Pratt C. 1971. Reproductive Anatomy in Cultivated Grapes - A Review. *Am. J. Enol. Vitic.* 22: 92–109.

Reynolds AG and Savigny C. 2004. Influence of girdling and gibberellic acid on yield components, fruit composition and vestigial seed formation of 'Sovereign Coronation' table grapes. *HortScience*. 39: 541–544.

Reynolds AG, Roller JN, Forgione A and De Savigny C. 2006. Gibberellic Acid and Basal Leaf Removal: Implications for Fruit Maturity, Vestigial Seed Development, and Sensory Attributes of Sovereign Coronation Table Grapes. *Am. J. Enol. Vitic.* 57: 41–53.

Roubelakis KA and Kliewer WM. 1976. Influence of Light Intensity and Growth Regulators on Fruit-Set and Ovule Fertilization in Grape Cultivars under Low Temperature Conditions. *Am. J. Enol. Vitic.* 27: 163–167.

Schneider GW. 1978. Abscission Mechanism Studies with Apple Fruitlets. *J Amer Soc Hort Sci*. 103: 455–458.

Sweetman C, Wong DC, Ford CM and Drew DP. 2012. Transcriptome analysis at four developmental stages of grape berry (*Vitis vinifera* cv. *Shiraz*) provides insights into regulated and coordinated gene expression. *BMC Genomics*. 13: 691.

Tripathi SK, Sane AP, Nath P, Tuteja N. 2008. Organ abscission in plants: Understanding the process through transgenic approaches. In: Rivera-Dominguez M, Troncoso-Rojas R, Tiznado-Hernandez ME. *A transgenic approach in plant biochemistry and physiology*, Research Signpost. 155–180.

Tugizimana F, Piater L and Dubery I. 2013. Plant metabolomics: A new frontier in phytochemical analysis. *S. Afr. J. Sci.* 109: 5–6.

Varoquaux F, Blanvillain R, Delseny M and Gallois P. 2000. Less is better: new approaches for seedless fruit production. *Trends Biotechnol.* 18: 233–242.

Vasconcelos MC, Greven M, Winefield CS, Trought MCT and Raw V. 2009. The Flowering Process of *Vitis vinifera*: A Review. *Am. J. Enol. Vitic.* 60: 411–434.

Velasco R, Zharkikh A, Troggio M, Cartwright DA, Cestaro A, Pruss D, Pindo M, et al. 2007. A high quality draft consensus sequence of the genome of a heterozygous grapevine variety. *PLoS One*. 2: e1326.

Venturini L, Ferrarini A, Zenoni S, Tornielli GB, Fasoli M, Dal Santo S, Minio A, et al. 2013. De novo transcriptome characterization of *Vitis vinifera* cv. Corvina unveils varietal diversity. *BMC Genomics*. 14: 41.

Wang Z, Gerstein M and Snyder M. 2009. RNA-Seq: a revolutionary tool for transcriptomics. *Nat. Rev. Genet.* 10: 57–63.

Wang X, Liu D, Li A, Sun X, Zhang R, Wu L, Liang Y, et al. 2013. Transcriptome analysis of tomato flower pedicel tissues reveals abscission zone-specific modulation of key meristem activity genes. *PLoS One*. 8: e55238.

Zamboni A, Di Carli M, Guzzo F, Stocchero M, Zenoni S, Ferrarini A, Tononi P, et al. 2010. Identification of putative stage-specific grapevine berry biomarkers and omics data integration into networks. *Plant Physiol.* 154: 1439–59.

Zenoni S, Ferrarini A, Giacomelli E, Xumerle L, Fasoli M, Malerba G, Bellin D, et al. 2010. Characterization of Transcriptional Complexity during Berry Development in *Vitis vinifera* Using RNA-Seq. *PLANT Physiol.* 152: 1787–1795.

Zhu H, Dardick C, Beers E, Callanhan A, Xia R and Yuan R. 2011. Transcriptomics of shading-induced and NAA-induced abscission in apple (*Malus domestica*) reveals a shared pathway involving reduced photosynthesis, alterations in carbohydrate transport and signaling and hormone crosstalk. *BMC Plant Biol.* 11: 138.

Zibordi M, Domingos S and Corelli Grappadelli L. 2009. Thinning apples via shading: an appraisal under field conditions. *J. Hort. Sci. Biotech.* 138–144.

Zinn KE, Tunc-Ozdemir M and Harper JF. 2010. Temperature stress and plant sexual reproduction: uncovering the weakest links. *J. Exp. Bot.* 61: 1959–1968.

Chapter 2

Molecular candidates for early-stage flower-to-fruit transition in stenospermocarpic table grape (*Vitis vinifera* L.) inflorescences ascribed by differential transcriptome and metabolome profiles

The data presented in this chapter were submitted to Plant Science:

Domingos S [1,2], Fino J [3], Paulo OS [3], Oliveira CM [1], Goulao FG[2]

[1] Linking Landscape, Environment, Agriculture and Food, Instituto Superior de Agronomia, Universidade de Lisboa, Lisbon, Portugal

[2] Instituto de Investigação Científica Tropical I.P., Lisbon, Portugal

[3] Computational Biology and Population Genomics Group, cE3c – Centre for Ecology, Evolution and Environmental Changes, Faculdade de Ciências, Universidade de Lisboa, Lisbon, Portugal

2. Molecular candidates for early-stage flower-to-fruit transition in stenospermocarpic table grape (*Vitis vinifera* L.) inflorescences ascribed by differential transcriptome and metabolome profiles

Abstract

Flower-to-fruit transition depends of nutrient availability and regulation at the molecular level by sugar and hormone signaling crosstalk. However, in most species, the identity of fruit initiation regulators and their targets are largely unknown. To ascertain the main pathways involved in stenospermocarpic table grapes fruit set, comprehensive transcriptional and metabolomic analyses were conducted specifically targeting the early phase of this development stage in 'Thompson Seedless'. The high-throughput analyses performed disclosed the involvement of 496 differentially expressed genes and 28 differently accumulated metabolites in the sampled inflorescences. Our data shows broad transcriptome reprogramming of molecule transporters, globally down-regulating gene expression and suggest that regulation of sugar- and hormone-mediated pathways determines the downstream activation of berry development. The most affected gene was *SWEET14* sugar transporter. Hormone-related transcription changes were observed, associated with increased indole-3-acetic acid, stimulation of gibberellin metabolism and cytokinin degradation, and regulation of MADS-box and AP2-like ethylene-responsive transcription factor expression. Secondary metabolism, the most representative biological process at transcriptome level, was predominantly repressed. The results add to the knowledge of molecular events occurring in grapevine inflorescences fruit set and provide a list of candidates, paving the way for genetic manipulation aiming at model research and plant breeding.

Keywords: fruit set, grapevine, metabolic pathways, RNA-seq, seedless

2.1 Introduction

Fruit set, or flower-to-fruit transition, is the stage in which the ovary progresses to a growing young fruit. Fruit cell number and the ultimate number of fruits formed are determined during this development stage, with decisive impact in the final fruit size and plant yield potential. During the first two to three weeks after full bloom, an abrupt increase in ovary size occurs due to cell multiplication and, to a lesser extent, to cell enlargement (Coombe, 1960; Dokoozlian, 2000; Ojeda et al., 1999; Pratt, 1971). During this period, reproductive organs are significantly

more sensitive to biotic and abiotic stresses than during later stages of berry development or vegetative growth (Boyer and McLaughlin, 2007; Jin et al., 2009; Kliewer, 1977; Suwa et al., 2010; Vasconcelos et al., 2009; Zinn et al., 2010), so the success of this developmental stage is critical both to species biological survival and agronomic sustainability.

Nowadays, an increase in table grape world production is clearly evident and, based on consumer preferences, is accompanied by a strong interest in seedless varieties for fresh consumption. Therefore, seedlessneess, is among the main focus of current table grape breeding programs (Nwafor et al., 2014). In seeded grapes, flower-to-fruit transition requires pollination and ovary fertilization towards seed formation. In seedless grapes, two mechanisms can be distinguished: parthenocarpy, which occurs when the ovary is able to develop without ovule fertilization (e.g. Black Corinth cv.) and stenospermocarpy, which progresses after pollination and fertilization, but the embryo aborts two to four weeks after fertilization (e.g. Thompson Seedless cv.) (Dokoozlian, 2000; Varoquaux et al., 2000). In the later case, partially developed seeds or seed traces can be found.

Fruit set is increasingly sustained by photoassimilates and other nutrients exported from photosynthetically active leaves through the phloem (Lebon et al., 2008) and photosynthesized by the inflorescence itself. Hence, the success of this developmental process depends on factors such as photoassimilates production, transport capacity, and phloem unloading to the fruit. Nonetheless, the main determinant is the fruit sink strength (Werner et al., 2011; Zhang et al., 2005). Based on transcript and metabolite analyses during fertilization-dependent and -independent fruit formation, it was further verified in the fruit model species tomato (*Solanum lycopersicon*) that, in addition to nutrient availability, common pathways of flower-to-fruit transition include modulation by sugar and hormone signaling crosstalk, and regulation by specific transcription factors from several families (De Jong et al., 2009, 2011; Olimpieri et al., 2007; Pascual et al., 2007; Ren et al., 2011; Serrani et al., 2007; Vriezen et al., 2008; Wang et al., 2005, 2009). However, only few components of the mechanism regulating fruit set have been identified so far. According to the hypothetical model for sugar signaling in seed and fruit set regulation (Ruan et al., 2012), glucose, as the product of sucrose hydrolysis, acts as a signal molecule to repress the expression of programmed cell death (PCD) genes and to promote cell division that, in turn, leads to fruit set. Under severe stress conditions, phloem sucrose import is blocked, which together with a depletion of starch reserves, results in reduced glucose levels, triggering the PCD pathway and inhibiting cell division, consequently leading to fruit abortion (McLaughlin and Boyer, 2004). Auxins, ethylene and gibberellins are other key players with a prominent role in triggering and coordinating the fruit set developmental process (Vriezen et al., 2008). Auxin signaling is recognized as one of the earliest events in the fruit initiation cascade, particularly the fine-tuning of *AUXIN/INDOLE-3-ACETIC ACID* (*Aux/IAA*), *AUXIN*

RESPONSE FACTOR (*ARF*) and MADS-box gene expression (Wang et al., 2009). In addition, fruit set is mediated by activating gibberellin (GA) biosynthesis mainly through the up-regulation of *GIBBERELLIN OXIDASE 20* (*GA20ox*) (Serrani et al., 2007). Polyamine (PA) metabolism showed different dynamics according to individual species. Levels of putrescine were showed to decreased in tomato while increasing in plum (*Prunus insititia*) during fruit set (De Dios et al., 2006; Wang et al., 2009). Alterations in secondary metabolism were also found during this stage, for instance, ascorbate antioxidant levels declined during the anthesis to postanthesis transition, while its direct precursor, galactonate 1,4-lactone, increased at postanthesis stage (Wang et al., 2009).

Despite the importance of grapevine, both from the economic point of view and as a genomic model for studying woody fruit species (Jaillon et al., 2007; Velasco et al., 2007), to date, the development-related global transcriptomic and metabolite analyses reported targeted only later stages of berry development (Cramer et al., 2014; Deluc et al., 2007; Grimplet et al., 2007; Sweetman et al., 2012; Venturini et al., 2013; Zenoni et al., 2010). In this work, through differential gene expression and metabolite analyses, we aimed at identifying the putative molecular cues responsible for initial flower-to-fruit transition in stenospermocarpic table grapes, which have a profound impact on the later stages of berry development.

2.2 Material and methods

2.2.1 Sample collection

Grape inflorescences were collected from seven-year-old cv. Thompson Seedless commercial vines (*Vitis vinifera* L.), grafted on 140 Ruggeri rootstock, spaced 3 x 3 m and grown under an overhead trellis system covered with plastic. The commercial vineyard is located in Ferreira do Alentejo, south of Portugal (38° 05' 23.80" N; 8° 04' 52.7 1" W) and was managed following standard fertilization, irrigation, and pest-management practices. Climate conditions (PAR, temperature and relative humidity) were monitored above the vines canopy (WatchDog MicroStation, Spectrum Tech., USA) and showed to be maintained during the sampling period (Supplementary Figure S2.1). To guarantee that the 2-3 days period required after pollination for fertilization to be completed (Vasconcelos et al., 2009), was spanned, inflorescence sampling was conducted at three time-points (Fig. 2.1): FS1 (3 days after 100% cap fall (3d)), FS2 (5d) and FS3 (7d). 100% cap fall corresponded to stage 69 of the BBCH scale (Lorenz et al., 1994). In each point, three biological replicates were randomly collected from the same five vines. Each biological replicate was, therefore, composed by one inflorescence, deprived from

rachis, immediately frozen in liquid nitrogen and subsequently powdered and stored at -80ºC until use.

FS1 (3 d) FS2 (5 d) FS3 (7 d)

Figure 2.1. Aspect of representative cv. Thompson Seedless inflorescences during fruit set. Samples were collected at fruit set stage 1 (FS1, 3 days after 100% cap fall (3d)), fruit set stage 2 (FS2, 5d) and fruit set stage 3 (FS3, 7d). Scale bar is 0.6 cm.

2.2.2 RNA whole transcriptome deep sequencing

Total RNA was extracted and purified from *ca*. 100 mg frozen material independently for each biological sample using the RNeasy Plant RNA Extraction Kit and RNase-Free DNase Set (Qiagen, Hilden, Germany) following manufacturer's instructions, modified by replacing the kit's extraction buffer by 100 mM Tris-HCl, 2% (w/v) CTAB, 25 mM EDTA and 2 M NaCl buffer (Chang et al., 1993). When traces of contaminant genomic DNA were detected after standard PCR amplification of the *Actin 1* (*ACT1*) gene (GenBank Accession: XM_002282480.3; primer forward: 5'-CTTCCAGCCATCTCTCATTGG-3' and primer reverse: 5'- TGTTGCCATAGAGGTCCTTCC-3'), RNA samples were further digested with RNase-free DNase I (Ambion, Life Techonologies, CA, USA). RNA integrity and purity were evaluated by visual inspection of ribosomal bands after 1.5% agarose gel electrophoresis and through 2100 Bioanalyzer system (Agilent Technologies, CA, USA) readings. Poly(A) mRNA isolation, cDNA synthesis, library generation, indexing, cluster generation and RNA-seq analyses by Illumina HiSeq 2000 RNA sequencing of 100-bp paired-end reads were carried out by LGC Genomics (Berlin, Germany), using commercial services.

2.2.3 Alignment and analysis of Illumina reads

The raw Illumina 100-bp pair-end sequences were deposited in the NCBI Sequence Read Archive (SRA) under accession numbers [SRS:853491, SRS:879704, SRS:879828, SRS:879847, SRS:879856, SRS:882229, SRS:882241, SRS:882246 and SRS:882247].

Poor quality-base reads and adapter sequences were trimmed using the Trimmomatic version 0.32 software (Bolger et al., 2014). Trimmed reads were mapped back to the reference genome (Jaillon et al., 2007) for quantification of gene expression levels and global transcript expression profiling within each time-point using Tophat2 version 2.0.12 (Kim et al., 2013) with the parameters -D 15 -R 2 -L 22 -i S,1,1.15 and end-to-end mode. The number of reads mapped to each gene per sample was extracted from the output bam files of Tophat2 using the in-house python script bamzinga (https://github.com/Nymeria8/bamzinga). Quantification and normalization of gene expression values by fragments per kilobase of exon per million fragments mapped (FPKM) was calculated by Cufflinks package cuffdiff version 2.2.1 (Trapnell et al., 2010). Mfuzz R package version 2.26.0 (Kumar and Futschik, 2007) processed the expression data to generate clustering plots with missing data and low standard deviation filtering, and number of centers set to 9.

The RNA-Seq data allowed comparison between the Thompson Seedless cultivar and the reference genome, related to the seeded variety Pinot Noir (Jaillon et al., 2007). Across the expressed genes in 'Thompson Seedless' inflorescences under the conditions of the assay, SNPs and posttranscriptional processing events, such as constitutive and alternative splicing, were identified. To mine for the existence of polymorphisms, the bam files from all the mapping steps were merged, and submitted to Atlas-SNP2 (Shen et al., 2010) version 1.4.3 with the parameters --Illumina -y 15 -m 5 -g 5. To extract the results from the output vcf file, together with the annotation gtf file, an in-house python script (https://github.com/Nymeria8/NGS_utilities/blob/master/polimorph_gtf.py), was used. Cufflinks program cuffmerge was used to identify new splicing events between the reference genome and our data set. To increase accuracy, we conservatively required that at least 10 independent reads mapped in the isoform and at least 10 reads mapped across the entire exon-exon junction.

2.2.4 Differential gene expression, functional annotation and pathway analysis

Statistical analysis to identify differential expressed genes (DEG) between time-points, was conducted using the R package version 3.0.2 from Bioconductor, DESeq2 version 1.4.5 (Love et al., 2014) considering estimation of size factors, a false discovery rate (FDR) of 0.05 and a $-1.5 \geq \log2$ fold-change ≥ 1.5.

Functional annotation of the grapevine genome (Jaillon et al., 2007) was obtained based on sequence homologies with KOG (euKaryotic Orthologous Groups) and NCBI databases. To obtain the KOG annotation of grapevine genes, Rapsearch2 (Zhao et al., 2012) was used to search against functional proteins from *Arabidopsis thaliana* in the database (Tatusov et al.,

2003) considering an e-value cut-off of 10^{-5}. From the total DEG identified, those that were not automatically assigned for a specific KOG functional category were either ascribed in the KOG categories according to the gene description or classified as other or of unknown function. For additional gene assignment in Kyoto Encyclopedia of Genes and Genomes (KEGG (Kanehisa et al., 2008)) and Gene Ontology (GO) annotation, Rapsearch2 similarity searches were locally conducted against non-redundant ("nr") peptide database (ftp://ftp.ncbi.nlm.nih.gov/blast/db/) downloaded at November 26, 2013, including all "nr" GenBank CDS translations + PDB + SwissProt + PIR+PRF). The output was submitted to an in-house developed script - Rapsearch2XML (https://github.com/Nymeria8/Rapsearch2Xml) and then to Blast2GO (Conesa et al., 2005) for enzyme identification, metabolic pathway assignment and functional annotation using GO terms. GO enriched categories were assigned using the R bioconductor package topGO version 2.18.0 (Alexa and Rahnenfuhrer, 2010), using a Fisher's exact test and *p*-value≤0.01.

Similarity of expression profiles between biological replicates was determined by Pearson correlation coefficient (PCC) analyses with R software using natural logarithm (ln)-transformed read counts for the DEG as input. All the analyses considered three independent biological replicates per treatment sequenced, providing higher statistical robustness and data validation.

2.2.5 Global metabolomic analysis

Circa 200 mg of powdered material from each of the three biological replicates collected in each time-point were lyophilized, extracted with methanol and analyzed using the integrated platform developed by Metabolon® (Durham, USA) consisting of a combination of three independent approaches: (1) ultrahigh performance liquid chromatography/tandem mass spectrometry (UHLC/MS/MS2) optimized for basic species, (2) UHLC/MS/MS2 optimized for acidic species, and (3) gas chromatography/mass spectrometry (GC/MS). Methods were performed as previously described (Evans et al., 2009, 2012; Ohta et al., 2009).

2.2.6 Differentially quantified metabolites and mapping on metabolic pathways

Raw area counts for each biochemical compound were rescaled by dividing each sample's value by the median value for the specific biochemical. Statistical analysis of the data was performed using Array Studio (Omicsoft). Welch's two-sample t-tests were then used to determine whether or not each metabolite had significantly increased or decreased in abundance. Mapping of named metabolites was performed onto general biochemical pathways, as provided in the KEGG databases (www.genome.jp/kegg/) and Plant Metabolic Network (PMN) (www.plantcyc.org/). Box plots were generated for those compounds that showed a significant change using both the Welch two-sample t-test (*p*-value≤0.05) and |log2 fold-change|≥1.

2.2.7 Global analysis of transcriptome and metabolome profiling

Data for transcript and metabolite profiling analyses was ln–transformed and Normal distribution was verified by histogram plotting the number of reads and metabolites per sample using the R software. For exploratory data analyses, Principal coordinate analysis (PCoA) was conducted based on the pair-wise correlation matrix using the NTsys-PC version 2.20e software package (Rohlf, 2005). The DCENTER module was used to transform the symmetric matrix to scalar product and EIGEN for eigenvalues decomposition to identify orthogonal components of the original matrix modules. A minimum-spanning tree was calculated and superimposed to facilitate the visualization of the distances between operational units. R statistical software was used for heatmap construction. Heatmap associated hierarchical clustering and approximately unbiased and bootstrap probability *p*-values were calculated using pvclust version 1.3.2 (Suzuki and Shimodaira, 2006) with the UPGMA method and 1000 bootstrap replications.

2.3 Results

2.3.1 Transcriptome analysis by RNA-Seq

Nine RNA-Seq 100-bp paired-end read libraries were prepared from poly(A) RNA extracted from grape inflorescences, corresponding to the 3 time-points sampled (FS1, FS2 and FS3), each represented by 3 independent biological replicates. Each cDNA library resulted in ≈ 29 million 100-bp paired end reads. An overview of the raw reads data is given in Table 2.1. The results showed that 8% of the reads were removed since they overpass the threshold cutoff after being trimmed based on the presence of Illumina adapters or low quality bases. The majority (62%) of the total number of reads could be mapped back to the reference genome. An additional 1.7% reads were mapped to multiple locations within the reference genome sequence and these reads were discarded. Statistics of each sample mapping are provided in detail in Table 2.2 and Supplementary Figure S2.2.

Transcription of 25703 grapevine genes was detected in at least one time transition, based on cuffdiff average FPKM across replicates. The class of 10-200 FPKM value included a higher number of genes in the three time-points sampled, with 11818, 11869 and 11875 genes at FS1, FS2 and FS3, respectively (Table 2.3).

Table 2.1. RNA-Seq data overview. Number of 100-bp reads obtained in each fruit set stage sequenced, before and after data trimming (mean of three independent biological replicates ± standard error (se)).

Fruit set stage	Raw read pairs (x1000)	Read pairs after trimming (x1000)	% of remaining reads
FS1	28494±1209	26517±1192	93.0±0.4
FS2	36342±5193	33045±4534	91.1±1.5
FS3	24725±603	22765±462	92.1±0.5

Table 2.2. Percentage (%) of mapped reads in each fruit set stage. Each value correspond to the mean of three independent biological replicates ± se. Reads singly mapped, are those that aligned concordantly while their mate pair was not mapped by the software.

Fruit set stage	Mapped reads	Paired reads align concordantly	Multiple alignments of read pairs	Reads singly mapped	Multiple alignments of single reads
FS1	61.5±4.8	54.6±4.4	1.63±0.03	6.90±0.44	1.70±0.06
FS2	66.0±3.1	58.7±2.8	1.63±0.03	7.30±0.37	1.73±0.03
FS3	59.8±3.4	53.0±3.1	1.63±0.03	6.77±0.35	1.73±0.03

Table 2.3. Classes of transcript abundance at each fruit set stage. Number of transcripts detected at various levels of abundance at each time-point, as calculated by fragments per kilobase of exon per million fragments mapped (FPKM), considering the data from three biological replicates.

	FS1	FS2	FS3
FPKM > 400	341	355	321
FPKM 200-400	484	473	471
FPKM 10-200	11818	11869	11875
FPKM 1-10	7098	6941	7082
FPKM < 1	4944	5240	4765
Total	24685	24878	24484

2.3.2 Genome Functional Annotation

Functional annotation of the genome was required for GO enrichment analyses and gene categorization. The overall functional annotation and gene assignment was made using sequence similarity searches by Rapsearch2 against the KOG and NCBI "nr" databases. The *Vitis* genome is 96.9% annotated, which corresponds to 29048 of the total 29971 identified genes in the grapevine genome. KOG annotation assignments classified 17385 genes (58.0% of the genome) distributed in 27 different categories, of which the most significant and representatives were signal transduction mechanisms (7.5%), posttranslational modification, protein turnover,

chaperones (5.0%) and transcription (3.1%). On the other hand, based on the KEGG annotation of the genome, 2281 genes were identified and assigned to at least one of the 130 pathways. Predominant pathways were purine metabolism, starch and sucrose metabolism and thiamine metabolism with 433, 274 and 226 assigned unigenes, respectively. Using GO-terms, 14915 genes were categorized, annotated and distributed in three main GO domains, with 3156 terms from biological process, 1786 from molecular function and 525 from cellular component (Supplementary Figure S2.3).

The 'Thompson Seedless' transcriptome was compared to the reference genome for polymorphisms. From the total 105614 SNPs identified, 72544 were found to be located in coding regions, 50 in introns and 33020 in uncharacterized regions. The analysis of the transcribed portion of the 'Thompson Seedless' genome also allowed identifying 509 new splice junctions (Supplementary Table S2.1).

2.3.3 Distribution of Gene Expression Patterns

The 25703 detected expressing genes were grouped into 9 pre-defined clusters, bringing together genes with similar expression pattern over the three time-points sampled, based on the FPKM results (Fig. 2.2). The cluster represented by the highest number of genes was Cluster 9, comprising a total of 3699 members, followed by Clusters 7 and 1 with 3199 and 3175 genes, respectively. On the opposite side, Cluster 3 was represented by 2044 genes. Selection of KOG annotations per clusters retrieved 24 categories associated to the genes represented. Except for Cluster 4, in which posttranslational modification, protein turnover, chaperones was the most represented category, all clusters were enriched in signal transduction mechanisms related genes. Cluster 4 was also differentiated by a higher representativeness of genes associated to translation, ribosomal structure and biogenesis. Annotated genes assigned under the category secondary metabolites biosynthesis, transport and catabolism were present at higher number in calls that followed Cluster 1 typical expression pattern.

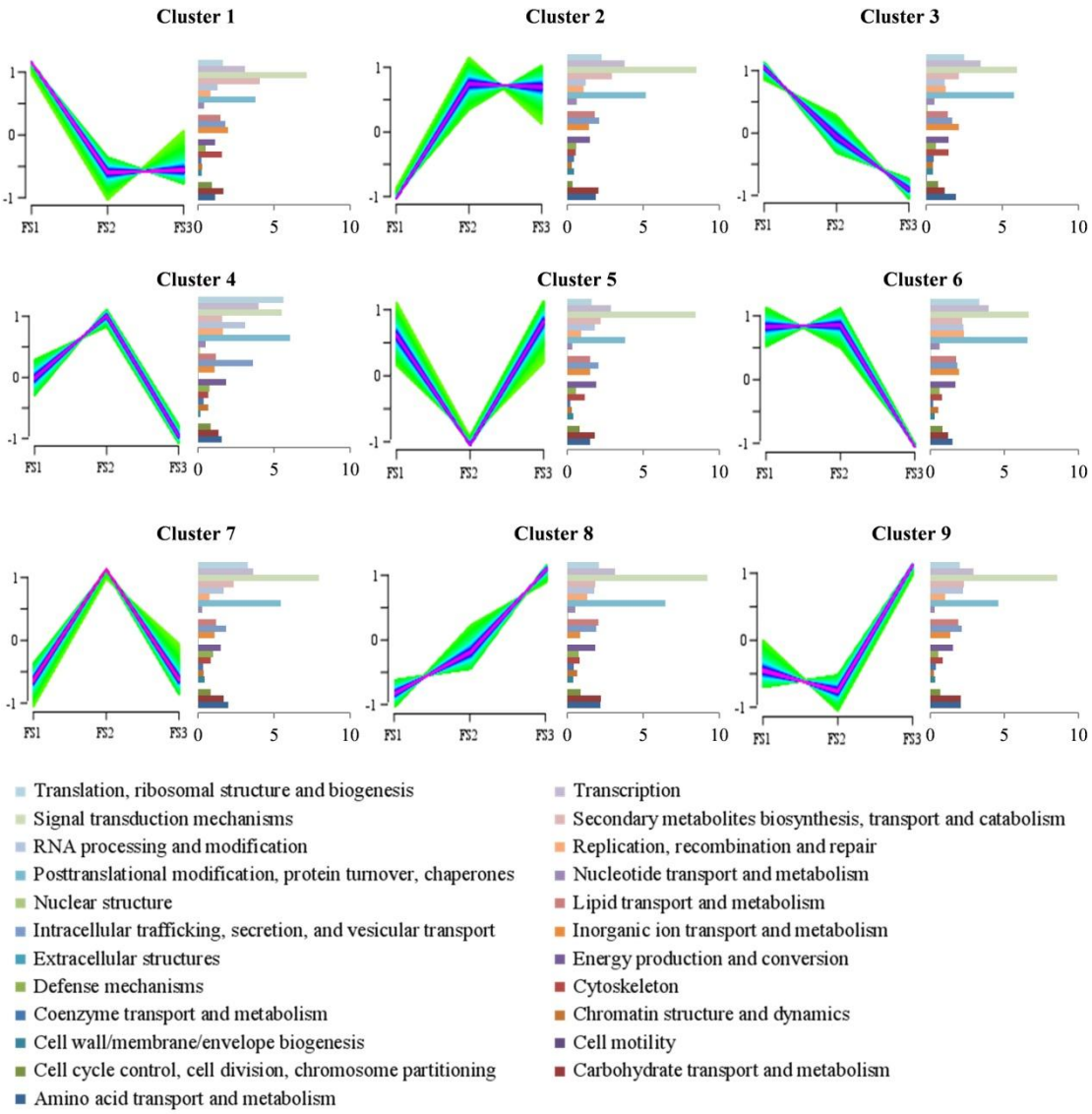

Figure 2.2. Clustering of genes according to the expression pattern. Clustering was performed for 25703 expressed genes in 9 pre-defined clusters with distinct expression profiles, using Mfuzz R package. Profiles are represented by expression changes and time-points (FS1, FS2 and FS3). Associated with the clusters are KOG annotated categories, with their respective percentage relatively to the total of genes of each cluster: Cluster 1 – 3175 genes; Cluster 2 – 2860 genes; Cluster 3 – 2044 genes; Cluster 4 – 2382 genes; Cluster 5 – 2915 genes; Cluster 6 – 2409 genes; Cluster 7 – 3199 genes; Cluster 8 – 3019; Cluster 9 – 3699.

2.3.4 Overall transcriptome profile

A total of 496 differentially expressed genes during at least one of the time transitions investigated (cut off FDR=0.05 and $-1.5>\log_2$ fold-change>1.5) were identified. The list of all genes significantly affected during fruit set, its annotation regarding functional categories and

gene code identification, the pattern-related gene cluster to which they were assigned and the respective fold-change are given in Supplementary Table S2.2. The expression pattern represented by Cluster 1 showed the highest number of DEG, with 181 genes.

During the 4-days period defined, the highest difference in gene expression occurred during the transition from FS1 to FS2 with 307 DEG observed, while in the following two days, from FS2 to FS3, only 137 genes showed differential expression. Considering the whole time span investigated, 108 additional genes showed statistical significance in expression from FS1 to FS3 (Fig. 2.3 and Supplementary Table S2.2).

PCoA and hierarchical clustering based on the 496 DEG are showed in Figure 2.4. PC1 and PC2 in combination explained 71.04 % of the total variance of the dataset (Fig. 2.4A). In general, PC1 differentiated FS1 from the remaining clusters, while PC2 allowed distinguishing FS2 from FS3 samples. In each case, biological samples were clustered together and are directly connected by the minimal spanning tree. These results indicate that inflorescences from the sampled time-points were affected significantly in the overall transcriptome dynamics, providing a suitable experimental dataset. Hierarchical clustering (Fig. 2.4B) showed the association between samples according to the overall transcriptome profile. Biological replicates collected in each stage were clustered together with strong confidence based on bootstrap analyses and Pearson correlations (Fig. 2.4B and Supplementary Figure S2.4).

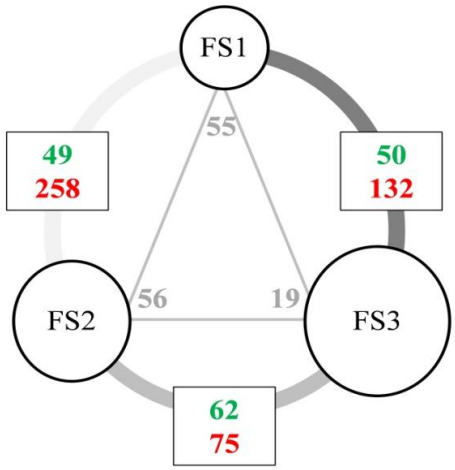

Figure 2.3. Diagram showing the number and trend of differentially expressed genes between each of the three time-points investigated during fruit set. Values indicate genes passing cutoff values of -1.5 ≥ log2 fold-change ≥1.5 and FDR=0.05. Green, red values indicate up-regulated and down-regulated genes, respectively. Grey values represent the number of gene shared between the two comparisons.

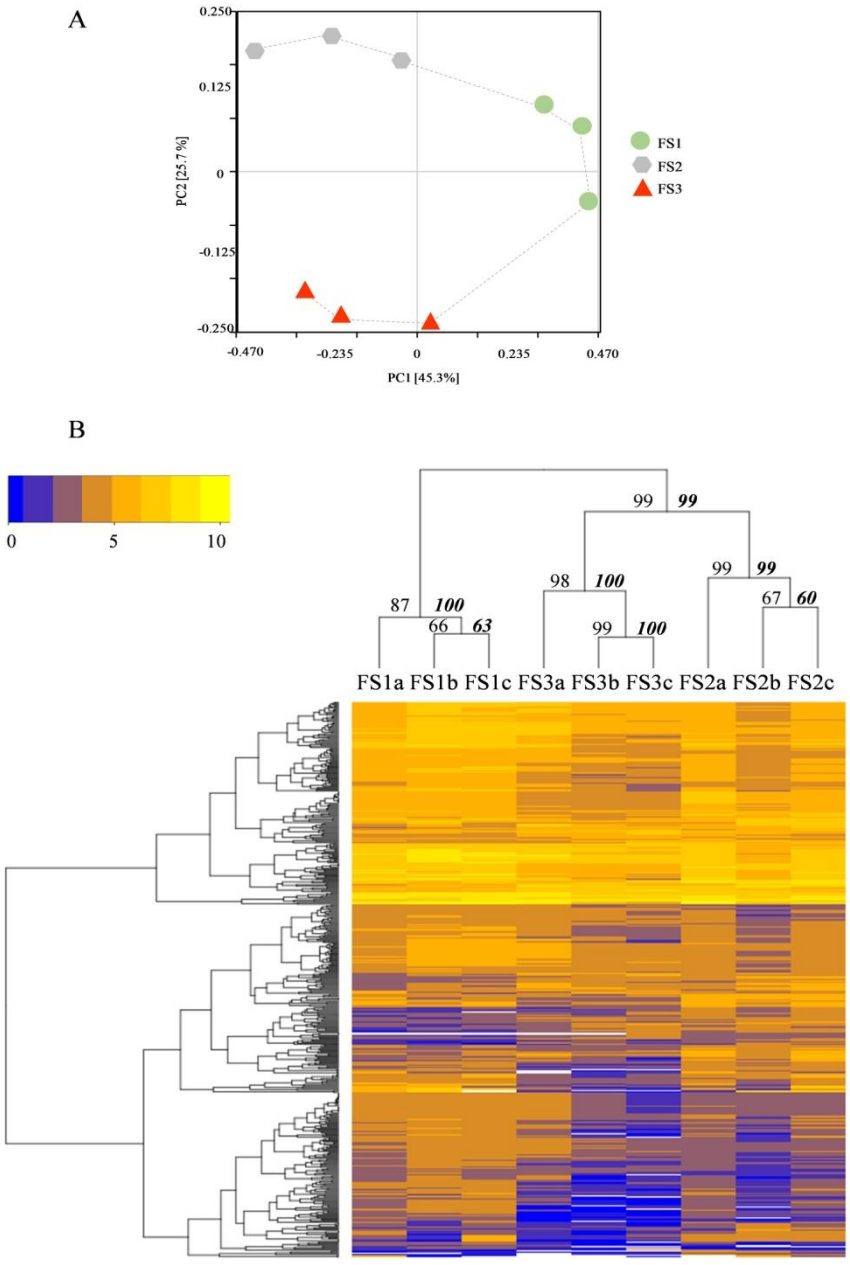

Figure 2.4. Principal coordinate analysis (A) and hierarchical clustering (B) of expression values at different sampled periods. A) Green, grey and red indicate the three different time-points – FS1, FS2, FS3 – and their respective replicates. Samples are connected by a minimal spanning tree. PC1 explains 45.32% and PC2 25.72% of the total variation. B) Each column represents one biological replicate. Yellow tones represent genes with higher expression while blue tones represent genes with lower expression. The strength of each dendrogram node was estimated with a bootstrap analysis using 1000 permutations. Values represented in the left side of internal nodes are the approximately unbiased *p*-values (AU), bold and italic values on the right side represented the bootstrap probability value.

2.3.5 GO enrichment analysis

Enriched categories are statistically well represented when compared to the genome, demonstrating that predominance of a given pathway is not observed by chance. The 496 DEG were found to be enriched in 188 GO terms, where 101 GO terms corresponded to biological processes, 81 to molecular function and 6 to cellular component (p-value≤0.01, Supplementary Table S2.3). Acyclic graphs resulting from the enrichment analysis and showing the top 5 and top 5-related biological processes, molecular functions and cellular components mostly affected in each time interval during early fruit set are provided in Supplementary Figure S2.5. Among biological processes, terms with reference to secondary metabolites biosynthesis and metabolism, cell wall (CW) components biosynthesis and organization, carbohydrates and lipid biosynthesis and metabolism were the most enriched in FS2 and FS3, followed by terms related to growth, morphogenesis, pollen germination and reproductive process. GO terms related to response to stress, abscission and dehiscence were enriched only in FS3 when compared to FS1. Regarding molecular functions, terms were mostly related to acyl transferase, secondary metabolites synthase, oxidoreductase, lyase and esterase activities. Regarding cellular components, the most enriched category was cell membrane. Among this category, pollen tube and mitochondrial membrane terms were found to be more present in FS2 and FS3 samples, respectively.

2.3.6 Overall metabolomic profile

From the 215 metabolites searched by the global metabolic analyses conducted, a total of 213 were detected in at least one of the conditions, and 40 changed in their abundance (p-value≤0.05) over the three fruit set stages (Supplementary Table S2.4). The relative content of about half (19) of the metabolites were altered between the first and second sampling points (9 and 10 were more and less abundant in FS2 comparing to FS1, respectively), and 28 in the transition from FS1 to FS3 (11 and 17 were more and less abundant in FS3 comparing to FS1, respectively) (Fig. 2.5).

PCoA showed that, based on 71.33% of the total variation explained by the combination of PC1 and PC2 endorsed by the metabolite profile, FS1 samples are different from FS2 and FS3, but these later two time points are indistinguishable based on their quantified metabolome (Fig. 2.6A). The observed dispersion between replicates of FS2 and FS3 in the plot can be explained only by biological variation. Individual plots pairwise comparing FS1 with FS2 and FS1 with FS3 (Supplementary Figure S2.6), highlighted that FS1 samples are distinguishable from both FS2 and FS3 and the transition from FS1 and FS3 would generate more clear information to understand metabolomic dynamics resulting from development than comparisons involving FS2. Hierarchical clustering (Fig. 2.6B) showed the association between samples according to

their metabolite profile. Likewise, only samples from FS1 formed a cluster that was significantly separated from the other samples. Regarding to metabolite association, a cluster composed by putrescine, 2-isopropylmalate, tartarate, adenosine 5'-monophosphate (AMP), galactinol and adenosine, which showed to be increased in the transition from FS1 to FS2 and FS3, was separated from the other metabolites. Diaminopropane and γ-tocotrienol showed the opposite pattern and were grouped in a different cluster.

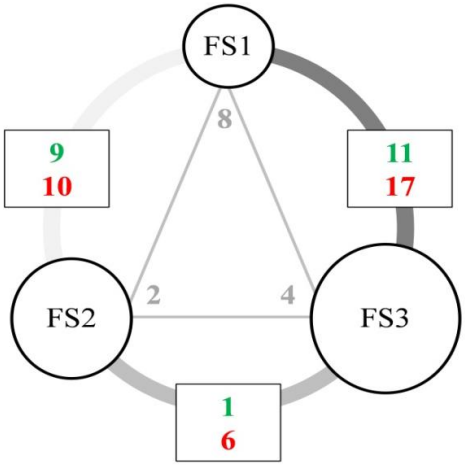

Figure 2.5. Diagram showing the metabolites with significantly different abundances in each of the three time-points sampled during early fruit set. Values indicate genes passing cutoff *p*-value≤0.05. Green and red values indicate number of metabolites with increased and decreased accumulation, respectively. Grey values represent the number of metabolites shared between the two comparisons.

2.3.7 Transcriptomic and metabolome profile by functional category

Figure 2.7 shows the functional annotation distribution of the 269 DEG, from which 64 and 205 were automatically and manually assigned to KOG categories, respectively. From the remaining 227 DEG, 13 were classified as other function and 214 as general and unknown function (Supplementary Table S2.2). Secondary metabolites biosynthesis, transport and metabolism, carbohydrates transport and metabolism and signal transduction mechanisms were the most representative functional categories of DEG during both FS1 to FS2 and FS2 to FS3 time intervals. In the transition from FS1 to FS3, secondary metabolites biosynthesis, transport and metabolism, carbohydrates transport and metabolism and posttranslational modification, protein turnover and chaperones category were enriched. Table 2.4 shows the summary of the DEG during fruit set aggregated by gene family and functional category, number of genes per family and number of genes up and down-regulated between each time point.

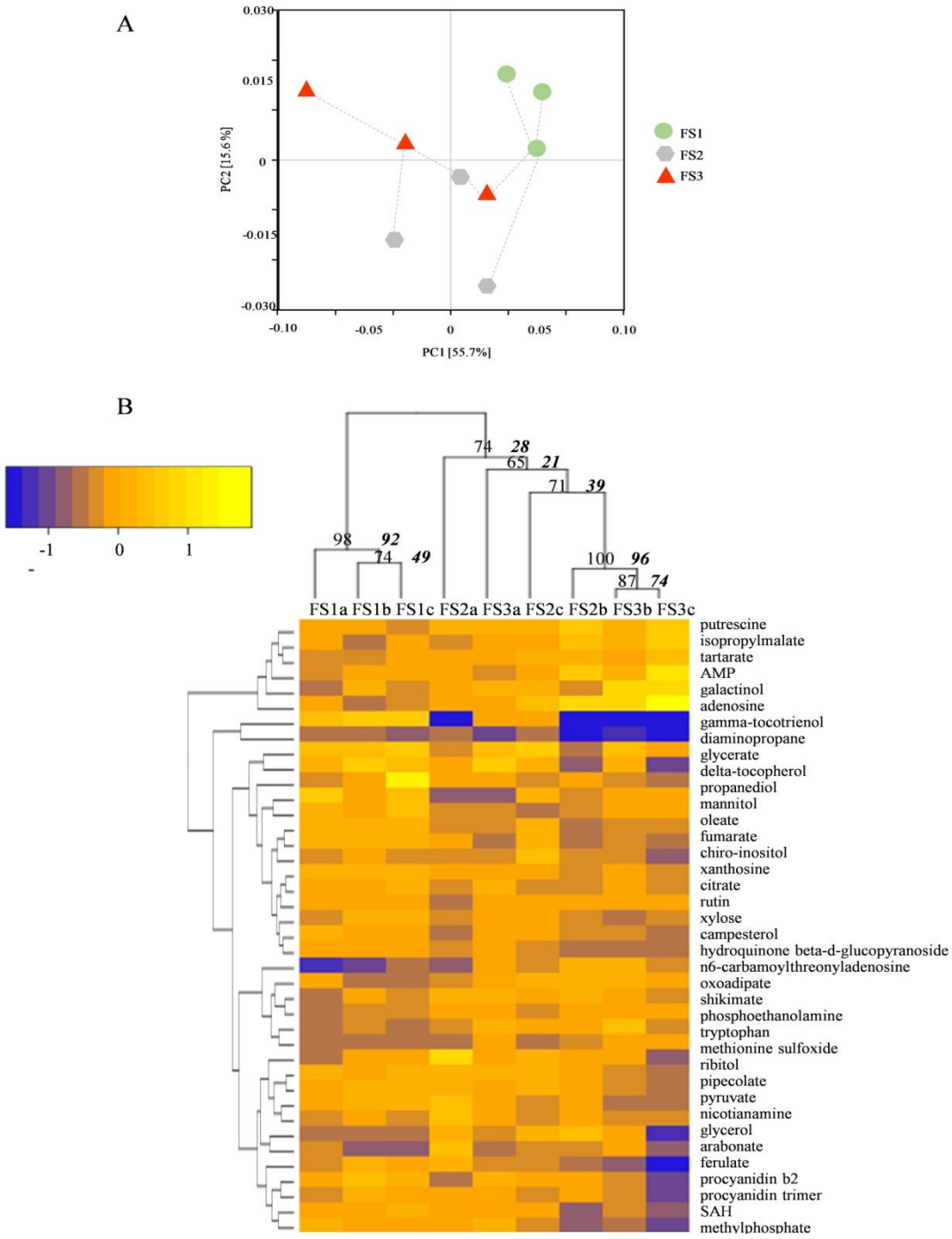

Figure 2.6. Principal coordinate analysis (A) and hierarchical clustering (B) of metabolite relative content. A) Green, grey and red indicate the three different time-points – FS1, FS2, FS3 – and their respective replicates. Samples are connected by a minimal spanning tree. PC1 and PC2 explain 71.33% of the total variation endorsed by metabolite profile. B) Each column represents one biological replicate. Yellow tones represent more abundant metabolites while blue represent less abundant ones. The strength of dendrogram nodes was estimated with a bootstrap analysis using 1000 permutations, in the left side are the approximately unbiased *p*-values (AU), bold and italic values on the right side represented the bootstrap probability value.

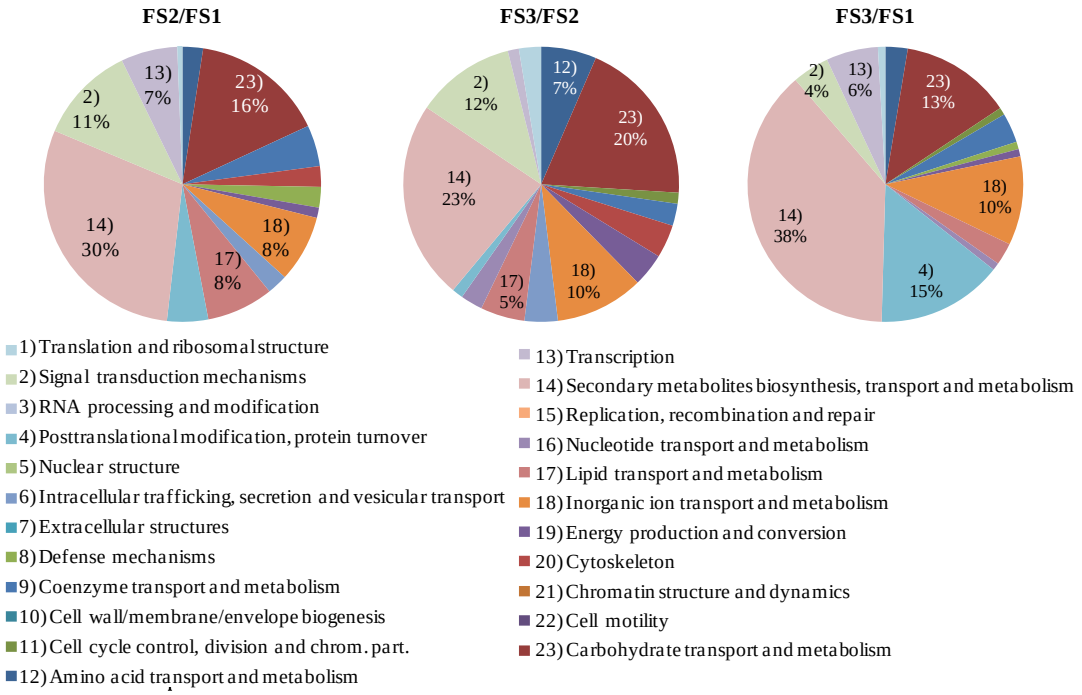

Figure 2.7. Functional annotation distribution for the 269 DEG assigned for a specific KOG functional category. Secondary metabolites biosynthesis, transport and metabolism and carbohydrates transport and metabolism were the most representative functional categories. In the transition from FS1 to FS3 also posttranslational modification, protein turnover and chaperones category was particularly enriched.

2.3.7.1 Amino acid transport and metabolism

Among the amino acid transport and metabolism functional category, genes encoding adenylylsulfate reductases (EC 1.8.4.8), a hypothetical protein involved in glutathione metabolism (EC 2.3.2.2) and amino acid and oligopeptide transporter related genes were down-regulated. Genes encoding gelatinases and peroxidases (EC1.11.1.7) involved in the phenylalanine metabolism and an endopeptidase were also differentially expressed. On the other hand, an increase of metabolites from amino acid metabolism was observed, comprising shikimate and tryptophan from shikimate pathway, 2-oxodipate and 2-isopropylmalate, involved in lysine and leucine biosynthesis, and putrescine. Aspartate accumulation showed the opposite pattern. Concerning metabolites involved in ethylene biosynthesis, an increase of methionine sulfoxide (the oxidized form of methionine) and a decrease of S-adenosylhomocysteine (SAH) were verified.

2.3.7.2 Carbohydrate transport and metabolism

All DEG involved in carbohydrates metabolism were down-regulated during the first time interval investigated, while in the second interval, the majority (12 in a total of 15 genes) was

up-regulated. Cluster 5 (Fig. 2.2) was highly represented by genes from this functional category, including genes encoding cellulose synthases (EC 2.4.1.12), β-galactosidases (EC 3.2.1.23) and a tonoplast intrinsic aquaporin. However, genes encoding eugenol synthase, sugar transporters, expansin, amylase (EC 3.2.1.2) and UDP-glucuronic acid decarboxylase (EC 4.1.1.35) were exclusively down-regulated during the fruit set stages studied. A hexokinase (EC 2.7.1.1), was up-regulated at FS3 comparing to FS2. Genes encoding proteins from glycosyl transferases (EC 2.4.1.14, E.C 2.4.1.134) and CW-related enzymes such as members from pectate lyase (EC 4.2.2.2), endoglucanase, polygalacturonase (EC 3.2.1.15), glucosidase and pectinesterase/pectinesterase inhibitor (EC 3.1.1.11) families were also differentially expressed during the period investigated. Regarding metabolites, pyruvate from glycolysis, citrate and fumarate from tricarboxylic acid (TCA) cycle, and chiro-inositol showed to be less abundant in FS3 than in FS1. Conversely, increased galactinol, ribitol and tartarate were measured.

2.3.7.3 Coenzime transport and metabolism

The coenzime transport and metabolism functional category included genes encoding thiazole, ketoacyl-CoA and chalcone synthase enzymes, which were down-regulated in FS2 comparing to FS1, while hydroxycinnamoyl-Coenzyme A shikimate/quinate was up-regulated in the same period. S-adenosylmethionine (SAM) synthase (EC 2.5.1.6) involved in the ethylene biosynthesis and blue copper proteins were also differentially expressed. Nicotinate ribonucleoside and methylphosphate relative content decreased during the stages investigated.

2.3.7.4 Inorganic ion transport and metabolism and intracellular trafficking

The majority of genes encoding inorganic ion transporter proteins (18 genes in a total of 24) showed a down-regulation pattern. Genes encoding K+/H+-antiporters and plasma membrane H+-transporting ATPase were down-regulated during the first time interval but shift to an up-regulation in the second one while carbonic anhydrases showed an up-regulated pattern during the whole period sampled. With respect to genes involved in intracellular trafficking, secretion and vesicular transport, a down-regulation of members encoding exocyst component and secretory carrier membrane proteins was perceived. Genes encoding SNARE and clathrin assembly proteins were down-regulated at the first time interval and up-regulated in the second one.

2.3.7.5 Lipid transport and metabolism

The majority of genes involved in lipid metabolism pathways (13 genes in a total of 15) were down-regulated at FS2 in comparison with FS1, including, among others, genes encoding medium-chain-fatty-acid--CoA ligase (EC 6.2.1.25), acyl-desaturases (EC 1.14.19.2) and a WAX protein. Two of these genes, encoding patellin and monoacylglycerol lipase proteins,

inverted the expression trend at FS3 comparing to FS2. Non-specific lipid transfer proteins were up-regulated in both time intervals. Two genes that encode O-acyltransferases, assigned under the different enzymatic classifications EC 2.3.1.20 and EC 2.3.1.75, were down- and up-regulated, respectively. Fatty acids, glycerolipids and sterols metabolites showed decreased amounts in the sampled inflorescences during the stages investigated.

2.3.7.6 Nucleotide transport and metabolism

Two genes with opposite expression patterns were assigned to the nucleotide transport and metabolism functional category. One gene classified to encode a dihydropyrimidinase (EC 3.5.2.2) was down-regulated and other encoding a putative RNA polymerase (EC 2.7.7.6) was up-regulated during the transition from FS2 to FS3. Adenosine and AMP were accumulated at FS3 compared to FS1, while N6-carbamoylthreonyladenosine relative content decreased.

2.3.7.7 Secondary metabolites biosynthesis, transport and catabolism

Most of the genes involved in secondary metabolism showed a down-regulation pattern. This set included 22 genes encoding stilbene synthases (EC 2.3.1.95), which are involved in the phenylpropanoid metabolism, and myrcene (EC 4.2.3.15) and limonene synthases (EC 4.2.3.16, EC 4.2.3.20), known to be involved in the terpenoids metabolism. On the other hand, genes encoding linalool and nerolidol synthase (EC 4.2.3.25), also involved in terpenoids metabolism, were up-regulated in the transition from FS1 to FS2. Genes encoding L-ascorbate oxidases, ABC transporter, cytochrome P450 related proteins, carotenoid cleavage dioxygenase and flavonol sulfotransferase were among the other DEG. All metabolites assigned to secondary metabolism functional category significantly decreased their abundance at FS3, namely γ-tocotrienol from tocopherol metabolism, ferulate involved in the phenylpropanoid metabolism, procyanidins B1 and trimer from the flavonoid metabolism and arbutin from benzenoids family.

2.3.7.8 Cell cycle control and cytoskeleton

Genes from the cell cycle control, cell division and chromosome partitioning category were up-regulated. Concerning the involvement in cytoskeleton function, genes encoding actin related proteins were down-regulated in FS2 comparing to FS1 and up-regulated in the second time interval, while kinesin protein-related genes were down-regulated in both time intervals.

2.3.7.9 Energy production and conversion

Genes encoding sarcosine oxidase (EC 1.5.3.1) and cytokinin dehydrogenase (EC 1.5.99.12) were up-regulated (Table 2.4 and Fig. 2.9) while genes coding for voltage-gated shaker and vacuolar H+-ATPase were down-regulated. One gene encoding a glycerophosphoryl diester

phosphodiesterase was down-regulated in FS2 comparing to FS1 and up-regulated in the last time interval.

2.3.7.10 Transcription factors

Genes from the MYB transcription factors superfamily were mostly up-regulated during the time span investigated while MADS-box, MEIS and related HOX domain, elongation factor SPT6, negative regulator of transcription and GATA-4/5/6 transcription factors were down-regulated. Genes encoding AP2-like ethylene-responsive factor, GT-2 and heat shock transcription factors were up-regulated in the transition from FS1 to FS2, FS2 to FS3, and FS1 to FS3, respectively.

2.3.7.11 Translation and posttranslational modification

Genes encoding a tRNA methyltransferase and ribosomal proteins, from translation, ribosomal structure and biogenesis functional category, were down-regulated in our samples set. Conversely, the majority of genes (14 genes in a total of 23) involved in posttranslational modification, protein turnover, chaperones showed an up-regulated pattern.

2.3.7.12 Signal transduction mechanisms

Concerning the signal transduction mechanisms functional category, the majority of DEG during the transition from FS1 to FS2 (18 in a total of 19 genes), were down-regulated and included genes encoding serine/threonine protein kinases, mitogen-activated protein kinase kinase kinase (MAPKKK) and calcium-binding messenger proteins. Among these genes, five encoding serine/threonine proteins kinases, two calcium-binding messenger proteins and one membrane protein were up-regulated from FS2 to FS3.

2.3.7.13 Defense mechanism, hormone metabolism and other functions

All DEG identified involved in defense mechanisms were down-regulated in the transition from FS1 to FS2, except a *CHITINASE* gene which was up-regulated under a pattern represented by Cluster 8 (Fig. 2.2 and Table 2.4). Genes involved in hormone metabolism, namely *1-AMINOCYCLOPROPANE-1-CARBOXYLATE OXIDASE, GA20ox* and *INDOLE-3-ACETATE-O-METHYLTRANSFERASE 1* (*IAMT1*) were differentially expressed. DEG with other functions were found, encoding a senescence related protein, MATE efflux family protein, major facilitator superfamily membrane transport proteins and major allergen proteins which were down-regulated during the time period targeted. Genes encoding a pollen specific protein were down-regulated in the transition from FS1 to FS2, and up-regulated in the following time interval.

Table 2.4. DEG combined by KOG functional annotation. The number of up- and down-regulated genes are indicated in the green and red squares, in each time interval. The identity of those genes is provided in Supplementary Table S2.2.

	Amino acid transport and metabolism	**FS2/FS1**		**FS3/FS2**		**FS3/FS1**	
4	amino acid and peptide transporters		2		1		1
3	adenylylsulfate reductase				3		
2	gelatinase	1	1				
2	peroxidase (phenylalanine metabolism)					1	1
1	endopeptidase (serine metabolism)			1			
1	glutathione metabolism-related protein				1		1
	Carbohydrate transport and metabolism						
10	glycosyl transferase		6	1	1	2	2
5	polygalacturonase		2	1		3	
5	sugar transporter		3				3
4	pectate lyase		4	1			
3	endoglucanase		1		1	1	
3	pectinesterase/ pectinesterase inhibitor		3	1	2		
2	eugenol synthase		1				2
2	cellulose synthase		2	2			
2	β-glucosidase/galactosidase		2	2			
1	aquaporin		1	1			
1	α-glucosidase				1		
1	amylase						1
1	hexokinase			1			
1	UDP-glucuronic acid decarboxylase						1
1	expansin		1				
	Inorganic ion transport and metabolism						
7	K+/H+-antiporter and plasma membrane H+-transporting ATPase		7	4			
5	copper, boron and phosphate transporter		2				4
3	sulfate/bicarbonate/oxalate exchanger				2		2
2	Ca2+-transporting ATPase and Ca2+/H+ antiporter						2
2	carbonic anhydrase	2				2	
2	Mn2+/Fe2+ and aluminum-activated malate transporter		2				1
1	ferric reductase				1		
1	porin						1
1	molybdopterin synthase catalytic				1		1
	Lipid transport and metabolism						
1	medium-chain-fatty-acid-CoA ligase		1				1
3	acyl-desaturase		3				
2	GDSL esterase		1	1			
2	lipid-transfer protein	1		1		1	
2	O-acyltransferase	1	1				
2	fatty acids biosynthesis-related proteins		2				1
1	patellin		1	1			
1	sphingolipid hydroxylase		1				
1	phosphatidylinositol transfer protein		1				
1	monoacylglycerol lipase		1	1			
1	WAX protein		1				1
	Nucleotide transport and metabolism						
1	dihydropyrimidinase-like				1		1
1	purine related protein			1			
	Secondary metabolites biosynthesis, transport and catabolism						
22	stilbene synthase		19				21
16	cytochrome P450 CYP2	5	3		7	3	7
12	ABC transporter		2	1	6	1	5
5	multicopper and copper amine oxidase		5				3
5	curcumene /myrcene / valencene synthase		4				1
2	L-ascorbate oxidase		2	2			
2	flavonol sulfotransferase	1	1				
2	linalool/nerolidol synthase	1					
2	carotenoid cleavage dioxygenase	1	1			1	1
1	flavin-containing monooxygenase		1				
1	flavonol synthase/flavanone hydroxylase		1				
1	alcohol dehydrogenase		1				
1	quercetin 3-O-methyltransferase		1				
1	naringenin,2-oxoglutarate 3-dioxygenase		1				1

Table 2.4 (continued). DEG combined by KOG functional annotation (continued). Number of up and down-regulated genes are indicated in the green and red squares in each time interval. The identity of those genes is provided in Supplementary Table S2.2.

	Cell cycle control, cell division, chromosome partitioning	**FS2/FS1**		**FS3/FS2**		**FS3/FS1**	
2	cullins and myosin assembly protein			1		1	
	Coenzyme transport and metabolism						
3	blue copper protein	1	1	1		1	
3	ketoacyl-CoA and thiazole synthase		3				1
1	S-adenosylmethionine and thiazole synthase		1	1			
1	chalcone synthase		1				1
1	hydroxycinnamoyl-Coenzyme A shikimate/quinate	1				1	
	Cytoskeleton						
3	actin related protein		3	1			
2	kinesin		1		1		
	Defense mechanisms						
2	pathogenesis and defense -related protein		2				
1	carboxylesterase		1				
1	chitinase	1				1	1
	Energy production and conversion						
1	sarcosine oxidase					1	
1	cytokinin dehydrogenase	1					
1	glycerophosphoryl diester phosphodiesterase		1	1			
1	voltage-gated shaker-like K+ channel				1		
1	vacuolar H+-ATPase				1		
	Intracellular trafficking, secretion, and vesicular transport						
2	SNARE protein		2	1			
2	exocyst and secretory carrier membrane protein		1		1		
1	clathrin assembly protein		1	1			
	Posttranslational modification, protein turnover, chaperones						
10	molecular chaperone/ heatshock protein					10	
4	E3 ubiquitin ligase	1	2				2
4	WD40 repeat-containing protein		1			2	1
2	Zn finger		1		1		
1	dnaJ homolog subfamily C		1				1
1	T-complex protein subunit gamma		1				1
1	glutaredoxin-related protein	1					
	Signal transduction mechanisms						
14	serine/threonine protein kinase	1	12	5	1		
7	Ca2+ binding proteins containing EF-Hand domain		3	2			4
1	mitogen-activated protein kinase kinase kinase		1				
1	NUDIX hydrolase FGF-2						1
1	N-methyl-D-aspartate receptor glutamate-binding		1				
1	membrane protein		1	1			
	Transcription						
7	MYB superfamily	5	1			3	
2	MADS-box		1				1
1	heat shock					1	
1	MEIS and related HOX domain						1
1	elongation factor SPT6		1				1
1	negative regulator of transcription		1				
1	GATA-4/5/6		1				
1	GT-2 and related protein			1			
1	AP2-like ethylene-responsive	1					
	Translation, ribosomal structure and biogenesis						
2	60S ribosomal protein		1		1		
1	tRNA methyltransferase				1		1
	Other functions						
3	major facilitator superfamily		3				
3	major allergen and MATE efflux family protein		1				2
2	1-aminocyclopropane-1-carboxylate oxidase	1	1				
2	pollen specific protein		2	2			
1	senescence related protein		1				
1	gibberellin 20 oxidase	1				1	
1	indole-3-acetate O-methyltransferase						1

A

Metabolite	Log_2 FS3/FS1	KEGG
Amino acid		
shikimate	0.51	C00493
tryptophan	0.49	C00078
2-oxoadipate	**1.43**	C00322
aspartate	-0.64	C00049
methionine sulfoxide	0.96	C02989
S-adenosylhomocysteine (SAH)	-0.62	C00021
2-isopropylmalate	0.75	C02504
putrescine	0.75	C00134
Carbohydrate		
pyruvate	-0.58	C00022
citrate	-0.43	C00158
fumarate	-0.74	C00122
tartarate	0.64	C00898
ribitol	0.75	C00474
chiro-inositol	-0.94	
galactinol	**1.29**	C01235
Lipids		
2-hydroxypalmitate	**-1.84**	
1,2-propanediol	**-1.29**	C00583
campesterol	-0.56	C01789
Cofactors. Prosthetic Groups. Electron Carriers		
nicotinate ribonucleoside	-0.47	C05841
methylphosphate	-0.64	
Nucleotide		
adenosine	**2.20**	C00212
adenosine 5'-monophosphate (AMP)	**1.20**	C00020
N6-carbamoylthreonyladenosine	-0.36	
Secondary metabolism		
arbutin	-0.54	C06186
procyanidin B2	-0.58	C17639
ferulate	**-1.18**	C01494
procyanidin trimer	-0.51	
gamma-tocotrienol	**-2.00**	C14155

B

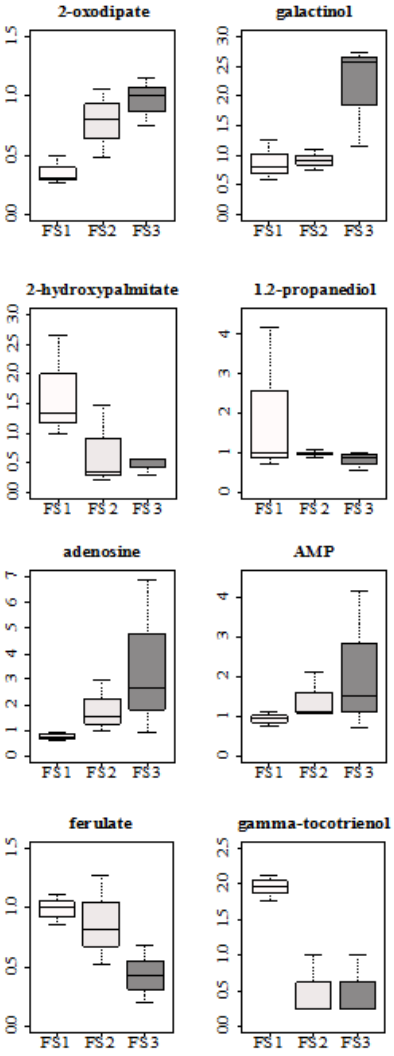

Figure 2.8. Summary of the metabolites that significantly changed during the early fruit set points investigated. A) List of metabolites significantly affected in FS3 comparing to FS1 (*p*-value≤0.05), assigned functional categories, KEGG compound number and respective accumulation fold-change. B) Relative content evolution of all metabolites with highly significantly differences (|fold-change| ≥1) between FS1 and FS3.

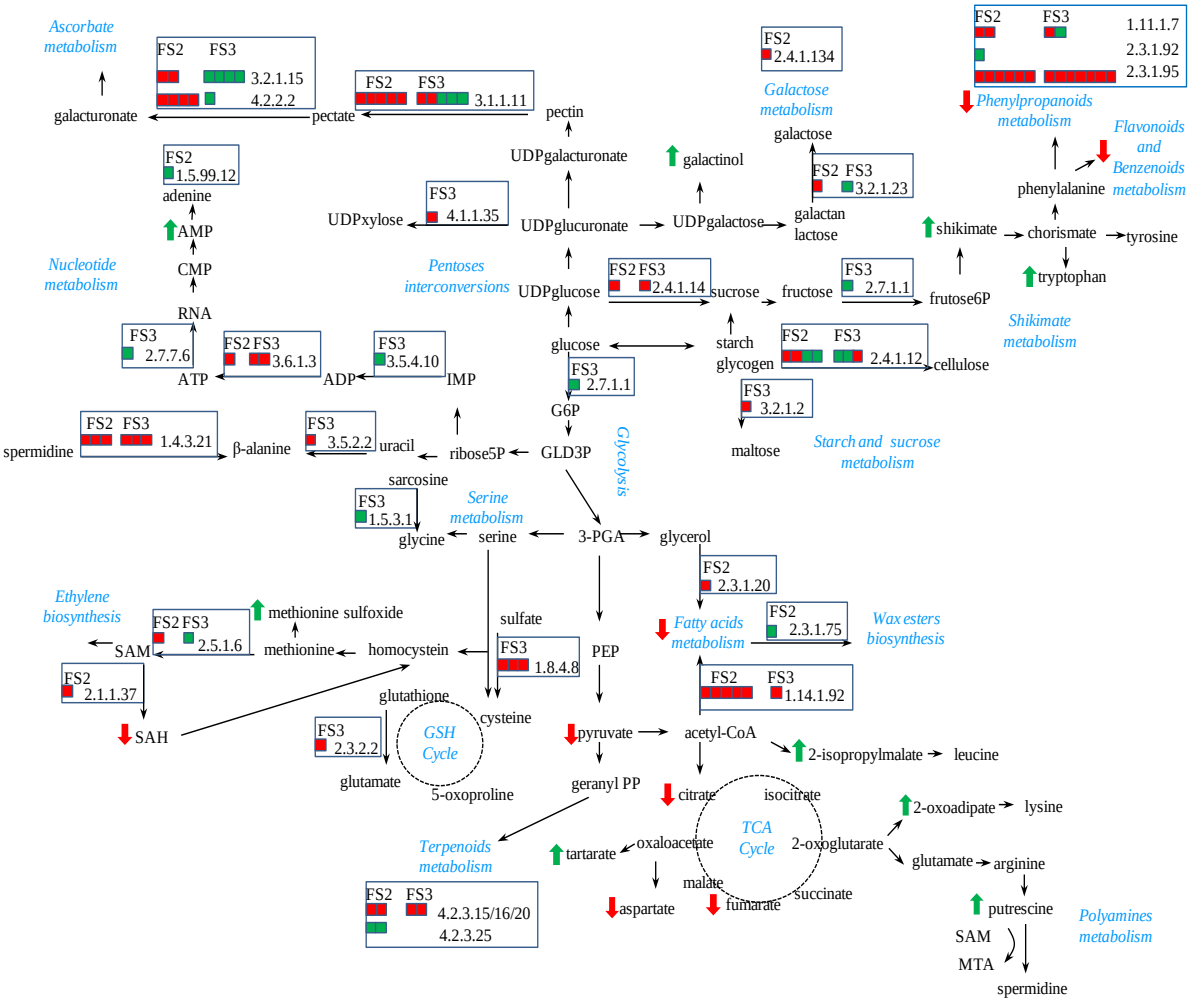

Figure 2.9. Changes on enzyme genes expression and metabolites quantification mapped onto simplified metabolic pathways. Red and green arrows represent changes in metabolite accumulation in FS3 comparing to FS1. Red and green squares represent down and up-regulation of the transcripts at FS2 stage (correspond to transition from FS1 to FS2) and FS3 (comprise transitions from FS1 to FS3 and from FS2 to FS3). Description of enzyme codes: 1.11.1.7 peroxidase; 1.14.19.2 acyl desaturase; 1.4.3.21 primary amine oxidase; 1.5.3.1 sarcosine oxidase; 1.5.99.12 cytokinin dehydrogenase; 1.8.4.8 adenylylsulfate reductase; 2.1.1.37 cytosine 5-methyltransferase; 2.3.1.20 acyltransferase; 2.3.1.75 wax-ester synthase; 2.3.1.92 sinapoyltransferase; 2.3.1.95 stilbene synthase; 2.3.2.2 γ-glutamyltransferase; 2.4.1.12 cellulose synthase; 2.4.1.134 β-galactosyltransferase; 2.4.1.14 sucrose-phosphate synthase; 2.5.1.6 S-adenosylmethionine synthase; 2.7.1.1 hexokinase; 2.7.7.6 RNA polymerase; 3.1.1.11 pectinesterase; 3.2.1.15 polygalacturonase; 3.2.1.2 β-amylase; 3.2.1.23 β-1,3-galactosidase; 3.5.2.2 dihydropyrimidinase; 3.5.4.10 IMP cyclohydrolase; 3.6.1.3 ATP monophosphatase; 4.1.1.35 UDP-glucuronate decarboxylase; 4.2.2.2 pectate lyase; 4.2.3.15 myrcene synthase; 4.2.3.16 (4S)-limonene synthase; 4.2.3.20 (R)-limonene synthase; 4.2.3.25 linalool synthase.

2.4. Discussion

2.4.1 RNA-Seq computational data validation by analysis of variability of biological replicates

Although RNA-Seq is now used in routine and as a convenient tool for comparative transcriptome analyses of species with or without genome sequences (Gao et al., 2013; Liu et al., 2013; Wang et al., 2009), understanding different sources of variability is of extreme importance, to allow it to be accounted in the experimental design. Following the approach previously proposed (Fasoli et al., 2012; Thakare et al., 2014), the significant correlation verified between biological replicates used as part of our experimental design (Supplementary Figure S2.4) confirms that our RNA-Seq data is reproducible and precise. With the development of next generation sequencing technology, the technical variability of the data is increasingly negligible while the establishment of biological replicates allows deciding whether observed differences between groups of organisms exposed to different treatments is simply random or represents a "true" biological difference induced by a given treatment. Previous studies addressing dichotomy between biological and technical replicates, showed that biological variation is often larger than technical variation, underscoring the importance of including biological replicates in the study design (Bullard et al., 2010). Taking advantage of the use of biological replicates, the PCoA and hierarchical clustering confirmed the samples separation into three classes sharing similar expression signatures, according to the specific time point during fruit set (Fig. 2.4).

2.4.2 Gene expression and metabolic patterns during fruit set

The general molecular dynamics occurred during fruit set highlighted a gene down-regulation pattern observed at 5d in most functional categories (Table 2.4), which was accompanied by decreased metabolites abundance, mainly concerning carbohydrates, cofactors, lipids and secondary metabolism, in the last investigated time point (Fig. 2.8). In addition, a total of 12.5% of DEG showed a trend inversion in expression patterns at FS2, indicating that at this time point a developmental or stress-resulting signal occurs. The same expression dynamics was observed in tomato in a short period ranging from 2 days before bloom to 4 days after full bloom, demonstrating lack of continuum in ovary development from flower bud to postanthesis (Wang et al., 2009).

2.4.3 Transcriptional and metabolic regulation of secondary metabolism

Functional annotation (Fig. 2.7) and top 5 GO enriched terms (Supplementary Table S2.3) highlighted secondary metabolism as the most representative biological process.

The large multigenic family of MYB transcription factors has members known to be regulated by sugars and to control flavonoids biosynthesis (Lecourieux et al., 2013), showed up-regulation during fruit set (Table 2.4). Based on our results, we can hypothesize that the signaling sugar galactinol and hexokinase enzyme can be involved in regulation of MYB expression. Specific MYB transcription factors, were previously described to be positive (Bogs et al., 2007; Gonzalez et al., 2008) or negative (Park et al., 2008) regulators of flavonoids biosynthesis, in several species. Our data revealed a repression of flavonoids and phenylpropanoids related pathways (Table 2.4, Fig. 2.8 and Fig. 2.9). Consistently, the biosynthesis of β-alanine, a phenylalanine precursor, via spermidine mediated by primary amine oxidase (EC 1.4.3.21) and via uracil mediated by dihydropyrimidinase (EC 3.5.2.2), was repressed (Fig. 2.9). The observed down-regulation of genes encoding ATP-binding cassette transporters (ABC transporters) (Table 2.4), indicated also reduced transport and accumulation of flavonoids in inflorescences during fruit set (Braidot et al., 2008).

The regulation of cytochrome P450-related genes, terpenoids metabolism (EC 4.2.3.15, EC 4.2.3.25), protection compounds biosynthesis as *EUGENOL SYNTHASE 1-LIKE*, *LACCASE-14-LIKE*, responsible for lignin degradation, *CHITINASE*, genes encoding ketoacyl-CoA synthases and WAX2 protein which contributes to cuticular wax and suberin biosynthesis, indicated that a response to environmental stimuli is activated during fruit set, agreeing with GO enriched terms associated to environmental stress responses and biotic stimuli (Table 2.4, Fig. 2.8 and Supplementary Table S2.3). The regulation of *L-ASCORBATE OXIDASE HOMOLOG* during the three fruit set investigated, with the change of expression pattern at FS2, to an up-regulation from FS2 to FS3, also indicates a response to oxidative stress conditions.

2.4.4 Regulation of nutrient transport in the developing fruit

The passive symplasmic phloem unloading pathway in the fruit wall and seed coats, through plamodesmata, predominates in the early and middle stages of berry development (Zhang et al., 2006). However, our data indication that fruit set induces extensive transcriptome reprogramming of nutrient transporters (Table 2.4) sounds with the evidence that nutrient transport across membranes requiring membrane-embedded amino acids, peptides, sugar, secondary metabolites and inorganic ions transporters is strongly regulated during fruit set (Ruan et al., 2012; Sanders et al., 2009; Shelden et al., 2009).

The observed down-regulation of membrane sugar transporter genes, namely those encoding sucrose transport protein SUC2 and bidirectional sugar transporter SWEET1, 4, 5 and 14 indicates a down-regulation at phloem long-distance transport (sucrose) and photosynthate short-term transport or accumulation (glucose) levels (Chen et al., 2010; Chong et al., 2014; Shiratke, 2007; Slewinski, 2011). Gene *VvSUC2/SUT2*, which participates in the phloem or

post-phloem unloading, firstly described as weakly expressed in berries (Afoufa-Bastien et al., 2010), showed to be involved in onset of berry development. In addition to *SWEET 1,4,5* genes previously described in grapevine flowers (Chong et al., 2014), the expression of *SWEET 14* was found in flower-to-fruit transition stage, with a 4-fold repression in FS3 comparing to FS1 (Supplementary Table S2.2).

In addition to the known impaired flower formation and berry set resulting from carbon limitation due to inadequate rates of source leaf photosynthesis (Domingos et al., 2015; Vasconcelos et al., 2009), these results suggest that also the sink strength limitation can be an important step during the flower-to-fruit transition stage.

2.4.5 Carbohydrates metabolism and other energy sources

The repression of carbohydrate related pathways at the transcriptome level during the first time interval investigated, which can be correlated with decreased metabolites content associated with glycolysis and TCA cycle, was inverted at FS2 with a predominantly stimulation of these pathways from this point (Fig. 2.8 and Table 2.4). The trend inversion observed can indicate the starting point of cell metabolism stimulation that will lead to berry formation. Among the genes encoding glycosyltransferases (Table 2.4), the perceived up-regulation of two genes encoding glycogenin enzymes (VIT_07s0005g01970, VIT_07s0005g01980) suggests that conversion of glucose to the energy storage polymer glycogen is favored (Supplementary Table S2.2). The demand for energy during fruit initiation can also be fulfilled by increased glycogen biosynthesis via sarcosine oxidase (EC 1.5.3.1). In addition, adenine synthesized via cytokinin dehydrogenase (EC 1.5.99.12) (Fig. 2.9), can be converted in adenosine, which is correlated with the increased levels observed (Fig. 2.8), and can be involved in energy transfer processes (ATP and ADP) and signal transduction (cyclic AMP).

CW biosynthesis accompanies the mandatory remodeling that provides the flexibility required for cell expansion during fertilized flower and pedicel development (Vriezen et al., 2008; Wang et al., 2009), and is fine-tuned to cope with the double sigmoid growth pattern of berry development (Goulão et al., 2012). Evidences of CW remodeling processes during fruit set were gained by changes in gene expression concerning members of glycosyltransferase and cellulose synthase (EC 2.4.1.12) families, required for pectin and cellulose biosynthesis, respectively, and other members, including expansins, endoglucanases, pectinesterases (EC 3.1.1.11), polygalacturonases (EC 3.2.1.15) and β-1,3-galactosidases (EC 3.2.1.23) that facilitate CW polymer modification (Table 2.4 and Fig. 2.9). In addition, genes encoding CW disassembly-associated enzymes can also be implicated in abscission of the non-fertilized flower organs (Ruperti et al., 2002), which are present in our whole inflorescence samples. This corroborates

with GO enrichment analysis (Supplementary Table 2.3) that revealed GO terms related to CW organization and modification and flower organ abscission biological processes.

2.4.6 Sugar signaling pathways

Sugars may directly or indirectly control a wide range of activities in plant cells, through transcriptional and post-translational regulation. The increased galactinol quantified along fruit set (Fig. 8) may affect expression of genes encoding different genes families as sugar transporters, components of the photosystems, enzymes of carbohydrate metabolism, enzymes of secondary metabolism and transcription factors (Lecourieux et al., 2013). The regulation of *HEXOKINASE-1* (VIT_09s0002g03390) (Table 2.4), was reported to be involved in sugar-sensing and signaling through CW invertase and sucrose synthase regulation (Wang et al., 2014) and sugar control of transporters (Lecourieux et al., 2013) in grape berries. Here, we could associate this regulation with early stages of fruit set in grapevine, during which hexose sugar signals that regulate cell cycle and cell division programs seemed to be generated (Bihmidine et al., 2013). The enhanced expression of heat-shock proteins (HSPs), disclosed by up-regulation of ten genes encoding heat-shock proteins (HSP90, HPS70 and sHPS26/42) and one heat stress transcription factor (Hsfs) (Table 2.4 and Supplementary Table S2.2), can be hypothesized to protect CW invertase from misfolding for correct targeting and function (Li et al., 2012). These proteins are known to be expressed in response to both stress conditions and during particular stages of the cell cycle and development (Vierling, 1991). Members of these classes perform chaperone function by stabilizing new proteins to ensure correct folding and play important roles in signaling, trafficking and pathogen resistance (Al-Whaibi, 2011).

2.4.7 Hormone biosynthesis and signaling pathways

In plants, sugar sensing and signaling are intimately interconnected with hormonal signaling pathways. The discerned regulation of auxin-, gibberellin- and ethylene-related genes during fruit set (Table 2.4) confirms the importance of plant hormones as mediators of the fruit developmental signal after pollination (Serrani et al., 2007; Vriezen et al., 2008; Wang et al., 2005, 2009). Our data also revealed the mediation of auxin biosynthesis and signaling (Li and Yuan, 2008) via down-regulation of IAMT, an enzyme responsible for inactivation of indole-3-acetic acid (IAA), and down-regulation of auxin-associated MADS-box genes (Wang et al., 2009). It can be speculated that these two MADS-box genes (VIT_14s0066g01640, VIT_18s0001g01760) (Supplementary Table S2.2) are instrumental in triggering the grapevine fruit set program. The up-regulation of *GIBBERELLIN 20 OXIDASE 2* (GA20ox2) (Table 2.4) suggests that GAs biosynthesis occurs during initial steps of fruit set, as previously proposed (Serrani et al., 2007). Gibberellins with a C20 carbon skeleton are converted in C19 products and in bioactive GAs through sequential oxidation involving GA20ox (Giacomelli et al., 2013).

Additionally, the observed regulation of genes encoding predicted ACC oxidase (Table 2.4) and S-adenosylmethionine synthase 1-like (EC 2.5.1.6) (Fig. 2.8) and the increased methionine sulfoxide content derived from the intermediate methionine, indicated changes on ethylene-related pathways, as previously reported by Wang et al. (2009). Likewise, the up-regulation of a gene encoding a AP2-like ethylene-responsive transcription factor suggested the activation of ethylene signaling pathway to act as fruit set trigger (Wang et al., 2009). Since PAs and ethylene share SAM as a common intermediate, SAM may be alternatively channeled towards the PAs pathway, which is also closely related to fruit set (Aziz, 2003). The observed increase in putrescine indicated an induction of PAs biosynthesis in the grapevine postanthesis stage, which contrasts with the previous observation in tomato (Wang et al., 2009).

Therefore, it can be discussed that the down-regulation of this IAA inhibitor probably results in increased levels of active IAA which, together with induction on ethylene signaling, will trigger fruit set and will stimulate the synthesis of bioactive GAs responsible for fruit growth through prompting cell division and expansion. On the other hand, the observed up-regulation of a cytokinin dehydrogenase (VIT_11s0016g02110) might be associated with a decrease on cytokinin (CK) levels. Contrastingly, previous work in grapevine demonstrated that an induction of CK biosynthetis occurs soon after, about 13 days after pollination (Dauelsberg et al., 2011).

2.4.8 Signal transduction mechanisms

The significant number of genes encoding proteins active in signal transduction that are regulated during fruit set (11% and 12% of DEG from FS1 to FS2 and from FS2 to FS3 stages; Fig. 2.7 and Table 2.4) was also previously reported (Vriezen et al., 2008). Serine/threonine kinases are known to play a role in the regulation of cell proliferation, PCD, cell differentiation, and embryonic development, and MAPKKK belongs to a signaling cascade that have evolved to transduce environmental and developmental signals into adaptive and programmed responses (Rodriguez et al., 2010). The observed regulation of genes encoding calcium-binding messenger proteins was previously described to be essential to rice pollen development (Zhang et al., 2011) and differentially expressed in grapevine in later stages of berry development (Nwafor et al., 2014).

2.4.9 Pollen viability, fertilization and cell division phase

On the Thompson Seedless stenospermocarpic cultivar, fruit set is dependent on successful pollination and fertilization, meaning that pollen must germinate and the pollen tubes must grow through the stylar tissue to the ovule and into the embryo sac. However, seed development aborts at an early stage after fertilization (Varoquaux et al., 2000). The observed regulation of

genes related to the pollen viability (Table 2.4), including genes encoding enzymes responsible for cellulose synthesis (EC 2.4.1.12), pectate lyase (EC 4.2.2.2), amilase (EC 3.2.1.2) and acyl-CoA synthase identified specific members for synthesis of energy, cellulose, callose and sporopollenin for pollen development (De Azevedo Souza et al., 2009, Krichevsky et al., 2007, Olek et al., 2014, Palusa et al., 2007). Pollen tube CW development also requires changes in lipid metabolism such as palmitate that can be converted in 2-hydroxypalmitate which showed decreased relative abundance from 3 to 7 days after 100% cap fall (Fig. 2.8). Changes on gene expression involved on active vesicle trafficking to deliver secretory vesicles, suggest the polarized rapid growth pollen tube regulation, via exo and endocytosis (Zonia and Munnik, 2009) (Table 2.4). These evidences and the regulation of genes encoding pollen specific proteins from MLP regulatory family (Lytle et al., 2009), agree the enriched GO terms corresponding to anther dehiscence biological processes and pollen tube cellular component.

Simultaneously, during fruit set stages investigated, a period of rapid cell division takes place, as verified by up-regulation of genes assigned to the cell cycle control, cell division and chromosome partitioning functional category (Table 2.4), corresponding to the ovary development (Ojeda et al., 1999).

2.5 Conclusions

During the decisive flower-to-fruit transition developmental stage, carbohydrate pathway, secondary metabolism and protein modification and turnover mechanisms were the most affected functional categories. An increased cell division-related gene expression, required for fruit growth initiation, was verified. Genes encoding signaling proteins as serine/threonine kinases and calcium-binding messenger proteins, L-ascorbate oxidase, chitinase and CW-modifying enzymes showed a discontinuous participation on this development stage with a change on expression pattern at FS2. It was also showed to be characterized by pathways that mediate sugar- and hormone-controlled responses. The participation of auxin, GA, ethylene and CK-related genes from the earlier fruit set stage investigated (FS1), maintaining the same expression pattern until FS3, suggested that the hormone action is one the constant trigger signals needed for the flower-to-fruit transition proceeding. Therefore, we propose that an increased level of active IAA together with induction on ethylene signaling will trigger fruit set and stimulate the synthesis of bioactive GAs, responsible for fruit growth through stimulation of cell division and expansion. Therefore this first global transcriptomic and metabolomic analysis helps elucidating the molecular mechanism occurring in inflorescences during the flower-to-fruit transition stage.

2.6 References

Afoufa-Bastien D, Medici A, Jeauffre J, Coutos-Thévenot P, Lemoine R, Atanassova R and Laloi M. 2010. The *Vitis vinifera* sugar transporter gene family: phylogenetic overview and macroarray expression profiling. *BMC Plant Biol.* 10: 245.

Alexa A and Rahnenfuhrer J. 2010. topGO: Enrichment analysis for gene ontology. *R Packag. version.* 2.

Al-Whaibi MH. 2011. Plant heat-shock proteins: A mini review. *J. King Saud Univ. - Sci.* 23: 139–150.

De Azevedo Souza C, Kim SS, Koch S, Kienow L, Schneider K, McKim SM, Haughn GW, et al. 2009. A novel fatty Acyl-CoA Synthetase is required for pollen development and sporopollenin biosynthesis in Arabidopsis. *Plant Cell*. 21: 507–525.

Aziz A. 2003. Spermidine and related metabolic inhibitors modulate sugar and amino acid levels in *Vitis vinifera* L.: possible relationships with initial fruitlet abscission. *J. Exp. Bot.* 54: 355–363.

Bihmidine S, Hunter CT, Johns CE, Koch KE and Braun DM. 2013. Regulation of assimilate import into sink organs: update on molecular drivers of sink strength. *Front. Plant Sci.* 4: 177.

Bogs J, Jaffé FW, Takos AM, Walker AR and Robinson SP. 2007. The grapevine transcription factor VvMYBPA1 regulates proanthocyanidin synthesis during fruit development. *Plant Physiol.* 143: 1347–61.

Bolger AM, Lohse M and Usadel B. 2014. Trimmomatic: a flexible trimmer for illumina sequence data. *Bioinformatics*. btu170.

Boyer JS and McLaughlin JE. 2007. Functional reversion to identify controlling genes in multigenic responses: analysis of floral abortion. *J. Exp. Bot.* 58: 267–277.

Braidot E, Zancani M, Petrussa E, Peresson C, Bertolini A, Patui S, Macrì F, et al. 2008. Transport and accumulation of flavonoids in grapevine (*Vitis vinifera* L.). *Plant Signal. Behav.* 3: 626–632.

Bullard JH, Purdom E, Hansen KD and Dudoit S. 2010. Evaluation of statistical methods for normalization and differential expression in mRNA-Seq experiments. *BMC Bioinformatics*. 11: 94.

Chang S, Puryear J and Cairney J. 1993. A simple and efficient method for isolating RNA from pine trees. *Plant Mol. Biol. Report.* 11: 113–116.

Chen L-Q, Hou B-H, Lalonde S, Takanaga H, Hartung ML, Qu X-Q, Guo W-J, et al. 2010. Sugar transporters for intercellular exchange and nutrition of pathogens. *Nature*. 468: 527–32.

Chong J, Piron M-C, Meyer S, Merdinoglu D, Bertsch C and Mestre P. 2014. The SWEET family of sugar transporters in grapevine: VvSWEET4 is involved in the interaction with Botrytis cinerea. *J. Exp. Bot.* 65: 6589–6601.

Coombe BG. 1960. Relationship of growth and development to changes in sugars, auxins, and gibberellins in fruit of seeded and seedless varieties of *Vitis Vinifera*. *Plant Physiol.* 35: 241–50.

Conesa A, Götz S, García-Gómez JM, Terol J, Talón M and Robles M. 2005. Blast2GO: a universal tool for annotation, visualization and analysis in functional genomics research. *Bioinformatics*. 21: 3674–3676.

Cramer GR, Ghan R, Schlauch KA, Tillett RL, Heymann H, Ferrarini A, Delledonne M, et al. 2014. Transcriptomic analysis of the late stages of grapevine (*Vitis vinifera* cv. Cabernet Sauvignon) berry ripening reveals significant induction of ethylene signaling and flavor pathways in the skin. *BMC Plant Biol.* 14: 370.

Dauelsberg P, Matus JT, Poupin MJ, Leiva-Ampuero A, Godoy F, Vega A and Arce-Johnson P. 2011. Effect of pollination and fertilization on the expression of genes related to floral transition, hormone synthesis and berry development in grapevine. *J. Plant Physiol.* 168: 1667–74.

De Dios P, Matilla AJ and Gallardo M. 2006. Flower fertilization and fruit development prompt changes in free polyamines and ethylene in damson plum (*Prunus insititia* L.). *J. Plant Physiol.* 163: 86–97.

Deluc LG, Grimplet J, Wheatley MD, Tillett RL, Quilici DR, Osborne C, Schooley DA, et al. 2007. Transcriptomic and metabolite analyses of Cabernet Sauvignon grape berry development. *BMC Genomics*. 8: 429.

Dokoozlian NK. 2000. Grape berry growth and development. *Raisin Production Manual.* University of California, Agricultural and Natural Resources. 30–37.

Domingos S, Scafidi P, Cardoso V, Leitao AE, Di Lorenzo R, Oliveira CM and Goulao LF. 2015. Flower abscission in *Vitis vinifera* L. triggered by gibberellic acid and shade discloses differences in the underlying metabolic pathways. *Front. Plant Sci.*6:457.

Evans A, DeHaven C and Barrett T. 2009. Integrated, nontargeted ultrahigh performance liquid chromatography/electrospray ionization tandem mass spectrometry platform for the identification and relative. *Anal. Chem.* 6656–6667.

Evans AM, Mitchell MW, Dai H and DeHaven CD. 2012. Categorizing ion –features in liquid chromatography/mass spectrometry metobolomics data. *Metabolomics:Open Access*. 2: 111.

Fasoli M, Dal Santo S, Zenoni S, Tornielli GB, Farina L, Zamboni A, Porceddu A, et al. 2012. The grapevine expression atlas reveals a deep transcriptome shift driving the entire plant into a maturation program. *Plant Cell*. 24: 3489–3505.

Gao L, Tu ZJ, Millett BP and Bradeen JM. 2013. Insights into organ-specific pathogen defense responses in plants: RNA-seq analysis of potato tuber-Phytophthora infestans interactions. *BMC Genomics*. 14: 340.

Giacomelli L, Rota-Stabelli O, Masuero D, Acheampong AK, Moretto M, Caputi L, Vrhovsek U, et al. 2013. Gibberellin metabolism in *Vitis vinifera* L. during bloom and fruit-set: functional characterization and evolution of grapevine gibberellin oxidases. *J. Exp. Bot.* 64: 4403–4419.

Gonzalez A, Zhao M, Leavitt JM and Lloyd AM. 2008. Regulation of the anthocyanin biosynthetic pathway by the TTG1/bHLH/Myb transcriptional complex in Arabidopsis seedlings. *Plant J.* 53: 814–27.

Goulão LF, Fernandes JC, Lopes P and Amâncio S. 2012. Tackling the cell wall of the grape berry. In Gerós H, Chaves M and Delrot S (Eds.), *The biochemistry of the grape berry*. Bentham science. 172–193.

Grimplet J, Deluc LG, Tillett RL, Wheatley MD, Schlauch KA, Cramer GR and Cushman JC. 2007. Tissue-specific mRNA expression profiling in grape berry tissues. *BMC Genomics*. 8: 187.

Jaillon O, Aury J-M, Noel B, Policriti A, Clepet C, Casagrande A, Choisne N, et al. 2007. The grapevine genome sequence suggests ancestral hexaploidization in major angiosperm phyla. *Nature*. 449: 463–467.

Jin Y, Ni D-A and Ruan Y-L. 2009b. Posttranslational elevation of cell wall invertase activity by silencing its inhibitor in tomato delays leaf senescence and increases seed weight and fruit hexose level. *Plant Cell*. 21: 2072–2089.

Dauelsberg P, Matus JT, Poupin MJ, Leiva-Ampuero A, Godoy F, Vega A and Arce-Johnson P. 2011. Effect of pollination and fertilization on the expression of genes related to floral transition, hormone synthesis and berry development in grapevine. *J. Plant Physiol.* 168: 1667–74.

De Jong M, Wolters-Arts M, Feron R, Mariani C and Vriezen WH. 2009. The *Solanum lycopersicum* auxin response factor 7 (SlARF7) regulates auxin signaling during tomato fruit set and development. *Plant J.* 57: 160–170.

De Jong M, Wolters-Arts M, García-Martínez JL, Mariani C and Vriezen WH. 2011. The *Solanum lycopersicum* auxin response factor 7 (SlARF7) mediates cross-talk between auxin and gibberellin signalling during tomato fruit set and development. *J. Exp. Bot.* 62: 617–626.

Kanehisa M, Araki M, Goto S, Hattori M, Hirakawa M, Itoh M, Katayama T, et al. 2008. KEGG for linking genomes to life and the environment. *Nucleic Acids Res.* 36: 480–484.

Kim D, Pertea G, Trapnell C, Pimentel H, Kelley R and Salzberg SL. 2013. TopHat2: accurate alignment of transcriptomes in the presence of insertions, deletions and gene fusions. *Genome Biol.* 14: 36.

Kliewer WM. 1977. Effect of high temperatures during the bloom-set period on fruit-set, ovule fertility, and berry growth of several grape cultivars. *Am. J. Enol. Vitic.* 28: 215–222.

Krichevsky A, Kozlovsky S V, Tian G-W, Chen M-H, Zaltsman A and Citovsky V. 2007. How pollen tubes grow. *Dev. Biol.* 303: 405–420.

Kumar L and E Futschik M. 2007. Mfuzz: a software package for soft clustering of microarray data. *Bioinformation*. 2: 5–7.

Lebon G, Wojnarowiez G, Holzapfel B, Fontaine F, Vaillant-Gaveau N and Clément C. 2008. Sugars and flowering in the grapevine (*Vitis vinifera* L.). *J. Exp. Bot.* 59: 2565–2578.

Lecourieux F, Kappel C, Lecourieux D, Serrano A, Torres E, Arce-Johnson P and Delrot S. 2013. An update on sugar transport and signalling in grapevine. *J. Exp. Bot.* 65: 821–832.

Li J and Yuan R. 2008. NAA and ethylene regulate expression of genes related to ethylene biosynthesis, perception, and cell wall degradation during fruit abscission and ripening in 'delicious' apples. *J. Plant Growth Regul.* 27: 283–295.

Li Z, Palmer WM, Martin AP, Wang R, Rainsford F, Jin Y, Patrick JW, et al. 2012. High invertase activity in tomato reproductive organs correlates with enhanced sucrose import into, and heat tolerance of, young fruit. *J. Exp. Bot.* 63: 1155–1166.

Liu J-J, Sturrock RN and Benton R. 2013. Transcriptome analysis of *Pinus monticola* primary needles by RNA-seq provides novel insight into host resistance to *Cronartium ribicola*. *BMC Genomics*. 14: 884.

Lorenz D, Eichhorn K, Bleiholder H, Klose R, Meier U and Weber E. 1994. Phänologische entwicklungsstadien der rebe (*Vitis vinifera* L. ssp. vinifera). – Codierung und beschreibung nach der erweiterten BBCH-Skala. *Vitic. Enol. Sci.*49: 66-70.

Love MI, Huber W and Anders S. 2014. Moderated estimation of fold change and dispersion for RNA-seq data with DESeq2. *Genome Biol.* 15: 550.

Lytle BL, Song J, de la Cruz NB, Peterson FC, Johnson KA, Bingman CA, Phillips GN, et al. 2009. Structures of two *Arabidopsis thaliana* major latex proteins represent novel helix-grip folds. *Proteins*. 76: 237–243.

McLaughlin JE and Boyer JS. 2004. Sugar-responsive gene expression, invertase activity, and senescence in aborting maize ovaries at low water potentials. *Ann. Bot.* 94: 675–689.

Mizutani M. 2012. Impacts of diversification of cytochrome P450 on plant metabolism. *Biol. Pharm. Bull.* 35: 824–832.

Nwafor CC, Gribaudo I, Schneider A, Wehrens R, Grando MS and Costantini L. 2014. Transcriptome analysis during berry development provides insights into co-regulated and altered gene expression between a seeded wine grape variety and its seedless somatic variant. *BMC Genomics*. 15: 1030.

Ohta T, Masutomi N, Tsutsui N, Sakairi T, Mitchell M, Milburn M V, Ryals J a, et al. 2009. Untargeted metabolomic profiling as an evaluative tool of fenofibrate-induced toxicology in Fischer 344 male rats. *Toxicol. Pathol.* 37: 521–535.

Ojeda H, Deloire A, Carbonneau A, Ageorges A and Romieu C. 1999. Berry development of grapevines: Relations between the growth of berries and their DNA content indicate cell multiplication and enlargement. *Vitis.* 38: 145-150.

Olek AT, Rayon C, Makowski L, Kim HR, Ciesielski P, Badger J, Paul LN, et al. 2014. The structure of the catalytic domain of a plant cellulose synthase and its assembly into dimers. *Plant Cell*. 26: 2996–3009.

Olimpieri I, Siligato F, Caccia R, Mariotti L, Ceccarelli N, Soressi GP and Mazzucato A. 2007. Tomato fruit set driven by pollination or by the parthenocarpic fruit allele are mediated by transcriptionally regulated gibberellin biosynthesis. *Planta*. 226: 877–888.

Palusa SG, Golovkin M, Shin S-B, Richardson DN and Reddy ASN. 2007. Organ-specific, developmental, hormonal and stress regulation of expression of putative pectate lyase genes in Arabidopsis. *New Phytol.* 174: 537–550.

Park J-S, Kim J-B, Cho K-J, Cheon C-I, Sung M-K, Choung M-G and Roh K-H. 2008. Arabidopsis R2R3-MYB transcription factor AtMYB60 functions as a transcriptional repressor of anthocyanin biosynthesis in lettuce (Lactuca sativa). *Plant Cell Rep.* 27: 985–94.

Pascual L, Blanca JM, Cañizares J and Nuez F. 2007. Analysis of gene expression during the fruit set of tomato: A comparative approach. *Plant Sci.* 173: 609–620.

Pratt C. 1971. Reproductive anatomy in cultivated grapes - a review. *Am. J. Enol. Vitic.* 22: 92–109.

Ren Z, Li Z, Miao Q, Yang Y, Deng W and Hao Y. 2011. The auxin receptor homologue in *Solanum lycopersicum* stimulates tomato fruit set and leaf morphogenesis. *J. Exp. Bot.* 62: 2815–2826.

Rodriguez MCS, Petersen M and Mundy J. 2010. Mitogen-activated protein kinase signaling in plants. *Annu. Rev. Plant Biol.* 61: 621–649.

Rohlf FJ. 2005. *NTSYS-pc: numerical taxonomy and multivariate analysis system*. Exeter Software, Setauket, New York, USA.

Ruan Y-L, Patrick JW, Bouzayen M, Osorio S and Fernie AR. 2012. Molecular regulation of seed and fruit set. *Trends Plant Sci.* 17: 656–665.

Ruperti B, Bonghi C, Ziliotto F, Pagni S, Rasori A, Varotto S, Tonutti P, et al. 2002. Characterization of a major latex protein (MLP) gene down-regulated by ethylene during peach fruitlet abscission. *Plant Sci.* 163: 265–272.

Sanders A, Collier R, Trethewy A, Gould G, Sieker R and Tegeder M. 2009. AAP1 regulates import of amino acids into developing Arabidopsis embryos. *Plant J.* 59: 540–552.

Serrani JC, Sanjuán R, Ruiz-Rivero O, Fos M and García-Martínez JL. 2007. Gibberellin regulation of fruit set and growth in tomato. *Plant Physiol.* 145: 246–257.

Shelden MC, Howitt SM, Kaiser BN and Tyerman SD. 2009. Identification and functional characterisation of aquaporins in the grapevine, *Vitis vinifera. Funct. Plant Biol.* 36: 1065.

Shen, Y, Wan Z, Coarfa C, Drabek R, Chen L, Ostrowski EA, Liu Y, Weinstock GM, Wheeler DA, Gibbs RA, Yu F. 2010. A SNP discovery method to assess variant allele probability from next-generation resequencing data. *Genome Res*. 20: 273–280.

Shiratke K. 2007. Genetics of sucrose transporter in plants. *Genes, genomes and genomics*. 74–80.

Slewinski TL. 2011. Diverse functional roles of monosaccharide transporters and their homologs in vascular plants: a physiological perspective. *Mol. Plant*. 4: 641–662.

Suwa R, Hakata H, Hara H, El-Shemy HA, Adu-Gyamfi JJ, Nguyen NT, Kanai S, et al. 2010. High temperature effects on photosynthate partitioning and sugar metabolism during ear expansion in maize (*Zea mays* L.) genotypes. *Plant Physiol. Biochem.* 48: 124–130.

Suzuki R and Shimodaira H. 2006. Pvclust: an R package for assessing the uncertainty in hierarchical clustering. *Bioinformatics*. 22: 1540–1542.

Sweetman C, Wong DC, Ford CM and Drew DP. 2012. Transcriptome analysis at four developmental stages of grape berry (*Vitis vinifera* cv. Shiraz) provides insights into regulated and coordinated gene expression. *BMC Genomics*. 13: 691.

Tatusov RL, Fedorova ND, Jackson JD, Jacobs AR, Kiryutin B, Koonin E V, Krylov DM, et al. 2003. The COG database: an updated version includes eukaryotes. *BMC Bioinformatics*. 4: 41.

Thakare D, Yang R, Steffen JG, Zhan J, Wang D, Clark RM, Wang X, et al. 2014. RNA-Seq analysis of laser-capture microdissected cells of the developing central starchy endosperm of maize. *Genomics Data*. 2: 242–245.

Trapnell C, Williams BA, Pertea G, Mortazavi A, Kwan G, van Baren MJ, Salzberg SL, et al. 2010. Transcript assembly and quantification by RNA-Seq reveals unannotated transcripts and isoform switching during cell differentiation. *Nat. Biotechnol.* 28: 511–515.

Varoquaux F, Blanvillain R, Delseny M and Gallois P. 2000. Less is better: new approaches for seedless fruit production. *Trends Biotechnol.* 18: 233–242.

Vasconcelos MC, Greven M, Winefield CS, Trought MCT and Raw V. 2009. The flowering process of *Vitis vinifera*: A review. *Am. J. Enol. Vitic.* 60: 411–434.

Velasco R, Zharkikh A, Troggio M, Cartwright DA, Cestaro A, Pruss D, Pindo M, et al. 2007. A high quality draft consensus sequence of the genome of a heterozygous grapevine variety. *PLoS One*. 2: 1326.

Venturini L, Ferrarini A, Zenoni S, Tornielli GB, Fasoli M, Dal Santo S, Minio A, et al. 2013. De novo transcriptome characterization of *Vitis vinifera* cv. Corvina unveils varietal diversity. *BMC Genomics*. 14: 41.

Vierling E. 1991. The roles of heat shock proteins in plants. *Annu. Rev. Plant Physiol. Plant Mol. Biol.* 42: 579–620.

Vriezen WH, Feron R, Maretto F, Keijman J and Mariani C. 2008. Changes in tomato ovary transcriptome demonstrate complex hormonal regulation of fruit set. *New Phytol.* 177: 60–76.

Wang H, Jones B, Li Z, Frasse P, Delalande C, Regad F, Chaabouni S, et al. 2005. The tomato Aux/IAA transcription factor IAA9 is involved in fruit development and leaf morphogenesis. *Plant Cell*. 17: 2676–2692.

Wang H, Schauer N, Usadel B, Frasse P, Zouine M, Hernould M, Latché A, et al. 2009. Regulatory features underlying pollination-dependent and -independent tomato fruit set revealed by transcript and primary metabolite profiling. *Plant Cell*. 21: 1428–1452.

Wang XQ, Li LM, Yang PP and Gong CL. 2014. The role of hexokinases from grape berries (*Vitis vinifera* L.) in regulating the expression of cell wall invertase and sucrose synthase genes. *Plant Cell Rep.* 33: 337–347.

Werner D, Gerlitz N and Stadler R. 2011. A dual switch in phloem unloading during ovule development in Arabidopsis. *Protoplasma*. 248: 225–235.

Zenoni S, Ferrarini A, Giacomelli E, Xumerle L, Fasoli M, Malerba G, Bellin D, et al. 2010. Characterization of transcriptional complexity during berry development in *Vitis vinifera* using RNA-Seq. *Plant Physiol.* 152: 1787–1795.

Zhang C, Tanabe K, Tamura F, Matsumoto K and Yoshida A. 2005. 13C-photosynthate accumulation in Japanese pear fruit during the period of rapid fruit growth is limited by the sink strength of fruit rather than by the transport capacity of the pedicel. *J. Exp. Bot.* 56: 2713–2719.

Zhang Q, Li Z, Yang J, Li S, Yang D and Zhu Y. 2011. A calmodulin-binding protein from rice is essential to pollen development. *J. Plant Biol.* 55: 18–14.

Zhang X-Y, Wang X-L, Wang X-F, Xia G-H, Pan Q-H, Fan R-C, Wu F-Q, et al. 2006. A shift of phloem unloading from symplasmic to apoplasmic pathway is involved in developmental onset of ripening in grape berry. *Plant Physiol.* 142: 220–232.

Zhao Y, Tang H and Ye Y. 2012. RAPSearch2: a fast and memory-efficient protein similarity search tool for next-generation sequencing data. *Bioinformatics*. 28: 125–126.

Zinn KE, Tunc-Ozdemir M and Harper JF. 2010. Temperature stress and plant sexual reproduction: uncovering the weakest links. *J. Exp. Bot.* 61: 1959–1968.

Zonia L and Munnik T. 2009. Uncovering hidden treasures in pollen tube growth mechanics. *Trends Plant Sci.* 14: 318–327.

Chapter 3

Flower abscission in *Vitis vinifera* L. triggered by gibberellic acid and shade discloses differences in the underlying metabolic pathways

The data presented in this chapter were published in Frontiers in Plant Science:

Domingos S[1,2], Scafidi P[3], Cardoso V[2], Leitão AE[2], DiLorenzo R[3], Oliveira CM[1] and Goulao LF[2]

[1] Linking Landscape, Environment, Agriculture and Food, Instituto Superior de Agronomia, Universidade de Lisboa, Lisbon, Portugal

[2] Instituto de Investigação Científica Tropical I.P., Lisbon, Portugal

[3] Dipartimento di Scienze Agrarie e Forestali, Universitá di Palermo, Palermo, Italy

Domingos S, Scafidi P, Cardoso V, Leitao AE, Di Lorenzo R, Oliveira CM and Goulao LF. 2015. Flower abscission in *Vitis vinifera* L. triggered by gibberellic acid and shade discloses differences in the underlying metabolic pathways. *Front. Plant Sci.* 6:457 doi:10.3389/fpls.2015.00457

3. Flower abscission in *Vitis vinifera* L. triggered by gibberellic acid and shade discloses differences in the underlying metabolic pathways

Abstract

Understanding abscission is both a biological and an agronomic challenge. Flower abscission induced independently by shade and gibberellic acid (GAc) sprays was monitored in grapevine (*Vitis vinifera* L.) growing under a soilless greenhouse system during two seasonal growing conditions, in an early and late production cycle. Physiological and metabolic changes triggered by each of the two distinct stimuli were determined. Environmental conditions exerted a significant effect on fruit set as showed by the higher natural drop rate recorded in the late production cycle with respect to the early cycle. Shade and GAc treatments increased the percentage of flower drop compared to the control, and at a similar degree, during the late production cycle. The reduction of leaf gas exchanges under shade conditions was not observed in GAc treated vines. The metabolic profile assessed in samples collected during the late cycle differently affected primary and secondary metabolisms and showed that most of the treatment-resulting variations occurred in opposite trends in inflorescences unbalanced in either hormonal or energy deficit abscission-inducing signals. Particularly concerning carbohydrates metabolism, sucrose, glucose, tricarboxylic acid (TCA) metabolites and intermediates of the raffinose family oligosaccharides pathway were lower in shaded and higher in GAc samples. Altered oxidative stress remediation mechanisms and indol-3-acetic acid (IAA) concentration were identified as abscission signatures common to both stimuli. According to the global analysis performed, we suggest that grape flower abscission mechanisms triggered by GAc application and C-starvation are not based on the same metabolic pathways.

Key-words: Abscission, gibberellic acid, grapevine, metabolomics, shade, thinning.

3.1 Introduction

Abscission is the process by which vegetative and reproductive organs can be detached from plants as an effect of developmental, hormonal and environmental cues. Abscission control is regarded as an important agricultural concern because it affects production yield and quality. In fruit species, fruit set is often excessive and the natural drop, which enables the plant to self-regulate its load, is not sufficient to satisfy fresh market quality standards (Bonghi et al., 2000).

Fruit thinning is a common practice, particularly in table grape production, in which the reduction of berry number per bunch is mandatory to guarantee improved bunch appearance and quality and decreased diseases incidence (Dokoozlian and Peacock, 2001). Excluding labor-demanding manual thinning, the most common thinning method for table grapes uses chemical treatments with gibberellic acid (GAc) sprays at bloom to induce flower abscission. The effectiveness of this practice is known to vary due to both internal (such as cultivar, phenologic stage, physiological condition and age) and external (such as nutrient availability, irrigation, temperature, irradiation and humidity) conditions (Dokoozlian, 1998; Dokoozlian and Peacock, 2001; Hed et al., 2011; Hopping, 1976; Looney and Wood, 1977; Reynolds and Savigny, 2004; Reynolds et al., 2006; Weaver et al., 1962). Gibberellins participate in biological processes such as cell elongation, dormancy breaking, parthenocarpy induction and seed germination (Davieré and Archard, 2013; Yamaguchi, 2008). However, despite the widespread use of GAc spraying, the mechanisms by which GAc works as thinning agent are not fully understood. According to the photosynthates competition hypothesis (Dokoozlian, 1998), GAc stimulates general organ growing, inducing competition for nutrients between flowers and shoots and/or among flowers within the inflorescence, which leads to reductions in the amount of nutrients available for berry set and growth. Alternatively, GAc can be responsible for unbalancing hormone relative concentrations, in agreement with the hormone balance hypothesis (Dokoozlian, 1998). Auxins are known to regulate gibberellin endogenous levels (Yamaguchi, 2008). A flow of inhibitory auxin in an organ destined to abscise prevents cell separation until its endogenous levels drop, de-repressing ethylene, which then activates the transcription of cell wall (CW) disassembly-related genes (Else et al., 2004; Dal Cin et al., 2005). The effect of shade imposition to promote berry set reduction has been first investigated by Roubelakis and Kliewer (1976) and Ferree et al. (2001). The use of this practice as an alternative thinning method was successful also in other species, such as apple (Basak, 2011; Byers et al., 1985, 1990, 1991; Corelli et al., 1990; Schneider, 1975; Widmer et al., 2008; Zibordi et al., 2009) and involves intercepted light reduction during a short period of time after bloom. The pronounced reduction of net photosynthetic rate under shading promotes the competition for photoassimilates between vegetative and reproductive organs, leading to shedding of the later, which have less sink strength at this early stage of development (Vasconcelos et al., 2009). Hence, abscission stands as challenging biological question since it can be induced by agents that apparently act by promoting opposite changes to the plant physiology. However, although the hormone and the assimilate theories may look contrasting, changes in assimilate availability may be the trigger required for changing hormone balances, leading to abscission. Moreover, sugars are more than an energy source as may also act as messengers operating in gene expression regulation or as signaling molecules (Lebon et al., 2008).

The mechanisms underlying organ abscission, were recently reviewed by Estornell et al. (2013), and involve signal peptides and specific receptors, mostly regulated by hormones, in which ethylene, ABA and jasmonic acid act as accelerating signals. Conversely, auxin, gibberellins, polyamines (PAs) and brassinosteroids act in abscission inhibiting signaling. The developmental phenomenon of physiological drop represents the natural reduction of fruit set and enables the plant to shed the weaker sinks, regulating the fruit load according to its capacity to produce the metabolic energy required to complete the development of reproductive and vegetative structures (Bonghi et al., 2000). Natural drop occurs after an increased abscisic acid (ABA) and ethylene production that induces a negative feedback in fruit development, as demonstrated in apple (Botton et al., 2011). In wine grapes, natural drop was showed to be related to lower sugar and PAs availability for developing flowers (Aziz, 2003; Lebon et al., 2004). Declines in the sugar supply at meiosis results in excessive flower abortion in this species (Lebon et al., 2008) which together with the expression of sucrose- or hexose-transporter genes (Davies et al., 1999), suggests a role for sugars in flower stress avoidance. Free-PA synthesis is also closely related to the onset of ovarian development and retards abscission (Aziz, 2003). Since PAs and ethylene share S-adenosylmethionine (SAM) as a common intermediate, SAM may be alternatively channeled towards the PA pathway, functioning as an alternative control. Free PAs fluctuate in parallel with sugars in the grape inflorescence, suggesting also a contribution in the modulation of their concentrations (Aziz, 2003).

Changes on the biochemical and transcriptome profiles during flower and fruit abscission triggered by growth regulators (Botton et al., 2011; Dal Cin et al., 2005, 2009; Li and Yuan, 2008; Meir et al., 2010; Giulia et al., 2013; Peng et al., 2013; Wang et al., 2013; Whitelaw et al., 2002) or by low light conditions (Aziz, 2003; Li et al., 2013; Zhou et al., 2008) have been studied in several species such as tomato (*Solanum lycopersicon*), apple (*Malus* × *domestica*), lychee (*Litchi chinensis*) or wine grapes aiming at understanding the effect caused by chemical/environmental perturbations. The above-cited studies revealed a coordinated response of hormones, reactive oxygen species (ROS), sugar metabolism and signaling pathways to determine the downstream activation of abscission which includes increased activity of CW-modifying enzymes. Nonetheless, to our knowledge, only one publication to date (Zhu et al., 2011) reports a direct comparison of the mechanisms underlying abscission triggered by two distinct cues. The authors compared napththaleneacetic acid (NAA) and shading treatments in inducing abscission in apple, through transcriptome analysis, and observed shared pathways involving reduction of photosynthesis, carbon transport and signaling, and hormone crosstalk. The aim of the present study was to provide a first global approach for understanding the changes occurring in vine inflorescences and canopy that explain flower abscission in *Vitis vinifera* L. (Black Magic table grape cultivar), triggered by two contrasting abscission-inducing

treatments (shade and GAc spraying) under conditions that leading to similar berry shed rates. The goal was to search for specificities and common links in metabolic pathways that control abscission.

3.2 Material and methods

3.2.1 Experimental conditions and design

The trails were carried out in a greenhouse in the south of Sicily, in a soilless table grape commercial production system (Di Lorenzo et al., 2014) of 'Black Magic' vines (*Vitis vinifera* L.) own-rooted in 2010 (Fig. 3.1A). Black Magic is a very early seeded table grape cultivar, with high fertility and yield, released by the National Research Institute of Grape and Wine in Chisinau, Moldova. The assays were performed during the late production cycle of 2011 and the early production cycle of 2012. Plants were spaced 1.60 m between lines x 0.40 m between plants, trained as unilateral cordon pruned with six buds and managed following integrated fertilization, irrigation, and pest-management practices (Di Lorenzo et al., 2009). The number of fertirrigations ranged between 5 and 20, judged by monitoring microclimate conditions. Nutritive solutions had the composition of 3, 1.25, 0.5, 0.65, 0.75, 0.5, 1.25, 7, 0.75, 2 and 0.5mM of Ca, Mg, Na, K, NH_4, Si, P, NO_3, HCO_3/CO_3, SO_4 and Cl, respectively, the pH was 5.0 and the electrical conductivity was maintained between 1.5 and 2 mS cm^{-1}. Treatments were: i) reduction of intercepted light and ii) chemical thinning with GAc, both established at bloom (50% cap fall, stage 65 of the BBCH scale (Lorenz et al., 1994)). Shade treatments entailed covering the vines with green polypropylene 90% nets (Serroplast, Italy) for a period of twelve days. Chemical treatment consisted in spraying GAc (Gibberellin 1.8% GA_3, Gobbi, Italy) at 15 ppm concentration. A group that remained untreated was included as control. Experiments were designed in three randomized blocks by treatment with 14 vines each, using single vines as replicates. Climate conditions were monitored above the canopy of shaded and control vines (WatchDog MicroStation, Spectrum Tech., USA) (Supplementary Figure S3.1).

Late production cycle: Plants were kept stored cold until June 2011 and the experiments started at 3rd July. The 50% cap fall stage (bloom) occurred after 34 days and harvest was carried out 67 days after bloom (DAB). This production cycle lasted a total of 101 days. The day (7 a.m. to 7 p.m.) / night (7 p.m. to 7 a.m.) mean temperatures registered were 32/23ºC, relative humidity was 41/64% and PAR was 5/504 μmol m^{-2} s^{-1}.

Early production cycle: The experiments were conducted in 2012 using the same plants as in the previous year. The early production cycle started at 9 February, 50% cap fall stage occurred

after 53 days and grapes were harvested 77 DAB. This cycle lasted a total of 130 days. The recorded day / night mean temperatures were 26/14ºC, relative humidity was 45/79% and PAR was 17/566 μmol m^{-2} s^{-1}.

3.2.2 Vine physiology monitoring

Flower and berry drop were monitored by positioning non-woven cloth bags around bunches at 50% cap fall after the imposition of each treatment, to collect the shed flowers (Fig. 3.1B and 3.1C). Flowers were collected and counted, 2, 4 and 12 DAB in 10 bunches per treatment. Bunches were selected taking uniformity of bloom in account. At harvest, the same bunches were collected and the final number of berries was recorded to calculate the cumulative and daily rate berry drop percentages. Net photosynthetic rate (P_n), transpiration rate (E) and stomatal conductance (g_s) were measured in the morning period (9:00 am - 11:00 am) using a portable infrared gas analyzer (CIRAS, PPsystems, UK) on twelve mature leaves from the central part of the shoot, twice during the shade period (at 3 and 10 DAB). Shoot length, estimated leaf chlorophyll content (SPAD-502 m, Minolta, Japan) and total (sum of primary and secondary) leaf area (WinDIAS leaf area measurement system, Delta-T Devices, UK) were determined 12 DAB, before removal of the shade nets, in nine shoots per treatment.

3.2.3 Metabolic analysis

3.2.3.1 Quantification of target metabolites

Sugar (glucose, sucrose, fructose and stachyose), free PAs (putrescine, spermine, spermidine and cadaverine) and hormone (indole-3-acetic (IAA) and abscisic acid (ABA)) contents extracted from inflorescence samples collected in the late cycle, 1, 3 and 4 DAB were quantified by high performance liquid chromatography (HPLC), aiming at determining the metabolic changes explaining flower abscission. The biochemical analyses were conducted using liquid nitrogen frozen powdered samples of whole inflorescences deprived from the rachis. Samples for soluble sugars quantification (100mg) were extracted according to Damesin and Lelarge (2003), and samples were injected into a HPLC (Beckman Coulter, USA) and separated on a Sugar-Pak I column I (300 x 6.5 mm, Waters) at 90 ºC under a 122μM EDTA-Ca solution and a flow rate of 0.5 ml min^{-1}. Peaks were detected by RI (Refractive Index Detector 2414, Waters). Free PAs were quantified according to Smith and Davies (1987) with modifications. Samples (100 mg) were mixed with 300 μL of a 5% perchloric acid solution, kept for 50 min in ice and centrifuged for 20 min at 20000 g at 4ºC. Saturated Na_2CO_3 (200 μl) and dansyl chloride (400 μL, 5 mg ml^{-1} in acetone) were added to 100μl of the supernatant, and mixtures were incubated in the dark at 60ºC for 1 h. Proline (10 mg) was then added and further incubated for 30 min. PAs were extracted with 500μl of toluene, the organic phase was dried under nitrogen and the

residue was dissolved in 300 µl acetonitrile. The resulting samples were injected into the HPLC (Ultimate 3000, Dionex, Sunnyville, CA, USA), eluted through a C18 column (particle size 5 µm, 4.6 x 150 mm, Thermo Scientific) at a flow rate of 1 ml min^{-1} with a mobile phase consisting of 10% acetonitrile solution, pH 3.5 (solvent A) and acetonitrile (solvent B) using a 60% to 90% of solvent A gradient, during 23 minutes. Peaks were detected with a diode array detector (DAD) at 346 nm. IAA and ABA were extracted according to Kelen et al. (2004) with modifications. Samples (200 mg) were extracted with 600 µL of 70% methanol and incubated at 4ºC overnight. The extraction was repeated twice and the methanol evaporated under vacuum. 0.1M phosphate buffer (800 µl) was added to the aqueous phase and partitioned with 300 µl of ethyl acetate 3 times. After ethyl acetate removal, the pH was adjusted to 2.5 with 1 N HCl. The solution was further partitioned 3 times with 450 µl of diethyl ether, passed through anhydrous sodium sulfate, evaporated at 50ºC under vacuum and the residue was dissolved in 100 µl of methanol. Aliquots were injected into the HPLC (Ultimate 3000, Dionex, Sunnyville, CA, USA), eluted through a C18 column (particle size 5 µm, 4.6 x 150 mm, Thermo Scientific) under a 30 mM phosphoric acid solution with 26% acetonitrile at 4 pH during 30 min at 0.8 ml min^{-1} and the peaks were detected with a DAD at 208 and 265 nm. In all cases, extractions were done in duplicate readings, each from three biological replicates per treatment. Standards for peak identification were purchased from Sigma-Aldrich®.

3.2.3.2 Global metabolomic profile

Sample points for metabolomic analysis were chosen based on the significant changes observed after target chromatography quantifications. Therefore, samples from three biological replicates (200mg) of GAc-, shaded-treated and control inflorescences collected at 4 DAB in the late production cycle, were lyophilized, methanol extracted and analyzed using the integrated platform developed by Metabolon® (Durham, USA) consisting of a combination of three independent approaches: (1) ultrahigh performance liquid chromatography/tandem mass spectrometry (UHLC/MS/MS2) optimized for basic species, (2) UHLC/MS/MS2 optimized for acidic species, and (3) gas chromatography/mass spectrometry (GC/MS). Methods were followed as previously described (Evans et al., 2009, Ohta et al., 2009).

3.2.4 Evaluation of productivity and berry quality attributes

The final number of shot berries (parthenocarpic small berries that remain green at harvest) and regular-sized berries, bunch weight, rachis length and weight, bunch compactness (ratio between total number of berries and length of the rachis) and yield per plant were recorded and calculated at harvest in the same 10 bunches per treatment used for flower drop monitoring. Ten berries per bunch were randomly selected to measure berries weight and diameter. The

remaining berries were distributed in 3 samples per treatment to measure soluble solids content (SSC) (in % using a PR-32 refractometer, Atago, Japan) and titratable acidity (TA; by potentiometric titration with 0.1 N NaOH up to pH 8.1).

3.2.5 Data imputation and statistical analysis

To access the significance of the differences observed between treatments and production cycles, variance analysis (one- and two-way ANOVA) and post-hoc (Tukey's HSD with α=0.05) tests were conducted using Statistix 9 (Analytical Software, Florida). To improve adjustment to the normal distribution, percentage values were arcsin sqrt(x) transformed and values of number of berries were square-root transformed. For global metabolomic analyses, raw area counts for each biochemical were rescaled by dividing each sample's value by the median value for the specific metabolite. Following $\log_2$ transformations, statistical analysis of the data was performed using Array Studio (Omicsoft). In order to visualize the results, a heat map was generated to show fold-change defined as the $\log_2$ of the means ratio of each treatment and control for each compound (Supplementary Table S3.1). Welch's two-sample t-tests were used to determine whether each metabolite had significantly increased or decreased in abundance. False Discovery Rates (FDR) were calculated as *q*-values according to Storey and Tibshirani (2003) to account for the large number of tests. Metabolites that significantly changed in response to at least one of the treatments were used to conduct correlation matrix-based principal coordinate analysis (PCoA) using the NTsys-PC version 2.20e software package (Rohlf, 2005). The DCENTER module was used to transform the symmetric matrix to scalar product and EIGEN for eigenvalues decomposition to identify orthogonal components of the original matrix modules. Hierarchical clustering, associated heatmap and approximately unbiased and bootstrap probability *p*-values were computed using pvclust version 1.3.2 (Suzuki and Shimodaira, 2006) with the UPGMA method and 1000 bootstrap replications. Box plots were generated for those compounds that were significant different using the Welch t-test, FDR significance values and |fold-change|≥1. Mapping of named metabolites was performed onto general biochemical pathways, provided in the Kyoto Encyclopedia of Genes and Genomes (KEGG) (www.genome.jp/kegg/) and Plant Metabolic Network (PMN) (www.plantcyc.org/).

3.3 Results

3.3.1 Effect of GAc and shade on flower abscission

The purpose of the treatments was to induce flower abscission, triggered by two distinct stimuli, with distinct physiological basis. In the late production cycle, both shade and GAc treatments

resulted in higher cumulative percentages of berry drop (95.9% in the shade and 94.3% in the GAc treatment) comparing to the natural drop values observed in control bunches (81.0%) (Table 3.1). Similarly, the average daily number of berries drop was highest in the shade treatment (115±20 berries dropped per bunch per day), followed by GAc (62±14 berries dropped per bunch per day) and lower in the control (28±4 berries dropped per bunch per day) between 2 and 4 DAB (Fig. 3.2A). In the early production cycle, shade imposition was the treatment that promoted the highest percentage of berries drop (49.4%) (Table 3.1). This effect was reflected by an average higher daily number of dropped berries during 2-4 DAB and 4-12 DAB intervals (13±5 and 104±26 berries dropped per bunch per day, respectively), when compared to control (1±0.5 and 29±10 berries dropped per bunch per day, respectively) and GAc treatments (0.3±0.2 and 10±3 berries dropped per bunch per day, respectively) (Fig. 3.2B). Based on these results, the metabolic composition of samples collected in the late cycle, treated with hormonal and light stress abscission-inducing signals, was analyzed.

3.3.2 Impacts on vine physiology

Natural flower drop was significantly affected by environmental factors, exerting a significant effect on fruit set (Table 3.1). A higher drop rate occurred in the late production cycle (81%) when compared to the early cycle (16.9%). Comparing shaded with unshaded conditions, a 90%PAR reduction was observed, while no significant differences in temperature and relative humidity were perceived (Supplementary Figure S3.1). On clear sunny day conditions, the 90%-interception shade cloth provided approximately a maximum PAR of 157 and 170 μmol m^{-2} s^{-1} in late and early cycles, respectively, which demonstrates the strong net photosynthetic rate (Pn) reduction achieved under shaded conditions, in the magnitudes of 90% and 99%, in the late and early cycle, respectively. Transpiration rate (E) (not shown) and stomatal conductance (g_s) decreased under shade, only during the early production cycle, by 23% and 54%, respectively, when compared to controls (Table 3.1). No differences in shoot length and total leaf area were observed between treatments. Nevertheless, in the early cycle, a higher estimated leaf chlorophyll content was perceived in shaded plants (31.2 spad units) when compared with plants treated with GAc (28.1 spad units) (Table 3.1). Production cycles and the interaction production cycles × treatment were statistically significantly different regarding cumulative flower drop and g_s (p-value<0.01). Production cycle also affected leaf area, shoot length and leaf chlorophyll content (p-value<0.01) (Table 3.1), impacting final bunch morphology and berry quality (Table 3.2).

Figure 3.1. Aspect of the experimental table grape vines (Black Magic cv) growing in greenhouse conditions (A), monitoring of flowers drop (B) and flowers detached from the base of flower pedicel (C) after abscission-inducing treatments application.

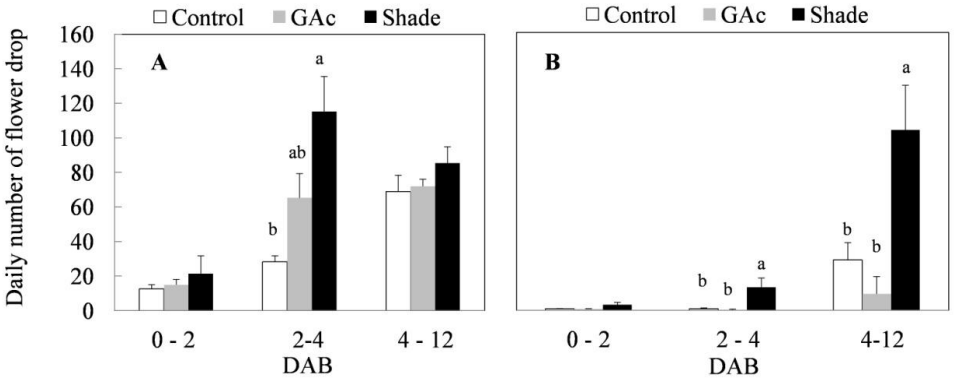

Figure 3.2. Average daily number of flower drop in summer (A) and spring (B) production cycles as effect of GAc and shade treatments on 'Black Magic' vines (mean ± se). Within each sampling date, different letters indicate statistically significant differences (p-values< 0.05).

Table 3.1. Effect of shade and GAc treatments on the average percentage of flower drop, total leaf area and estimated leaf chlorophyll content at 12 DAB, on net photosynthetic rate (P_n) and stomatal conductance (g_s) during the shade period in 'Black Magic' vines in late and early cycles. Within each column, different letters indicate significant differences (p-value<0.05) among treatments, independently in each production cycle, according to Tukey's HSD test.

Production cycle	**Treatment**	**Cumulative flower drop (%)**	**Leaf area (m^2 $vine^{-1}$)**	**Shoot length (cm)**	**Leaf chlorophyll content (spad units)**	**P_n (µmol m^{-2} s^{-1})**	**g_s (mmol m^{-2} s^{-1})**
Late	Control	81.0 b	0.52	79.4	30.5	2.72 a	227.57
	GAc	94.3 a	0.62	96.3	30.3	2.12 a	251.81
	Shade	95.9 a	0.58	86.8	31.7	0.26 b	153.4
Early	Control	16.9 b	1.86	174.6	28.7 ab	3.23 a	576.96 a
	GAc	5.4 b	1.83	183.4	28.1 b	3.18 a	613.69 a
	Shade	49.4 a	1.92	158.7	31.2 a	0.04 b	268.89 b

Table 3.2. Effect of shade and GAc treatments on bunch and berries characteristics at harvest in Black Magic table grape cultivar in the late and early cycles. Values represent the average of the appropriate number of replicates. Within each column, different letters indicate significant differences (*p*-value<0.05) among treatments individually in each production cycle according to Tukey's HSD test.

Production cycle	Treatment	Yield (kg plant^{-1})	Bunch weight (g)	No berries	No shot berries	Rachis length (cm)	Rachis weight (g)
Late	Control	1.9 a	315.9 a	96.8 a	22.3	15.0 ab	7.7 b
	GAc	1.1 b	193.2 b	62.1 b	29.1	17.4 a	10.4 a
	Shade	0.9 b	148.3 b	46.2 b	14.3	12.0 b	4.2 c
Early	Control	8.9 a	879.8 a	173.0 a	188.3 b	24.1 a	12.9 a
	GAc	5.6 b	555.0 b	105.5 b	407.1 a	23.2 a	10.5 ab
	Shade	5.7 b	562.3 b	93.4 b	117.6 b	20.2 b	7.8 b

		Bunch compactness	Berry diameter (cm)	Berry weight (g)	SSC (%)	TA (g L^{-1})
Late	Control	8.0 a	14.1 a	3.83 a	12.5 b	5.7
	GAc	6.1 ab	13.2 c	3.47 b	14.1 ab	5.1
	Shade	5.1 b	13.7 b	3.36 b	15.5 a	5.4
Early	Control	15.5 b	17.2 ab	5.15 c	13.9	3.8
	GAc	22.1 a	16.6 b	5.18 b	14.3	4.7
	Shade	10.5 c	17.8 a	5.78 a	15.8	3.8

3.3.3 Impacts on metabolite content

Regarding the metabolites analyzed in inflorescences sampled from untreated vines 1, 3 and 4 DAB during the late cycle, the results showed reduced sucrose levels between 1 and 4 DAB (Fig. 3.3A) and increased ABA concentrations, peaking at 3 DAB (Fig. 3.3E). Conversely, compared to the control, in shade-treated inflorescences, sucrose concentration decreased at 3 and 4 DAB and fructose and glucose at 4 DAB. In GAc-treated inflorescences, sucrose concentration was highest at 4 DAB (Fig. 3.3B). A significant increase of putrescine content was also observed in the same samples, 4 DAB. In samples submitted to the shade treatment, this PA decreased 3 and 4 DAB (Fig. 3.3D). Cadaverine was not detected. Concerning hormones, IAA concentration was significantly increased in result of both treatments 4 DAB and no differences in ABA levels were observed between treated inflorescences and controls (Fig. 3.3F). From the 215 metabolites investigated by the global metabolic analyses conducted in samples collected 4 DAB, a total of 211 were detected (Supplementary Figure S3.1) and 48 showed to be differentially changed in abundance (*p*-value<0.05) in inflorescences induced for abscission. A total of 34 and 23 metabolites showed differential abundance in shade and GAc treatments, respectively, of which 9 metabolites were common in the different treatments (Table 3.3). Hierarchical clustering (Fig. 3.4A) showed the association between samples according to

the metabolite profile. Samples resulting from each treatment were significantly clustered together. Oleonate, the only metabolite that highly decreased with GAc treatments (fold-change= -2) was separated from the other metabolites. Raffinose, sucrose and benzoyl-O-glucose, showed a distinct pattern according to the imposed treatment, and were grouped in a different cluster. Principal coordinate analysis (Fig. 3.4B) showed that all samples could be separated according to the treatment to each they were submitted to. The first coordinate allows distinguishing inflorescences developing under shade from all the other samples. GAc samples were separated from controls by the second coordinate. Differentially quantified metabolites were mapped onto general biochemical pathways, and categorized into functional classes as showed in Fig. 3.5. Among the 34 metabolites significantly altered in abundance in shaded inflorescences, those assigned to carbohydrates composed the most prevalent class (38%), followed by products of secondary metabolism (26%), amino acid (15%), nucleotide (9%), peptide (7%), cofactors (3%) and lipids (3%). Among the 23 metabolites that significantly changed in response to GAc, products from carbohydrate metabolism was also the most prevalent class (52%), followed by amino acid (18%), secondary metabolism (13%), nucleotide (9%), cofactor (4%) and hormone (4%). A list of all metabolites significantly affected by GAc and shade treatments (p-value<0.05), assigned functional categories, KEGG compound number and respective fold-change is provided in Table 3.3. Shade and GAc treatments were responsible for a decreased concentration of 24 and 4 metabolites, respectively, sharing two metabolites derived from the carbohydrate pathway, namely myo-inositol tetrakisphosphate and erythrulose. On the opposite trend, the imposed treatments induced increased concentration of 10 and 19 metabolites, in shade and GAc, respectively. N6-carbamoylthreonyladenosine, a metabolite from the nucleotide class, was common to both sample sets. Six metabolites concurrently increased in response to GAc and decreased under shade. Four were derived from carbohydrates metabolism, namely sucrose, glucose, raffinose and malate and the other two were derived from secondary metabolism, and included benzyl alcohol and benzyl-O-glucose. Regarding amino acid pathway, decreased quinate, shikimate and putrescine concentrations and increased metabolites derived from aspartate family (methionine and S-adenosylhomocysteine (SAH)) were observed in shade-derived samples. In the GAc treated samples, an increase of phenethylamine, aspartate and alanine and a decrease of 2-aminobutyrate occurred. All metabolites from the carbohydrate pathway were reduced in shaded inflorescences except arabonate. Conversely, in GAc-treated samples, all metabolites increased except myo-inositol tetrakisphosphate and erythrulose. Glycerol, a product from the lipids metabolism, highly increased in result of shade conditions. Gibberelate was detected only in the GAc-derived samples, probably as the result of the exogenous application. Several metabolites from coenzyme and nucleotide metabolisms increased in both treatments except adenosine that was

reduced in shade. Likewise, γ-glutamylisoleucine (γ-glu-lleu) and γ-glutamylvaline (γ-glu-val), from peptides metabolism, increased in the shade treatment. The concentration of metabolites derived from secondary metabolism was reduced in both treatments except two aromatic benzenoids (benzyl alcohol and benzyl-O-glucose) that increased in the GAc treatment and rutin that was increased in the shaded samples. Focusing on the metabolites with more pronounced changes (fold-change (|log 2 (treatment/control)|)≥1), it was observed that raffinose, inositol, glycolysis, TCA cycle, shikimate, phenylalanine and PA pathways were involved in the changes that occurred in inflorescences treated to enhance abscission rates (Fig. 3.6). Sucrose and raffinose amounts changed in opposite directions in shade and GAc treated inflorescences, and a down- and up-regulation of the raffinose family oligosaccharides (RFO) pathway was found in shade and GAc, respectively. Inositol and metabolites from the shikimate pathway (quinate and shikimate) were reduced in shade. Erythrulose and 1,3-dihydroxyacetone derived from glucose and glyceraldeyde-3-P in the glycolysis pathway were also reduced in this treatment. Concerning compounds associated with the TCA cycle, 2-ketogulonate, derived from oxaloacetate, was reduced in shaded samples and 2-aminobutyrate, derived from α-ketoglutarate (via glutamate), was reduced in response to GAc spraying. PA metabolism, likewise derived from glutamate, was reduced in result of the shade treatment. Compounds from benzenoids family increased in GAc treated inflorescences whereas oleanolate was decreased. Flavonoids (catechin and catechin gallate), phenylpropanoids (resveratrol and gallate), benzyl-O-glucose and loganin were reduced in response to shade.

3.3.4 Impacts on bunch and berry quality

Shade and GAc treatments reduced yield per plant, bunch weight and number of regular sized berries, in both cycles, when compared to untreated vines (Table 3.2). In the late production cycle, no differences in shot berries number were observed while in the early cycle, GAc promoted a higher number of these berries (407.1 shot berries), which was reflected in the increased number of total berries (512.6 berries per bunch) measured. Rachis length was shorter in bunches from vines submitted to shade and GAc, in the early production cycle. Nevertheless, bunch compactness was lower in plants that were shaded during flowering in both production cycles (5.1 and 10.5 berries cm^{-1}) and higher in GAc treated plants in the early production cycle (22.1 berries cm^{-1}) when compared with control. Rachis weight was lower in both production cycles in bunches from shaded vines, and was higher in GAc treated bunches in late cycle. Regarding berry quality parameters, the weight and transversal diameter of the berries were reduced in grapes from GAc treated and shaded vines in late cycle, when compared with controls. In the early cycle, no significant differences were observed in berry diameter but shade lead to increased berry weight. Berry SSC content was higher in shaded vines comparing to the

control in the late cycle, while differences in titratable acidity were not observed (Table 3.2). Both production cycle and the interaction production cycles × treatment significantly affected yield per plant, number of berries, number of shot berries, bunch compactness and berry diameter and berry weight (p-value<0.05). Production cycle also affected average bunch weight and titrable acidity (p-value<0.001).

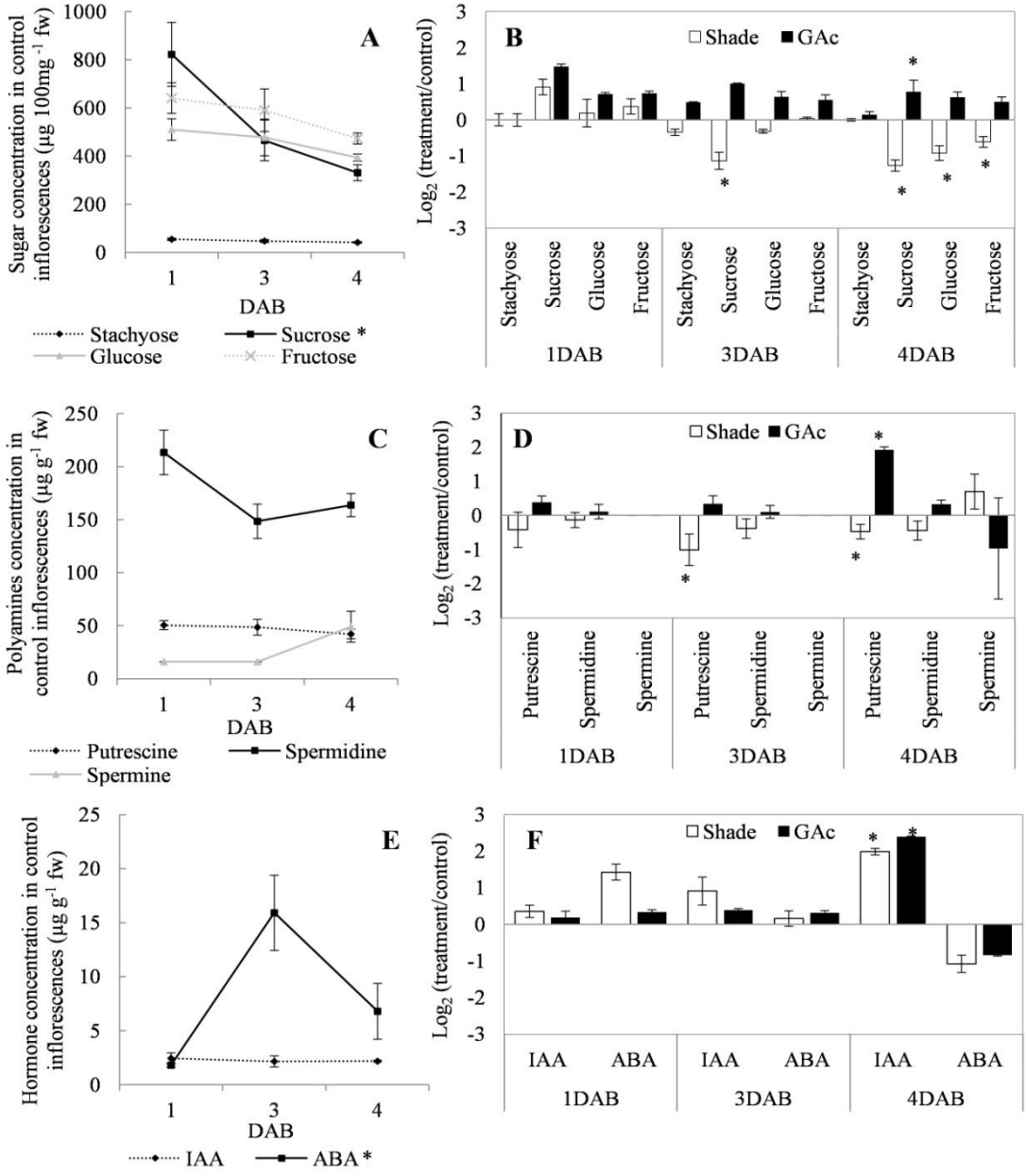

Figure 3.3. Fluctuation in sugar (A), polyamine (C) and hormone (E) concentrations in control and fold-change variations [Log_2 (treatment/control)] in sugar (B), polyamine (D) and hormone (F) concentrations in shade and GAc treated inflorescences at 1, 3 and 4 DAB. Statistical significances of different time points in metabolites concentration in control inflorescences, and of treatments comparing to control were assessed by one-way ANOVA (* mean significantly different at p-value<0.05).

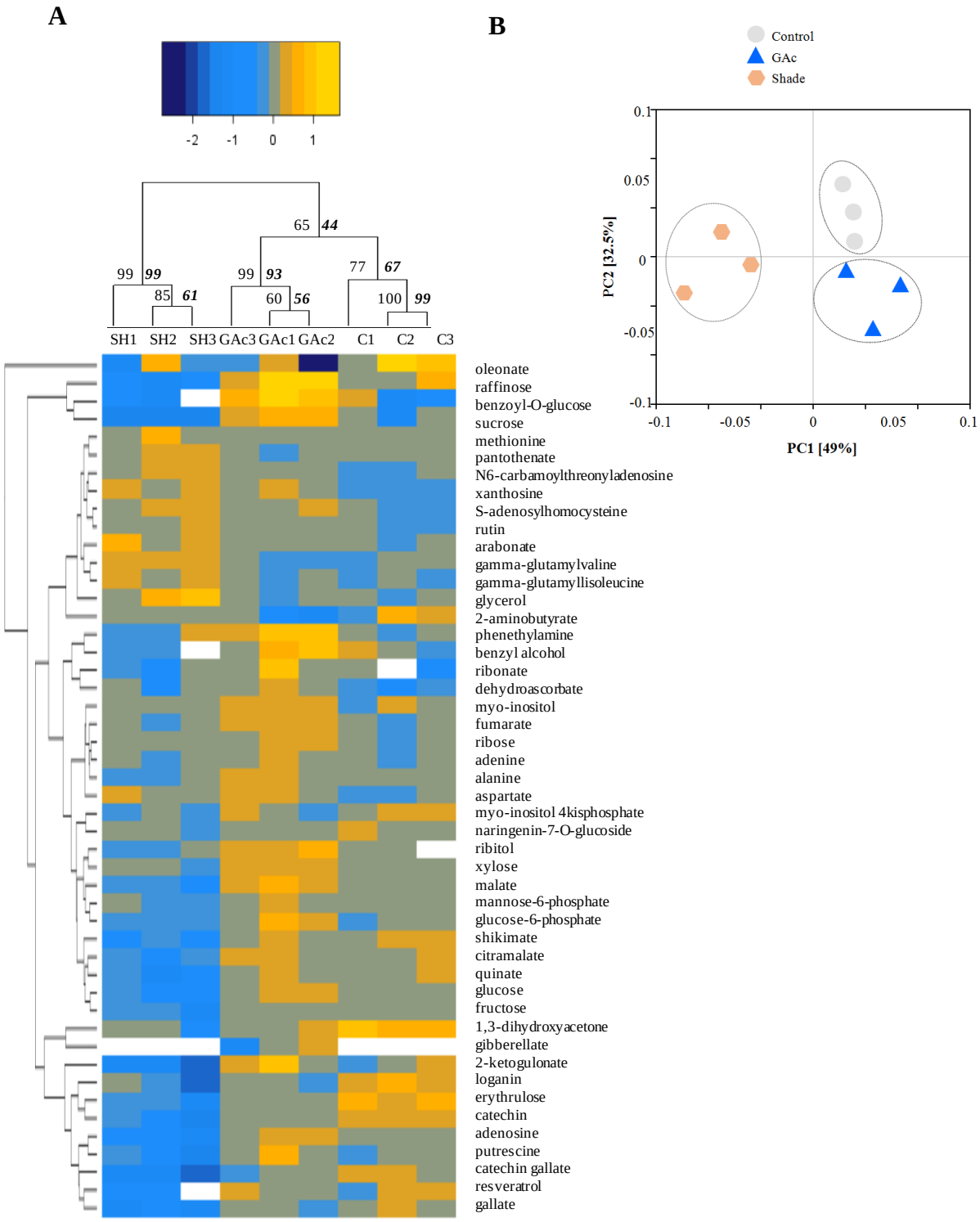

Figure 3.4. Hierarchical cluster (A) and principal coordinate analysis (B) of the significantly changed metabolites. A) Yellow and blue tones represent metabolites more and less abundant, respectively. The significance of dendrogram nodes was estimated by bootstrap analyses using 1000 permutations. Values in the left side of internal nodes are the approximately unbiased *p*-values (AU), bold and italic values on the right side represented the bootstrap probability value. B) PC1 and PC2 explain 81.5% of the total variation endorsed by the metabolite profile. Gray, blue and orange represent replicates from control, GAc and shade treatments, respectively.

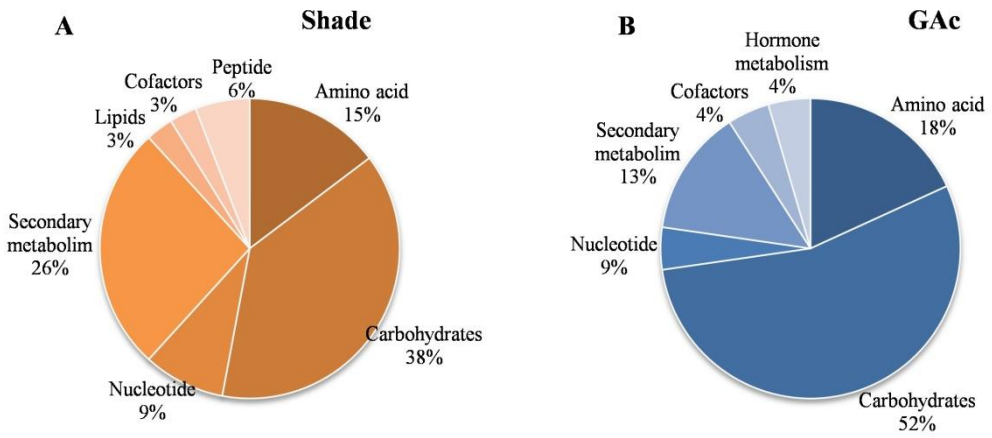

Figure 3.5. Functional categorization of the 48 metabolites that showed significantly changes (*p*-value< 0.05) in abundance. In shaded inflorescences (A), 34 metabolites from carbohydrate, secondary metabolism, amino acid, nucleotide, peptide, cofactors and lipids functional pathways were significantly affected. Meanwhile in GAc-treated inflorescences (B), 23 metabolites content from carbohydrate, amino acid, secondary metabolism, hormone, cofactors and nucleotide pathways changed. There were nine metabolites that changed in both treatments.

Table 3.3. List of metabolites significantly affected by GAc and shade treatments (*p*-value<0.05), functional categories, KEGG compound number and respective fold-change. Bold letters correspond to the highly significant different metabolites fold-change (|log 2 (treatment/control)|)≥1.

Super Pathway	Compound	KEGG	Log_2 (GAc/ Control)	Log_2 (Shade/ Control)
Amino acid	**2-aminobutyrate**	**C02261**	**-1.0**	
	phenethylamine	**C02455**	**1.6**	
	quinate	**C00296**		**-1.1**
	shikimate	**C00493**		**-1.2**
	putrescine	**C00134**		**-1.3**
	alanine	C00041	0.5	
	aspartate	C00049	0.6	
	methionine	C00073		0.7
	S-adenosylhomocysteine (SAH)	C00021		0.6
Carbohydrate	**2-ketogulonate**	**C02261**		**-1.8**
	ribonate		**1.3**	
	raffinose	**C00492**	**1.4**	**-1.6**
	glucose	C00031	0.3	-0.9
	glucose-6-phosphate (G6P)	C00668		-0.5
	fumarate	C00122	0.8	
	malate	C00149	0.7	-0.8
	arabonate	C00878		0.8
	ribitol	C00474	0.8	
	xylose	C00181	0.5	
	ribose	C00121	0.5	
	sucrose	**C00089**	**1.3**	**-1.7**
	erythrulose	**C02045**	**-**0.8	**-1.6**
	fructose	C00095		-0.8
	mannose-6-phosphate	C00275		-0.5
	citramalate	C00815		-0.8
	1,3-dihydroxyacetone	**C00184**		**-1.5**
	myo-inositol	C00137	0.5	
	myo-inositol 4kisphosphate (1,3,4,6/3,4,5,6/ 1,3,4,5)	**C01272**	-0.7	**-1.1**
Lipids	**glycerol**	**C00116**		**1.3**
Coenzyme	**dehydroascorbate**	**C05422**	**1.0**	
	pantothenate	C00864		0.7
Nucleotide	**adenosine**	**C00212**		**-1.3**
	adenine	C00147	0.5	
	N6-carbamoylthreonyladenosine		0.4	0.9
	xanthosine			0.8
Hormone	**gibberellate**	**C01699**	**3.3**	
Peptide	γ-glutamylisoleucine			0.7
	γ-glutamylvaline			0.7
Secondary metabolism	**oleanolate**		**-2.0**	
	benzyl alcohol	**C00556**	**1.1**	-0.8
	benzoyl-O-glucose		**2.0**	**-1.4**
	catechin	**C06562**		**-1.6**
	naringenin-7-O-glucoside			-0.5
	rutin	C05625		0.4
	catechin gallate			**-2.3**
	gallate	**C01424**		**-1.7**
	resveratrol	**C01424**		**-1.9**
	loganin	**C01433**		**-1.5**

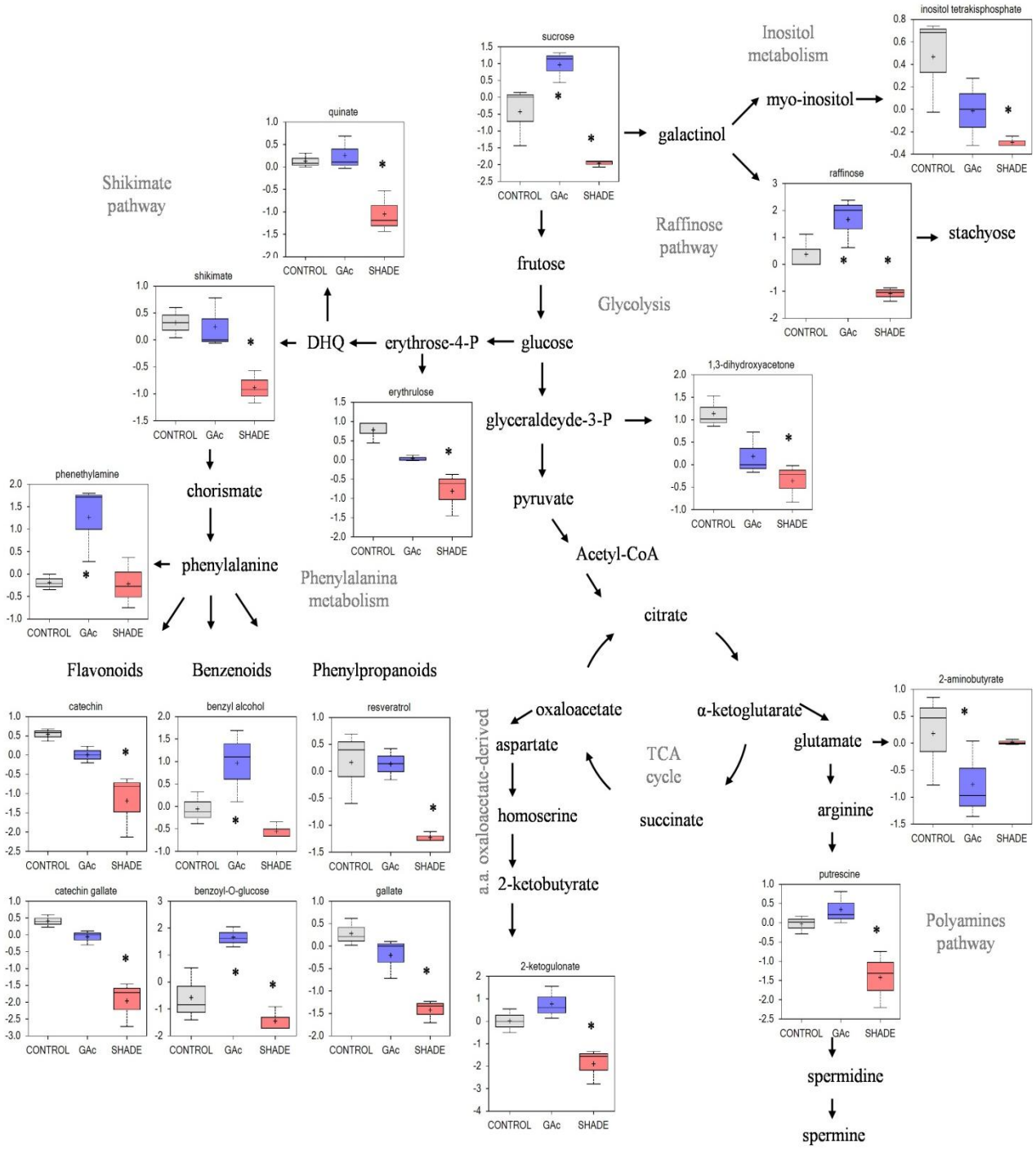

Figure 3.6. Changes in metabolic profile in table grape inflorescences treated with GAc and Shade. Metabolites with highly significant differences are represented in the box plots and asterisks identify which treatment is different from the control (p-value<0.05, fold-change (|log 2 (treatment/control)|)≥1). Data were log $_2$ transformed after scale imputation median=1. Grey, blue and orange represent samples from control, GAc and shade treatments, respectively.

3.4 Discussion

3.4.1 Flower abscission induced by hormonal and C-starvation stimuli

The direct comparison of the changes in *Vitis vinifera* L. inflorescences metabolite abundance that resulted from the imposition of two different abscission-triggering treatments was possible due to controlled conditions allowed from the experimental model used. Using potted plants growing under soilless greenhouse conditions, it was possible to apply both treatments to homogenous biological material. Moreover, this system allowed achieving improved plant growth and grape productivity, extending the harvest schedule and, relevant to the objectives of this work, obtaining more than one production cycle in the same agronomic year (Di Lorenzo et al., 2009).

The significant effect of climatic conditions on fruit set, revealed by the differences observed in natural flower drop rates between the two production cycles, can be explained by the influence exerted by the maximum temperatures registered during bloom in the late cycle that exceeded 35ºC in the majority of the days during the bloom period (Supplementary Figure S3.1). Under these range of temperatures, fruit set is known to decrease due to reduction of ovule fertility (Kliewer, 1977) and pollen germination rates (Vasconcelos et al., 2009).

The Black Magic table grape cultivar showed to be sensitive to shade imposed during bloom, resulting in increased flower drop percentages in both production cycles while the response to GAc application showed to be dependent of microclimate conditions. Under this treatment, fruit set was impaired in the late production cycle while an increase was observed in the early cycle, which agrees with previous results (Reynolds and Savigny, 2004; Reynolds et al., 2006) in three-year trials. The significant reduction of fruit set induced by the twelve-days period shading during bloom (Table 3.1) suggests that this approach can be exploited as an effective method for thinning in table grape production, relying on the pronounced decline of net photosynthetic rate, which promotes a decrease on carbon resources available to both vegetative and reproductive sinks and increases the competition between them (Corelli Grappadelli et al., 1990; Byers et al., 1991; Zibordi et al., 2009). The moment of shade imposition matched a stage during which the vine carbon reserves reached a minimum, which coincides with the onset of bloom in grapevines (Zapata et al., 2004). During this sensible period, interruptions or partial sugar supply declines are known to promote flower abortion (Lebon et al., 2008). In the present study, monitoring daily rate of berry drop during the shade imposition period enabled us to verify that the maximum rate of berries drop depends on the global environmental conditions, occurring between 2-4 DAB in late cycle and between 4-12 DAB in early cycle, indicating precocity in C-shortage in the former cycle. Shading did not affect leaf area nor shoot growth, confirming

previous observations that indicate that reproductive growth is more sensitive to environmental stress or limitation of resources than vegetative growth (Chiarello and Gulmon, 1991). The increased estimated leaf chlorophyll content in result from intercepted light reduction when compared with GAc treated vines, agrees with Ferree et al. (2001), and suggests an adaptability of the grapevine to low light intensity by increasing the PAR trapping efficiency (Cartechini and Palliotti, 1995).

The evidence that disturbances in growth regulators internal concentrations have an important influence on fruit set has been exploited in table grape production. In fact, GAc exogenous bloom application is commonly used as a mean to achieve cluster loosening (Dokoozlian and Peacock, 2001). Nonetheless, environment was demonstrated to play a major role in modulating the responses to growth regulator treatments, in particular the temperature. Low temperatures lead to sub-optimal response while, under high temperature conditions, the response may be excessive (Wertheim and Webster, 2005). Thus, we suggest that the observed differences on GAc effectiveness to induce flower abscission and increase shot berries number was related to the environmental conditions and physiological stage of the vines. During the late production cycle, vines are developing under more intense stress conditions, and had a smaller leaf area and shoot length than in the early cycle. Plants are expected to have lower carbohydrates and endogenous GA levels, resulting in a higher sensitivity to exogenously applied GAc and a reduction of fruit set comparing to control. Sensitivity to exogenously applied GAc was reported to be inversely related with endogenous gibberellins levels (Boll et al., 2009).

3.4.2 Sugar metabolism and other energy sources

Sucrose, glucose and fructose are the major phloem sap sugars which feed the developing vine inflorescences (Lebon et al., 2008). The reduction on the sucrose content in inflorescences developing under control conditions observed 4 DAB, at the onset of natural drop, agrees with previous observations (Glad et al., 1992) reporting that this sugar, predominant in this stage, represents 85% in sap flow at full bloom and declines thereafter to 60% at the end of fertilization, explaining natural drop. Our results were expected in confirming that decreased light intensity inhibits photosynthesis and sugar accumulation in inflorescences but showed that, in contrast, GAc treatment did not affect photosynthesis and even increased the inflorescence sugar content. Noticeably, both treatments resulted in similar rates of flower abscission (Table 3.1 and Fig. 3.3). Shade induced more pronounced effects than GAc spraying concerning the number of changed metabolites (Table 3.3). Essentially, all carbon metabolites identified showed to be present in lower amounts in shaded and in higher levels in GAc samples, including sucrose and glucose, as well as TCA intermediates (malate, citramalate and fumarate), and intermediates of the RFO pathway, such as raffinose (Table 3.3 and Fig. 3.6). The decline

of carbohydrate transport metabolism that occurred in shade agrees with abscission modulation induced by NAA and by shade in apple (Zhu et al., 2011). It was also verified that under shade, as in other stress conditions, the synthesis of glycerol may be favored via starch degradation, as an energy resource, and decrease of the carbon flow into TCA cycle (Xia et al., 2014). Regarding amino acid pathways, in shaded samples, the concentration of quinate, shikimate and putrescine decreased while methionine and SAH increased (Table 3.3 and Fig. 3.6). In addition, adenosine, which plays an important role in biochemical processes as energy transfer (adenosine triphosphate and diphosphate (ATP and ADP) and in signal transduction (cyclic adenosine monophosphate (cAMP)), also decreased. Shade conditions led to a signature of carbon/nitrogen (C/N) imbalance with lower energy and carbon metabolites, biosynthetic precursors such as shikimate and nitrogen-rich compounds associated with anabolic activity such as putrescine, and higher proteinogenic amino acid such as methionine that may result from protein turnover to free up amino acid carbon backbones for energy utilization. Likewise, the increased amount of pantheonate (vitamin B_5) whose biosynthetic pathway involves valine and alanine amino acids (Raman and Rathinasabapathi, 2004) observed in shade-derived inflorescences support the hypothesis of proteinogenic amino acids abundance from protein turnover. On the other hand, since all Calvin cycle metabolites were present in lower amounts in shaded samples, the pathway of pantheonate functioning as CoA biosynthesis precursor needs a more detailed evaluation. Our results are in accordance with Baena-González and Sheen (2008), which review physiological and molecular responses associated with plant energy deficit, including activation of catabolic pathways to provide alternative nutrient, metabolite and energy sources, and a decline in the activity of biosynthetic enzymes to preserve energy, and with Aziz (2003) showing that shading the vines at full bloom causes a decrease in both sugars and free polyamines and leads to a substantial increase of abscission.

Gibberellins are involved in pathways of regulation of flowering and fruit-set in grapes, as active GAs, mainly GA_1, peaks at anthesis and decrease thereafter (Perez et al., 2000; Giacomelli et al., 2013). GAc is commonly applied during bloom to reduce fruit set but the molecular mechanisms underlying this process are largely unknown. In *Arabidopsis thaliana*, GAc induces increased 3-P-glycerate and promotes plant growth rate (Meyer et al., 2007; Ribeiro et al., 2012). In this study, GAc application led to generalized up-regulation of both primary (carbohydrates, amino acid, coenzyme and nucleotide pathways) and secondary metabolisms (Table 3.3 and Fig. 3.6). Since no changes in photosynthetic rate (source) were detectable in samples submitted to this treatment, we hypothesize that an increase on inflorescences sink strength occurs after GAc treatments, resulting in the formation of king berries, with higher potential to compete for carbohydrates and other metabolites and higher growth rate, inhibiting the development and inducing abscission of later flowers. Regarding

TCA cycle-derived metabolites, only 2-aminobutyrate from glutamate family decreased as a result of GAc while, on the other hand, metabolites derived from aromatic amino acid phenylalanine and from aspartate family (alanine and aspartate) showed the opposite trend (Table 3.3 and Fig. 3.6). Glutamate derives from α-ketoglutarate and can be involved in the biosynthesis of 2-aminobutyrate or, alternatively, in the biosynthesis of arginine and polyamines biosynthesis. According to our results, it can be hypothesized that the pathway from glutamate to PAs is favored when vines are treated with GAc, in contrast with biosynthesis of 2-aminobutyrate.

3.4.3 Cell wall modifications

The recorded increase of CW monosaccharides in samples from both abscission-triggering treatments (Table 3.3) sounds with the known CW remodeling processes that occur during pedicel AZ formation as part of the coordinated series of modifications that ultimately lead to CW loosening, cell separation and differentiation of a protective layer on the proximal side after organ detachment (Lee et al., 2008). The increased arabonate concentration, which is a metabolite derived from arabinose, as consequence of the shade treatment contrasts with the observations in GAc treated inflorescences where xylose was the increased monosaccharide (Table 3.3). These differences are likely to reflect differences on target CW polymers, with pectins and xyloglucans more affected by shade or GAc, respectively. Pectin changes depends on the type of substitutions and branches in their backbone and are considered a central event (Fukuda et al., 2013) since the continuity between AZ cells is preserved by the middle lamellae, which is rich in this class of polymers, responsible for cell-cell adhesion. Pectins are additionally responsible for modulating the CW porosity, controlling the enzymes access to their substrates (Baron-Epel et al., 1988). Augmented arabinose levels may also indicate a higher substitution of pectic polysaccharides with arabinosyl residues which can work as plasticizers (Harholt et al., 2010) and be involved in the formation of the protective layer in the proximal area. In fact, during abscission, CWs of the proximal area are relatively richer in cellulose, arabinose-rich polymers and pectin, and poorer in xylan-rich polysaccharides and lignin when compared with AZ CWs (Lee et al., 2008). Regarding the detection of increased concentrations of xylose in samples from GAc-treated inflorescences, it may similarly reflect CW loosening processes needed for organ shed or CW strengthening requirements, but through action on cellulose-xyloglucan contact points. Xyloglucans are closely intertwined with cellulose at limited sites designed as “biomechanical hotspots”, promoting selective targets majorly modulating CW loosening (Park and Cosgrove, 2012). These assumptions are further supported by gene expression assays since it has been demonstrated that the activation of the abscission molecular machinery involves alterations of genes encoding CW remodeling

enzymes acting on structural polysaccharides leading to the middle lamellae breakdown, accompanied by distortion and dissolution of primary CWs along the abscission plane (Agusti et al., 2009; Lashbrook and Cai, 2008; Lee et al., 2008; Meir et al., 2010; Peng et al., 2013; Wang et al., 2013; Zhu et al., 2011) and glycosyl hydrolysis (Lashbrook and Cai, 2008; Singh et al., 2011, 2013). The pattern of differential temporal regulation of distinct classes of CW-related genes (Lashbrook and Cai, 2008) additionally suggests that the differences observed between treatments may be the result of triggering their action at different stages of the process. It should be noted that the samples here investigated include cells other than AZ. Hence, as CWs represent primarily communication between the plant and the environment, a role in adaptation to the imposed abiotic stress can be discussed. The observed difference in CW composition are known to be related to events such as localized cell division, arrestment of elongation and modifications in the differentiation status, to impact anatomy and development (Braidwood et al., 2013).

3.4.4 Markers of oxidative stress

Likewise, both abscission-triggering stimuli lead to oxidative stress related metabolism, but the results suggest that different pathways are tracked. Some of the significant increases observed are related to metabolites associated with oxygen stress remediation. Gamma-glutamyl amino acids, observed in shaded samples, are intermediates in the glutathione synthesis cycle (Table 3.3) and dehydroascorbate, observed in GAc treated samples, indicates responses to elevated oxidative stress conditions related to the ROS scavenging coupled ascorbate/dehydroascorbate cycle (Table 3.3). During abscission a continuous increase of ROS production is known to occur. ROS role in abscission encompasses multiple steps of signaling (Sakamoto et al., 2008) associated with ROS-sugar-hormone cross talk (Botton et al., 2011) and ROS-mediated oxidative damage/cleavage on CW components leading to cell separation (Cohen et al., 2014). Regulation of excessive ROS by the free radical scavenging systems comprises essential enzymatic components and non-enzymatic molecules such as ascorbate and glutathione. Glutathione and ascorbate play important roles individually or through the ascorbate glutathione cycle, having specific functions besides interchangeable antioxidants (Bohnert and Sheveleva, 1998). Our results suggest that distinct metabolite-dependent responses are triggered by each treatment agreeing with the independence and interdependence of glutathione and ascorbate in peroxide metabolism model proposed by Foyer and Noctor (2011).

3.4.5 Hormone regulation

The occurrence of an ABA peak 3 DAB in control inflorescences (Fig. 3.3E) preceding the rise of natural flower drop (4-12 DAB) (Fig. 3.2A) is in accordance with previous works describing

ABA as a component of the self-regulatory mechanism that adjusts fruit load to carbon supply occurring under natural conditions or following treatments (Gomez-Cadenas et al., 2000). On the other hand, ABA might promote cell expansion after pollination and fertilization in untreated inflorescences. According to what has been described for tomato, ABA possibly regulates processes related to organ formation and cell expansion during fruit set (Nitsch et al., 2012).

The increase of inflorescence IAA (auxin) concentration registered in both treatments (Fig. 3.3F) may suggest that IAA was accumulated on the proximal side of abscission and the auxin flux to the distal organ predict to abscise was interrupted. It has been showed that a constant auxin transport through the AZ is needed to prevent abscission (Taylor and Whitelaw, 2001) and a auxin depletion linked with acquisition of ethylene sensitivity within AZ cells is needed to its induction (Meir et al., 2010, Basu et al., 2013). Our results are also consistent with the auxin gradient theory (Addicott et al., 1955) based on the evidence that auxin application in the proximal end of AZ explants accelerates abscission whereas when applied at the distal end delays it, and suggesting that changes in auxin gradients may act in signaling the onset of senescence and abscission. Ethylene and auxins are critical factors that regulate the onset of abscission (Basu et al., 2013) in a mechanism where the auxin depletion inside AZs and an altered expression of auxin-regulated genes induce the acquisition of sensitivity to ethylene and AZ activation. The increase of methionine and SAH, which are intermediates in the ethylene biosyntheses, observed in shaded-treated samples (Table 3.3) can be associated with the increase of ethylene, acting as a trigger in the abscission process (Meir et al., 2010). SAM, derived from methionine, is also the precursor of the spermidine and spermine biosynthesis pathway or alternatively can be used on the synthesis of 1-aminocyclopropane-1-carboxylic acid (ACC) which is the immediate precursor of ethylene (Wang et al., 2002).

3.4.6 Secondary metabolism

In shade, decreased loganin content, which is a monoterpenoid intermediate in the production of indole alkaloids, and several phenylpropanoids, benzenoids and flavonoids was observed (Table 3.3 and Fig. 3.6), indicating suppression of biosynthesis of secondary metabolites and a slowdown of biochemical reactions in the AZ and neighboring tissues (Wang et al., 2013). This significant reduction can also mean an initial delay flower development and fruit set process under these conditions due to drastic reductions in carbon supply during this period, when compared to control samples. In this later situation, the accumulation of compounds characteristics of berry development, mainly in red and black varieties as 'Black Magic', is known to be already started (Braidot et al., 2008). The decreased catechin can be also the result of the condensation of such flavanols, as observed after ethylene exogenous application (Rizzuti

et al., 2015). Among the metabolites analyzed, flavonoid rutin was the exception in the general trade, showing a slightly increase in shade, probably due to its potential as strong radical scavenger and inhibitor of lipid peroxidation (Kumar and Pandey, 2013). On the other hand, GAc application led to a general advance in flower development in this stage and can have the opposite effect in ripening, depending on the cultivar (Tészlák et al., 2005). Comparing to the control, the aromatic compounds (benzenoids) showed increased accumulation in GAc treated samples (Table 3.3). Also in GAc, the decreased terpenoid oleonate levels measured suggests a reduction of steroids synthesis, which are membrane components that appears to control membrane fluidity and permeability and, in some plants, have a specific function in signal transduction (Piironen et al., 2000).

3.4.7 Final development of reproductive structures

The treatments imposed to produce biological samples enriched in abscission signals affected final yield and quality in both production cycles and some implications can be ascertain with relevance for table grape production (Table 3.2). The reduction of the number of berries in the late production cycle in shade and GAc treatments lead to reductions of bunch weight and yield per plant, indicating that the two approaches were efficient in inducing abscission. However, in the late cycle, both treatments affected berry weigh and diameter in a detrimental way, which can be the result of a decreased seed number and weight (Reynolds et al., 2006). In early cycle, shade resulted in a successful thinning method reducing total berries number and improving berry weight and diameter. The shade treatment affected bunch characteristics, reducing rachis length and weight and still reducing the number of berries per centimeter of rachis, in both cycles. The observed effect on the rachis can result from competition for photoassimilates favoring vegetative growth in detriment of the development of reproductive organs (Chiarello and Gulmon, 1991). In the early cycle, GAc treatment showed to be ineffective as thinning method due to the increased number of shot berries, total berries number and bunch compactness. The high number of shot berries observed as a negative effect of GAc application was also described by Dokoozlian and Peacock (2001). Recently, in a study performed by Abu-Zahra and Salameh (2012) aimed at evaluating the impact of GAc spray (50 ppm at the end of bloom, 18 and 40 days after end of bloom) on 'Black Magic' grape quality, an increase of berries number, berry size, SSC, titratable acidity and decreased colour intensity was observed. Although, according to Cartechini and Palliotti (1995), shade during flowering has no effect on final berries sugar content, under our conditions, the shade treatments increased SSC in the late production cycle, which can be a direct result of the reduction of berries weight and diameter.

3.4.8 A mechanistic view of flower abscission control in *Vitis vinifera* L.

The analysis performed in the late cycle, when both treatments were efficient in inducing abscission, showed that GAc responses comprised a relatively low numbers of significant changes, while the shade treatment conduced to more dramatic physiological and metabolomic alterations (Table 3.3). These results allowed us to propose a mechanistic model to explain differences and common links for flower abscission determination in response to two stimuli (Fig. 3.7). Comparing the composition in metabolites of grapevine inflorescences treated with the different abscission inducers (shade and GAc) and the control, we can conclude that abscission mechanisms triggered by hormonal application and via C-starvation are not based in the same metabolic changes. A new insight on the mode of action of GAc during bloom is here provided, showing that it is based on a generally stimulation of cell metabolism and gene expression revealed by ribose and its derived metabolites, sugar, amino acid and PA metabolisms in the whole inflorescence and a highly significant inhibition of a glutamate sub-pathway related with 2-aminobutirate (Table 3.3), which can be a key step in the GAc metabolism in inflorescences at bloom stage and may participate in a cross talk between IAA and gibberellate. As it as been described for other biological processes (Yamaguchi, 2008), bioactive gibberellins and auxins can positively regulate flower abscission triggered by GAc spraying. On other hand, shade induced abscission through energy deprivation mechanisms showed by the decline of photosynthesis, carbon metabolism and biosynthetic activity. The increased accumulation of ethylene precursors suggests that these events may participate together with ethylene production (Table 3.3). The common markers of abscission were increased IAA concentration in inflorescences, which can be a result of an auxin gradient change through the AZ, and increases in oxidative stress marker metabolites agreeing with previous studies in other species (Estornell et al., 2013). Despite the grapevine economic value and scientific relevance as a model species, this study provides the first mechanistic view of the metabolomic changes responsible for the flower abscission regulation in this species (Fig. 3.7), triggered by exogenous GAc application and reduction of the intercepted light, unraveling the complexity of its opposite effects and contributing to the advance in knowledge that will ultimately may lead to improved control of grapevine fruit set.

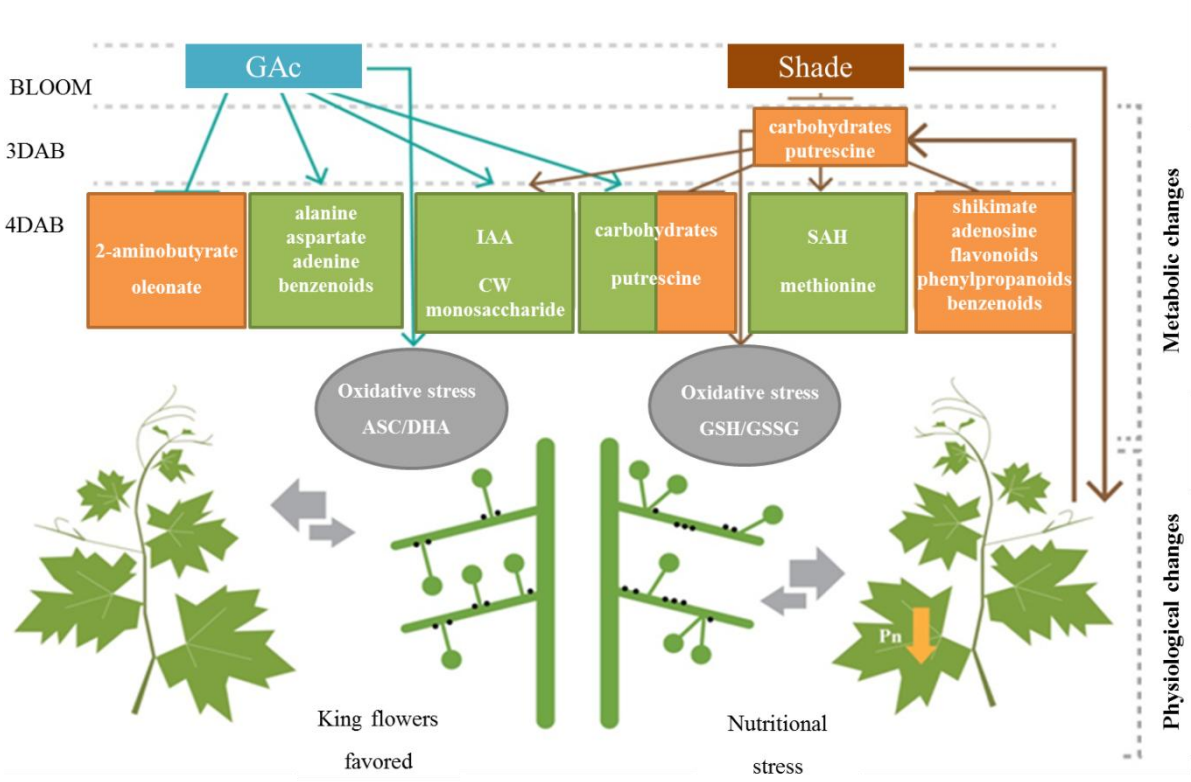

Figure 3.7. A proposed mechanistic model for flower abscission in *Vitis Vinifera* L. inflorescences triggered by GAc and shade. Shade treatment reduced net photosynthetic rate which lead to significant alterations 3 and 4 DAB, including global carbohydrates starvation, repressing on shikimate, putrescine and secondary metabolisms and increasing oxidative stress, revealed by glutathione remediation cycle. GAc induced an increase on carbohydrates, putrescine, amino acids and secondary metabolisms and oxidative stress, revealed by ascorbate/dehydroascorbate remediation couple at 4 DAB. Both treatments induced IAA and CW monosaccharide accumulation. The thickness of the arrows related to inter-organ competition is proportional to the sink strength at bloom stage. According to this model, flower abscission in shade is due to a general nutritional stress and, in GAc treatment to the induced metabolism of king flowers which inhibits the development of lateral flowers. Abscission layer in plant side is represented by black dots. Green and orange boxes indicate the increase and decrease on metabolite concentrations, respectively, as response of imposed treatments.

3.5 References

Abu-Zahra TR, and Salameh NM. 2012. Influence of gibberellic acid and cane girdling on berry size of black magic grape cultivar. *Middle East J. Sci. Res.* 11:718–722.

Addicott FT, Lynch RS, and Carns HR. 1955. Auxin gradient theory of abscission regulation. *Science.* 121: 644–645.

Agusti J, Merelo P, Cercos M, Tadeo F, and Talon M. 2009. Comparative transcriptional survey between laser-microdissected cells from laminar abscission zone and petiolar cortical tissue during ethylene-promoted abscission in citrus leaves. *BMC Plant Bio.* 9: 127.

Aziz A. 2003. Spermidine and related metabolic inhibitors modulate sugar and amino acid levels in *Vitis vinifera* L.: possible relationships with initial fruitlet abscission. *J. Exp. Bot.* 54: 355–363.

Baena-González E, and Sheen J. 2008. Convergent energy and stress signaling. *Trends Plant Sci.*13:474–482.

Baron-Epel O, Gharyal PK, and Schindler M. 1988. Pectins as mediators of wall porosity in soybean cells. *Planta*. 175: 389–95.

Basak A. 2011. Efficiency of fruitlet thinning in apple Gala must by use of metamitron and artificial shading. *J. Fruit Ornam. Plant Res.* 19: 51–62.

Basu MM, González-Carranza ZH, Azam-Ali S, Tang S, Shahid AA, and Roberts JA. 2013. The manipulation of auxin in the abscission zone cells of Arabidopsis flowers reveals that indoleacetic acid signaling is a prerequisite for organ shedding. *Plant Physiol.*162: 96–106.

Bohnert HJ, and Sheveleva E. 1998. Plant stress adaptations — making metabolism move. *Curr. Opin. Plant Biol.* 1: 267–274.

Boll S, Lang T, Hofmann H, and Schwappac P. 2009. Correspondence between gibberellin-sensitivity and pollen tube abundance in different seeded vine varieties. *Mitteilungen Klosterneub.* 59: 129–133.

Bonghi C, Tonutti P, and Ramina A. 2000. Biochemical and molecular aspects of fruitlet abscission. *Plant Growth Regul*. 31: 35–42.

Botton A, Eccher G, Forcato C, Ferrarini A, Begheldo M, Zermiani M, *et al*. 2011. Signaling pathways mediating the induction of apple fruitlet abscission. *Plant Physiol.* 155: 185–208.

Braidot E, Zancani M, Petrussa E, Peresson C, Bertolini A, Patui S, *et al*. 2008. Transport and accumulation of flavonoids in grapevine (*Vitis vinifera* L.). Plant signaling & behavior 3: 626–32.

Braidwood L, Breuer C, and Sugimoto K. 2013. My body is a cage: mechanisms and modulation of plant cell growth. *New Phytol*. 201: 388–402.

Byers R, Barden J, Polomski R, Young R, and Carbaugh D. 1990. Apple thinning byphotosynthetic inhibition. *J. Amer. Soc. Hort. Sci.*115: 14–19.

Byers R, Carbaugh DCP, and Wolf T. 1991. The influence of low light on apple fruit abscission. *J. Hort. Sci. Biotech*. 66: 7–18.

Byers R, Lyons J, and Yoder K. 1985. Peach and apple thining by shading andphotosynthetic inhibition. *J. Hort. Sci.*4: 465–472.

Cartechini A, and Palliotti A. 1995. Effect of shading on vine morphology and productivity and leaf gas exchange characteristics in grapevines in the field. *Am. J. Enol. Vitic.* 46: 227–234.

Chiarello NR, and Gulmon SL. 1991. Stress effects on plant reproduction. In Mooney HA, Winner WE, Pell AJ (Eds.). R*esponse of plants to multiple stresses*. New York: Academic Press. 161–188.

Cohen MF, Gurung S, Fukuto JM, and Yamasaki H. 2014.Controlled free radical attack in the apoplast: a hypothesis for roles of O, N and S species in regulatory and polysaccharide cleavage events during rapid abscission by Azolla. *Plant Sci*. 217-218, 120–126.

Corelli L, Sansavini S and Ravaglia GF. 1990. Effects of shade and sorbitol on fruit growth andabscission in apple. *Proc. XXIII Int. Congr.,* Florence. 620.

Davies C, Wolf T, Robinson SP. 1999. Three putative sucrose transporters are differentially expressed in grapevine tissues. *Plant Sci.* 147: 93–100.

Dal Cin V, Danesin M, Boschetti A, Dorigoni A, and Ramina A. 2005. Ethylene biosynthesis and perception in apple fruitlet abscission (*Malus domestica* L. Borck). *J. Exp. Bot.* 56: 2995–3005.

Dal Cin V, Velasco R, and Ramina A. 2009. Dominance induction of fruitlet shedding in *Malus* x *domestica* (L. Borkh): molecular changes associated with polar auxin transport. *BMC Plant Biol.* 9: 139.

Damesin C, and Lelarge C. 2003. Carbon isotope composition of current-year shoots from *Fagus sylvatica* in relation to growth, respiration and use of reserves. *Plant, Cell Environ.* 26: 207–219.

Davière J-M, and Achard P. 2013. Gibberellin signaling in plants. *Development*. 140: 1147–1151.

Di Lorenzo R, Gambino C, and Dimauro B. 2009. La coltivazione dell'uva da tavola in fuori suolo: stato attuale e prospettive. *Proc.XXXIst World Congr. Vine Wine,* Verona. 82: 33-44.

Di Lorenzo R, Scafidi P, and Gambino C. 2014. Soiless table grape production. *Proc. VII International Table Grape Symposium,* Mildura. 24–25.

Dokoozlian NK. 1998.Use of plant growth regulators in table grape production in California. *Proc.Univ. Calif. Table Grape Prod. Course,* Visalia. 200–210.

Dokoozlian NK, and Peacock .L. 2001. Gibberellic acid applied at bloom reduces fruit set and improves size of Crimson Seedless table grapes. *HortSci.* 36: 706–709.

Else MA, Stankiewicz-Davies AP, Crisp CM, and Atkinson CJ. 2004. The role of polar auxin transport through pedicels of *Prunus avium* L. in relation to fruit development and retention. *J. Exp. Bot.* 55: 2099–2109.

Estornell LH, Agustí J, Merelo P, Talón M, and Tadeo FR. 2013. Elucidating mechanisms underlying organ abscission. *Plant Sci.*199–200, 48–60.

Evans A, DeHaven C, and Barrett T. 2009. Integrated, nontargeted ultrahigh performance liquid chromatography/electrospray ionization tandem mass spectrometry platform for the identification and relative. *Anal. Chem.* 16: 6656–6667.

Ferree DC, McArtney SJ, and Scurlock DM. 2001. Influence of Irradiance and Period of Exposure on Fruit Set of French-American Hybrid Grapes. *J. Am. Soc. Hortic. Sci.*126: 283–290.

Foyer CH, and Noctor G. 2011. Ascorbate and glutathione: the heart of the redox hub. *Plant Physiol*. 155: 2–18.

Fukuda K, Yamada Y, Miyamoto K, Ueda J, and Uheda E. 2013. Separation of abscission zone cells in detached Azolla roots depends on apoplastic pH. *J. Plant Physiol.* 170: 18–24.

Giacomelli L, Rota-Stabelli O, Masuero D, Acheampong AK, Moretto M, Caputi L, *et al*. 2013. Gibberellin metabolism in *Vitis vinifera* L. during bloom and fruit-set: functional characterization and evolution of grapevine gibberellin oxidases. *J. Exp. Bot.* 64: 4403–4419.

Giulia E, Alessandro B, Mariano D, Andrea B, Benedetto R, and Angelo R. 2013. Early induction of apple fruitlet abscission is characterized by an increase of both isoprene emission and abscisic acid content. *Plant Physiol.*161: 1952–1969.

Glad C, Regnard J-L, Querou Y, Brun O, and Morot-Gaudry J-F. 1992. Phloem sap exudates as a criterion for sink strength appreciation in *Vitis vinifera* cv. Pinot noir grapevines. *Vitis.* 31: 131–1138.

Gomez-Cadenas A, Mehouachi J, Tadeo FR, Primo-Millo E, and Talon M. 2000. Hormonal regulation of fruitlet abscission induced by carbohydrate shortage in citrus. *Planta.* 210: 636–643.

Harholt J, Suttangkakul A, and Scheller HV.2010. Biosynthesis of pectin. *Plant physiol*. 153: 384–395.

Hed B, Ngug HK and Travis JW. 2011. Use of Gibberellic acid for management of bunch rot on Chardonnay and Vignoles grape. *Plant Dis.* 95: 269–278.

Hopping ME. 1976. Effect of bloom applications of gibberellic acid on yield and bunch rot of the wine grape 'Seibel 5455'. *NZJ. Exp. Agric.* 4: 103–107.

Kelen M, Demiralay EÇ, Şen S, and Alsancak GÖ. 2004. Separation of abscisic acid, indole-3-acetic acid, gibberellic acid in 99 R (*Vitis berlandieri* x *Vitis rupestris*) and Rose oil (*Rosa damascena* Mill.) by reversed phase liquid chromatography. *Turkish J. Chem.* 28: 603–610.

Kliewer WM. 1977. Effect of high temperatures during the bloom-set period on fruit-set, ovule fertility, and berry growth of several grape cultivars. *Am. J. Enol. Vitic.*28: 215–222.

Kumar S, and Pandey AK. 2013. Chemistry and biological activities of flavonoids: an overview. *ScientificWorldJournal.* 2013: 16.

Lashbrook CC, and Cai S. 2008. Cell wall remodeling in Arabidopsis stamen abscission zones: Temporal aspects of control inferred from transcriptional profiling. *Plant Signal Behav.* 3: 733–736.

Lebon G, Duchêne E, Brun O, Magné C, and Clément C. 2004. Flower abscission and inflorescence carbohydrates in sensitiveand non-sensitive cultivars of grapevine. *Sex Plant Reprod*. 17: 71–79.

Lebon G, Wojnarowiez G, Holzapfel B, Fontaine F, Vaillant-Gaveau N, and Clément C. 2008. Sugars and flowering in the grapevine (*Vitis vinifera* L.). *J. Exp. Bot.*59: 2565–2578.

Lee Y, Derbyshire P, Knox JP, and Hvoslef-Eide AK. 2008. Sequential cell wall transformations in response to the induction of a pedicel abscission event in *Euphorbia pulcherrima* (poinsettia). *Plant J*. 5: 993–1003.

Li C, Wang Y, Huang X, Li J, Wang H, and Li J. 2013. De novo assembly and characterization of fruit transcriptome in *Litchi chinensis Sonn* and analysis of differentially regulated genes in fruit in response to shading. *BMC Genomics.* 14: 552.

Li J and Yuan R. 2008. NAA and ethylene regulate expression of genes related to ethylene biosynthesis, perception, and cell wall degradation during fruit abscission and ripening in 'delicious' apples. *J. Plant Growth Regul.* 27: 283–295.

Looney NE, and Wood DF. 1977. Some cluster thinning and gibberellic acid effects on fruit set, berry size, vine growth and yiels of De Chaunac grapes. *Can. J. Plant Sci.* 57: 653–659.

Lorenz D, Eichhorn K, Bleiholder H, Klose R, Meier U, and Weber E. 1994. Phänologische entwicklungsstadien der rebe (*Vitis vinifera* L. ssp. vinifera) – codierung und beschreibung nach der erweiterten bbch-skala. *Vitic. Enol. Sci.* 49: 66–70.

Meir S, Philosoph-Hadas S, Sundaresan S, Selvaraj KSV, Burd S, Ophir R, *et al*. 2010. Microarray analysis of the abscission-related transcriptome in the tomato flower abscission zone in response to auxin depletion. *Plant Physiol.*154: 1929–1956.

Meyer RC, Steinfath M, Lisec J, Becher M, Witucka-Wall H, Törjék O, *et al*. 2007. The metabolic signature related to high plant growth rate in *Arabidopsis thaliana*. *Proc. Natl. Acad. Sci.* 104: 4759–4764.

Nitsch L, Kohlen W, Oplaat C, Charnikhova T, Cristescu S, Michieli P, Wolters-Arts M, *et al*. 2012. ABA-deficiency results in reduced plant and fruit size in tomato. *J. Plant Physiol.* 169: 878–83.

Ohta T, Masutomi N, Tsutsui N, Sakairi T, Mitchell M, Milburn, MV, *et al*. 2009. Untargeted metabolomic profiling as an evaluative tool of fenofibrate-induced toxicology in Fischer 344 male rats. *Toxicol. Pathol.* 37: 521–535.

Park YB, and Cosgrove DJ. 2012. A revised architecture of primary cell walls based on biomechanical changes induced by substrate-specific endoglucanases. *Plant Physiol*.158: 1933–1943.

Peng G, Wu J, Lu W, and Li J. 2013. A polygalacturonase gene clustered into clade E involved in lychee fruitlet abscission. *Sci. Hortic.* 150: 244–250.

Perez FJ, Viani C, and Retamales J. 2000. Bioactive gibberellins in seeded and seedless grapes: identification and changes in content during berry development. *Am. J. Enol. Vitic.* 51: 315–318.

Piironen V, Lindsay DG, Miettinen TA, Toivo J, and Lampi A-M. 2000. Plant sterols: biosynthesis, biological function and their importance to human nutrition. *J. Sci. Food Agric.* 80: 939–966.

Raman SB, and Rathinasabapathi B. 2004. Pantothenate synthesis in plants. *Plant Sci.* 167: 961–968.

Reynolds AG, Roller JN, Forgione A, and De Savigny C. 2006. Gibberellic acid and basal leaf removal: implications for fruit maturity, vestigial seed development, and sensory attributes of sovereign coronation table grapes. *Am. J. Enol. Vitic.* 57: 41–53.

Reynolds AG, and Savigny C. 2004. Influence of girdling and gibberellic acid on yield components, fruit composition and vestigial seed formation of 'Sovereign Coronation' table grapes. *HortScience.* 39: 541–544.

Ribeiro DM, Araújo WL, Fernie AR, Schippers JHM, and Mueller-Roeber B. 2012. Translatome and metabolome effects triggered by gibberellins during rosette growth in Arabidopsis. *J. Exp. Bot.* 63: 2769–2786.

Rizzuti A, Aguilera-Sáez LM, Gallo V, Cafagna I, Mastrorilli P, Latronico M, *et al*. 2015. On the use of ethephon as abscising agent in cv. crimson seedless table grape production: combination of fruit detachment force, fruit drop and metabolomics. *Food Chem*. 171: 341-350.

Rohlf FJ. 2005. *NTSYS-pc: numerical taxonomy and multivariate analysis system*. Exeter Software, Setauket, New York, USA.

Roubelakis KA, and Kliewer WM. 1976. Influence of light intensity and growth regulators on fruit-set and ovule fertilization in grape cultivars under low temperature conditions. *Am. J. Enol. Vitic.* 27: 163–167.

Sakamoto M, Munemura I, Tomita R, and Kobayashi K. 2008. Reactive oxygen species in leaf abscission signaling. *Plant Signal Behav*. 3: 1014–1015.

Schneider G. 1975. C-sucrose translocation in apple. *J. Amer. Soc. Hort. Sci.* 103: 455–458

Singh AP, Tripathi SK, Nath P, and Sane AP. 2011. Petal abscission in rose is associated with the differential expression of two ethylene-responsive xyloglucan endotransglucosylase/hydrolase genes, RbXTH1 and RbXTH2. *J Exp. Bot.* 62: 5091–5103.

Singh AP, Dubey S, Lakhwani D, Pandey SP, Khan K, Dwivedi UN *et al*. 2013. Differential expression of several xyloglucan endotransglucosylase/hydrolase genes regulates flower opening and petal abscission in roses. *AoB Plants*. 5: plt030.

Smith, MA, and Davies, PJ. 1987. Monitoring polyamines in plant tissues by high performance liquid chromatography. In Linskens HF and Jackson JF (Eds.). *High Perform. Liq. Chromatogr. Plant Sci. (Modern Methods Plant Anal. New Ser. Vol 5)*. New York. 209–227.

Storey J, and Tibshirani R. 2003. Statistical significance for genomewide studies. *Proc. Natl. Acad. Sci.*100: 9440–9445.

Suzuki R, and Shimodaira H. 2006. Pvclust: an R package for assessing the uncertainty in hierarchical clustering. *Bioinformatics.* 22: 1540–1542.

Taylor JE, and Whitelaw CA. 2001. Signals in abscission. *New Phytol.* 151: 323–340.

Teszlák P, Gaál K, and Nikfardjam PMS. 2005. Influence of grapevine flower treatment with gibberllic acid (GA_3) on polyphenol content of *Vitis vinifera* L. wine. *Anal. Chim.Acta. 543*. 275-281.

Vasconcelos MC, Greven M, Winefield CS, Trought MCT, and Raw V. 2009. The flowering process of *Vitis vinifera*: a review. *Amer. J.Enol.Vitic.* 60: 411–434.

Wang KL-C, Li H, and Ecker JR. 2002. Ethylene biosynthesis and signaling networks. *Plant Cell.* 14: 131–151.

Wang X, Liu D, Li A, Sun X, Zhang R, Wu L, *et al*. 2013. Transcriptome analysis of tomato flower pedicel tissues reveals abscission zone-specific modulation of key meristem activity genes. *PLoS One* 8: e55238.

Weaver RJ, McCune SB, and Hale CR. 1962. Effect of plant regulators on set and berry development in certain seedless varieties of *Vitis vinifera* L. *Vitis.* 3: 84–96.

Wertheim SJ and Webster AB. 2005. Manipulation of growth and development by plant bioregulators. In Tromp J, Webster AD, and Wertheim SJ (Eds.). *Fundamentals of temperate zone tree fruit production.* Universidade de Cornell:Backhuys. 267-294.

Whitelaw CA, Lyssenko NN, Chen L, Zhou D, Mattoo AK, and Tucker ML. 2002. Delayed abscission and shorter internodes correlate with a reduction in the ethylene receptor LeETR1 transcript in transgenic tomato. *Plant Physiol.* 128: 978–987.

Widmer A, Kockerols K, Schwan S, Stadler W, and Bertschinger L. 2008. Towards grower-friendly apple crop thinning by tree shading. *Proc. Int. Conf. Cultiv. Tech. Phytopatho. Probl. Org. Fruit-Growing* .Weinsberg. 314–318.

Xia B-B, Wang S-H, Duan J-B, and Bai L-H. 2014. The relationship of glycerol and glycolysis metabolism patway under hyperosmotic stress in *Dunaliella salina*. *Cent. Eur. J. Biol*. 9: 901–908.

Yamaguchi S. 2008. Gibberellin metabolism and its regulation. *Annu. Rev. Plant Bio*. 59: 225–225.

Zapata C., Deléens E., Chaillou S., and Magné C. 2004. Partitioning and mobilization of starch and N reserves in grapevine (*Vitis vinifera* L.). *J. Plant Physiol.* 161: 1031–1040.

Zhou C, Lasko AN, Robinson TL, and Gan S. 2008. Isolation and characterization of genes associated with shade-induced apple abscission. *Mol. Genet. Genomics.* 280: 83–92.

Zhu H, Dardick C, Beers E, Callanhan A, Xia R, and Yuan R. 2011. Transcriptomics of shading-induced and NAA-induced abscission in apple (*Malus domestica*) reveals a shared pathway involving reduced photosynthesis, alterations in carbohydrate transport and signaling and hormone crosstalk. *BMC Plant Biol.* 11: 138.

Zibordi M., Domingos S. and Corelli Grappadelli L. 2009. Thinning apples via shading: an appraisal under field conditions. *J. Hort. Sci. Biotech.*84: 138–144.

Chapter 4

Shared and divergent pathways for flower abscission are triggered by gibberellic acid and carbon starvation in seedless *Vitis vinifera* L.

The data presented in this chapter is in preparation to be submitted to BMC Plant Biology:

Domingos S[1,2], Fino J[2,3], Cardoso V[2], Sánchez C[4], Ramalho JC[2], Larcher R[5], Paulo OS[3], Oliveira CM[1], Goulao LF[2]

[1] Linking Landscape, Environment, Agriculture and Food, Instituto Superior de Agronomia, Universidade de Lisboa, Lisbon, Portugal.

[2] Instituto de Investigação Científica Tropical, I.P., Lisbon, Portugal.

[3] Computational Biology and Population Genomics Group, Centre for Ecology, Evolution and Environmental Changes, Faculdade de Ciências, Universidade de Lisboa, Lisbon, Portugal.

[4] Instituto Nacional de Investigação Agrária e Veterinária, I.P., Oeiras, Portugal

[5] FEM-IASMA, Fondazione Edmund Mach, Istituto Agrario di San Michele all'Adige, San Michele all'Adige, Italy.

.

4. Shared and divergent pathways for flower abscission are triggered by gibberellic acid and carbon starvation in seedless *Vitis vinifera* L.

Abstract

Abscission is a highly coordinated developmental process by which plants control vegetative and reproductive organs load. Aiming at get new insights on flower abscission regulation, changes in the global transcriptome, metabolome and physiology were analyzed in 'Thompson Seedless' grapevine (*Vitis vinifera* L.) inflorescences, using gibberellic acid (GAc) spraying and shading as abscission stimuli, applied at bloom. Natural flower drop rates increased from 63.1% in non-treated vines to 83% and 99% in response to GAc and shade treatments, respectively. Both treatments had a broad effect on inflorescences metabolism. Specific impacts from shade included photosynthesis inhibition, associated nutritional stress, carbon/nitrogen imbalance and cell division repression, whereas GAc spraying induced energetic metabolism simultaneously with induction of nucleotide biosynthesis and carbon metabolism, therefore, disclosing alternative mechanisms to regulate abscission. Regarding secondary metabolism, changes in flavonoid metabolism related pathways were mostly represented in the GAc while phenylpropanoid and stilbenoid biosynthetic pathways were predominantly affected in the inflorescences by the shade treatment. However, both GAc and shade treated inflorescences revealed also shared pathways, that involved the regulation of putrescine catabolism, the repression of gibberellin biosynthesis, the induction of auxin biosynthesis and the activation of ethylene signaling pathways and antioxidant mechanisms, although often the quantitative changes occurred on specific transcripts and metabolites of the pathways. Globally, the results suggest that chemical and environmental cues induced contrasting effects on inflorescence metabolism, triggering flower abscission by different mechanisms and pinpointing the participation of novel abscission regulators. Stenospermocarpic grapevine showed to be considered a valid model to study molecular pathways of flower abscission competence acquisition, noticeably responding to independent stimuli.

Key-words: flower shedding, gibberellin, grapevine, light reduction, metabolomics, RNA-Seq

4.1 Introduction

Abscission is the developmental mechanism by which plants are able to shed damaged and excessively formed organs, regulating the metabolic energy required to successfully attain the

formation of vegetative and reproductive structures (Bonghi et al., 2000). Abscission encompasses a complex but precise regulation of cell separation that occurs in a specific layer of specialized cells known as abscission zone (AZ) and is simultaneously activated by and responsive to endogenous signals and to exogenous stimuli, such as environmental abiotic and biotic interactions or exposure to chemical molecules (Sawicki et al., 2015; Taylor and Whitelaw, 2001). Once the AZ is properly differentiated, AZ cells acquire competence to respond to triggering-abscission signals in a hormone-mediated way, by modulating the expression of genes involved, among others, in cell wall (CW) remodeling and protein metabolism, and a high number of transcription factors (Estornell et al., 2013). After this activation phase, cell separation and differentiation of a protective layer on the proximal side after organ detachment advance as last steps of the abscission pathway (Patterson, 2001). Increased ethylene biosynthesis is associated with the final events of abscission activation, namely by promoting CW disassembly-related genes transcription (Dal Cin et al., 2005; Singh et al., 2011). Abscisic acid (ABA) is involved by acting as modulator of 1-aminocyclopropane-1-carboxylic acid (ACC) levels, and therefore of ethylene biosynthesis (Gomez-Cadenas et al., 2000). According to the currently accepted model, the endogenous flow level of inhibitory auxin in an organ destined to abscise must drop to acquire sensitivity to ethylene (Else et al., 2004; Meir et al., 2010).

In reproductive organs, abscission is related to lower carbohydrate and polyamine (PA) availability to developing flowers and fruits (Aziz, 2003; Gomez-Jimenez et al., 2010; Lebon et al., 2008; Zhu et al., 2011). Together with its role as energy source, glucose acts as a repressing signal of programmed cell death (PCD) (Ruan et al., 2012). A glucose gradient in the AZ was recently reported, suggesting a mechanism similar to the auxin flux that regulates ethylene signaling (Sawicki et al., 2015).

In addition, the inflorescence deficient in abscission (IDA) peptide signals and interacting receptor-like-kinases, HAESA and HAESA-like2, where showed to activate mitogen-activated protein kinase (MAPK) cascades leading to the abscission of floral organs in *Arabidopsis thaliana* L. (Cho et al., 2008; Niederhuth et al., 2013), in a signaling system that was proposed to be conserved and was hypothesized to regulate cell separation also in other plant species (Tucker and Yang, 2012). Increased levels of reactive oxygen species (ROS) resulting from unbalances caused by abscission-inducers have a pivotal role in organ abscission control, encompassing multiple steps of signaling, downstream from ethylene, and associated with ROS-sugar-hormone cross talk (Botton et al., 2011; Domingos et al., 2015; Giulia et al., 2013; Sakamoto et al., 2008).

Strategies that stimulate enhanced natural flower and fruit abscission are widespread horticultural practices, collectively known as thinning. In seedless table grape (*Vitis vinifera* L.) production, reduction of the number of berries per bunch is mandatory to guarantee acceptable bunch appearance and improved quality, and decreased fungal diseases incidence (Dokoozlian and Peacock, 2001). In grapevines, the natural separation process takes place at AZs formed at the base of each floral pedicel and begins at flowering, progressing for two weeks (Bessis et al., 2000).

Flower abscission rates are known to be enhanced by chemical thinner applications. Gibberellic acid (GAc) spraying during bloom, often followed by hand adjustments, is the most common method for thinning in grapevine (Dokoozlian and Peacock, 2001; Hed et al., 2011; Looney and Wood, 1977; Reynolds and Savigny, 2004; Reynolds et al., 2006), although the mechanisms by which GAc induces abscission remains largely unknown. Gibberellin (GA) perception and signaling investigated in model plants (Sun, 2010) disclosed early recognition *via* the GA INSENSITIVE DWARF1 (GID1) receptor and interaction between GA-GID complex and DELLA transcription factor responsible for GA signaling repression. Binding of GA-GID1 to DELLA induces recognition of DELLA for ubiquitination by a specific F-box protein (GID2) that results in a rapid degradation of DELLAs *via* the ubiquitin-proteasome pathway. More recently, GA-induced changes in the transcriptome of pre-bloom inflorescences and of berry enlargement stages in grapevine, inducing seed abortion and increased berry size, respectively, were investigated (Chai et al., 2014; Cheng et al., 2015). The overall observations suggest that GAc application to grape flowers and berries has a fairly comprehensive impact on their metabolism mediated by hormone biosynthesis and signaling, suggesting a negative feedback regulation of bioactive GAs (Chai et al., 2014; Cheng et al., 2015).

Flower abscission can also be boosted by shading conditions (70-90% light interception) during bloom (Domingos et al., 2015; Ferree et al., 2001; Roubelakis and Kliewer, 1976), paving the way to explore light management as an alternative thinning method. The pronounced reduction of net photosynthetic rates under shading promotes the competition for photoassimilates between vegetative and reproductive organs, leading to shedding of the later, which have less sink strength at this early stage of development (Vasconcelos et al., 2009). Shade-induced changes in the transcriptome of apple (*Malus* × *domestica*) revealed that photosynthesis repression and associated nutrient stress is perceived at the fruit level, its growth is inhibited by a sugar transport blockage, which results in lower sink strength, decreased auxin transport to the AZ and concomitant increased sensitivity to ethylene, leading to fruit abscission (Zhu et al., 2011).

Therefore, abscission is a challenging biological question that can be induced by at least two distinct stimuli, with distinct physiological and molecular basis. Recently, using an experimental assay with potted seeded vines managed under a greenhouse hydroponic controlled production system, and thinned with GAc spraying or *via* shade nets to reduce intercepted light, we established an efficient method to produce sample sets with predictable abscising potential triggered by different (chemical and environmental) cues, which allowed us to disclose the participation of different metabolic pathways according to the imposed treatment in flower abscission regulation (Domingos et al., 2015). We now report the investigation of the effect of the same abscission-inducers using a different genetic background under field conditions. The rationale was that, by using a seedless variety, deprived of the main endogenous source of bioactive GAs (Perez et al., 2000), developed while adapting to field multiple stresses, the major signals for abscission triggering would be perceived, providing new insights on this subject. Hence, comprehensive cutting-edge metabolomics and RNA-Seq transcriptomics combined with physiological measurements, were performed to allow discussing how environmental (C-shortage) and GAc application act to trigger flower abscission. This will prompt the identification of the routes linking the aptitude of an organ to become competent for cell separation and the culmination on abscission, further identifying specificities and communication between different pathways leading to organ drop. In addition, the present study provides the first sequential transcriptomic atlas of GAc-induced flower abscission.

4.2 Material and Methods

4.2.1 Experimental conditions and sample collection

The trail was conducted in a commercial table grape vineyard in south of Portugal (38° 05' 23.80" N; 8° 04' 52.7 1" W), using seven-year-old 'Thompson Seedless' (*Vitis vinifera* L.) vines grafted on '140 Ruggeri' rootstock, spaced 3x3 m, grown under an overhead trellis system covered with plastic, and managed following standard fertilization, irrigation, and pest-management practices.

The imposed treatments were: thinning *via* reduction of intercepted light and chemical thinning with GAc, in five vines per treatment. An additional group of five vines remained untreated to be used as control. Shade was imposed at 50% cap fall (stage 65 of the BBCH scale (Lorenz et al., 1994)) by covering the vines with polypropylene shading nets (Hubel, Portugal) that intercept 100% of the incident photosynthetic active radiation (PAR), for a period of fourteen days. Chemical treatment consisted in spraying a GAc solution (Berelex with 9% of gibberellic acid, Kenogard) of 10 ppm, 12.5 ppm and 12.5 ppm, which was applied at 20%, 50% and 100%

cap fall (stages 62, 65 and 69 of the BBCH scale), respectively. Climate conditions during the assay were monitored above the canopy of shaded and control vines (WatchDog MicroStation, Spectrum Tech., USA) (Supplementary Figure S4.1).

Grape inflorescence samples were collected in a time-course assay, at three time-points: 5, 7 and 10 days after 100% cap fall (referred to as 5d, 7d and 10d) (Fig. 4.1). In each point, three independent biological replicates were collected per treatment. Each biological replicate was composed by one inflorescence, deprived from rachis, and immediately frozen in liquid nitrogen. Samples were subsequently fine-powdered and stored at -80ºC until use.

4.2.2 RNA deep sequencing

Total RNA was extracted and purified from *ca.* 100 mg frozen inflorescences from each 5d and 7d biological sample, using the RNeasy Plant RNA Extraction Kit and RNase-Free DNase Set (Qiagen, Hilden, Germany) following the manufacturer's instructions, but replacing the extraction solution for a 100 mM Tris-HCl, 2% (w/v) CTAB, 25 mM EDTA and 2 M NaCl buffer (Chang et al., 1993). When traces of contaminant genomic DNA were detected after standard PCR amplification of the *ACTIN* 1 (*ACT1*) gene (GenBank Accession: XM_002282480.3), samples were further digested with RNase-free DNase I (Ambion, Life Techonologies, CA, USA). RNA integrity and purity were evaluated by visual inspection of ribosomal bands in 1.5% agarose gel electrophoresis and by 2100 Bioanalyzer (Agilent Technologies, CA, USA) readings. Poly(A) mRNA isolation, cDNA synthesis, library generation, indexing, cluster generation and RNA-Seq analyses by Illumina HiSeq 2000 RNA sequencing of 100 bp paired-end reads was carried out by LGC Genomics (Berlin, Germany), using commercial services.

4.2.3 Computational biology analyses

The raw Illumina 100-bp pair-end sequences were deposited in the NCBI Sequence Read Archive (SRA) under accession numbers SRX964421, SRX964430, SRX966723, SRX966735, SRX966740, SRX966742, SRX966755, SRX1008101, SRX1008174, SRX1008177, SRX1008181, SRX1008185, SRX1008211, SRX1008213, SRX1008214, SRX1008217, SRX1010114 and SRX1010115.

The reads were quality trimmed using Trimmomatic version 0.32 (Bolger et al., 2014), and surveyed for the presence of rRNA contamination using homology searches against rRNA databases (Quast et al., 2013). The reads were then aligned against the *Vitis vinifera* reference genome (Jaillon et al., 2007) with the software Tophat2 version 2.0.12 (Kim et al., 2013) set with the parameters -D 15 -R 2 -L 22 -i S,1,1.15 and end-to-end mode. Quantification and normalization of gene expression values by Fragments Per Kilobase Of Exon Per Million

Fragments Mapped (FPKM) was calculated by Cufflinks version 2.2.1 (Trapnell et al., 2010). Differential expression calculations were handled by DESeq2 version 1.4.5 (Love et al., 2014) considering estimation of size factors, a false discovery rate (FDR) of 0.05 and a -1.5≥ log2 fold-change ≥1.5, using the raw read counts.

EuKaryotic Orthologous Groups (KOG) (Tatusov et al., 2003), Gene Ontology (GO) and Kyoto Encyclopedia of Genes and Genomes (KEGG) (Kanehisa et al., 2007) functional annotations were based on sequence homologies against public databases. Rapsearch2 (Zhao et al., 2012) with an e-value cut-off of 10^{-5} was used to search against Arabidopsis thaliana sequences in the KOG database and non-redundant ("nr") peptide database (ftp://ftp.ncbi.nlm.nih.gov/blast/db/ downloaded at November 26, 2013, including all "nr" GenBank CDS translations + PDB + SwissProt + PIR+PRF). To GO and KEGG annotations, the output was submitted to an in-house developed script - Rapsearch2XML (https://github.com/Nymeria8/Rapsearch2Xml) and then to Blast2GO (Conesa et al., 2005). GO enriched categories were identified using the R bioconductor package topGO version 2.18.0 (Alexa and Rahnenfuhrer, 2010), using a Fisher's exact test and a *p*-value cut-off of 0.01.

4.2.4 Data validation by gene expression quantification and correlation between replicates analyses

Aliquots (150 ng) of the same RNA samples extracted as per 2.1 were used for first-strand cDNA synthesis by M-MLV Reverse Transcriptase (Invitrogen), according to the manufacturer's instructions. The expression of eight genes with significant differences on RNA-seq analysis, involved in auxin and ethylene signaling pathways (Basu et al., 2013; Dal Cin et al., 2005) and mitogen-activared protein kinase cascades (Cho et al., 2008), and putatively related to flower abscission regulation, was assessed by quantitative real-time PCR (q-rtPCR). Their specific primer sequences and properties are given in Supplementary Figure S4.3. Q-rtPCR amplifications were conducted in a qTOWER 2.0 (Analytikjena, Germany) thermal cycler in 15 µL reactions containing 1× SsoAdvanced™ SYBR®Green Supermix (Bio-Rad, United States of America), 0.3 µM each primer and 90 ng cDNA.

The amplification cycling profile was: 95°C during 30 s; then 40 cycles at 95°C for 5 s and 60°C for 30 s. Melting curves were generated to confirm amplification of single products and absence of primer dimerization. For each primer pair, PCR amplification efficiencies were calculated *via* a calibration dilution curve and slope calculation, using the equation $E(\%)=(10^{[-1/slope]})\times100$ (Rasmussen, 2001). Data normalization was conducted based on quantification threshold cycle (Ct) values with respect to the geometric average of the Ct of 3 reference genes (Vandesompele et al., 2002), polyubiquitin (XM_002282083.2), actin (XM_002282480.3) and glyceraldehyde-3-phosphate dehydrogenase (XM_002263109.2), as

suggested to have invariable expression by Faccoli et al. (2010) and Coito et al. (2012). Each analysis was performed in duplicate technical reactions, in each of the three biologic replicates per treatment and condition. To obtain measurements of the correlation between RNA-seq and q-rtPCR data, linear regression and determination coefficient (R^2) were determined between the two methods obtained $\log_2$ fold-changes for the same eight genes.

To further investigate the robustness of our RNA-seq dataset, similarity of expression profiles between the three biological replicates was determined by Pearson correlation coefficient (PCC) analyses with R software using natural logarithm (ln)-transformed read counts for the differentially expressed genes (DEG) as input.

4.2.5 Global and targeted metabolomic profiling

Circa 200 mg of powdered material from each of the three biological replicates collected at 5 and 7 days after 100% cap fall, in each treatment were lyophilized, extracted with methanol and analyzed using the integrated platform developed by Metabolon® (Durham, USA) consisting of a combination of three independent approaches: (1) ultrahigh performance liquid chromatography/tandem mass spectrometry (UHLC/MS/MS2) optimized for basic species, (2) UHLC/MS/MS2 optimized for acidic species, and (3) gas chromatography/mass spectrometry (GC/MS). Methods were performed as previously described (Evans et al., 2009, 2012; Ohta et al., 2009).

Hormone (indole-3-acetic acid (IAA), abscisic acid (ABA), GA_1, GA_4, GA_8, GA_9, GA_{12}, GA_{20}, GA_{34}, GA_{53}) extraction and quantification were performed according to Giacomelli et al. (2013) in 5d, 7d and 10d inflorescence samples. Starting from lyophilized *ca.* 300 mg weighed aliquots per sample, 15 µL samples were injected on an Acquity UPLC BEH C18 column (1.7 µm film thickness, 2.1 mm × 100 mm; Waters) mounted into an Acquity UPLC Waters equipped with a Xevo TQ MS mass spectrometer (Waters Corporation, Milford, USA). Flow rate was set at 0.45 $mLmin^{-1}$ and column temperature at 40°C. Eluent A was a 0.1 % formic acid in a 2mM ammonium acetate solution and eluent B was methanol with 0.1% formic acid in a 2mM ammonium acetate solution. Chromatographic separation was obtained using the following gradient for solvent B: 2% for 0.5 minutes, raised to 95% in 7.25 minutes, then held at 95% for 1 minute, and back to 2% in 0.01 minutes. Column reconditioning was performed holding B at 2% per 3 minutes before each injection. The transitions are reported in Table S1.

Sugar (glucose, sucrose, fructose and stachyose) and free PA (putrescine, spermine, spermidine and cadaverine) contents from inflorescence samples collected at same time points were extracted and quantified by high performance liquid chromatography (HPLC) as previous described by Domingos et al. (2015). To access the significance of the differences between

treatments, one-way ANOVA and Tukey HSD test at p-value≤0.05 were performed using Statistix9 software. Box plots were generated for the five compounds that showed the higher significant change in its relative content, using both the Welch two-sample t-test (p-value≤0.05) and |log2 fold-change|≥1.

4.2.6 Metabolomic data imputation and statistical analyses

Raw area counts for each biochemical compound were rescaled by dividing each sample's value by the median value for the specific biochemical. Welch's two-sample t-tests were then used to determine whether or not each metabolite had significantly increased or decreased in abundance using Array Studio software (Omicsoft) and Microsoft Excel® spreadsheets. Mapping of metabolites was performed onto general biochemical pathways, as provided in the Kyoto Encyclopedia of Genes and Genomes (KEGG) (www.genome.jp/kegg/) and Plant Metabolic Network (PMN) (www.plantcyc.org/).

4.2.7 Exploratory analysis of transcriptome and metabolome profile

Data regarding transcript and metabolite quantification was natural logarithm (ln) –transformed for adjustment to normal distribution, and verified by histogram plotting the number of reads and metabolites per sample, using the R software version 3.1.2 before and after the transformation. Principal Coordinate Analysis (PCoA) was conducted based on the pair-wise correlation matrix using the NTsys-PC version 2.20e software package (Rohlf, 2005). The DCENTER module was used to transform the symmetric matrix to scalar product and EIGEN for eigenvalues decomposition to identify orthogonal components of the original matrix modules. The minimum-spanning tree was calculated allow the visualization of the distances between operational units. R software was used for heatmap construction and associated hierarchical clustering. Approximately unbiased and bootstrap probability p-values were calculated using pvclust version 1.3.2 (Suzuki and Shimodaira, 2006) with UPGMA method and 1000 bootstrap replications.

4.2.8 Vine physiology and final bunch morphology assessment

Flower drop was monitored with resource to non-woven cloth bags positioned around 10 bunches per treatment at full bloom and kept until 10d (days after 100% cap fall). Shoot length and primary and secondary leaf areas were determined at bloom and 15 after in six shoots per treatment following non-destructive methods (Lopes and Pinto, 2005). Estimated leaf chlorophyll content (SPAD-502 m, Minolta, Japan) was measured twice during the shade period (2 and 9d). Leaf gas exchange were measured in the morning period (9:00 am - 11:00 am) using a portable infrared gas analyzer (CIRAS-1, PPSystems, USA), on eight mature leaves from the central part of the shoots, twice during the shade period (8 and 10d) and twice after removal of

the shading nets (30 and 43d). At harvest (which corresponded to 96d), the same bunches used for flower drop monitoring, were collected and the final number of berries was recorded to calculate the cumulative and daily rate berry drop percentages. Bunch weight, rachis length and bunch compactness (number of berries/cm of rachis) were also determined. To access the significance of the differences between treatments, one-way ANOVA and Tukey HSD test were performed as previous described for targeted metabolite analysis.

4.3 Results

4.3.1 Effects of GAc and shade on leaf gas exchanges, vegetative and reproductive organs development

Vine physiology was monitored in the interval from bloom until berries with 6 mm, corresponding to the time during which the shade nets were placed, and *ca.* 36 days after shade removal. During that period, the day/night mean temperature and relative humidity measured above the nets were 26/15 ºC and 57/71%, respectively. No significant differences in these environmental conditions were perceived between treatments (Supplementary Figure S4.1). Conversely, during the shading period a 100% PAR interception was observed in the shaded vines. Leaf net photosynthetic rate (P_n), stomatal conductance (g_s), vegetative growth and chlorophyll content were reduced, only under shaded conditions (Table 4.1). Increased shoot growth was observed in vines submitted to GAc treatments, when compared with shade-treated vines.

GAc and shade treatments resulted in the drop of 887±74 and 955±9 flowers per inflorescence, respectively, corresponding to 99% and 83%. In both cases, these values were significantly higher as compared to the control (natural drop flower drop of the untreated plants) that showed a loss of 569±81 flowers, corresponding to 63.1%.. Therefore, both GAc and shade imposed treatments significantly induced flower abscission, although with a higher magnitude resulting from light interception, validating our experimental setup. After shade removal, leaf gas exchange rates recovered to values not significantly different from control.

At harvest, the increased flower abscission was translated in a reduced berry number and bunch compactness in both treatments (Table 4.2). Rachis length and bunch weight and yield were also reduced in bunches from shade-treated plants.

Figure 4.1. Aspect of representative 'Thompson Seedless' grapevine inflorescences from 50% cap fall to 10 days after 100% cap fall (d)). Samples were collected at 5, 7 and 10 d. Scale bar corresponds to 0.6cm.

Table 4.1. Effect of GAc and shade treatments on net photosynthetic rate (P_n), stomatal conductance (g_s), estimated leaf chlorophyll content , total (primary and secondary) leaf area growth, shoot growth and total percentage of flower drop during shade period (average values are reported). Within each column, different letters indicate significant differences (*p*-value≤0.05) among treatments according to Tukey's HSD test.

	P_n (µmol CO_2 m^{-2} s^{-1})	**g_s (mmol H_2O m^{-2} s^{-1})**	**Leaf chlorophyll content (SPAD units)**	**Total leaf area growth (m^2 $vine^{-1}$ day^{-1})**	**Shoot growth (cm day^{-1})**	**Flower drop (%)**
Control	8.7 a	83.5 a	25.6 a	0.914 a	2.9 ab	63.1 c
GAc	8.8 a	83.4 a	24.2 a	0.917 a	3.8 a	83.0 b
Shade	0.0 b	7.4 b	22.5 b	0.052 b	1.6 b	99.0 a

Table 4.2. Effect of shade and GAc treatments on net photosynthetic rate (P_n) and stomatal conductance (g_s) after shade period, bunch weight, number of berries, rachis length and bunch compactness at harvest (averages values are reported). Within each column, different letters indicate significant differences (*p*-value≤0.05) among treatments according to Tukey's HSD test.

	P_n (µmol CO_2 m^{-2} s^{-1})	**g_s (mmol H_2O m^{-2} s^{-1})**	**Bunch weight (g)**	**Number of berries**	**Rachis length (cm)**	**Bunch compactness**
Control	7.3	69.7	1479.6 a	324.2 a	48.5 a	6.8 a
GAc	8.6	81.8	821.8 ab	168.0 b	44.9 a	3.9 b
Shade	7.0	92.6	97.0 b	14.8 c	20.8 b	0.7 c

4.3.2 Transcriptome analysis

Three biological replicates from each treatment, enriched in abscission-signaling of different origin, and from the control were collected in two time-points (5 and 7 days after 100% cap fall) to be used for transcriptomic and metabolomic analysis. Eighteen RNA-seq 100-bp paired-end read libraries were prepared from poly(A) RNA extracted from grapevine inflorescences and an average of 27 million paired end reads were collected per each library (Table 4.3). Approximately 8% of the reads were trimmed based on the presence of Illumina adapters or low quality bases. After removing rRNA contamination, clean reads were obtained and the statistics of each sample mapping are showed in Supplementary Figure S4.2. Reads mapping to the genome sequence made up approximately 76.8±1.8% of the reads (Table 4.3).

Table 4.3. RNA-Seq data overview. Number of 100-bp reads obtained in each fruit set stage sequenced, percentage of reads after data trimming and of successfully mapped reads (mean of three independent biological replicates ± standard error (se)).

	Raw read pairs (x1000)	**Remaining reads after trimming (%)**	**Mapped reads (%)**
C5d	36342±5193	91.1±2.5	76.9±0.7
C7d	24725±603	92.1±0.8	76.1±0.7
GAc5d	23705±1936	93.2±0.8	77.9±2.2
GAc7d	20957±1580	91.1±1.3	76.0±0.7
SH5d	26103±1920	92.4±1.0	80.0±5.5
SH7d	30549±1242	92.2±1.6	74.1±1.0

A total of 5581 genes were identified as differentially expressed between control and at least one of the libraries from treated samples (Supplementary Table S4.2). The abbreviations GAc5d, GAc7d mean the log2 fold-change between gene relative expression obtained in GAc treated and control inflorescences, from samples collected at 5 and 7 days after 100% cap fall. The abbreviations SH5d, SH7d mean the log2 fold-change between gene relative expression of shade treatment and control, at the same collected time than GAc treated vines. As shown in Figure 4.2A, the shade treatment was responsible for the highest number of DEG, with 1781 and 5060 genes significantly showing differential expression at 5 and 7d, respectively. On the other hand, GAc treatment led to the differential expression of 192 and 173 genes, in 5d and 7d samples, respectively. For all comparisons, except for SH7d, a prevalence of gene up-regulation was verified (Supplementary Table S4.2). According to hierarchical clustering analysis, means of expression values of samples collected in the two time points investigated from each thinning

treatment, were significantly clustered together (Fig. 4.3A). Regarding PCoA, the shade-treated biological replicates were differentiated from GAc and control ones by PC1 in both time points, whereas PC2 separated the 7d GAc-treated biological replicates from the controls (Fig. 4.3B). These results indicate that, while shade treatment affected significantly the overall transcriptome dynamics both at 5 and 7d, in GAc, only in the second time sampled the treatment effect was above the biological variation between replicates. Thus, transcriptome analysis was targeted to the 7d time-point for GAc-treated inflorescences.

A positive significant correlation was found between the log2 fold-changes from q-rtPCR and RNA-Seq transcriptomic datasets, confirming the reproducibility of RNA-Seq data (Supplementary Figure S4.3). In agreement, the robustness of the generated RNA-Seq dataset was further revealed by a high correlation of the transcriptome profiles among three biological replicates per treatment (Supplementary Figure S4.4).

4.3.3 Metabolome analysis

Regarding global metabolomic analysis, from the 215 metabolites searched by the global metabolic analyses conducted, a total of 105 changed its relative content in at least one of the conditions (p-value$\leq$0.05) (Supplementary Table S4.3). For the Figure 4.2B, the abbreviations GAc5d, GAc7d mean the log2 fold-change between metabolite relative content obtained in GAc treated and control inflorescences, collected after 5 and 7 days after 100% cap fall. The abbreviations SH5d, SH7d mean the log2 fold-change between metabolite relative content of shade treatment and control at the same collected time than GAc treated vines. In samples from the GAc treatment, 30 and three metabolites changed respectively at 5 and 7d, while in shaded vines, 50 and 62 metabolites changed in the same time points (Fig. 4.2B). For the majority of metabolites the concentration increased in treated inflorescences comparing to control. According to hierarchical clustering, the two time points of each treatment were clustered together and the different treatments were separated with strong confidence based on bootstrap analyses (Fig. 4.3C). Figure 4.3D shows the association between biological replicates from all samples. PC1 separated shade from GAc treatment, while PC2 distinguished control replicates from treated ones, in both time points.

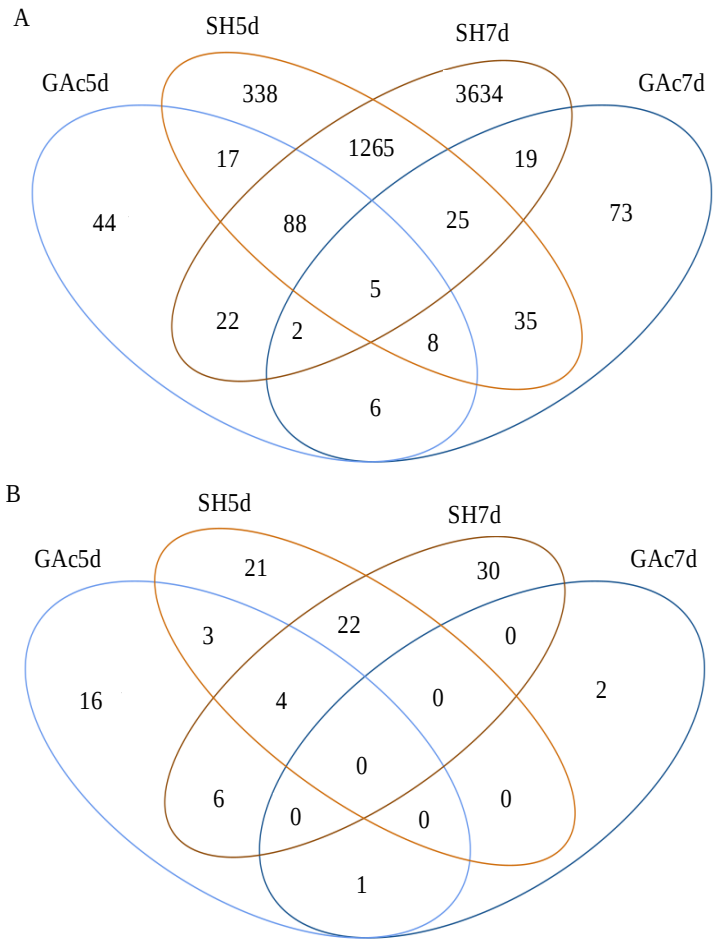

Figure 4.2. Venn diagram representing the number of differentially expressed genes (A) and differentially changed metabolites (B) in inflorescences sampled at 5 and 7 days after 100% cap fall (d), induced by GAc and shade treatments relatively to the control. Values indicate unigenes passing cutoff values of -1.5 ≥ log2 fold-change ≥1.5and *p*-value≤0.05for transcripts, and *p*-value≤0.05 for metabolites. The list of all DEG, their respective annotation, fold-change and KOG functional category are given in Supplementary Table S4.2.

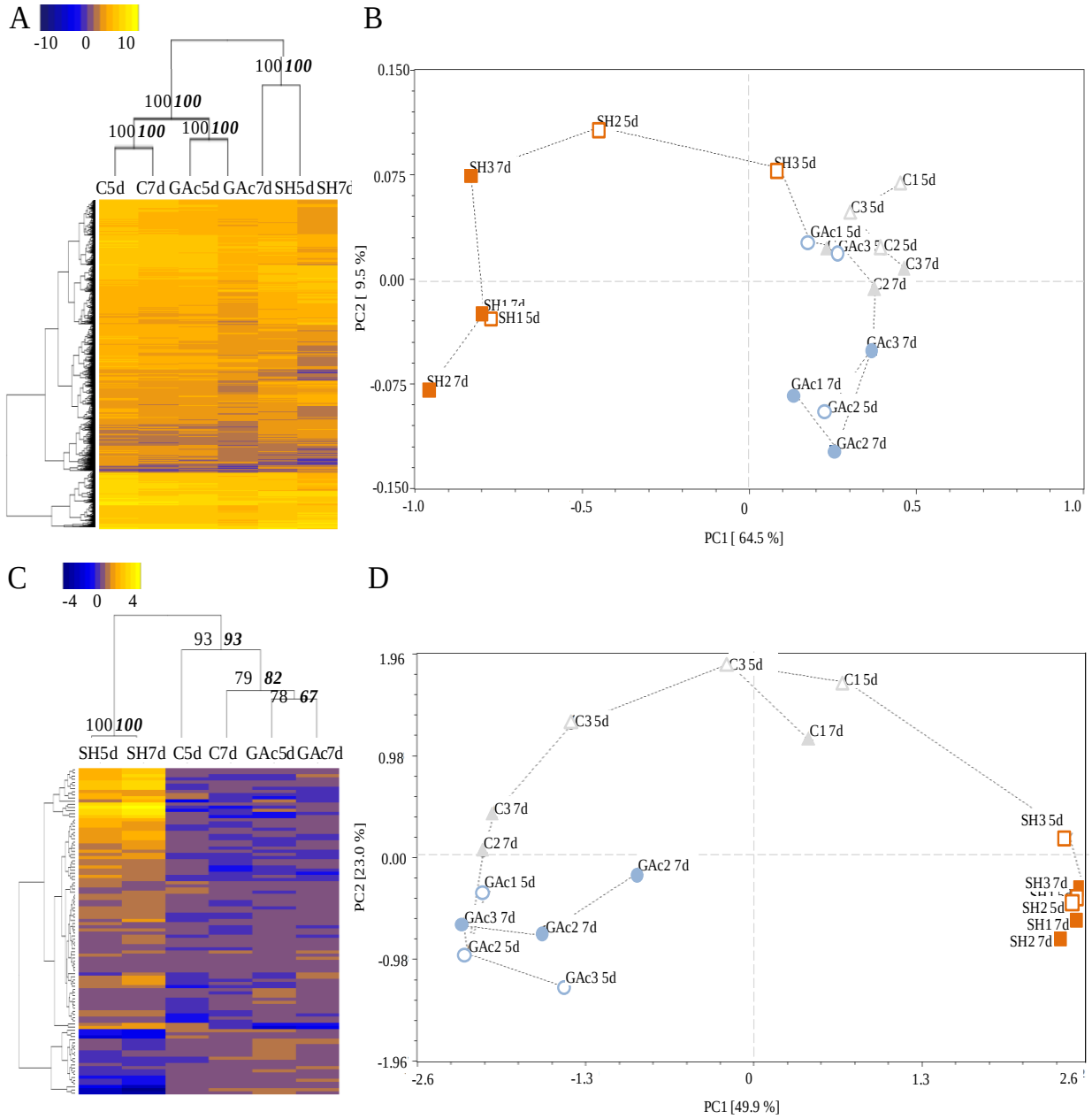

Figure 4.3. Hierarchical clustering and principal coordinate analysis (PCoA) of transcriptomic and metabolomic profile. Hierarchical clustering of expression values (A) and metabolite content (C) at different sampled stages. Each column represents the mean value for each treatment at each sampled stage (5 and 7 days after cap fall (d)). Yellow tones represent higher values while blue tones represent lower values. The strength of dendrogram nodes was estimated with a bootstrap analysis using 1000 permutations, values represented in the left side of internal nodes are the approximately unbiased *p*-values (AU), bold and italic values on the right side represented the bootstrap probability value. Principal coordinate analysis of expression values (B) and metabolite content (D) of control (triangles), GAc (circles) and shade (squares) treated inflorescences, at 5d (open) and 7d (close), and respective biological replicates. The variance explained by each coordinate (%) is given under brackets.

4.3.4 Functional annotation and enrichment analysis

Figure 4.4 represents the functional annotation distribution for the DEG and metabolites differentially abundant assigned for a specific KOG functional category and KEGG super pathway, respectively. From the total 5581 DEG, 2079 were automatically classified in KOG functional categories, 748 were manually assigned to the same categories according to the similarity with the automatically annotated, 393 were assigned to other functions and 2361 were classified as general or unknown function (Supplementary Table S4.2). The most representative functional categories in shade-treated samples at both time points investigated were: signal transduction mechanisms, secondary metabolites biosynthesis, transport and catabolism, carbohydrates transport and metabolism, transcription and posttranslational modification, protein turnover, and chaperones (Fig. 4.4). Regarding metabolites, the most representative pathways included amino acid and peptide, carbohydrate, lipid and cofactors metabolism in both time points, whereas secondary metabolism and nucleotide metabolism were most representative only at 5d and 7d, respectively. On the other hand, in GAc-treated samples the most representative functional categories changed from 5 to 7d.

To cope with the exploratory analysis results observed at transcriptome level (Fig. 4.3A), only GAc-treated samples collected at 7d will be discussed. In this sample set, energy production and conversion, translation and ribosomal structure, carbohydrates transport and metabolism, transcription and signal transduction mechanism functional categories were enriched (Fig. 4.4). Based on metabolome analysis, carbohydrates, amino acid and peptide, secondary metabolism, nucleotide and cofactor, prosthetic group and electron carrier were the most representative functional categories at 5d, while nucleotide, hormone and cofactors metabolisms were the only classes represented at 7d.

In addition, enzyme identification among DEG and its KEGG metabolic pathway assignment allowed identifying 24 and 205 enzymatic classes and 32 and 113 KEGG pathways for GAc- and shade-abscission inducing treatments, respectively (Supplementary Table S4.4). The most representative KEGG metabolic pathways were oxidative phosphorylation and purine metabolism in GAc-treated inflorescences, and starch and sucrose metabolism and purine metabolism in shade-treated inflorescences.

According to GO enrichment analysis, which demonstrate if a given pathway is predominant in our data set comparing to whole-genome background (p-value ≤ 0.01, Supplementary Table S4.5), 460 terms were found to be enriched, of which 267 GO terms corresponded to biological processes, 113 to molecular function and 89 to cellular component. Acyclic graphs showing the top 5 and top 5-related GO terms mostly affected in treatment and time point (Supplementary Figure S4.5) suggested that genes related to electron and proton transport, oxidative

phosphorylation were enriched in GAc-treated inflorescences while genes involved in response to light signal and secondary metabolism were enriched in shade samples, concerning biological processes. Among molecular functions, terms were mostly related to NADH oxidoreductase and dehydrogenase and rRNA binding in GAc-treated inflorescences, and to oxidoreductase, electron carrier, tetrapyrrole binding, hydrolase, glycosyl transferase and phenylalanine ammonia-lyase activities in shade-treated inflorescences. Regarding cellular components, the most enriched categories induced by GAc treatment were intracellular membrane-bounded organelle, chloroplast and cytoplasm, while apoplast, thylakoid and CW terms were enriched in shade treatment.

4.3.5 Effect of GAc treatment on metabolic pathways

As shown in Table 4.4, the specific genes most affected by GAc treatment were all up-regulated. The most representative category was energy production and conversion, comprising genes encoding ATP synthases, cytochrome *c* biosgenesis protein, cytochrome oxidase, NADH dehydrogenases, an ATPase, and ribosomal proteins.

The most abundant metabolites specifically altered in result of the GAc treatment, were β-alanine and guanine from nucleotide metabolism, carnitine from cofactor metabolism and mannitol and galactose from carbohydrates functional category (Fig. 4.5). It should be noted that GAc was only detected in GAc treated samples at both time points, presumably of exogenous origin. Targeted metabolite analysis, allowed detecting increased putrescine and GA_8 molecules and to confirm the rise of GAc in GAc-treated inflorescences at 7d (Table 4.5). Cadaverine, IAA, GA_1, GA_4, GA_9, GA_{12}, GA_{20}, GA_{34}, GA_{53} readings were below the detection threshold, so could not be quantified. Spermine, spermidine, glucose and fructose contents were not different between treated inflorescences and control. Due to the relatively lower number of GAc-induced alterations particularly when compared to those triggered by shade imposition, it was possibly to map it onto simplified metabolic pathways (Fig. 4.6).

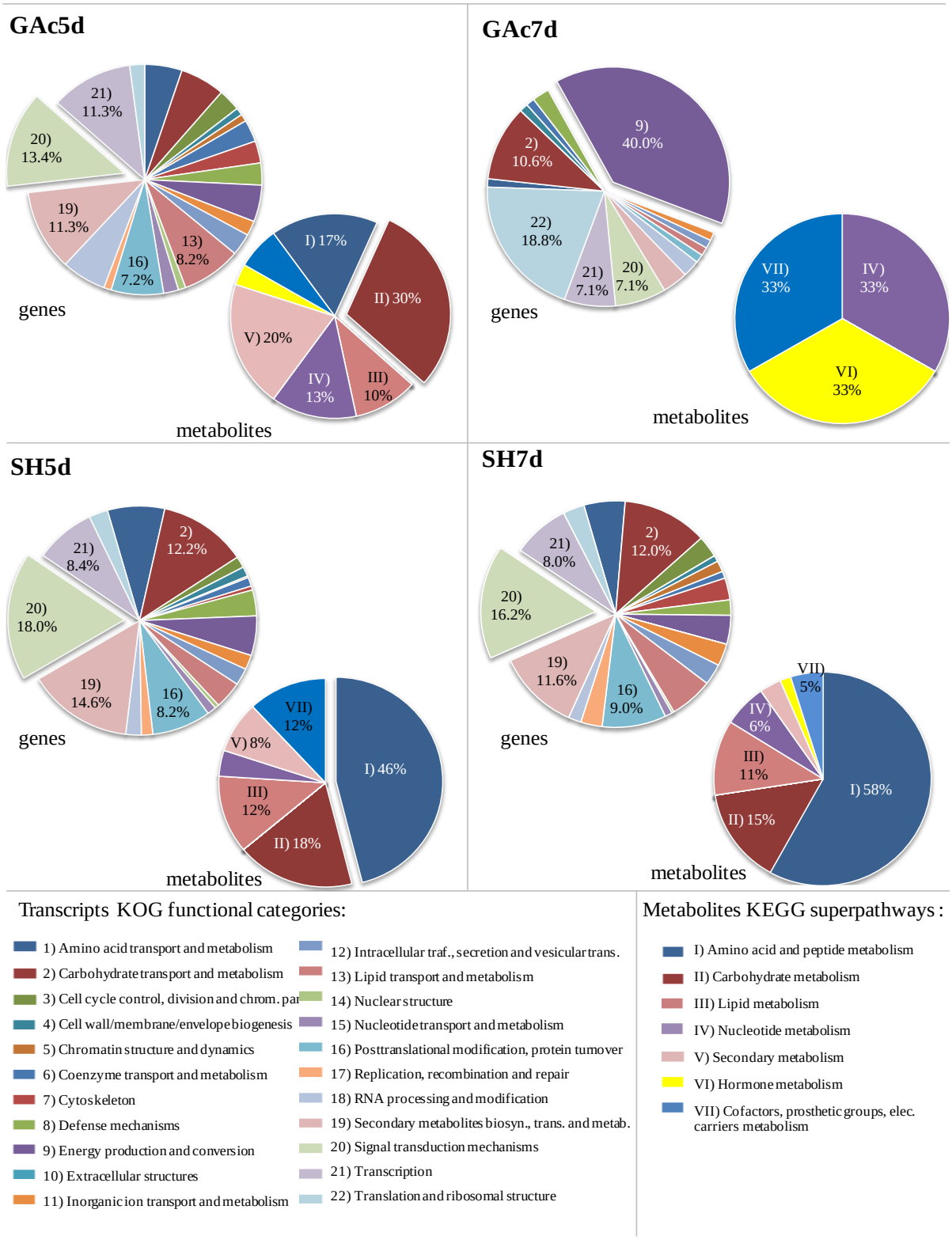

Figure 4.4. Distribution of differentially changed transcripts according to KOG functional category and metabolites according to functional class, as response to GAc and shade treatments at 5 and 7days after 100% cap fall (d).

Table 4.4. List of top ten DEG specific of GAc treatment. Gene code identification, fold-change, annotation, UniProtKB accession number and KOG functional category. Data were obtained from 3 independent biological replicates.

Gene ID	GAc 5d	GAc 7d	Annotation	UniprotKB	Functional category
VIT_09s0070g00890		1.96	ribosomal protein S7	F6I3F7	Translation, rib. struct. and biog.
VIT_00s0246g00230		1.98	cytochrome oxidase subunit III, predicted	F6HML2	Energy product. and conversion
VIT_10s0003g04310		2.00	vacuolar H+-ATPase V0 sector, subunits c/c'	D7TKE9	Energy product. and conversion
VIT_08s0056g01050		2.03	NAD dehydrogenase subunit 1 (chloroplast)	F6HMW3	Energy product. and conversion
VIT_14s0030g00680		2.05	ribosomal protein S4, predicted	D7TUX0	Translation, rib. struct. and biog.
VIT_00s0198g00060		2.06	ribosomal protein S7, predicted	F6I245	Translation, rib. struct. and biog.
VIT_00s0246g00170		2.10	cytochrome c biogenesis protein (chloroplast)	F6HMK6	Energy product. and conversion
VIT_00s0854g00040	1.50	2.11	NADHdehydrogenase subunit 4 (mitochondrion)	F6HWW5	Energy product. and conversion
VIT_09s0002g00310		2.21	ATP synthase F0 subunit 6, predicted	D7TZJ7	Energy product. and conversion
VIT_14s0036g01270	1.55	2.44	ATP synthase F0 subunit 6, predicted	E0CU73	Energy product. and conversion

Table 4.5. Metabolites with statistically significant changes assessed by target chromatography in GAc and shade-treated inflorescence comparing to control, respective fold-change and super pathway. Data were obtained from 3 independent biological replicates.

Metabolite	GAc 5d	GAc 7d	GAc 10d	SH 5d	SH 7d	SH 10d	Super pathway
sucrose				-1.19	-1.60	-1.63	Carbohydrate
putrescine		0.52		-1.69	-1.40		Polyamine
asbscisic acid				-0.94	-0.71		Hormone
gibberellic acid		2.36					
gibberellin 8		1.81					

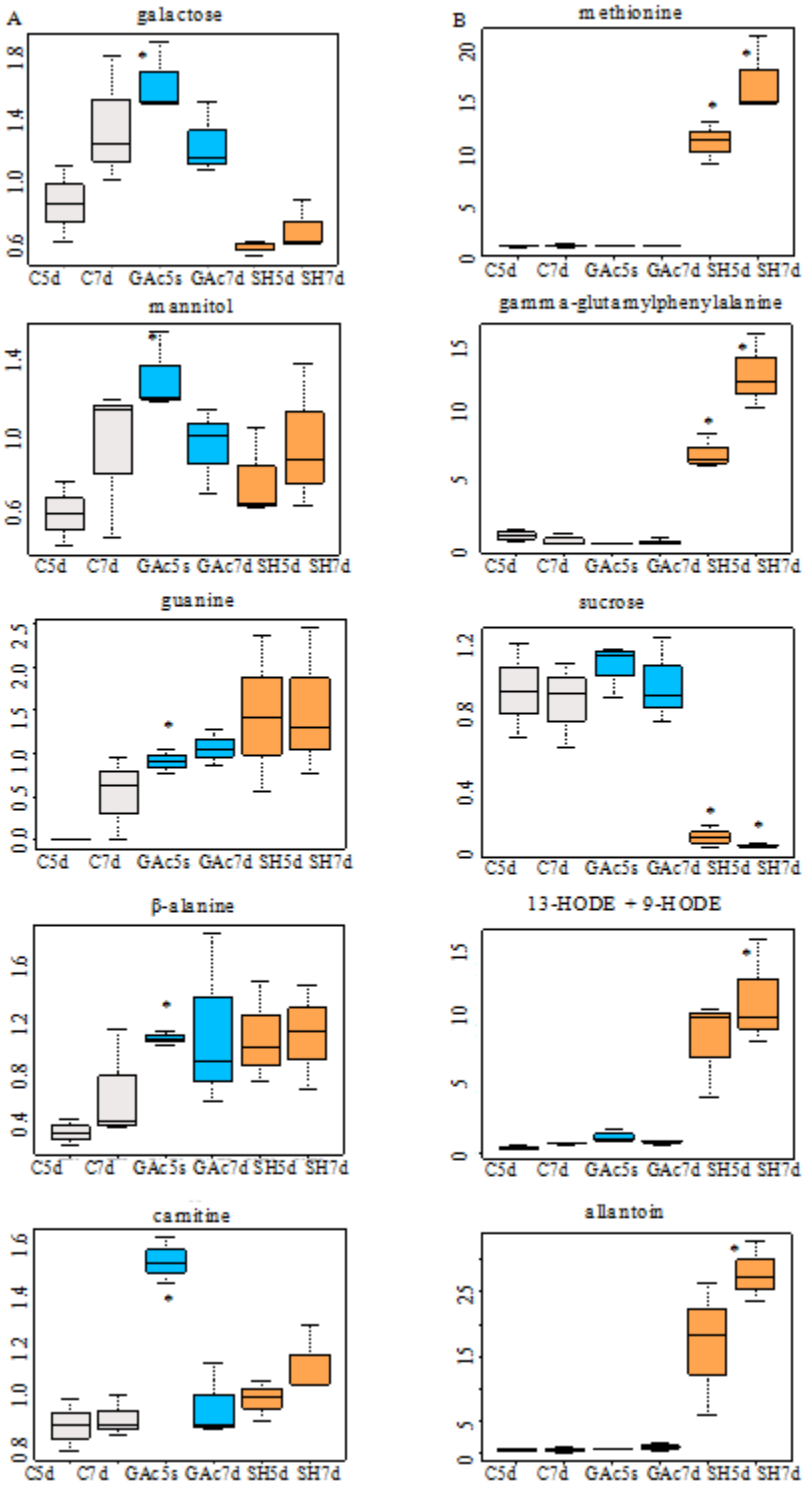

Figure 4.5. Relative content evolution of the metabolites with highly significantly differences (*p*-value≤0.05) as effect of GAc (A) and shade (B) treatments during bloom and specific of these treatments. Asterisks identify which treatment is different from the control. Data were scale imputed median = 1. Gray, blue, and orange represent samples from control, GAc and shade treatments, respectively. Data were obtained from 3 independent biological replicates.

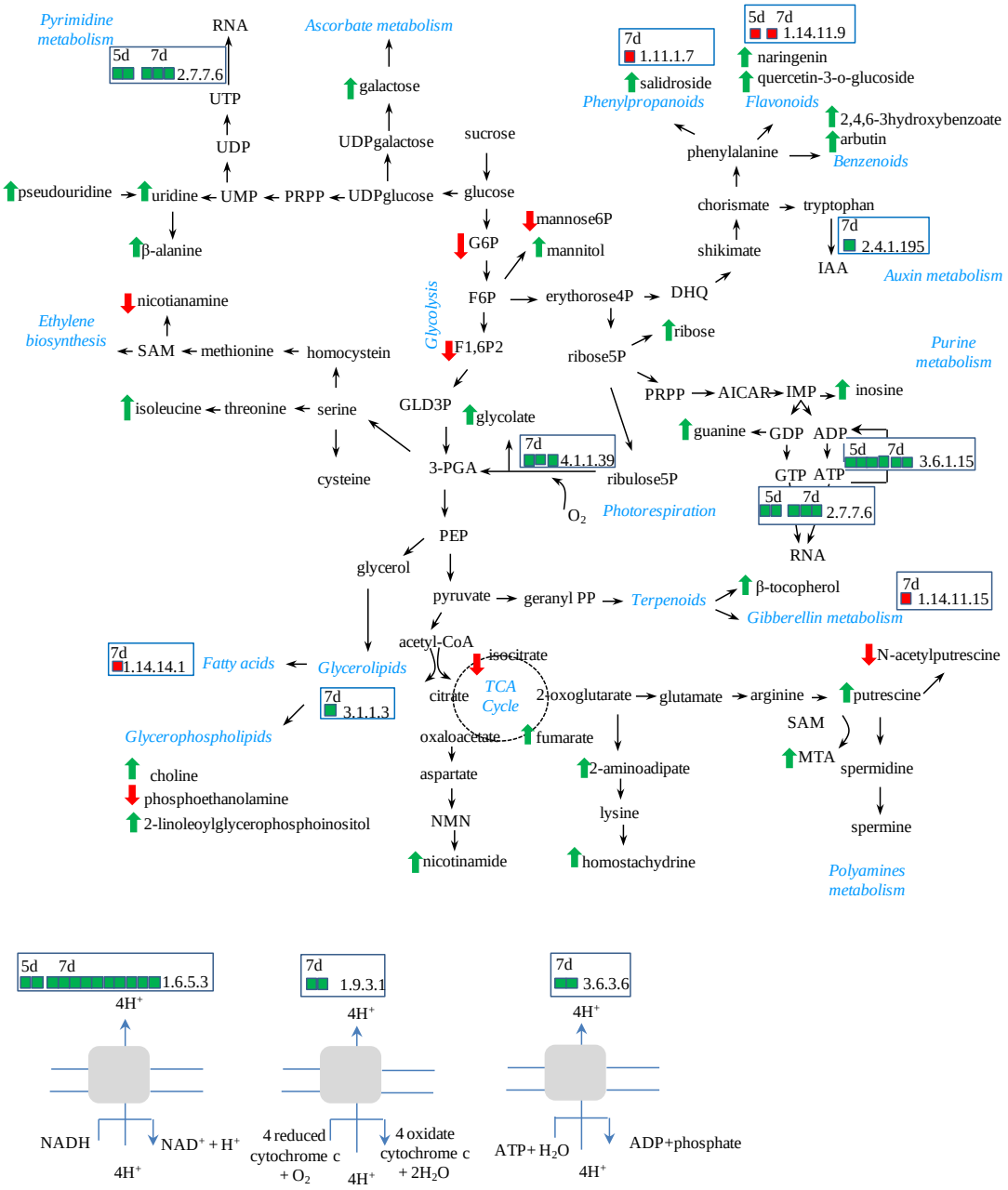

Figure 4.6. Changes on enzyme genes expression and metabolites quantification mapped onto simplified metabolic pathways, observed in GAc treated inflorescences. Red and green squares represent down and up-regulation of the transcripts, respectively. Gene description and fold-change corresponding to enzyme codes are given in Supplementary Table S4.4. Red and green arrows represent decreased and increased metabolite accumulation, respectively. Description of enzyme codes: 1.11.1.7 - peroxidase; ec:1.14.11.15 - 3β-dioxygenase; 1.14.11.9 - 3-dioxygenase; 1.14.14.1 - monooxygenase; 1.6.5.3 - reductase (H+-translocating); 1.9.3.1 - cytochrome-c oxidase; 2.4.1.195 - Sβ-glucosyltransferase; 3.1.1.3 - lipase; 3.6.1.15 - nucleoside-triphosphatase; 3.6.3.6 - ATPase; 4.1.1.39 - carboxylase.

4.3.5.1 Changes on carbohydrates, amino acid and nucleotide metabolism and energy production processes

Glucose-6-phosphate, fructose-1,6-bisphosphate and mannose-6-phosphate (M6P) and fructose and mannose levels were reduced, while mannitol, which can be synthesized *via* M6P degradation, and galactose increased in inflorescences from GAc-treated vines. Enhanced photosynthetic and respiratory metabolisms can be hypothesized based on the up-regulation of genes encoding photosystem I and II associated proteins, ribulose-1,5-bisphosphate carboxylase-oxygenase (RuBisCO, EC 4.1.1.39), NADH dehydrogenases (EC 1.6.5.3) and cytochrome-c oxidases (EC 1.9.3.1) and increased glycolate relative content (Supplementary Table S4.2). Concerning compounds associated with the TCA cycle, a isocitrate relative content decrease and fumarate increase were observed. Cofactors metabolism was also affected, as disclosed by decreased relatives contents of nicotianamine and increased nicotinamide and carnitine, which is involved in the mitochondrial transport of long-chain free fatty acids and in antioxidant activity (Gülçin, 2006).

Amino acid and nucleotide pathways were favored in response to GAc treatment comparing to controls, as revealed by increased lysine, isoleucine and PA metabolisms and increased pyrimidine and purine metabolisms, respectively (Fig. 4.6). Conversely N-acetylputrescine levels. Genes encoding nucleoside-triphosphatase (EC 3.6.1.15) enzymes involved in purine and thiamine metabolisms, RNA polymerases (EC 2.7.7.6) and H^+-translocating ATPase (EC 3.6.3.6) from the oxidative phosphorylation pathway were up-regulated.

4.3.5.2 Changes on hormone, lipid and secondary metabolism

A gene encoding an S-β-glucosyltransferase (EC 2.4.1.195) also known as UDP-glycosyltransferase74B1, and involved in indole-3-acetic acid (IAA) biosynthesis and secondary metabolism, was up-regulated. Secondary metabolic pathways were also significantly altered following GAc treatment, with the increase of salidroside, naringenin and quercetion-3-O-glucoside, 2,4,6-trihydroxybenzoate and arbutin contents and down-regulation of genes encoding a peroxidase (EC 1.11.1.7) and a hyoscyamine 6-dioxygenase (EC 1.14.11.9), acting in phenylpropanoids, flavonoids and benzenoids biosynthesis and metabolism pathways. Regarding transcription factors, two genes from MYB family, known to control anthocyanin biosynthesis (Lecourieux et al., 2014), were down-regulated (Supplementary Table S4.2).

Regarding hormone metabolism, the down-regulation of a gene encoding a gibberellin 3-β-dioxygenase (GA3ox) (EC 1.14.11.15) involved in GA biosynthesis, was disclosed. In addition, *ETHYLENE-RESPONSIVE TRANSCRIPTION FACTOR RAP2-3(ERF RAP2-3)* was the only transcript of hormone signaling pathways affected by GAc and was down-regulated (Table

4.11). The expression of a gene encoding a thioredoxin peroxidase (EC 1.11.1.15) and the relative content of β-tocopherol, associated to ROS detoxification mechanism, were found to be affected by this treatment.

As showed in Figure 4.6, among lipid-related pathways, glycerolipid metabolism, fatty acid degradation and linoleic acid metabolism were represented as down-regulation of *CYTOCHROME P450 94A1-LIKE* and up-regulation of a gene encoding a predicted lipase. Glycerophospholipid metabolism was also affected, as choline and 2-linoleoylglycerophosphoinositol levels increased and phosphoethanolamine relative contents decreased in GAc-treated inflorescences.

4.3.6 Effect of shade treatment on metabolic pathways

Shade imposition resulted in a more pronounced change in the number of genes differentially transcribed (up to 7 fold) and metabolites differentially accumulated (up to 5 fold) than GAc spraying (Table 4.4 and 4.6, Fig. 4.5). As shown in Table 4.6, secondary metabolism-related genes encoding a specific MYB transcription factor, flavonol synthase and chalcone synthase, genes encoding a cullin protein which have crucial roles in the post-translational modification of cellular proteins involving ubiquitin and cell cycle (Dieterle et al., 2005), a sugar transporter, stem-specific proteins and a small GTPase protein were the most significantly induced genes, specific for the shade treatment.

The most affected metabolites, specifically as result of the shade treatment (Fig. 4.5B) derived from amino acid and peptide (methionine and γ-glutamylphenylalanine), carbohydrate (sucrose), lipid (13-HODE + 9HODE) and nucleotide (allantoin) metabolisms. Targeted metabolite analysis were also performed in samples collected at 10d, in both treatments, confirmed the reduction of putrescine and sucrose contents detected in global metabolomic analysis, and provided additional data of a significant decrease of ABA levels 5 and 7d in inflorescences sampled from shade treated plants.

4.3.6.1 Changes on amino acid, peptide and nucleotide metabolism

A map of putative enzymes coded by the DEG is given in Supplementary Table S4.4. Amino acids metabolism was largely affected by shade treatment at the transcriptomic level, inducing a higher number of alterations in phenylalanine, cysteine, methione, glycine, serine and threonine-related pathways, followed by alanine, aspartate, arginine, glutamate, glutamine, tyrosine, tryptophan, valine, leucine, isoleucine, proline and PA related paths. Regarding metabolite accumulation (Table 4.5 and Supplementary Table S4.3), which encompass increased abundance of 30 amino acids or amino acid-related metabolites and reduced shikimate, putrescine and 4-acetamidobutanoate relative contents in shaded inflorescences, compared to

untreated organs. Glutathione and γ-glutamil peptides accumulation was likewise favored in shade treatment. DEG associated with purine and pyrimidine nucleotides metabolisms were predominantly up-regulated in result of the shade treatment (Supplementary Table S4.2 and S4.5) and the same pattern was observed in associated metabolites, except for guanosine and inosine abundance. In particular, genes encoding nucleoside-triphosphatase (EC 3.6.1.15) and adenosine triphosphatase (EC 3.6.1.3) were highly represented.

4.3.6.2 Changes on carbohydrate metabolism, transport and signaling pathways

Regarding carbohydrate-related pathways, photosynthesis, chlorophyll metabolism, carbon fixation, glycolysis, pyruvate metabolism, TCA cycle, starch and sucrose metabolism, pentose phosphate pathway, fructose and mannose metabolism, amino sugar and nucleotide sugar metabolism, galactose metabolism, pentose and glucuronate interconversions and inositol phosphate metabolisms were mostly repressed in shaded inflorescences. In particular, DEG encoding CW-modifying enzymes such as pectinesterase (EC 3.1.1.11), polygalacturonase (EC 3.2.1.15) and cellulose synthase (EC 2.4.1.12) were highly represented. Genes encoding callose synthase (EC 2.4.1.34), α and β-amylase (EC 3.2.1.2, 3.2.1.1) and chitinase enzymes (EC 3.2.1.14) were predominantly up-regulated. At the metabolomic level, malate and citromalate from TCA cycle, 2-ketogulonate, gluconate, xylose from amino sugar metabolism, inositol, glucose and sucrose decreased and fumarate from TCA cycle, and arabonate and xylonate from amino sugar metabolism were showed to increase in samples from the shade treatment.

Alterations on sugar signaling pathways and transport were induced by shade treatment during bloom, as displayed in Table 4.7. Sucrose nonfermenting-1 (SNF1)-related protein kinases (SnRKs) are a major family of signaling proteins in plants and include SnRK1, SnRK2, and SnRK3 sub-families (Kulik et al., 2011). Genes encoding SnRK1, hexokinases and fructokinase enzymes were significantly affected by the shade treatment. Other genes encoding sugar metabolizing enzymes such as threalose-6-phosphate synthases, sucrose synthases and invertases were represented among DEG and showed a global up-regulation pattern. Consistently, a gene encoding an invertase inhibitor was down-regulated. Genes encoding other monosaccharide-kinases were up-regulated, such as arabinose kinase and fructose-6-phosphate kinase (Supplementary Table 4.2). Regarding sugar transport, genes encoding glucose-6-phosphate translocators and sugar transporter SWEET1 and 3 were predominantly down-regulated, whereas genes encoding sugar transporter SWEET2 and 10, putative hexose transporter and sugar transporters ERD6-like, implicated in transport of sugars out of the vacuole in C-starvation conditions (Büttner, 2007), were up-regulated.

The expression of genes encoding other molecules involved in signal transduction mechanisms such as serine/threonine-protein phosphatase (EC 3.1.3.16), protein-tyrosine kinases (EC

2.7.10.2), and MAPKs (EC 2.7.11.24) was predominantly up-regulated (Supplementary Table S4.4) while MAPKKs were down-regulated (Table 4.8).

4.3.6.3 Changes on hormone metabolism and signaling pathways

In what concerns hormone metabolism and signaling pathways, genes involved in ethylene and auxin related pathways were the most represented in samples from the thinning by shade treatment, followed by genes involved in GA, cytokinin (CK), ABA, brassinosteroid (BR) and salicylic acid (SA) and jasmonic acid (JA)-related pathways (Table 4.8). Regarding ethylene biosynthesis, genes encoding S-adenosylmethionine synthase (SAM-S) were down-regulated while the expression of genes encoding ACC oxidases showed predominantly an up-regulation. Moreover, cyano-alanine relative content, which is a co-product of ethylene biosynthesis *via* the ACC pathway (Yip and Yang, 1998) increased in these samples. The expression of *ETHYLENE INSENSITIVE 3-LIKE* (*EIN3*) and *ERFs*, which act as transcriptional activators or repressors in ethylene-signal transduction, was significantly affected by shade.

Auxin biosynthetic pathway from thyptophan was favored as suggested by the up-regulation of a tryptophan aminotransferase-related gene. Genes encoding auxin binding proteins (ABP) and transport inhibitor response 1 auxin receptor (TIR1) were up-regulated. TIR1 mediates Aux/IAA proteins degradation, which are repressors of auxin responsive genes, and auxin-regulated transcription (Peer, 2013). Genes encoding g Aux/IAA proteins, auxin responsive factor (ARF) and auxin efflux carriers (AEC) were down-regulated resulting in affected expression of genes encoding other auxin and IAA-induced proteins by shade treatment. The synthesis of IAA-amino acid conjugates was induced by the *GH3.9* gene at 5d.

Genes encoding gibberellin 20-oxidase (GA20ox) were down-regulated whereas gibberellin 3-β -dioxygenase (GA3ox) was up-regulated. The expression of genes encoding gibberellin 2-oxidase (GA2ox) involved in GA metabolism was also significantly regulated. GA signaling pathway was repressed, with a concomitant up-regulation of a *DELLA* gene and down-regulation of *GID2*, responsible for DELLA degradation (Acheampong et al., 2015; Davière and Achard, 2013).

Genes involved in CK activation, such as those encoding a UDP-glycosyltransferase 85A1 (EC 2.4.1.215), zeatin-O-glucosyltransferase and CK riboside 5'-monophosphate phosphoribohydrolase were significantly affected by the imposition of the shade treatment. Genes encoding the CK receptors histidine kinases and histidine-containing phosphotransferase, and CK dehydrogenase enzyme, involved in its degradation, were induced. Shade also promoted the up-regulation of genes involved in brassinosteroids (BR) signal transduction, such as members encoding serine/threonine-protein phosphatase BSL3-like, and a gene encoding a

brassinosteroid-regulated protein BRU1. In addition, the expression of genes encoding cyclin-D3 (CYCD3) proteins, which are downstream components of the CK and BR-signaling pathways promoting cell division (Zhiponova et al., 2013), were down-regulated, and a *SENESCENCE RELATED GENE* (*SRG1*) was up-regulated at 7d (Supplementary Table S4.2).

Genes encoding ABA synthesis and degradation enzymes, such as aldehyde oxidase and abscisic acid 8'-hydroxylase, were up-regulated. These changes on ABA metabolism were also verified as decreased ABA relative content in shaded inflorescences (Table 4.5). In the ABA-signal transduction pathway, down-regulation of protein phosphatase 2C, which is a negative regulator of ABA response, up-regulation of SnRK2 (serine/threonine-protein kinase SAPK2 and SRK2I) which are the main positive regulators of abscisic acid signaling (Fujita et al., 2009), were observed, suggesting a de-repression of ABA signaling in shaded inflorescences.

The expression of genes encoding methyltransferase enzymes responsible for conversion of jasmonic (JA) and salicylic acids (SA) in methyljasmonate and methylsalicylate, was down-regulated, suggesting accumulation of JA and SA. JA-mediated signaling pathway was also affected, as revealed by the up-regulation of a gene encoding TIFY9 which negatively regulates a key transcriptional activator of jasmonate responses (Chung and Howe, 2009).

4.3.6.4 Changes on lipid, cofactor and secondary metabolism

Impact on lipid-related pathways was disclosed as glycerolipid, glycerophospholipid and sphingolipid metabolism, fatty acid biosynthesis, elongation and degradation, linoleic, α-linoleic acid and arachidonic acid metabolism, unsaturated fatty acids biosynthesis, alkaloid biosynthesis, ether lipid metabolism and cutin, suberine and wax biosynthesis, were affected in shade-treated inflorescences (Supplementary Table S4.4). In particular, genes encoding lipoxygenase (EC 1.13.11.12) and lipase (EC 3.1.1.3) enzymes were highly represented and mostly up-regulated. At the metabolite level, a global increase of fatty acids, oxylipins (HODE), glycerolipids, sterols and glycerophospholipids was verified (Supplementary Table S4.3).

Cofactors metabolism-related pathways were also significantly altered, of which thiamine metabolism was the most represented, followed by vitamin B6 metabolism, riboflavin metabolism, pantothenate and CoA biosynthesis and nicotinate and nicotinamide metabolism. In particular, and regarding oxidative phosphorylation, the expression of genes encoding inorganic pyrophosphatases (EC 3.6.1.1) genes encoding cytochrome *c* oxidases (EC 1.9.3.1), NADH dehydrogenases (EC 1.6.5.3) was affected, and phosphate and methylphosphate metabolite levels increased in shade-treated inflorescences.

Secondary metabolic pathways such as phenylpropanoid, stilbenoid, monoterpenoid, diterpenoids, carotenoids, benzenoids, flavonoids and anthocyanin biosynthesis and degradation

and cytochrome P450-related pathways were significantly affected during shade in both time points. In particular, DEG encoding phenylalanine ammonia-lyases (EC 4.3.1.25) which catalyse the first step of phenylpropanoids biosynthetic pathway, and stilbene synthases (EC 2.3.1.95) were the most represented and were predominantly up-regulated. Genes encoding myrcene synthases (EC 4.2.3.20), involved in monoterpenoids biosynthetic pathway, were up-regulated while (3S)-linalool/(E)-nerolidol /(E,E)-geranyl linalool synthases (EC 4.2.3.25) were down-regulated. Flavonoids and diterpenoids biosynthetic pathways were, conversely, repressed. At the metabolomic level, oleanolate from terpenoids metabolism, ferulate from phenylpropanoid metabolism, and both α- and γ-tocopherols increased, while arbutrin (benzenoid) and salidroside (phenylpropanoid) were reduced in result of shaded inflorescences.

Shade altered the accumulation of non-enzymatic markers of oxidative stress, including increased reduced glutathione (GSH) relative content and decreased ascorbate-related metabolites, namely 5-ketogluconate and threonate (Supplementary Table S4.3). The expression of genes encoding enzymatic antioxidants comprising superoxide dismutase, ascorbate oxidase, ascorbate peroxidase, glutathione peroxidase, peroxiredoxin, thioredoxin, glutaredoxin and glutathione S-transferase was also significantly affected (Table 4.9). In addition, genes encoding laccase (EC 1.10.3.3), involved in ascorbate metabolism and lignin biosynthesis, were exclusively down-regulated in shade treatment.

4.3.6.5 Shade-responsive transcription factors

A high number of differentially expressed transcription factors induced by shade treatment was identified, predominantly at 7d, including MYB,GATA, MADS-box, HEX, GT-2, WRKY, CCAAT, ZF-HD, HSF, WOX, E2F/DP, bHLH, MOT2, MEIS1, RF2b and ZFF (Table 4.10). In particular, genes encoding MYB and GATA families were the most represented and were predominantly down- and up-regulated, respectively.

Table 4.6. List of top ten DEG specific of shade treatment. Gene code identification, fold-change, annotation, UniProtKB accession number and KOG functional category. Data were obtained from 3 independent biological replicates.

Gene ID	SH 5d	SH 7d	Annotation	UniprotKB	Functional category
VIT_11s0016g01320		-6.51	transcription factor MYB, predicted	F6HGP6	Transcription
VIT_18s0001g03470	-3.26	-5.70	flavonol synthase, predicted	F6H0T8	Secondary metab. bios. transp. cat.
VIT_04s0043g00650		-5.63	cullin-1 isoform 1, predicted		Cell cycle control, cell div., chrom. part.
VIT_14s0068g00930	-2.50	-5.32	chalcone synthase		Secondary metab. bios. transp. cat
VIT_18s0001g11010		5.42	Ca^{2+}independent phospholipase A2, pred.	F6H017	Lipid transport and metabolism
VIT_13s0019g03070	3.31	5.46	small heat-shock protein Hsp26, predicted	F6HNN6	Posttranslational mod., protein turn., chap.
VIT_05s0020g02170	3.99	5.73	sugar transporter ERD6-like, predicted	F6HDJ1	Carbohydrate transport and metabolism
VIT_00s0561g00020	3.86	5.73	stem-specific protein TSJT1-like	D7TYY3	Other
VIT_02s0033g00830		5.75	GTPase Rab11/YPT3, predicted	F6I079	Intracellular traff., secretion, vesic. transp.
VIT_00s0586g00030	3.91	5.80	stem-specific protein TSJT1-like , pred.	D7UE87	Other

Table 4.7. DEG involved in sugar signaling pathway and sugar transport induced by shade treatment during bloom and respective fold-change. Up-regulation is marked as red and down-regulation as green background. Data were obtained from 3 independent biological replicates.

Gene family	GID	SH5d	SH7d
SnRK1	VIT_01s0026g01740		-1.61
	VIT_06s0009g01930	1.69	2.35
HK	VIT_06s0061g00040		2.14
	VIT_18s0001g14230		-2.57
FK	VIT_05s0102g00710		-1.60
T6PS	VIT_00s0173g00110	2.03	
	VIT_00s0233g00030		2.13
	VIT_01s0011g05960	1.67	2.05
	VIT_01s0026g00280	2.05	2.87
	VIT_02s0012g01680		-1.54
	VIT_02s0154g00110		2.40
	VIT_06s0009g01650	2.47	3.11
	VIT_10s0003g01680	1.76	2.55
	VIT_10s0003g02160		-2.38
	VIT_12s0028g01670	1.83	2.25
	VIT_17s0000g08010	2.92	3.83
SUS	VIT_07s0005g00750	1.90	2.66
INV	VIT_00s0233g00010	1.60	2.46
	VIT_00s2527g00010		2.27
	VIT_02s0154g00090		1.63
	VIT_05s0077g00510	2.31	3.18
	VIT_14s0060g00860	1.52	2.25
	VIT_16s0022g00670		-2.90
INV-I	VIT_18s0075g00280	-2.05	
G6PT	VIT_01s0011g00590		-2.64
	VIT_06s0004g02710	-2.64	-3.46
	VIT_06s0004g07960		-1.73
	VIT_10s0116g00760		-1.60
	VIT_14s0066g01000		-2.13
	VIT_15s0024g01440		-2.31
	VIT_17s0000g08560		-2.35
	VIT_18s0001g06300		1.72
SWEET	VIT_16s0050g02540		-2.03
	VIT_17s0000g00830	1.92	1.62
	VIT_18s0001g15330	-1.60	-1.92
	VIT_19s0014g00280		2.54
HT	VIT_00s0181g00010	1.83	2.60
	VIT_16s0013g01950	1.76	2.43
ERD6	VIT_05s0020g02170	3.99	5.73
	VIT_07s0104g00830		1.80

SnRK1: serine/threonine-protein kinase SnRK1; HK: hexokinase; FK: fructokinse; T6PS: trehalose-6-phosphate synthase; SUS: sucrose synthase; ÍNV: invertase; INV-I: invertase inhibitor; G6PT: glucose-6-phosphate/phosphate translocator 2; SWEET: bidirectional sugar transporter SWEET; HT: hexose transporter; EDR6: sugar transporter ERD6-like.

Table 4.8. DEG involved in hormone biosynthesis, metabolism and signaling pathways induced by shade at 5 and 7 days after 100% cap fall, and respective fold-change. Up-regulation is marked as green and down-regulation as red. Data were obtained from 3 independent biological replicates.

	Gene family	GID	SH5d	SH7d		Gene family	GID	SH5d	SH7d
ABA	AO	VIT_18s0041g02410	2.19	2.66	**ET**	SAM-S	VIT_07s0005g02230		-3.02
	ABAX	VIT_03s0063g00380	2.03	2.63			VIT_14s0060g00480	-1.50	-2.58
	PP 2C	VIT_08s0007g06510		-1.51		ACO	VIT_05s0049g00310	1.56	1.98
		VIT_16s0050g02680	-1.82				VIT_07s0005g03060		-2.25
	SnRK2	VIT_07s0197g00080	1.87	1.73			VIT_08s0007g03040	2.14	2.54
		VIT_18s0001g06310		1.64		EIN3	VIT_13s0047g00250		1.66
AUX	TRY-ATF	VIT_18s0157g00140	1.81	4.65		ERF	VIT_00s0772g00020	1.65	2.00
	TIR	VIT_05s0020g04830	2.36	3.12			VIT_01s0011g03070		2.24
	ABP	VIT_07s0005g05910		1.71			VIT_01s0150g00120	1.56	1.87
		VIT_07s0005g05930		1.75			VIT_02s0234g00130		2.02
		VIT_09s0002g01320		4.42			VIT_04s0008g06000		-2.02
		VIT_18s0086g00590		2.93			VIT_04s0023g00970		-1.83
	Aux/IAA	VIT_04s0008g00220	-2.03	-2.70			VIT_05s0049g00510		1.79
		VIT_07s0141g00270		-1.64			VIT_05s0077g01860		1.68
		VIT_07s0141g00290	-2.21	-3.33			VIT_07s0031g01980		2.65
	Aux-IP	VIT_03s0038g00930	-1.77	-2.94			VIT_07s0141g00690	-1.60	
		VIT_03s0038g00940		-2.71			VIT_08s0040g03180		-2.60
		VIT_04s0023g00560	3.45				VIT_09s0018g01650		-2.46
		VIT_18s0001g13360		-1.72			VIT_12s0059g00280		1.80
		VIT_18s0072g00660	-1.57	-2.32			VIT_13s0019g03550		1.55
	IAA-IP	VIT_07s0005g00660		1.89			VIT_14s0006g02290	-2.32	-2.90
		VIT_18s0001g13980		-1.92			VIT_15s0021g01630		2.63
	ARF	VIT_06s0004g03130		-2.52			VIT_15s0046g00310	-2.12	-2.50
	GH3.9	VIT_07s0005g00090	1.56				VIT_15s0046g01390		1.77
	AEC	VIT_11s0052g00440		-1.92			VIT_16s0013g00950		1.64
		VIT_17s0000g02420		-1.67			VIT_16s0013g01000	1.63	
BR	BSL	VIT_00s1197g00010	2.03				VIT_16s0013g01030		2.09
		VIT_00s1427g00010	2.30				VIT_16s0013g01070		2.10
	BRU1	VIT_05s0062g00250	2.04	3.82			VIT_16s0013g01120		2.01
CK	UDP-GTF	VIT_18s0001g05990		-2.84			VIT_16s0100g00400		1.51
	zeatin-GTF	VIT_08s0007g08920	1.63	3.35			VIT_17s0000g04480	1.58	1.93
	CYT	VIT_18s0001g14030		-1.61			VIT_18s0001g10150		1.64
	CH	VIT_13s0158g00320		1.73			VIT_18s0001g03240		2.04
	HK	VIT_01s0010g03780		2.22			VIT_18s0001g05850		1.71
		VIT_04s0008g03460		1.96			VIT_18s0001g08610		-1.58
		VIT_12s0057g00690	1.69	1.53	**JA**	JA-MTF	VIT_18s0001g12880	-1.62	-3.29
	AHP	VIT_09s0002g03520	-1.67	-3.25			VIT_18s0001g12890	-1.70	-3.61
GA	DELLA	VIT_14s0006g00640		1.74			VIT_18s0001g12900	-1.64	-1.93
	GID2	VIT_07s0129g01000		-1.82		TIFY	VIT_01s0146g00480		2.26
		VIT_18s0001g09700		-1.69	**SA**	SA-MTF	VIT_04s0023g02220		2.55
	GA20ox	VIT_03s0063g01150	-3.21	-2.12			VIT_04s0023g02230	-2.40	-1.92
		VIT_03s0063g01260	-2.55	-1.91			VIT_04s0023g02240	-2.35	-1.77
		VIT_09s0002g05280	-1.56	-2.23			VIT_04s0023g02260	-2.64	-2.09
		VIT_15s0046g02550		-2.28			VIT_04s0023g02310		2.44
	GA3ox	VIT_04s0008g04920		1.76			VIT_04s0023g03810		-2.10
	GA2ox	VIT_05s0077g00520		1.99	**MAPKs**	MAPK	VIT_06s0004g03540		2.101
		VIT_06s0004g06790	-1.82				VIT_04s0023g02420		1.512
		VIT_10s0116g00410		-3.39		MAPKK	VIT_11s0016g02970		-2.239
		VIT_19s0140g00120		3.05			VIT_05s0020g02910		-3.101
		VIT_19s0177g00030		-2.59					
	GA-R	VIT_14s0108g00740		-2.97					

ABA: abscisic acid; AO: aldehyde oxidase; ABAX: abscisic acid 8'-hydroxylase; PP 2C: protein phosphatase 2C; SnRK2: serine/threonine-protein kinase SnRK2; **AUX:** auxin; TRY-ATF: tryptophan aminotransferase-related protein; TIR1 : transport inhibitor response 1; ABP: auxin-binding protein; Aux/IAA: Aux/IAA proteins; Aux-IP: other auxin induced proteins; IAA-IP: other IAA induced proteins; GH3.9: putative indole-3-acetic acid-amido synthetase GH3.9; AEC: auxin efflux carrier component; **BR:** brassinosteroid; BRU1: brassinosteroid-regulated protein BRU1; BSL: serine/threonine-protein phosphatase BSL3-like; **CK:** cytokinin, UDP-GTF: UDP-glycosyltransferase 85A1; ZEA-GTF: zeatin O-glucosyltransferase; CYT: cytokinin riboside 5'-monophosphate phosphoribohydrolase; CYH: cytokinin dehydrogenase; HK: histidine kinase; AHP: histidine-containing phosphotransfer protein; **GA:** gibberellin; DELLA: DELLA protein GAI1; GID2: F-box protein GID2; GA20ox: gibberellin 20 oxidase; GA3ox: gibberellin 3-β-dioxygenase; GA2ox: gibberellin 2-β-dioxygenase; GA-R: gibberellin-regulated protein; **ET:**

ethylene, SAM-S: S-adenosylmethionine synthase; ACO: 1-aminocyclopropane-1-carboxylate oxidase; EIN3: ethylene insensitive 3-like; ERF: ethylene-responsive transcription factor; **JA:** jasmonic acid; JA-MTF: jasmonate O-methyltransferase; TIFY: TIFY 9 protein; **SA:** salicylic acid; SA-MTF: salicylate O-methyltransferase; MAPKs: mitogen-activated protein kinase cascade: MAPK: mitogen-activated protein kinase; MAPKK: mitogen-activated protein kinase kinase.

Table 4.9. DEG encoding oxidative stress-related enzymes induced by shade treatment during bloom and respective fold-change. Up-regulation is marked green and down-regulation is marked red. Data were obtained from 3 independent biological replicates.

Gene family	GID	SH5d	SH7d	Gene family	GID	SH5d	SH7d
AO	VIT_00s0253g00040		-2.19	GST	VIT_01s0026g01340	-2.67	-4.08
	VIT_06s0009g01320		-2.20		VIT_01s0026g01340	-2.67	-4.08
	VIT_10s0116g01610		-2.80		VIT_05s0049g01090	-1.75	
	VIT_18s0001g00470		-2.46		VIT_05s0049g01120	-1.74	
APX	VIT_06s0004g03550		-1.86		VIT_05s0051g00180		2.01
PX	VIT_02s0012g00540		2.04		VIT_05s0051g00240		2.87
	VIT_03s0063g01040	2.63	2.90		VIT_06s0004g03690	-1.66	-2.78
	VIT_05s0077g00880		-2.47		VIT_06s0004g05690		2.32
	VIT_06s0004g07770		-2.05		VIT_06s0004g05700		2.11
	VIT_07s0129g00360		1.91		VIT_07s0005g04880		2.41
	VIT_07s0130g00220		-2.87		VIT_07s0005g04880		2.41
	VIT_10s0116g01780	-1.81	-3.41		VIT_07s0005g04890		2.01
	VIT_14s0066g01850		-2.70		VIT_07s0104g01800	-2.09	-3.16
	VIT_19s0085g01040	-1.69			VIT_07s0104g01800	-2.09	-3.16
SOD	VIT_16s0013g00260		-2.29		VIT_07s0104g01810	-2.43	-3.62
PXR	VIT_05s0020g00600		1.91		VIT_07s0104g01810	-2.43	-3.62
	VIT_11s0016g00560	-2.00	-3.69		VIT_07s0104g01820		-2.61
	VIT_11s0016g03630		-2.47		VIT_07s0104g01820		-2.61
TR	VIT_00s0532g00030		1.98		VIT_07s0104g01830		-1.77
	VIT_03s0038g04160		2.18		VIT_08s0007g01420		-1.96
	VIT_04s0008g02900		2.00		VIT_08s0007g01420		-1.96
	VIT_04s0023g02700		-1.58		VIT_12s0028g00920		3.56
	VIT_08s0007g07620		1.52		VIT_13s0067g03470		-1.80
	VIT_17s0000g06370		1.66		VIT_16s0039g01070		2.53
	VIT_18s0001g00820		-2.08		VIT_18s0001g00690		-2.03
	VIT_18s0001g13240	-2.05	-2.08		VIT_18s0001g00690		-2.03
	VIT_18s0001g15310	-2.93	-3.94		VIT_19s0015g02590		2.53
	VIT_19s0014g05090	3.31	3.14		VIT_19s0015g02690		2.44
GR	VIT_02s0025g01710	-4.39	-2.30		VIT_19s0015g02730		1.58
	VIT_02s0025g02700		-3.42		VIT_19s0015g02730		1.58
	VIT_04s0008g01120	-1.76	-1.81		VIT_19s0015g02880		2.60
	VIT_05s0020g01750	3.18			VIT_19s0015g02890		1.54
	VIT_05s0020g01760	2.63	3.18		VIT_19s0015g02890		1.54
	VIT_07s0104g01390	-2.15	-3.33		VIT_19s0027g00460		2.00
	VIT_07s0104g01400	2.37			VIT_19s0027g00460		2.00
	VIT_08s0007g03220		-3.53		VIT_19s0093g00160		2.57
	VIT_11s0052g00500		-1.64		VIT_19s0093g00220		1.98
	VIT_13s0067g01650		1.68		VIT_19s0093g00220		1.98
	VIT_13s0073g00520		-3.50		VIT_19s0093g00260		2.18
GPX	VIT_05s0102g00120		-3.97		VIT_19s0093g00320	2.05	1.86

AO: ascorbate oxidase; APX: ascorbate peroxidase; PX: peroxidase; SOD: superoxide dismutase; PXR: peroxiredoxin; TR: thioredoxin; GR: glutaredoxin; GPX: glutathione peroxidase; GST: glutathione S-transferase.

Table 4.10. DEG encoding transcription factors induced by shade treatment during bloom and respective fold-change. Up-regulation is marked by green and down-regulation by red. Transcription factors directly involved in hormone signal transduction pathways were represented in Table 4.8.

	GID	SH5d	SH7d		GID	SH5d	SH7d
bHLH	VIT_14s0128g00110	-1.86	-3.82	MOT2	VIT_13s0019g02510	-1.80	-2.42
	VIT_18s0001g06650		-1.86	MEIS1	VIT_06s0009g00410		1.59
CCAAT	VIT_00s0956g00020		-2.12	MYB	VIT_00s0341g00050		-2.10
	VIT_01s0010g03550		-4.39		VIT_00s1241g00010	-1.85	
	VIT_06s0080g00460		-2.19		VIT_02s0025g02210	-2.26	-3.75
	VIT_09s0002g01590		1.71		VIT_02s0025g02220		-2.72
	VIT_11s0016g01480		-1.85		VIT_04s0008g01800	-1.69	
E2F/DP	VIT_08s0007g00170		-1.94		VIT_04s0008g01810	-1.61	-3.81
	VIT_17s0000g07630		-2.62		VIT_04s0008g01820	-1.82	
	VIT_18s0001g14110		-1.76		VIT_04s0008g01830		-1.90
GATA-4/5/6	VIT_01s0011g03520	2.09	2.96		VIT_04s0008g03780		-2.10
	VIT_01s0011g04240	1.56			VIT_05s0020g01100	-1.74	
	VIT_01s0150g00410		1.81		VIT_05s0049g01020		2.13
	VIT_02s0033g00300	-1.53	-2.76		VIT_05s0049g02260	2.26	
	VIT_03s0038g00340		-2.44		VIT_05s0077g00500		2.04
	VIT_04s0023g01840		-2.19		VIT_06s0004g04140	2.20	1.96
	VIT_08s0007g06310	1.65	1.59		VIT_07s0005g01210		-5.21
	VIT_09s0002g03750		-2.60		VIT_07s0005g01950		2.16
	VIT_09s0054g00530	-1.80			VIT_08s0007g00410		-1.69
	VIT_09s0054g01620		1.91		VIT_08s0007g04830		2.90
	VIT_11s0016g02210	1.92			VIT_09s0002g01380		-1.97
	VIT_11s0103g00760		-2.24		VIT_09s0002g01670	-2.18	-3.21
	VIT_11s0206g00060	1.50			VIT_10s0116g01760		1.52
	VIT_12s0028g00980		1.85		VIT_11s0016g01300	-1.91	-2.50
	VIT_12s0134g00400	-1.94	-2.12		VIT_11s0016g01320		-6.51
	VIT_13s0067g03390		1.70		VIT_11s0016g03750		-2.02
	VIT_15s0048g02540		1.83		VIT_12s0134g00490		-2.35
	VIT_16s0098g00360	-2.03	-2.50		VIT_13s0064g00570		1.75
	VIT_16s0098g00900		1.59		VIT_13s0067g01630	1.74	2.22
	VIT_17s0000g06570		1.55		VIT_14s0006g01280	-2.03	
	VIT_18s0001g13520		1.54		VIT_14s0006g01290	-2.50	
	VIT_19s0014g05120	1.62			VIT_14s0006g01340	-2.40	
GT-2	VIT_00s0558g00020		1.75		VIT_14s0006g01620	-2.73	-4.46
	VIT_02s0025g03220		1.87		VIT_14s0066g01220		-2.09
	VIT_04s0008g01850		-2.03		VIT_14s0083g00120		-1.88
	VIT_08s0007g04180		-3.95		VIT_14s0108g01010	-1.63	-2.47
	VIT_08s0058g00200		1.62		VIT_15s0046g00170	-2.65	-3.42
	VIT_13s0084g00800		-2.26		VIT_17s0000g02660	-2.53	-3.53
	VIT_17s0000g10420		-1.72		VIT_17s0000g03560		1.87
HSF	VIT_04s0008g01110		-2.10		VIT_18s0117g00200	-1.84	-4.32
	VIT_06s0009g02730		-2.25		VIT_18s0117g00210	-1.96	-2.47
	VIT_12s0028g01410		2.03	RF2b	VIT_06s0004g08070		-1.54
	VIT_18s0001g10380		-3.12	WOX	VIT_01s0011g05020		-1.92
HEX	VIT_01s0026g01950		-1.80		VIT_17s0000g02460		-2.17
	VIT_04s0023g01330		1.91		VIT_18s0001g10160	-1.55	-3.72
	VIT_08s0007g04200		-4.21	WRKY	VIT_01s0010g03930		2.70
	VIT_10s0003g00380		1.93		VIT_06s0004g07500		2.59
	VIT_13s0156g00260		1.60		VIT_07s0005g01710		2.29
	VIT_14s0066g01440	-1.56			VIT_08s0058g00690		2.64
	VIT_18s0001g06430		-2.65		VIT_09s0018g00240		3.26
MADS-box	VIT_00s0211g00110	-2.40	-4.92		VIT_12s0059g00880		1.81
	VIT_00s0211g00180	1.78		ZF-HD	VIT_12s0035g00650	1.86	2.55
	VIT_14s0068g01800		2.04		VIT_12s0035g01880		-1.76
	VIT_14s0083g01030		-1.96		VIT_17s0000g00810		-2.10
	VIT_16s0022g02380		1.84		VIT_18s0001g12580		2.10
	VIT_17s0000g04990		1.86	ZFF	VIT_06s0004g03180		2.06
	VIT_17s0000g06340		1.72				

4.3.7 Common DEG and metabolites that significantly changed in response to GAc and shade

In addition to the DEG found to be specific for each treatment, 36 annotated genes were differentially expressed in both abscission inducing treatments, from which 5 DEG changed with a opposite expression pattern, whereas 31 changed followed the same trend (Table 4.11). The latter ones could be candidate genes involved in shared pathways leading to abscission Among the treatment-independent DEG, genes encoding a matrix metalloendoproteinase, acidic endochitinase, RuBisCO, glycogenin, lipase, mitochondiral maturases, enzymes from oxidative phosphorylation pathway, molecules involved in signal transduction, RNA polymerases**,** ribosomal proteins and a 1-cys peroxiredoxin involved in ROS scavenging mechanism were up-regulated in response to both stimulus. Genes encoding a cooper transporter, subtilisin-like protease, cytochrome P450, a subunit of exocyst complex, and MYB transcription factor were down-regulated. Genes that showed an opposite change in expression pattern encode a UGT74B1, glucose-6-phosphate translocator, blue Cu-protein and were up-regulated in GAc treatment and down-regulated in shade. Additionally, a gene encoding an ethylene-responsive transcription factor was up-regulated in shade while was repressed in samples from the GAc-treatment.

Among the 13 commonly altered metabolites in response to both thinning strategies, eight showed the same pattern in both imposed treatments, belonging mostly to the amino acids pathway, followed by fumarate from TCA cycle, 2-linoleoylglycerophosphoinositol derived from phospholipid metabolism, and pseudouridine from pyrimidine metabolism (Table 4.12).

On other hand, the phospholipid phosphoethanolamine and nicotianamine from cofactor functional category decreased in GAc treated samples and increased in those from shaded vines, while putrescine, inosine from purine pathway and arbutine and salidorise from secondary metabolism were increased in GAc- and reduced in shade-treated inflorescences (Table 4.5 and 4.12). Other gene family, vacuolar H^+-ATPase, was affected by GAc (VIT_10s0003g04310) and shade (VIT_00s0187g00310, VIT_13s0175g00200, VIT_17s0000g00460, VIT_18s0001g13630) treatments, although not exactly the same genes have been involved (Supplementary Table S4.2).

Table 4.11. List of DEG simultaneous affected by GAc and shade treatments (p-value≤0.05), respective gene code identification, fold-change, annotation, UniProtKB accession number and KOG functional category. Data were obtained from 3 independent biological replicates. Bold letters indicate the metabolites showing opposite trend in both treatments.

Gene ID	GAc 5d	GAc 7d	SH 5d	SH 7d	Annotation	UniprotKB	NCBI	Functional category
VIT_14s0066g01960	1.71	1.77		3.51	metalloendoproteinase 1, predicted	F6HV36		Amino acid transport and metabolism
VIT_14s0060g00740		1.81		1.80	glycosyl transferase, family 8 - glycogenin, predicted	D7UA70		Carbohydrate transport and metabolism
VIT_07s0129g00790		2.02	1.77		ribulose-1,5-bisphosphate carboxylase /oxygenase subunit	F6HSX2		
VIT_01s0026g00630		**1.65**	**-1.99**	**-2.71**	**UDP-glycosyltransferase 74B1, predicted**	**F6HPK7**	**XM_002267629.2**	
VIT_06s0004g02710		**1.60**	**-2.64**	**-3.46**	**glucose-6-phosphate/phosphate antiporter, predicted**	**D7SKZ8**	**XM_002285193.2**	
VIT_15s0046g01600		2.11		2.77	acidic endochitinase, predicted	F6I685	XM_002279522.2	Cell wall/membrane/envelope biogenesis
VIT_18s0001g06580		**1.60**	**-3.04**	**-3.11**	**blue copper protein-like, predicted**	**F6H0Y2**	**XM_002285700.3**	Coenzyme transport and metabolism
VIT_00s0733g00010		1.83	2.60		ATPase subunit 1 (mitochondrion)	F6I2F8		Energy production and conversion
VIT_00s0332g00170		1.78	2.04		NADH:ubiquinone oxidoreductase, NDUFS2/49 k subunit (mitochondrion), predicted	F6HSD9		
VIT_08s0056g01060		2.25	2.29		NADH dehydrogenase subunit 1 (chloroplast)	F6HMW4		
VIT_14s0108g01640	1.64	2.27	2.56		NADH-plastoquinone oxidoreductase subunit 2 (chloroplast)	F6H5N4		
VIT_13s0067g03310		2.15	1.67		ATPase subunit, predicted	F6HC65		
VIT_01s0011g04110		1.75	2.22	2.39	NADH dehydrogenase subunits 2, 5, predicted	F6HEV2		
VIT_00s0246g00050		1.93	2.32	2.17	NADH dehydrogenase subunits 2, 5, predicted	D7TKT1		
VIT_00s0332g00140		1.61	1.70		NADH:ubiquinone oxidoreductase, NDUFS2/49 kDa subunit, predicted	D7TSH3		
VIT_00s0246g00070		1.96		2.22	NADH:ubiquinone oxidoreductase, NDUFS2/49 kDa subunit, predicted	F6HMJ6		
VIT_10s0116g00060		2.04	2.18		NADH:ubiquinone oxidoreductase, NDUFS2/49 kDa subunit, predicted	E0CVJ6		
VIT_10s0092g00770	1.68	2.27	2.79		cytochrome c biogenesis C (mitochondrion)	F6I3K0	XM_010657573.1	
VIT_03s0110g00360		-2.04		-1.88	copper transporter 6-like, predicted	A5AQX0	XM_003631673.2	Inorganic ion transport and metabolism
VIT_18s0072g00740		-1.55	-1.68	-1.75	sec5 subunit of exocyst complex, predicted	F6GY22		Intracellular traff., secretion, vesic. transp.
VIT_07s0031g00570		1.66		3.41	lipase, predicted	D7SVX1		Lipid transport and metabolism
VIT_18s0001g10330		-1.60		-4.02	subtilisin-like protease	F6H1C2		Posttranslational modification, protein turnover, chaperones
VIT_00s0332g00010		1.81	2.13		mitochondrial mRNA maturase	F6HSC8		RNA processing and modification
VIT_00s0332g00030	1.57	1.83	2.23		mitochondrial mRNA maturase, predicted	F6HSD0		
VIT_08s0007g01910		**1.90**	**-3.05**	**-4.22**	**laccase-4, predicted**	**D7THA7**	**XM_002278602.3**	Secondary metabolites biosynthesis, transport and catabolism
VIT_17s0000g01490		-1.81	-1.88	-2.05	cytochrome P450 94A1-like, predicted	F6GST7	XM_002279945.2	

Table 4.11 (continued). List of DEG simultaneous affected by GAc and shade treatments (*p*-value≤0.05), respective gene code identification, fold-change, annotation, UniProtKB accession number and KOG functional category. Data were obtained from 3 independent biological replicates. Bold letters indicate the metabolites showing opposite trend in both treatments.

Gene ID	GAc 5d	GAc 7d	SH 5d	SH 7d	Annotation	UniprotKB	NCBI	Functional category
VIT_02s0012g00820		2.60	2.08		serine/threonine protein kinase, predicted	F6HTC0		Signal transduction mechanisms
VIT_02s0012g00720		2.65	2.14		serine/threonine protein kinase, predicted	D7TTF6		
VIT_12s0028g02570		1.80	2.60	3.46	calmodulin and related proteins (EF-Hand superfamily), predicted	E0CTM8	XM_002279084.2	
VIT_08s0056g00900	1.76	1.87	2.03	2.12	RNA polymerase II, second largest subunit, predicted	F6HMV9		Transcripton
VIT_14s0108g01010	-1.50	-1.90	-1.63	-2.47	transcription factor, Myb superfamily, predicted	F6H5U7		
VIT_09s0002g04540	1.81	2.02	1.96		DNA-directed RNA polymerase subunit beta	D7U0K0		
VIT_15s0024g01960		2.39	2.28		RNA polymerase III, large subunit, predicted	D7UBC3		
VIT_05s0077g01860		**-1.56**		**1.68**	**ethylene-responsive transcription factor RAP2-3, predicted**	**D7SYA3**	**XM_002272390.2**	
VIT_00s0173g00170		2.10	1.74	2.33	30S ribosomal protein S7, chloroplastic, predicted	F6HD03		Translation
VIT_10s0092g00790		2.04	2.42		ribosomal protein S19, mitochondrial-like, predicted	D7U8H6		
VIT_02s0033g00990		2.55	2.71		ribosomal protein S7 (chloroplast)	F6I086		
VIT_16s0039g00380		1.77	1.85		mitochondrial/chloroplast ribosomal protein S14/S29, predicted	F6GZ45		
VIT_12s0028g00970		2.20	1.80	2.33	ribosomal protein S7, predicted	F6HRD9		
VIT_09s0070g00900		1.87	1.92	2.37	ribosomal protein S7, predicted	D7U8C4		
VIT_09s0070g00920		1.79	1.84	2.41	ribosomal protein S7, predicted	D7U8C4		
VIT_13s0047g00220		2.12	2.60		mitochondrial/chloroplast ribosomal protein S19, predicted	D7TF26		
VIT_02s0033g00980		2.79	2.88		ribosomal protein S7, predicted	F6I085		
VIT_00s0396g00050		1.81	2.67		ribosomal protein S4 (mitochondrion)	F6HRU1	XM_010648649.1	
VIT_05s0020g00600		1.66		1.91	1-cys peroxiredoxin	D7T674	NM_001281268.1	Other

Table 4.12. List of metabolites simultaneous affected by GAc and shade treatments (*p*-value≤0.05), respective functional class and pathway, KEGG compound number and fold-change. Data were obtained from 3 independent biological replicates. Bold letters indicate the metabolites with opposite trend.

Metabolite	GAc 5d	GAc 7d	SH 5d	SH 7d	KEGG	Pathway	Super pathway
2-aminoadipate	0.52			1.09	C00956	Aspartate family	Amino acid and peptide
N-acetylputrescine	-0.25		-0.92	-1.39	C02714	Glutamate family	
Homostachydrine	0.71		1.39	0.84	C08283		
Isoleucine	0.49		2.26	1.83	C00407	Branched Chain Amino Acids	
5-methylthioadenosine (MTA)	1.17		1.42		C00170	Amine	
Fumarate	0.57			0.46	C00122	TCA cycle	Carbohydrate
Phosphoethanolamine	**-0.39**			**1.52**	**C00346**	Phospholipids	Lipid
2-linoleoylglycerophosphoinositol	0.91		0.98			Phospholipids	
Nicotianamine	**-1.04**		**1.49**	**1.70**	**C05324**	Nicotinamide	Cofactor
Inosine	**0.80**			**-0.55**	**C00294**	Purine	Nucleotide
Pseudouridine	0.85			0.82	C02067	Pyrimidine	
Arbutine	**0.51**		**-0.72**		**C06186**	Benzenoids	Secondary metabolism
Salidroside	**2.02**		**-2.69**			Phenylpropanoids	

4.4 Discussion

4.4.1 What makes a flower to abscise?

Flower abscission depicted by –OMIC approaches disclosed complex cross-talk between different regulatory levels, including adjustments of metabolism, gene expression and physiology. In grapevine, natural flower drop occurs between 6 and 12 days after 100% cap fall (d) (Bessis and Fournioux, 1992) and peaks at 10 d under our experimental conditions (data not shown). Our data revealed that GAc and shade induced flower abscission by opposite effects on cell metabolism at 5 and 7 d, but converging on some common pathways leading to abscission.

As previously reported, PA metabolism pathway have a key role in reproductive organs abscission (Aziz, 2003; Domingos et al., 2015; Gomez-Jimenez et al., 2010; Malik and Singh, 2003; Parra-Lobato and Gomez-Jimenez, 2011). Changed putrescine inflorescence content varied with the imposed treatment, increasing and decreasing in result of GAc- and shade-treatment, respectively. Whereas putrescine catabolism, by conversion on N-acetylputrescine and/or biosynthesis of downstream PAs spermidine and spermine with the accumulation of MTA, was affected in the same direction in both treatments (Table 4.12). MTA is produced from SAM mainly through the spermidine and spermine biosynthetic pathway, where it behaves as a powerful inhibitory product (Bagga et al., 1997), suggesting that the regulation of the downstream PAs biosynthetic step, but not the biosynthesis of its precursor putrescine, is a common signal of abscission. In addition, in inflorescences developing under shaded conditions,

the observed up-regulation of a gene encoding SAM decarboxylase (EC 4.1.1.50) and repression of the subsequent step of spermidine biosynthesis, by the down-regulation of a putative *SPERMIDINE SYNTHASE* 2 gene (VIT_17s0000g08030) indicates that this step of PAs metabolism was also regulated at transcriptome level (Supplementary Table S4.2). This is in accordance with observations of abscission inhibition by application of exogenous spermidine, but not of putrescine, prior to flowering (Aziz, 2003). MTA is also a by-product of nicotianamine, a chelator of metals which was accumulated in response to shade and reduced after GAc treatment (Table 4.12), and ethylene biosynthesis pathways (Waduwara-Jayabahu et al., 2012). Ethylene biosynthetic pathway was significantly affected only by shade treatment (Table 4.8), while the expression of *ERF RAP2-3* was induced by shade and repressed by GAc treatment, thus suggesting that the ethylene signal transduction pathway was differentially regulated according to the treatment (Table 4.11).

Two common events were the up-regulation of both genes involved in RNA metabolism, such as those encoding RNA polymerases and ribosomal proteins, and energy production related genes, such as NADH dehydrogenases, cytochrome *c* and ATPase (Table 4.11), suggesting an increased demand for energy. NADH:ubiquinone oxidoreductase, a member of NADH dehydrogenase family, and cytochrome *c* are members of the respiratory chain, acting to generate a proton gradient which is thereafter used for ATP synthesis through H^+-transporting ATPase. The up-regulation of chloroplastic NADH dehydrogenases suggested that chlororespiration, which is associated with ROS alleviation around photosystems (Rumeau et al., 2007), is also induced as response to both treatments.

In addition to genes encoding serine/threonine protein kinases and calmodulin protein, which are components of signal transduction pathways, a gene encoding a subtilisin-like protease, described to be involved in protein turnover, generation and processing of peptide signals and PCD (Butenko et al., 2009; Cao et al., 2014; Schaller et al., 2012; Srivastava et al., 2008), was commonly affected by abscission-inducing stimulus (Table 4.11). The higher transcript accumulation of a gene encoding a specific antioxidant 1-cys peroxiredoxin enzyme (EC 1.11.1.15), which is prone to be reduced by ascorbic acid or glutathione, was additionally found to be common after both abscising inducing treatments. This observation agrees with previous works that described the multiple ROS roles in abscission including signaling, ROS-sugar-hormone cross talk and induction of the expression of CW-degrading enzymes (Botton et al., 2011; Sakamoto et al., 2008). Other changes on enzymatic and non-enzymatic oxygen stress remediation mechanisms were found to be specific from each abscission-triggering *stimulus*. In particular, the accumulation of the antioxidants arbutin, salidroside, and the expression of genes encoding a laccase 4 and other blue Cu-protein were contrasting between the two treatments,

indicating different ROS detoxification instruments triggered by GAc or by shade in treated inflorescences (Table 4.11 and 4.12).

Regarding amino acid metabolism, the observed induction of lysine and isoleucine biosynthetic pathways revealed that both treatments are abiotic stress-impacted. In addition to its function as a building block of proteins, lysine is also a precursor for glutamate, an important signaling amino acid that regulates plant growth and plant-environment responses (Galili, 2003). On the other hand, isoleucine is accumulated as an compatible osmolyte, playing a role in plant stress tolerance (Joshi et al., 2010).

In lipid-related pathways, changes in glycerolipids and phospholipids metabolism indicated alterations on cell membrane stability and signaling lipids content (Jouhet et al., 2007; Zhu, 2002), as candidates to common markers of abscission.

The common event of increased transcription of genes encoding glycogenin and RuBisCO enzymes, suggests that, in what concerns carbohydrate metabolism, conversion of glucose to the energy storage polymer glycogen and CO_2/O_2 fixation were affected in both samples (Table 4.11). At the metabolite level, the accumulation of fumarate from TCA cycle (Table 4.12) was also reported to be associated to flower shedding in response to the same treatments, under greenhouse conditions (Domingos et al., 2015). Among the multiple functions of fumarate, are the involvement in pH regulation, nitrogen assimilation and growth, stomatal movement and signaling and as a respiratory substrate during carbon starvation (Araújo et al., 2011; Arias et al., 2013). Expression of genes encoding vacuolar H^+-ATPase genes involved in pH regulation was affected by both treatments, although exclusive up-regulation was only found in GAc treated inflorescences (Supplementary Table S4.2). This overexpression agrees with the recent findings of cytosolic alkalization as part of abscission pathways and occurring concomitantly with the execution of organ abscission (Sundaresan et al., 2015).

Pathogenesis-related genes, as the *ACIDIC ENDOCHITINASE* up-regulation in inflorescences submitted to both treatments (Table 4.11), are reportedly expressed at the site where organs will be shed during abscission (Meir et al., 2011; Nakano et al., 2013), and proposed to act in establishing a defense system at the plant's side.

4.4.2 The GAc abscission inducing mechanism requires energy production and a global metabolism stimulation

Although the GAc effect is known to be largely dependent on the microclimate conditions (Domingos et al., 2015), GAc application at bloom was a successful treatment to promote flower abscission (Table 4.1), and cluster loosening at harvest (Table 4.2), in 'Thompson Seedless' vines growing in open field at south Portugal conditions.

The process by which exogenous application of GAc significantly increased flower abscission, seemed to be primarily activated by a non-enzymatic mechanism, resulting in a higher number of changes on metabolites content at 5d comparing to 7d (Supplementary Table S4.3), and a significant transcriptomic reprogramming noticed at 7d (Fig. 4.3B). Non-enzymatic reactions are non-targetable reactions widespread and integral part of metabolism, occurring spontaneously as a consequence of the chemical properties of the metabolites and including reaction of synthesis, redox, decomposition, replacement and isomerisation analogous to principal enzyme categories (Iuliano, 2011; Keller et al., 2015; Nagase et al., 1997; Signorelli et al., 2015).

Thus, our data suggests that GAc spraying led to different levels of metabolism regulation in the grape inflorescences, predominantly *via* non-enzymatic pathway at 5d and a combination of gene-dependent and -independent pathway at 7d. This resulted in modifications on the levels of amino acids and peptides, nucleotide, carbohydrates, lipids, cofactor and secondary metabolisms, energy production and conversion and signal transduction mechanisms (Fig. 4.4).

Although the leaf P_n values have not been significantly affected by GAc treatment (Table 4.1), in inflorescences it was observed the up-regulation of two genes encoding photosystem I assembly protein and photosystem II reaction center, as well as three genes encoding RuBisCO, as disclosed by RNA-Seq (Supplementary Table S4.2). These indicators suggested a global reinforcement of the photosynthetic machinery in inflorescences, what might have been accompanied also by an increase in photorespiration and chlororespiration, since glycolate contents increased accompanied by the up-regulation of seven genes encoding chloroplastic NADH dehydrogenase complex units (Fig. 4.6 and Supplementary Table S4.2). Photorespiration and chlororespiration both involve the oxidation of carbohydrates, the consumption of oxygen and are associated with light energy dissipation (Guan et al., 2004; Quiles and López, 2004; Rumeau et al., 2007). Likewise, respiration seemed be enhanced in GAc treated inflorescences, as revealed by the up-regulation of other 13 genes encoding NADH dehydrogenases, one encoding cytochrome b and two encoding cytochrome c oxidase from respiratory electron transport chain in mitochondria (Fig. 4.6 and Supplementary Table S4.2). These results concerning the photosynthetic and respiration pathways suggested therefore a stimulation of the energy metabolism on inflorescences.

This hypothesis is further supported by the accumulation of the precursor ribose, purine and pyrimidine nucleotides (Supplementary Table S4.3), which play a central role as energy carriers and subunits of nucleic acids, therefore indicating not only a global increased in cell metabolism, but also in gene expression. The up-regulation of DEG assigned to sugar and polysaccharide-related pathways also pinpoints an induction of carbohydrates metabolism.

Accordingly, the decreased glucose 6-phosphate, fructose-1,6-biphosphate and mannose-6-phosphate (Fig. 4.6) suggests a degradation of these molecules to generate ribulose-5-phosphate, which is a precursor of the nucleotides synthesis. Furthermore, the overall induction of nucleotide and carbohydrates metabolism in response to GAc used as abscission inducing treatment in grapevine was previously reported (Domingos et al., 2015).

The increase of mannitol content is known be related to stress tolerance due to the osmoprotectant function (Keunen et al., 2013). In addition to the compounds with antioxidant activity previously discussed as having similar or opposite patterns in response to the two treatments, only GAc promoted an accumulation of the ascorbate-precursor galactose (Smirnoff and Wheeler, 2000), in agreement with the observed increase in dehydroascorbate, previously reported in a different genetic background (Domingos et al., 2015).

GAc caused changes in the inflorescences levels of transcripts and metabolites involved in the secondary metabolism at bloom (Fig. 4.6), similarly to what was previously observed in an earlier phenological stage (pre-bloom) (Cheng et al., 2015). The quercetin-3-O-glucoside and naringenin accumulation and repression of a gene encoding a hyoscyamine 6-dioxygenase suggests induced flavonoids metabolism. In particular, a gene encoding an UDP-glycosyltransferase 74B1, proposed to be involved in the secondary metabolism and as a defense response by callose deposition into the CW, is also part of IAA biosynthetic pathway. Hence, the up-regulation of this gene suggests that the increment of auxin contents might be needed for the GAc-induced responses (Chai et al., 2014). On the other hand, taking into account the down-regulation of *GIBBERELLIN 3-β-DIOXYGENASE 1* and the increased GA_8 content which results from GA_1 inactivation (Fig. 4.6 and Table 4.5), a reduction of the endogenous bioactive GA level can be suggested, probably due to a negative-feedback regulation promoted by GAc spraying, as previously observed after GAc treatments in different phenological stages (Chai et al., 2014; Cheng et al., 2015). An auxin regulation of bioactive GAc levels has been suggested, corroborating this assumption (Yamaguchi, 2008).

4.4.3 Shade induced abscission by nutritional stress and global metabolism repression

The Thompson Seedless cultivar showed to be sensitive to shade imposed at 50% cap fall and during 14 days, resulting in increased flower drop percentages (Table 4.1). These observations at bloom stage together with depicted shorter rachis and less compact bunches, with a lower total number of berries and bunch weight (Table 4.2), suggests that this approach can be exploited as an alternative method for thinning berries on table grape production. The observed decline of P_n to zero will consequently decrease C-resources availability available to both vegetative and reproductive sinks. This will increase the competition between sinks (Corelli Grappadelli *et al.*, 1990; Byers *et al.*, 1991; Zibordi *et al.*, 2009), and promote flower abortion

(Lebon et al., 2008). Our results highlighted also the importance of the P_n during bloom to the developing cluster, despite the carbohydrate reserves (Caspari et al., 1998). Shading also affected leaf chlorophyll content, total leaf area and shoot growth (Table 4.1), showing a more pronounced effect in vegetative growth comparing to previously observations under in greenhouse conditions (Domingos et al., 2015). This might have been related to a higher percentage of light intercepted, to the different genetic background and to the field growing conditions, in the present work.

Shade induced flower abscission by C-starvation, as result of the down-regulation of a large group of genes involved in photosynthesis, carbohydrates metabolism and transport (Li et al., 2013; Zhu et al., 2011), and reduced carbon and carbon derived metabolites content (Aziz, 2003; Domingos et al., 2015) (Supplementary Table S4.2 and S4.4). The accumulation of arabonate and xylonate were the only exceptions at the metabolite level. These monosaccharides decorate CW polymers, such as pectins or xyloglucans, and its presence can result from CW remodeling processes that occur during pedicel AZ formation, protective layer differentiation on the proximal side after organ detachment (Lee et al., 2008) and alterations on CW structure and growth in adaptation to the imposed abiotic stress (Braidwood et al., 2013). Their accumulation is also in accordance to the differentially expression of pectinesterases (EC 3.1.1.11), polygalacturonases (EC 3.2.1.15), expansins, cellulose synthase (EC 2.4.1.12) and callose synthase (EC 2.4.1.34). Consistently, starch and sucrose metabolisms were the most represented affected pathways (Supplementary Table S4.4). These metabolisms are reported to be very sensitive to environment changes, which promote the mobilization of stored carbohydrates to provide sugars with different roles in the cell metabolism (Krasensky and Jonak, 2012). The analysis of the impact of shade on sugar signaling pathway and transport (Table 4.7) showed that expression of genes from SnRK1 family was significantly affected. This family genes was identified as central regulator of the transcriptome in response to darkness and multiple types of stress signals triggering extensive transcriptional changes (Baena-González et al., 2007). The predominant up-regulation of trehalose-6-phosphate synthase (EC 2.4.1.15) genes, putatively promotes the synthesis of trehalose 6-phosphate to inhibit SnRK1 family, inducing gene expression growth-associated *via* SnRK1 signaling (Nunes et al., 2013). Hexose kinases, which phosphorylate glucose (hexokinase) and fructose (fructokinase), and invertases (EC 3.2.1.26, 3.2.1.48) involved in sugar signaling (Bihmidine et al., 2013; Granot et al., 2013; Lastdrager et al., 2014) showed to be implicated in organ abscission *via* shading, as previously reported (Zhu et al., 2011). Sucrose mobilization was also induced during shade *via* the up-regulation of a gene encoding the reversible sucrose synthase (EC 2.4.1.13), indicating altered sucrose and sucrose-derived metabolites, such as UDP-glucose, necessary for CW and glycoprotein biosynthesis, and sucrose-specific signaling pathway (Gupta and Kaur, 2005).

At transcriptomic and metabolomic levels, shade imposition led to a classic signature of carbon/nitrogen (C/N) imbalance due to carbon deficit, with a stimulation of amino acids metabolism, a repression of energy metabolites and carbon metabolites pathways and increased accumulation of oxidative stress markers (Baena-González and Sheen, 2008; Krasensky and Jonak, 2012). According to the amino acid and peptide biosynthesis, metabolism and transport associated pathways affected by the shade treatment (Supplementary Table S4.3), the increased content of the proteinogenic amino acids may result from amino acid biosynthesis and from enhanced protein turnover to free up amino acid carbon backbones for energy utilization. Particularly, the increased aromatic amino acids phenylalanine, tyrosine and tryptophan contents might result from stress-induced protein breakdown, as revealed by the decline of the biosynthetic precursor shikimate levels, simultaneous with the down-regulation of genes encoding enzymes of the shikimate pathway, as shikimate kinase (EC 2.7.1.71) and the bi-functional enzyme 3-dehydroquinate dehydratase/shikimate 5-dehydrogenase (EC 4.2.1.10) (Supplementary Table S4.4). Our results are in accordance with previous studies which demonstrate that abiotic stresses enhance accumulation of beatine, proline and allantoin (Alamillo et al., 2010; Krasensky and Jonak, 2012; Wang et al., 2012). Allantoin, which was the mostly increased metabolite in inflorescences developing under shade (Supplementary Table S4.3), often accumulates as a response to C/N imbalances, and results from purine degradation is implicated in nitrogen metabolism and stress tolerance by activation of abscisic acid metabolism (Watanabe et al., 2014).

Our data suggests that, under shade imposition, ABA biosynthesis, catabolism and signaling pathways were stimulated (Table 4.8). The effect of ABA in abscission can be directly related to the activation of ABA-signaling genes and/or indirectly associated to an ACC increase and to ethylene biosynthesis (Botton et al., 2011; Gomez-Cadenas et al., 2000). On the other hand, ethylene accumulation can promote ABA catabolism as a consequence of increased ABA 8′-hydroxylase activity (Saika et al., 2007), which resulted in a reduced net ABA content (Table 4.5). The decreased ABA content was also observed by Zhang et al. (2011), as response from the soybean reproductive structures to shading.

Ethylene-auxin balance is recognized as one of the most important regulators of organ abscission determination (Basu et al., 2013; Dal Cin et al., 2005). The acquisition of sensitivity to ethylene by the AZ cells has been associated with an altered expression of auxin-regulated genes as a result of auxin depletion (Meir et al., 2010). Moreover, (Basu et al., 2013) showed that auxin regulates the timming of organ abscission and that a functional IAA signaling pathway is required for setting up the event. Our data shows that auxin biosynthesis was induced in shaded-treated inflorescences, and the auxin signaling pathway was active with the up-regulation of genes encoding auxin receptors TIR1 and ABP and down-regulation of

Aux/IAA and *ARF* genes which mediate the expression of several genes encoding auxin and IAA induced proteins in both time points investigated (Table 4.8). On the other hand, the up-regulation of a gene encoding an IAA-amido synthetase GH3.9 only at 5d, as previously observed in shade-induced lychee abscission (Li et al., 2013), indicated that auxin conjugation reducing the free IAA content, can exert an important role in auxin-ethylene balance. Accordingly, auxin transport showed to be repressed by down-regulation of *AEC* genes only at 7d, as previously reported by (Zhu et al., 2011) in response to the fruit abscission induction by naphthaleneacetic acid application.

Ethylene biosynthesis and signal transduction pathways were induced in shade treated inflorescences, involving the accumulation of cyano-alanine (Supplementary Table S4.3) and the predominantly up-regulation of genes encoding ACC oxidases and *EIN3* and differentially regulation of ERF family of transcription factors involved in activation or repression of transcription activity (Nakano et al., 2014; Taylor and Whitelaw, 2001) (Table 4.8). In particular key elements of MAPK cascades related to ABA and ethylene signal transduction pathways (Harrison, 2012), and known to be involved in floral organ abscission (Cho et al., 2008) were regulated, as those coding for MAPK3, MAPK4, MAPKK5 and MAPKK6 (Table 4.8). In addition, GTPase mediated signal transduction, upstream of MAPK cascades (Xin et al., 2005), was induced during shade treatment (Table 4.6) and was previously shown to be involved in leaf abscission signaling and ethylene biosynthesis (Yuan et al., 2005) and to regulate the movement of key molecules required for abscission (Liljegren, 2012). GAs biosynthetic and signaling pathways were predominantly repressed, accordingly with Mahouachi et al. (2009) that demonstrated that fruit abscission is enhanced by low carbohydrates and GAs availability.

The significant impact on CKs activation, perception and degradation caused by light reduction during bloom (Table 4.8) highlights the role of this hormones class, and is in accordance with the described CKs action as abscission-accelerating signal (Botton et al., 2011), although following the hypothesis of having ethylene regulation (Dal Cin et al., 2007). Also BR, SA and JA metabolism were correlated with the abscission boost caused by shade (Table 4.8). The accumulation of SA content agrees with the down-regulation of genes encoding salicylate-O-methyltransferase and the general up-regulation of genes encoding phenylalanine ammonia-lyase (Supplementary Table S4.4) involved in its own biosynthesis (Chen et al., 2009). In addition, the accumulation of oxidized lipids confirmed to occur in response to shade, as 13-HODE and 9-HODE, products of elevated oxidative status, have been linked to the JA biosynthetic pathway (Kunkel and Brooks, 2002).

Some of the most striking changes observed in shaded inflorescence samples were represented by DEG and accumulation of metabolites associated with oxygen stress remediation (Table 4.9

and Supplementary Table 4.4), and amongst them, the intermediates of the glutathione synthesis cycle were the most represented, as previously reported (Domingos et al., 2015). On the other hand, ascorbate metabolism seemed to be inhibited, as suggested by the down-regulation of genes encoding ascorbate oxidase, ascorbate peroxidase and GDP-l-galactose phosphorylase, concomitantly with decreased levels of metabolites related with ascorbate metabolism. Regarding secondary metabolism, the fact that flavonoids and dipertenoids-related pathways had been predominantly repressed, while phenylpropanoids and stilbenoid-related pathways were predominantly induced (Supplementary Table S4.2 and S4.4), pinpoints a slowdown of biochemical reactions while promoting the activation of stress responses and defense systems during abscission (Wang et al., 2013).

Among the transcription factors differentially regulated by shade treatment, members of MADs-box, AP2, MYB, WRKY, zinc finger transcription factor families were previously described to participate in abscission regulation (Botton et al., 2011; Chen et al., 2011; Li et al., 2013; Meir et al., 2010; Zhu et al., 2011).

4.5 Conclusions

The two imposed treatments induced flower abscission by exerting different effects on grapevine inflorescences metabolism, agreeing with the mechanistic model previously proposed (Domingos et al., 2015). GAc treatment response suggested a reinforcement of the energetic metabolism simultaneously with induction of nucleotide biosynthesis and carbon metabolism. A global metabolism stimulation of the central flower (king flower), which open before the smaller lateral ones (Vasconcelos et al., 2009), by GAc application, can be hypothesize, promoting the fruit set of these flowers and the developmental inhibition and abscission of the later ones. On the other hand, shade imposition induced carbohydrate metabolism repression, promoting flower drop by the previously described abscission process *via* nutritional stress (Botton et al. 2011; Zhu et al., 2010) associated with sugar-, ethylene- and auxin-responsive signaling pathways engage in crosstalk with each other and with other signaling pathways to coordinate abscission. Regulation of PAs metabolism, activation of ROS scavenging mechanisms, alterations on ethylene signaling pathway and bioactive GA biosynthesis repression were identified as candidate common signatures of abscission.

Our data provided a new insight on alternative pathways leading to abscission, which can assist the development and optimization of strategies for abscission control in fruit crop species.

4.6 References

Acheampong AK, Hu J, Rotman A, Zheng C, Halaly T, Takebayashi Y, Jikumaru Y, et al. 2015. Functional characterization and developmental expression profiling of gibberellin signalling components in *Vitis vinifera*. *J. Exp. Bot.* 66: 1463–1476.

Alamillo JM, Díaz-Leal JL, Sánchez-Moran MV and Pineda M. 2010. Molecular analysis of ureide accumulation under drought stress in *Phaseolus vulgaris* L. *Plant. Cell Environ.* 33: 1828–1837.

Alexa A and Rahnenfuhrer J. 2010. topGO: enrichment analysis for gene ontology. *R Package version* 2.

Araújo WL, Nunes-Nesi A and Fernie AR. 2011. Fumarate: Multiple functions of a simple metabolite. *Phytochemistry*. 72: 838–843.

Arias CL, Andreo CS, Drincovich MF and Gerrard Wheeler MC. 2013. Fumarate and cytosolic pH as modulators of the synthesis or consumption of C(4) organic acids through NADP-malic enzyme in *Arabidopsis thaliana*. *Plant Mol. Biol.* 81: 297–307.

Aziz A. 2003. Spermidine and related metabolic inhibitors modulate sugar and amino acid levels in *Vitis vinifera* L.: possible relationships with initial fruitlet abscission. *J. Exp. Bot.* 54: 355–363.

Baena-González E, Rolland F, Thevelein JM and Sheen J. 2007. A central integrator of transcription networks in plant stress and energy signalling. *Nature*. 448: 938–942.

Baena-González E and Sheen J. 2008. Convergent energy and stress signaling. *Trends Plant Sci.* 13: 474–482.

Bagga S, Rochford J, Klaene Z, Kuehn GD and Phillips GC. 1997. Putrescine aminopropyltransferase is responsible for biosynthesis of spermidine, spermine, and multiple uncommon polyamines in osmotic stress-tolerant alfalfa. *Plant Physiol.* 114: 445–454.

Basu MM, González-Carranza ZH, Azam-Ali S, Tang S, Shahid AA and Roberts JA. 2013. The manipulation of auxin in the abscission zone cells of Arabidopsis flowers reveals that indoleacetic acid signaling is a prerequisite for organ shedding. *Plant Physiol.* 62: 96–106.

Bessis R, Charpentier N, Hilt C and Fournioux J-C. 2000. Grapevine fruit set: Physiology of the abscission zone. *Aust. J. Grape Wine Res.* 6: 125–130.

Bessis R and Fournioux JC. 1992. Abscission zone and berry drop in grapevine. *Vitis*. 31: 9–21.

Bihmidine S, Hunter CT, Johns CE, Koch KE and Braun DM. 2013. Regulation of assimilate import into sink organs: update on molecular drivers of sink strength. *Front. Plant Sci.* 4: 177.

Bolger AM, Lohse M and Usadel B. 2014. Trimmomatic: a flexible trimmer for illumina sequence data. *Bioinformatics*. btu170.

Bonghi C, Tonutti P and Ramina A. 2000. Biochemical and molecular aspects of fruitlet abscission. *Plant Growth Regul*. 31: 35–42.

Botton A, Eccher G, Forcato C, Ferrarini A, Begheldo M, Zermiani M, Moscatello S, et al. 2011. Signaling pathways mediating the induction of apple fruitlet abscission. *Plant Physiol.* 155: 185–208.

Braidwood L, Breuer C and Sugimoto K. 2013. My body is a cage: mechanisms and modulation of plant cell growth. *New Phytol.* 201: 388–402.

Butenko MA, Vie AK, Brembu T, Aalen RB and Bones AM. 2009. Plant peptides in signalling: looking for new partners. *Trends Plant Sci.* 14: 255–263.

Büttner M. 2007. The monosaccharide transporter(-like) gene family in Arabidopsis. *FEBS Lett.* 581: 2318–2324.

Byers R, Carbaugh D, C. P and Wolf T. 1991. The influence of low light on apple fruit abscission. *J. Hort. Sci. Biotech*. 66: 7-17.

Cao J, Han X, Zhang T, Yang Y, Huang J and Hu X. 2014. Genome-wide and molecular evolution analysis of the subtilase gene family in *Vitis vinifera*. *BMC Genomics*. 15: 1116.

Caspari HW, Lang A and Alspach P. 1998. effects of girdling and leaf removal on fruit set and vegetative growth in grape. *Am. J. Enol. Vitic.* 49: 359–366.

Chai L, Li Y, Chen S, Perl A, Zhao F and Ma H. 2014. RNA sequencing reveals high resolution expression change of major plant hormone pathway genes after young seedless grape berries treated with gibberellin. *Plant Sci.* 229: 215–224.

Chang S, Puryear J and Cairney J. 1993. A simple and efficient method for isolating RNA from pine trees. *Plant Mol. Biol. Report.* 11: 113–116.

Chen M-K, Hsu W-H, Lee P-F, Thiruvengadam M, Chen H-I and Yang C-H. 2011. The MADS box gene, FOREVER YOUNG FLOWER, acts as a repressor controlling floral organ senescence and abscission in Arabidopsis. *Plant J.* 68: 168–185.

Chen Z, Zheng Z, Huang J, Lai Z and Fan B. 2009. Biosynthesis of salicylic acid in plants. *Plant Signal. Behav.* 4: 493–496.

Cheng C, Jiao C, Singer SD, Gao M, Xu X, Zhou Y, Li Z, et al. 2015. Gibberellin-induced changes in the transcriptome of grapevine (*Vitis labrusca* × *V. vinifera*) cv. Kyoho flowers. *BMC Genomics*. 16: 128.

Cho SK, Larue CT, Chevalier D, Wang H, Jinn T-L, Zhang S and Walker JC. 2008. Regulation of floral organ abscission in *Arabidopsis thaliana*. *Proc. Natl. Acad. Sci.* 105: 15629–15634.

Chung HS and Howe GA. 2009. A critical role for the TIFY motif in repression of jasmonate signaling by a stabilized splice variant of the JASMONATE ZIM-domain protein JAZ10 in Arabidopsis. *Plant Cell*. 21: 131–145.

Coito JL, Rocheta M, Carvalho L, Amancio S. 2012. Microarray-based uncovering reference genes for quantitative real time PCR in grapevine under abiotic stress. *BMC Res. Notes.* 5: 220.

Colebrook EH, Thomas SG, Phillips AL and Hedden P. 2014. The role of gibberellin signalling in plant responses to abiotic stress. *J. Exp. Biol.* 217: 67–75.

Conesa A, Götz S, García-Gómez JM, Terol J, Talón M and Robles M. 2005. Blast2GO: a universal tool for annotation, visualization and analysis in functional genomics research. *Bioinformatics*. 21: 3674–3676.

Corelli Grappadelli L, Sansavini S and Ravaglia GF. 1990. Effects of shade and sorbitol on fruit growth andabscission in apple. *Proc. XXIII Int. Congr.*, Florence. 620.

Dal Cin V, Danesin M, Boschetti A, Dorigoni A and Ramina A. 2005. Ethylene biosynthesis and perception in apple fruitlet abscission (*Malus domestica* L. Borck). *J. Exp. Bot.* 56: 2995–3005.

Dal Cin V, Boschetti A, Dorigoni A and Ramina A. 2007. Benzylaminopurine application on two different apple cultivars (*Malus domestica*) displays new and unexpected fruitlet abscission features. *Ann. Bot.* 99: 1195–1202.

Davière J-M and Achard P. 2013. Gibberellin signaling in plants. *Development*. 140: 1147–1151.

Dieterle M, Thomann A, Renou J-P, Parmentier Y, Cognat V, Lemonnier G, Müller R, et al. 2005. Molecular and functional characterization of Arabidopsis Cullin 3A. *Plant J.* 41: 386–399.

Dokoozlian NK and Peacock WL. 2001. Gibberellic acid applied at bloom reduces fruit set and improves size of 'crimson seedless' table grapes. *HortScience*. 36: 706-709.

Domingos S, Scafidi P, Cardoso V, Leitao AE, Di Lorenzo R, Oliveira CM and Goulao LF. 2015. Flower abscission in *Vitis vinifera* L. triggered by gibberellic acid and shade discloses differences in the underlying metabolic pathways. *Front. Plant Sci.* 6: 457.

Else MA, Stankiewicz-Davies AP, Crisp CM and Atkinson CJ. 2004. The role of polar auxin transport through pedicels of *Prunus avium* L. in relation to fruit development and retention. *J. Exp. Bot.* 55: 2099–2109.

Estornell LH, Agustí J, Merelo P, Talón M and Tadeo FR. 2013. Elucidating mechanisms underlying organ abscission. *Plant Sci.* 199–200: 48–60.

Evans A, DeHaven C and Barrett T. 2009. Integrated, nontargeted ultrahigh performance liquid chromatography/electrospray ionization tandem mass spectrometry platform for the identification and relative. *Anal. Chem.* 6656–6667.

Evans AM, Mitchell MW, Dai H and DeHaven CD. 2012. Categorizing ion –features in liquid chromatography/mass spectrometry metobolomics data. *Metabolomics:Open Access*. 2: 111.

Faccioli P, Stanca AM, Morcia C, Alberici R, Terzi V. 2010. Identification of a set of widely expressed genes in grape (*Vitis vinifera* L.) and its functional characterisation: a multi-evidence based study. *Vitis.* 49: 175–179.

Ferree DC, McArtney SJ and Scurlock DM. 2001. Influence of irradiance and period of exposure on fruit set of french-american hybrid grapes. *J. Am. Soc. Hortic. Sci.* 126: 283–290.

Fujita Y, Nakashima K, Yoshida T, Katagiri T, Kidokoro S, Kanamori N, Umezawa T, et al. 2009. Three SnRK2 protein kinases are the main positive regulators of abscisic acid signaling in response to water stress in Arabidopsis. *Plant Cell Physiol*. 50: 2123–32.

Galili G. 2003. New insights into the regulation and functional significance of lysine metabolism in plants. *Annu. Rev. Plant Biol.* 53: 27-43.

Giacomelli L, Rota-Stabelli O, Masuero D, Acheampong AK, Moretto M, Caputi L, Vrhovsek U, et al. 2013. Gibberellin metabolism in *Vitis vinifera* L. during bloom and fruit-set: functional characterization and evolution of grapevine gibberellin oxidases. *J. Exp. Bot.* 64: 4403–19.

Giulia E, Alessandro B, Mariano D, Andrea B, Benedetto R and Angelo R. 2013. Early induction of apple fruitlet abscission is characterized by an increase of both isoprene emission and abscisic acid content. *Plant Physiol.* 161: 1952–1969.

Gomez-Cadenas A, Mehouachi J, Tadeo FR, Primo-Millo E and Talon M. 2000. Hormonal regulation of fruitlet abscission induced by carbohydrate shortage in citrus. *Planta*. 210: 636–643.

Gomez-Jimenez MC, Paredes MA, Gallardo M and Sanchez-Calle IM. 2010. Mature fruit abscission is associated with up-regulation of polyamine metabolism in the olive abscission zone. *J. Plant Physiol.* 167: 1432–1441.

Granot D, David-Schwartz R and Kelly G. 2013. Hexose kinases and their role in sugar-sensing and plant development. *Front. Plant Sci.* 4: 44.

Guan XQ, Zhao SJ, Li DQ and Shu HR. 2004. Photoprotective function of photorespiration in several grapevine cultivars under drought stress. *Photosynthetica*. 42: 31–36.

Gülçin I. 2006. Antioxidant and antiradical activities of L-carnitine. *Life Sci.* 78: 803–11.

Gupta AK and Kaur N. 2005. Sugar signalling and gene expression in relation to carbohydrate metabolism under abiotic stresses in plants. *J. Biosci.* 30: 761–776.

Harrison MA. 2012. Phytohormones and Abiotic Stress Tolerance in Plants. in Khan NA, Nazar R, Iqbal N and Anjum N. (Eds.), *Phytohormones and abiotic stress tolerance in plants*. Springer-Verlag Berlin Heidelberg. 49–76.

Hed B, Ngug HK and W. TJ. 2011. Use of gibberellic acid for management of bunch rot on chardonnay and vignoles grape. *Plant Dis.* 95: 269-278.

Iuliano L. 2011. Pathways of cholesterol oxidation via non-enzymatic mechanisms. *Chem. Phys. Lipids*. 164: 457–68.

Jaillon O, Aury J-M, Noel B, Policriti A, Clepet C, Casagrande A, Choisne N, et al. 2007. The grapevine genome sequence suggests ancestral hexaploidization in major angiosperm phyla. *Nature*. 449: 463–467.

Joshi V, Joung J-G, Fei Z and Jander G. 2010. Interdependence of threonine, methionine and isoleucine metabolism in plants: accumulation and transcriptional regulation under abiotic stress. *Amino Acids*. 39: 933–947.

Jouhet J, Maréchal E and Block MA. 2007. Glycerolipid transfer for the building of membranes in plant cells. *Prog. Lipid Res.* 46: 37–55.

Kanehisa M, Araki M, Goto S, Hattori M, Hirakawa M, Itoh M, Katayama T, et al. 2007. KEGG for linking genomes to life and the environment. *Nucleic Acids Res.* 36: 480–484.

Keller MA, Piedrafita G and Ralser M. 2015. The widespread role of non-enzymatic reactions in cellular metabolism. *Curr. Opin. Biotechnol.* 34: 153–161.

Keunen E, Peshev D, Vangronsveld J, Van Den Ende W and Cuypers A. 2013. Plant sugars are crucial players in the oxidative challenge during abiotic stress: extending the traditional concept. *Plant. Cell Environ.* 36: 1242–1255.

Kim D, Pertea G, Trapnell C, Pimentel H, Kelley R and Salzberg SL. 2013. TopHat2: accurate alignment of transcriptomes in the presence of insertions, deletions and gene fusions. *Genome Biol.* 14: 36.

Krasensky J and Jonak C. 2012. Drought, salt, and temperature stress-induced metabolic rearrangements and regulatory networks. *J. Exp. Bot.* 63: 1593–1608.

Kulik A, Wawer I, Krzywińska E, Bucholc M and Dobrowolska G. 2011. SnRK2 protein kinases—key regulators of plant response to abiotic stresses. *Omi. A J. Integr. Biol.* 15: 859–872.

Kunkel BN and Brooks DM. 2002. Cross talk between signaling pathways in pathogen defense. *Curr. Opin. Plant Biol.* 5: 325–331.

Lastdrager J, Hanson J and Smeekens S. 2014. Sugar signals and the control of plant growth and development. *J. Exp. Bot.* 65: 799–807.

Lebon G, Wojnarowiez G, Holzapfel B, Fontaine F, Vaillant-Gaveau N and Clément C. 2008. Sugars and flowering in the grapevine (*Vitis vinifera* L.). *J. Exp. Bot.* 59: 2565–2578.

Lecourieux F, Kappel C, Lecourieux D, Serrano A, Torres E, Arce-Johnson P and Delrot S. 2014. An update on sugar transport and signalling in grapevine. *J. Exp. Bot.* 65: 821–832.

Lee Y, Derbyshire P, Knox JP and Hvoslef-Eide AK. 2008. Sequential cell wall transformations in response to the induction of a pedicel abscission event in *Euphorbia pulcherrima* (poinsettia). *Plant J.* 54: 993–1003.

Li C, Wang Y, Huang X, Li J, Wang H and Li J. 2013. De novo assembly and characterization of fruit transcriptome in *Litchi chinensis* Sonn and analysis of differentially regulated genes in fruit in response to shading. *BMC Genomics*. 14: 552.

Liljegren SJ. 2012. Organ abscission: exit strategies require signals and moving traffic. *Curr. Opin. Plant Biol.* 15: 670–676.

Looney NE and Wood DF. 1977. Some cluster thinning and gibberellic acid effects on fruit set, berry size, vine growth and yiels of De Chaunac grapes. *Can. J. Plant Sci.*57: 653-659.

Lopes C and Pinto PA. 2005,April15. Easy and accurate estimation of grapevine leaf area with simple mathematical models. *Vitis.* 44: 55–61.

Lorenz D, Eichhorn K, Bleiholder H, Klose R, Meier U and Weber E. 1994. Phänologische entwicklungsstadien der rebe (*Vitis vinifera* L. ssp. vinifera). – codierung und beschreibung nach der erweiterten BBCH-Skala. *Vitic. Enol. Sci.*49: 66-70.

Love MI, Huber W and Anders S. 2014. Moderated estimation of fold change and dispersion for RNA-seq data with DESeq2. *Genome Biol.* 15: 550.

Mahouachi J, Iglesias DJ, Agustí M and Talon M. 2009. Delay of early fruitlet abscission by branch girdling in citrus coincides with previous increases in carbohydrate and gibberellin concentrations. *Plant Growth Regul.* 58: 15–23.

Malik A and Singh Z. 2003. Abscission of mango fruitlets as influenced by biosynthesis of polyamines. *J. Hortic. Sci. Biotechnol.*78: 721-727.

Meir S, Philosoph-Hadas S, Sundaresan S, Selvaraj KSV, Burd S, Ophir R, Kochanek B, et al. 2010. Microarray analysis of the abscission-related transcriptome in the tomato flower abscission zone in response to auxin depletion. *Plant Physiol.* 154: 1929–1956.

Meir S, Philosoph-Hadas S, Sundaresan S, Selvaraj KSV, Burd S, Ophir R, Kochanek KSB, et al. 2011. Identification of defense-related genes newly-associated with tomato flower abscission. *Plant Signal. Behav.* 6: 590–593.

Nagase S, Takemura K, Ueda A, Hirayama A, Aoyagi K, Kondoh M and Koyama A. 1997. A novel nonenzymatic pathway for the generation of nitric oxide by the reaction of hydrogen peroxide and D- or L-arginine. *Biochem. Biophys. Res. Commun.* 233: 150–153.

Nakano T, Fujisawa M, Shima Y and Ito Y. 2013. Expression profiling of tomato pre-abscission pedicels provides insights into abscission zone properties including competence to respond to abscission signals. *BMC Plant Biol.* 13: 40.

Nakano T, Fujisawa M, Shima Y and Ito Y. 2014. The AP2/ERF transcription factor SlERF52 functions in flower pedicel abscission in tomato. *J. Exp. Bot.* 65: 3111–3119.

Niederhuth CE, Patharkar OR and Walker JC. 2013. Transcriptional profiling of the Arabidopsis abscission mutant hae hsl2 by RNA-Seq. *BMC Genomics*. 14: 37.

Nunes C, O'Hara LE, Primavesi LF, Delatte TL, Schluepmann H, Somsen GW, Silva AB, et al. 2013. The trehalose 6-phosphate/SnRK1 signaling pathway primes growth recovery following relief of sink limitation. *Plant Physiol.* 162: 1720–1732.

Ohta T, Masutomi N, Tsutsui N, Sakairi T, Mitchell M, Milburn M V, Ryals J a, et al. 2009. Untargeted metabolomic profiling as an evaluative tool of fenofibrate-induced toxicology in Fischer 344 male rats. *Toxicol. Pathol.* 37: 521–535.

Parra-Lobato MC and Gomez-Jimenez MC. 2011. Polyamine-induced modulation of genes involved in ethylene biosynthesis and signalling pathways and nitric oxide production during olive mature fruit abscission. *J. Exp. Bot.* 62: 4447–4465.

Patterson SE. 2001. Cutting Loose. Abscission and dehiscence in Arabidopsis. *Plant Physiol.* 126: 494–500.

Peer WA. 2013. From perception to attenuation: auxin signalling and responses. *Curr. Opin. Plant Biol.* 16: 561–568.

Perez FJ, Viani C and Retamales J. 2000. Bioactive gibberellins in seeded and seedless grapes: identification and changes in content during berry development. *Am. J. Enol. Vitic.* 51: 315–318.

Quast C, Pruesse E, Yilmaz P, Gerken J, Schweer T, Yarza P, Peplies J, Glöckner FO. 2013. The SILVA ribosomal RNA gene database project: improved data processing and web-based tools. *Nucl. Acids Res*. 41: 590-596.

Quiles MJ and López NI. 2004. Photoinhibition of photosystems I and II induced by exposure to high light intensity during oat plant growth. *Plant Sci.* 166: 815–823.

Rasmussen R. 2001. Quantification on the LightCycler. In Meuer S, Wittwer C and Nakagawara K-I (Eds.), *Rapid cycle real-time PCR, Methods and applications.* Springer Berlin Heidelberg, Berlin, Heidelberg. 21–34.

Reynolds AG, Roller JN, Forgione A and De Savigny C. 2006. Gibberellic acid and basal leaf removal: implications for fruit maturity, vestigial seed development, and sensory attributes of sovereign coronation table grapes. *Am. J. Enol. Vitic.* 57: 41–53.

Reynolds AG and Savigny C. 2004. Influence of girdling and gibberellic acid on yield components, fruit composition and vestigial seed formation of 'Sovereign Coronation' table grapes. *HortScience*. 39: 541-544.

Rohlf FJ. 2005. *NTSYS-pc: numerical taxonomy and multivariate analysis system*. Exeter Software, Setauket, New York, USA.

Roubelakis KA and Kliewer WM. 1976. Influence of light intensity and growth regulators on fruit-set and ovule fertilization in grape cultivars under low temperature conditions. *Am. J. Enol. Vitic.* 27: 163–167.

Ruan Y-L, Patrick JW, Bouzayen M, Osorio S and Fernie AR. 2012. Molecular regulation of seed and fruit set. *Trends Plant Sci.* 17: 656–665.

Rumeau D, Peltier G and Cournac L. 2007. Chlororespiration and cyclic electron flow around PSI during photosynthesis and plant stress response. *Plant. Cell Environ.* 30: 1041–1051.

Saika H, Okamoto M, Miyoshi K, Kushiro T, Shinoda S, Jikumaru Y, Fujimoto M, et al. 2007. Ethylene promotes submergence-induced expression of OsABA8ox1, a gene that encodes ABA 8'-hydroxylase in rice. *Plant Cell Physiol.* 48: 287–98.

Sakamoto M, Munemura I, Tomita R and Kobayashi K. 2008. Reactive oxygen species in leaf abscission signaling. *Plant Signal. Behav.* 3: 1014–1015.

Sawicki M, Aït Barka E, Clément C, Vaillant-Gaveau N and Jacquard C. 2015. Cross-talk between environmental stresses and plant metabolism during reproductive organ abscission. *J. Exp. Bot.* 66: 1707–1719.

Schaller A, Stintzi A and Graff L. 2012. Subtilases - versatile tools for protein turnover, plant development, and interactions with the environment. *Physiol. Plant.* 145: 52–66.

Signorelli S, Dans PD, Coitiño EL, Borsani O and Monza J. 2015. Connecting proline and γ-aminobutyric acid in stressed plants through non-enzymatic reactions. *PLoS One*. 10: e0115349.

Singh AP, Tripathi SK, Nath P and Sane AP. 2011. Petal abscission in rose is associated with the differential expression of two ethylene-responsive xyloglucan endotransglucosylase/hydrolase genes, RbXTH1 and RbXTH2. *J. Exp. Bot.* 62: 5091–5103.

Smirnoff N and Wheeler GL. 2000. Ascorbic acid in plants: biosynthesis and function. *Crit. Rev. Biochem. Mol. Biol*. 35:291-314

Srivastava R, Liu J-X and Howell SH. 2008. Proteolytic processing of a precursor protein for a growth-promoting peptide by a subtilisin serine protease in Arabidopsis. *Plant J.* 56: 219–227.

Sun T. 2010. Gibberellin-GID1-DELLA: a pivotal regulatory module for plant growth and development. *Plant Physiol.*154: 567–570.

Sundaresan S, Philosoph-Hadas S, Riov J, Belausov E, Kochanek B, Tucker ML and Meir S. 2015. Abscission of flowers and floral organs is closely associated with alkalization of the cytosol in abscission zone cells. *J. Exp. Bot.* 66: 1355–1368.

Suzuki R and Shimodaira H. 2006. Pvclust: an R package for assessing the uncertainty in hierarchical clustering. *Bioinformatics*. 22: 1540–1542.

Tatusov RL, Fedorova ND, Jackson JD, Jacobs AR, Kiryutin B, Koonin E V, Krylov DM, et al. 2003. The COG database: an updated version includes eukaryotes. *BMC Bioinformatics*. 4: 41.

Taylor JE and Whitelaw CA. 2001. Signal in abscission. *New Phytol.* 151: 323–339.

Trapnell C, Williams BA, Pertea G, Mortazavi A, Kwan G, van Baren MJ, Salzberg SL, et al. 2010. Transcript assembly and quantification by RNA-Seq reveals unannotated transcripts and isoform switching during cell differentiation. *Nat. Biotechnol.* 28: 511–515.

Tucker ML and Yang R. 2012. IDA-like gene expression in soybean and tomato leaf abscission and requirement for a diffusible stelar abscission signal. *AoB Plants*. pls035.

Vandesompele J, Kubista M and Pfaffl M. 2009. Reference gene validation software for improved normalization. In Logan J, Edwards K, Saunders N (Eds.), *Real-time PCR: current technology and applications.* Caister Academic, Norfolk. 47–63

Vasconcelos MC, Greven M, Winefield CS, Trought MCT and Raw V. 2009. The flowering process of *Vitis vinifera*: A Review. *Am. J. Enol. Vitic.* 60: 411–434.

Waduwara-Jayabahu I, Oppermann Y, Wirtz M, Hull ZT, Schoor S, Plotnikov AN, Hell R, et al. 2012. Recycling of methylthioadenosine is essential for normal vascular development and reproduction in Arabidopsis. *Plant Physiol.* 158: 1728–1744.

Wang P, Kong C-H, Sun B and Xu X-H. 2012. Distribution and function of allantoin (5-ureidohydantoin) in rice grains. *J. Agric. Food Chem.* 60: 2793–2798.

Wang X, Liu D, Li A, Sun X, Zhang R, Wu L, Liang Y, et al. 2013. Transcriptome analysis of tomato flower pedicel tissues reveals abscission zone-specific modulation of key meristem activity genes. *PLoS One*. 8: e55238.

Watanabe S, Matsumoto M, Hakomori Y, Takagi H, Shimada H and Sakamoto A. 2014. The purine metabolite allantoin enhances abiotic stress tolerance through synergistic activation of abscisic acid metabolism. *Plant. Cell Environ.* 37: 1022–1036.

Xin Z, Zhao Y and Zheng Z-L. 2005. Transcriptome analysis reveals specific modulation of abscisic acid signaling by ROP10 small GTPase in Arabidopsis. *Plant Physiol.* 139: 1350–1365.

Yamaguchi S. 2008. Gibberellin metabolism and its regulation. *Annu. Rev. Plant Biol.* 259: 225–251.

Yip WK and Yang S-F. 1998. Ethylene biosynthesis in relation to cyanide metabolism. *Bot. Bull. Acad. Sin.* 39: 1-7

Yuan R, Wu Z, Kostenyuk IA and Burns JK. 2005. G-protein-coupled alpha2A-adrenoreceptor agonists differentially alter citrus leaf and fruit abscission by affecting expression of ACC synthase and ACC oxidase. *J. Exp. Bot.* 56: 1867–1875.

Zhao Y, Tang H and Ye Y. 2012. RAPSearch2: a fast and memory-efficient protein similarity search tool for next-generation sequencing data. *Bioinformatics*. 28: 125–126.

Zhiponova MK, Vanhoutte I, Boudolf V, Betti C, Dhondt S, Coppens F, Mylle E, et al. 2013. Brassinosteroid production and signaling differentially control cell division and expansion in the leaf. *New Phytol.* 197: 490–502.

Zhu H, Dardick C, Beers E, Callanhan A, Xia R and Yuan R. 2011. Transcriptomics of shading-induced and NAA-induced abscission in apple (*Malus domestica*) reveals a shared pathway involving reduced photosynthesis, alterations in carbohydrate transport and signaling and hormone crosstalk. *BMC Plant Biol.* 11: 138.

Zhu J-K. 2002. Salt and drought stress signal transduction in plants. *Annu. Rev. Plant Biol.* 53: 247–273.

Zibordi M, Domingos S and Corelli Grappadelli L. 2009. Thinning apples via shading: an appraisal under field conditions. *J. Hort. Sci. Biotech.*84: 138-144.

Chapter 5

Light management and gibberellic acid spraying as thinning methods in seedless table grapes (*Vitis vinifera* L.): cultivar responses and effects on the final quality

The data presented in this chapter were submitted to VITIS- Journal of Grapevine Research:

Domingos S[1,2], Nobrega H[1], Raposo A[2], Cardoso V[2], Soares I[1], Ramalho JC[2], Leitão AE[2], Oliveira CM[1] and Goulao F.[2]

[1] Linking Landscape, Environment, Agriculture and Food, Instituto Superior de Agronomia, Universidade de Lisboa, Lisbon, Portugal

[2] Instituto de Investigação Científica Tropical, I.P., Lisbon, Portugal

5. Light management and gibberellic acid spraying as thinning methods in seedless table grapes (*Vitis vinifera* L.): cultivar responses and effects on the final quality

Abstract

In seedless table grapes, the excessive natural fruit set leads to compact bunches, small berries, with poor colour, low uniformity of maturation and higher incidence of diseases, requiring flower and fruit thinning to attain a profitable production. Here, gibberellic acid spraying (GAc) and imposition of shading nets, cutting incident irradiance by 90 or 100% at flowering were tested in consecutive years aiming to examine their influence on flower drop and consequent quality of ‘Sugraone’, 'Thompson Seedless' and 'Crimson Seedless' bunches and grapes. Concerning physiological responses during bloom, it was observed that shade treatments reduced leaf gas exchange and leaf growth rates while no differences were found in GAc-treated vines. Effects on leaf gas exchange showed to be reversible after shading net removal. Flower drop percentages increased in 'Sugraone' in response to 90% light reduction imposed at 50% bloom, and in 'Thompson Seedless' in response to GAc spraying and shade imposition, when compared to untreated vines. GAc treatment resulted in lower bunch compactness and improved berry quality in 'Thompson Seedless', while the effects on berry quality observed in 'Sugraone' and 'Crimson Seedless' were not consistent across the trials conducted in different years. Regarding shade treatments, bunches were significantly less compact by reducing the incident light by 90% and 100% at 50% bloom on 'Sugraone' and 'Crimson Seedless', respectively. In 'Thompson Seedless' vines, bunch compactness was improved after shade imposed both at 50 and 100% bloom. 'Thompson Seedless' was the more sensitive cultivar to GAc and shade thinning methods. In general, shade-promoted thinning induced a decrease on berry weight and diameter compared to untreated vines, to GAc treatments and to hand-thinning practices, leading to desired values of bunch compactness were achieved but without improvement of other bunch and berry quality characteristics.

Keywords: berry size, bunch compactness, fruit set, gibberellins, shade, phenolic composition, yield.

5.1 Introduction

In table grapes, natural fruit set is often excessive, requiring berry thinning practices to improve final bunch aspect and grape quality and to decrease the incidence of diseases and physical damages. Table grape overall quality encompasses quality parameters of both bunches and

berries. Major quality factor for bunches include weight and compactness (ratio between number of berries and rachis length). For berries, external colour uniformity, size and firmness, and internal features such as soluble solids content (SSC), SSC/Acidity ratio and phytochemicals content, namely polyphenols that contribute to organoleptic characteristics and have beneficial health effects (Xia et al., 2010), are among the most important quality attributes.

Hence, control of fruit set is mandatory to seedless table grape production because of its influence on yield and fruit quality. Berries removal can be achieved manually, in a very expensive and labour-consuming operation (50 to 80 labour days/ha) and/or chemically through the application of the growth regulator gibberellic acid (GAc). The choice for GAc sprays for thinning is common in seedless table grape varieties (Dokoozlian, 1998; Dokoozlian and Peacock, 2001) but the success of the applications depends on both endogenous (such as vine cultivar, phenological stage, physiological status and age) and exogenous conditions (such as nutrient and water availability, temperature, irradiation and humidity) during flowering (Weaver and Pool, 1971; Dokoozlian, 1998; Dokoozlian and Peacock, 2001). Therefore, for berry thinning using GAc optimum doses and treatment timings must be individually optimized for the different cultivars, and a large body of practical knowledge is required in order to tailor the treatment according to each year environmental conditions. On the other hand, GAc application can have several drawbacks like retardation of colour development, induction of post-harvest berries drop or causing physiological damages to the fruits (Zoffoli et al., 2009). Under this scenario, and due to nowadays market and consumer demand for safer environmental practices, alternative thinning methods have emerged or have been revisited in recent years. The effect of shade imposition at berry set, aiming at thinning via light management, was firstly investigated in grapevines by Roubelakis and Kliewer (1976), which succeeded in attainting a decreased number of berries per cluster by reducing the incident light (72% and 82%) in 'Carignane' vines, what was attributed to competition caused by carbon shortage. More recently, it was further verified that carbon shortage resulting from shade imposition during bloom and other practices, such as defoliation could reduce berry set and the final number of berries per bunch at harvest (Ferree et al., 2001; Lohitnavy et al., 2010; Intrigliolo et al., 2014). The alternative thinning via shade method was also successfully reported in apple (*Malus* × *domestica*), in which a higher number of studies were published (Byers et al., 1985, 1991; Byers, 2003; Schneider, 1975; Widmer et al., 2008; Zhou et al., 2008; Zibordi et al., 2009; Zhu et al., 2011), which modifies the balance source/sink for carbon. In fact, according to these authors, carbon balance in the tree stands was the most important factor that influences fruit abscission. Shading near bloom, in the specific and well determined period when the stored carbohydrates reach a minimum and the early fruit growth still depends primarily on current rates of photosynthesis, leads to a deficit in the carbon availability. This C-deficit will increase the competition between shoots and berries

for photosynthetic resources, reducing the amount of carbon partitioned to young fruitlets and ultimately causing fruit abscission. Also in grapevines, the moment of shade imposition is critical to induce suitable rates of flower abscission, which is caused by energy deprivation (Domingos et al., 2015). Similarly to apples, in this species, at bloom, the C-reserves are known to reach the minimum and a lack of newly sugar synthesis through photosynthesis would severelly reduce C-availability in flowers what may lead to drastic flower abortion (Zapata et al., 2004; Lebon et al., 2008). Yet, more experimental data is needed to increase the knowledge of the involved mechanism and to allow translating these physiological observations into a commercial thinning practice.

Therefore, the aim of this study was to investigate the potential of light reduction using shading nets and GAc application during bloom in Sugraone, Thompson Seedless and Crimson Seedless table grape cultivars as thinning methods, to reduce berry set and consequently improve bunch compactness and berries quality.

5.2 Material and methods

5.2.1 Plant material and experimental design

The experimental work was conducted in a commercial vineyard, established in 2006 in the south of Portugal (38° 05' 23,80" N, 8° 04' 52,7 1" W), with Sugraone, Thompson Seedless and Crimson Seedless (*V. vinifera* L.) cultivars, using five vines per treatment. Vines were grafted on ‘140 Ruggeri’ rootstock, spaced 3 x 3 m and grown on an overhead trellis system covered with plastic. The vineyard was managed following integrated fertilization, irrigation, and pest-management. Plant hydration was maintained at a high level, as reflected by the predawn leaf water potential values close to 0.2 MPa for the entire experiment.

Two experiments were conducted, each in two trials. In all cases, the second trial was optimized based on the results obtained in the previous year of experiments.

5.2.1.1 Experiment 1 - 'Sugraone' and 'Crimson Seedless' trials

Trials were performed in two consecutive years (trial 1 in 2012 and trial 2 in 2013). Treatments consisted in commercial thinning with GAc spraying (Berelex with 9% of gibberellic acid, Kenogard, Spain) at recommend doses for both cultivars (1 ppm) (Dokoozlian, 1998) at 100% cap fall and imposition of 90% and 100% of photosynthetic active radiation (PAR) reduction with polypropylene shading nets (Hubel, Portugal).

In both cultivars, in trial 1, 90% of PAR reduction was imposed at two moments during bloom: 50% and 100% cap fall, corresponding to stage 65 and 69 of the BBCH scale (S50B-90% and S100B-90% treatments). Vines were shaded for 14 and 11 days ('Sugraone'), or 23 and 19 days ('Crimson Seedless'), for S50B-90% and S100B-90% treatments, respectively. In both cultivars, in trial 2, 100% of PAR reduction was imposed at 50% and 100% cap fall (S50B-100% and S100B-100% treatments). The total number days during which the vines were submitted to was 24 and 21 in S50B-100% and S100B-100% treatments, for both cultivars. GAc was applied by spraying 1 ppm (GAc-1ppm) at 100% bloom in both trials.

Non-treated GAc vines, without shading net, were used as control.

5.2.1.2 Experiment 2 - 'Thompson Seedless' trials

Trials were performed in two consecutive years (trial 1 in 2013 and trial 2 in 2014). GAc spraying and the effect of 98% and 100% PAR reduction were investigated and compared to hand thinning performed 10 days after full bloom.

In trial 1, total PAR reduction was enforced at 50% and 100% cap fall (S50B-100% and S100B-100% treatments) and the total number of shaded days was 14 and 10, respectively. The GAc treatment was done by spraying at the recommended doses of 10ppm + 12.5ppm + 12.5ppm, sequentially at 20%, 50% and 100% cap fall (GAc-35ppm). Non-treated GAc vines, without shading net, were used as control.

In the second trial, shade nets were instaled at 50% cap fall, providing 98% (S50B-98%) and 100% (S50B-100%) of light interception for 14 days. GAc treatment was identical to trial 1 but the control was hand thinning executed at 10 days after 100% cap fall.

Aspects of the shading imposition are given in Supplementary Figure S5.1.

5.2.2 Physiological measurements

Climate conditions of temperature, relative humidity (RH) and PAR were monitored above the canopy of shaded and control vines (WatchDogMicroSta., Spectrum Tech., USA) during the bloom period for each cultivar and in each year. Flower drop rates were monitored with resource to non-woven cloth bags positioned around 10 bunches per treatment at full bloom. Cloth bags and shading nets were removed when berries were 6 mm diameter (stage 75 of the BBCH scale according to Lorenz et al.(1994)).

Leaf net photosynthetic (P_n) and stomatal conductance to water vapour (g_s) rates were obtained under steady-state conditions at *ca.* (10:00-12:00 a.m.) in eight mature leaves per treatment tagged from the central part of the main shoot, using a portable infrared gas analyzer (CIRAS 1;

PP Systems, USA), under external CO_2 of 380 L CO_2 L^{-1} and natural irradiance of *ca.*1200 μmol m^{-2} s^{-1}. Measurements were repeated during and 20 days after shading nets removal, on the three cultivars.

Primary leaf area was calculated at 100% cap fall and 15 after, in six shoots per treatment on 'Crimson Seedless' and 'Thompson Seedless', according to the non-destructive method described by Lopes and Pinto (2005).

Phloem exudates were collected from leaf pedicels using the method described by Zhang et al. (2006). Pedicels were cut under water and incubated in 20 mM EDTA solution pH 7.5 for 4 h, in a humid chamber at 20°C and stored at −80°C until use. The samples were analyzed for total sugars by an adapted anthrone method (DuBois et al., 1956; Devaux et al., 2009). Briefly, the solutions obtained by exudation were centrifuged at 11,000 g for 2 min, diluted 1:3 in distilled water and 50 μL aliquots were added to 2.5 mL of anthrone reagent. The colorimetric reaction was accelerated by heating at 80°C for 30 min and the total sugar content was determined spectrophotometrically (Unicam UV/Vis UV2, UK) by 560 nm absorbance readings and quantification based on known concentration sucrose standard curves.

5.2.3 Final quality and yield assessment

Harvest was done at commercial maturity of each variety, determined by the SSC. Bunch weight, total number of berries per bunch, and rachis length were determined in the same 10 bunches per treatment used for flower drop monitoring. The bunch compactness, determined as the number of berries cm^{-1} of rachis, the estimated initial number of flowers, calculated as the sum of the number of dropped flowers and the number of berries at harvest, and the percentage of flower drop, corresponding to the ratio between the number of dropped collected flowers and the initial number of flowers were also assessed. Eighteen berries per bunch were randomly sampled, to compose a pool from which forty-eight berries per treatment were used to measure weight, longitudinal and transversal diameters and firmness. Firmness values were obtained by compressing each berry with a flat probe to 5% deformation, with resource to a texture analyzer (TA-XT Plus, Stable Micro Systems, UK). The remaining berries were distributed in six samples per treatment and converted into juice to measure the SSC, using a hand refractometer (PR-32, Atago, Japan) and the titratable acidity (TA), by potentiometric titration with 0.1 N NaOH of each lot. Colour was measured by calculating the hue angle (h°), according to McGuire (1992). Berries skin composition on total polyphenols, and malvidin-3-O-glucoside, trans-resveratrol and (+)-catechin contents were determined in 'Thompson Seedless' and 'Crimson Seedless' samples. Total polyphenols extraction was performed according to Di Stefano et al. (1989) and Di Stefano and Cravero (1991). Briefly, thirty berries per treatment were peeled and the skins of each group of five berries were weighted and homogenized with 25

mL hydrochloric ethanol solution (ethanol-water-concentrated HCl 70:30:1, v/v/v). After twenty-four hours at room temperature, the homogenates were paper filtered. For total polyphenol content quantification the extracts were diluted 1.3 times with the same solution and it was determined by spectrophotometry (Unicam UV/Vis UV2, UK) absorbance readings at 700 nm. Malvidin-3-O-glucoside quantification was performed according to Ristic et al., (2007). Briefly, the initial extracts were clarified by centrifugation at 1,500 g for 5 minutes and filtration (0.45 μm), then diluted with twice their volume distilled water, and injected (20 μl) into a high performance liquid chromatography (HPLC, Beckman Coulter, USA) and separated on a C18 column (250 × 4 mm, 5 μm, SunFire, Waters, USA) with a flow rate of 0.4 mL min^{-1} and a binary gradient with mobile phases containing 20% solvent A (1.5% orthophosphoric acid) and 80% solvent B (acetonitrile). Anthocyanin was detected by a photodiode array detector (DAD, Beckman Coulter, USA) at 520 nm. Trans-resveratrol and (+)-catechin quantification was adapted from the methods described by Burns et al. (2002) and Lutz et al. (2011). Weighed aliquots of *ca.* 300 mg of berry skins were freeze-dried and homogenized with 0.5 mL methanol containing 2% formic acid. Samples were centrifuged at 10000g for 10 min and the supernatant was filtered (0.45 μm), injected (20 μl) and separated using the previously described HPLC and C18 column, with a flow rate of 1 mL min^{-1} with 25% acetonitrile in 0.5% aqueous formic acid. Trans-resveratrol was detected and quantified using a fluorescence detector (Jasco, Japan) operating at 298 nm excitation and 385 nm emission and (+)-catechin contents were measured using the DAD at 280 nm. In all cases, extractions were performed in duplicates, each one from three biological replicates. Standards used for peak identification and for standard curve plotting for quantification were purchased from Sigma-Aldrich®.

5.2.4 Statistical analysis

To access the significance of the differences between treatments, one-way ANOVA and Tukey HSD test (α=0.05) were performed using Statistix9 (Analytical Software, Tallahassee, Florida). To adjust data to the normal distribution, percentage values were transformed to arcsin square-root (x) and values concerning count number of berries were square-root transformed.

5.3 Results

5.3.1 Effects on leaf physiology and vegetative growth

Microclimate conditions to which vines were exposed during bloom period were similar in the three years assayed. The mean temperatures from day (from 7 am to 7 pm)/night (from 7 pm to 7 am) were 25/16, 26/14 and 25/16 ºC in 2012, 2013 and 2014, respectively. The mean relative

humidity values for the day/night periods were 57/72, 49/63 and 60/68% for the same year order.

As expected, during the period of shade imposition, P_n and g_s were significantly reduced in all trials and varieties, in shaded vines (Fig.5.1). 'Sugraone', which is the earliest cultivar assayed, tended to higher levels of P_n when compared to 'Crimson Seedless' and 'Thompson Seedless' under both control or with the application of GAc conditions. When a level of 90% shade was imposed, the reduction in P_n was in average 92%, while total shade provoked a 100% P_n reduction. For the same shading conditions, the reduction in g_s was 75%, 85% and 93% in 'Sugraone', 'Crimson Seedless' and 'Thompson Seedless' cultivars, respectively. Neither Pn nor g_s were affected (p-value>0.05) in GAc treated vines, when compared to control plants. After the removal of shade nets, the vines thinned *via* shade showed to recover their leaf gas exchange parameters and, in 'Crimson Seedless' g_s was even significantly higher (p-value≤0.05) comparing to both control and GAc-treated vines (Fig.5.1). The P_n results were confirmed by measuring the total sugar content in the phloem sap of 'Thompson Seedless' leaf pedicels along the treatments. The results showed that 7 days after full boom, a significant decrease was observed only for shaded vines. In fact, at early stages (5 days after 100% cap fall), the average was determined to be 211.5 ± 53.4 mg sucrose mg^{-1} fresh weight (FW), which, 7 days after bloom, decreased from values of 579.6 ± 88.7 mg sucrose mg^{-1} FW in control and plants from GAc treatment to 151.6 ± 45.2 mg sucrose mg^{-1} FW for both shade treatments. Likewise, 3 days later, a similar 76.0 % decrease of photoassimilates was observed in petioles from shaded vines.

In 'Thompson Seedless' untreated vines, primary leaf area growth and main shoot growth rates were 2.6 (Fig.5.2) and 4 fold higher, compared with the ones observed in 'Crimson Seedless'. Shade treatments resulted in a significant reduction on leaf area growth rate in both cultivars, whereas GAc treatment did not produce any effect.

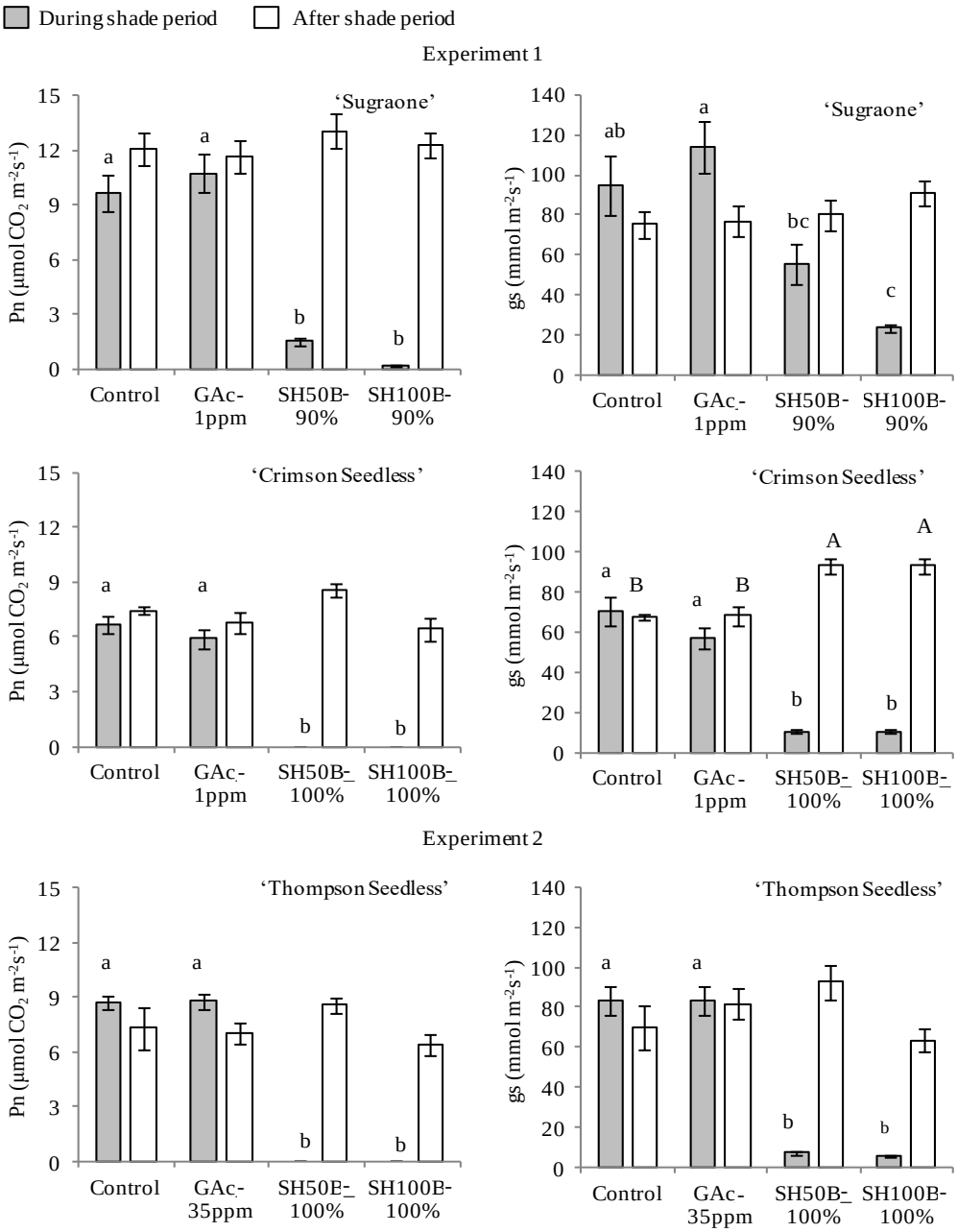

Figure 5.1. Effects of GAc and shade treatments on the net photosynthetic (P_n) and stomatal conductance to water vapour (g_s) rates in 'Sugraone', 'Crimson Seedless' and 'Thompson Seedless' vines during and 20 days after shading nets removal (mean values±se of 8 leaves, twice during and after shade). Different letters means that treatments were significantly different by Tukey's HSD test (p-value≤ 0.05), lowercase was used for comparison during shade and uppercase for comparison after shade.

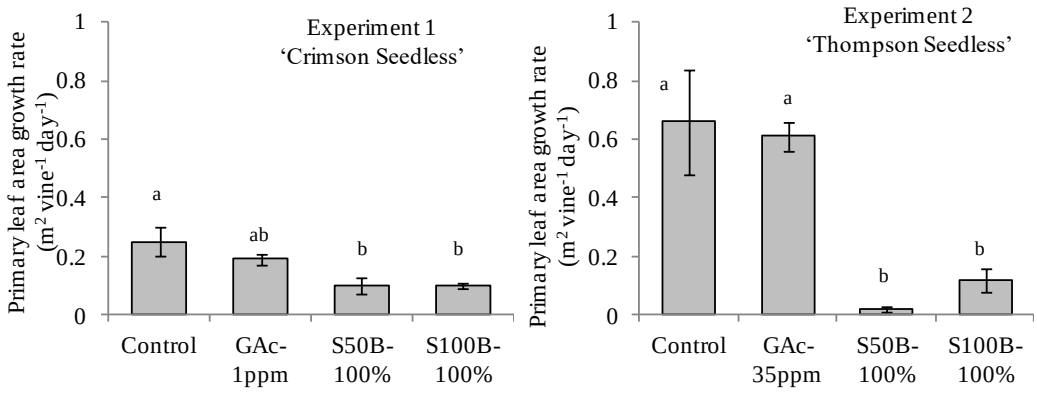

Figure 5.2. Effect of GAc and shade treatments on primary leaf area growth in 'Crimson Seedless' and 'Thompson Seedless' (bars represent mean values±se in 6 shoots, twice during the shade period). Different letters means that treatments were significantly different by Tukey's HSD test (*p*-value≤ 0.05).

5.3.2 Effect on flower drop, bunch and berry quality

5.3.2.1 Sugraone cultivar

The effect of shade on flower drop (monitored from full bloom until 6 mm berry size) was significant (*p*-value≤0.01) in trial 1 but not in trial 2 (Table 5.1). The growth regulator produced no significant effect on natural flower drop percentages in none of the trials. Flower drop ranged from 78.6% in GAc-1ppm to 90.6% in S50B-90% in trial 1, while the mean percentage of flower drop was 73.6 in trial 2. The effect of the treatments on trial 1 flower drop resulted in differences on number of berries and bunch compactness observed at harvest, which were significantly reduced (*p*-value≤0.05) in S50B-90%. In agreement to the absence of significant impact on the % of flower drop in trial 2, no significant differences on neither number of berries nor bunch compactness were found (Table 5.1 and Fig. 5.3).

Nonetheless, the result on bunch weight and yield per plant was influenced by shade treatments in both trials. In trial 1, in GAc-treated and control vines, the mean bunch weight was 762.1 ± 20.7 g, while in shade-treated it was reduced to 535.1 ± 73.9 g. In trial 2, bunch weight from control and GAc-treated vines was 756.8 ± 46.8 g, and in shade-treated plants the average was 490.9 ± 14.1 g. S50B-90% and S100B-90% conditions resulted, in trial 1, in yields per plant corresponding to 60.6% and 62.4% of the produce obtained in untreated vines. A similar value of 66.3% was obtained in trial 2 under S50B-100% conditions.

In what concerns trial 1 berry quality, GAc and shade treatments were responsible for reduced berry weight and transversal diameter, whereas only the S100B-90% condition led to reduced berry longitudinal diameter (Table 5.2). Soluble solids content (SSC) and berry skin colour were significantly altered between the two times of shade imposition since SCC in S100B-90% was higher (18.5%) comparing to S50B-90% (16.2%) and to control (16.8%). Hue angle in S100B-90% berries (114.8) was lower than in S100B-90% (116.9). Titratable acidity (TA) was lower in S100B-90% (4.3 g L^{-1}) than in control grapes (4.8 g L^{-1}). None of these parameters was significantly different from the control in grapes harvested in GAc-treated vines.

Even though no differences in flower drop have been disclosed until the 6 mm berry size stage, in trial 2, treatments resulted in significant effects (p-value≤0.01) on berry weight, diameters, colour and firmness (Table 5.2). Berry weight and longitudinal and transversal diameters were similar in the two shade treatments but showed to be significantly lower than those observed on GAc-1 ppm treated and on control vines. GAc treatments resulted in the heavier berries with longer longitudinal diameter. No significant differences in SSC and TA were observed. Both shade and GAc thinning treatments produced berries with higher skin colour hue angle compared to the control. Regarding firmness, grapes developing under GAc-1 ppm and SH50B-90% conditions showed higher values than the respective controls.

5.3.2.2 Crimson Seedless cultivar

In both trials, the thinning methods investigated did not promoted flower drop when compared to the respective controls (Table 5.1). Nonetheless, in trial 1 and under SH100B-90% conditions, bunch weight and yield per plant were 56.1% and 53.2% of the control, respectively, but no significant differences in berry number and bunch compactness were found. Conversely, in trial 2, bunch weight and yield per plant were unaffected by the shade treatments. S50B-100% treatment induced less compact bunches, representing 54.5% of the control, what was related to a lower berry number per bunch (Table 5.1 and Fig. 5.3). GAc treatments did not influence bunch characteristics in none of the trials.

In trial 1, shade treatments at bloom caused lighter and smaller berries at harvest, comparing to GAc-1 ppm treated and control vines. This effect was more pronounced in SH100B-90% (Table 5.2). All thinning treatments had a significant effect on SSC (p-value≤0.05) and berry colour (p-value≤0.01), but not in TA. The measured grape mean SSC was 17.8% in result of the thinning treatments, while this content was 17.1% in control grapes. The hue angle was significantly lower (between 45.7 and 47.6) in grapes that developed in thinned vines when compared to untreated plants (54.7), but only S100B-100% conditions influenced berry firmness, as grapes showed 75% firmness values than control.

In trial 2, all berry characteristics were affected by some of the imposed treatments (*p*-value≤0.01) (Table 5.2). GAc treatment resulted in a reduction on berry weight, transversal diameter, SSC and an increase on TA, colour hue angle and firmness, associated with delayed maturation date. The SH100B-100% showed reduced berry weight, longitudinal diameter, SSC and an increased hue angle were measured. The SH50B-100% treatment did not induce significant differences in any of these parameters (Table 5.2).

5.3.2.3 Thompson Seedless cultivar

In trial 1, all thinning treatments caused increased rates of flower drop, which resulted in decreased bunch weight, berry number, bunch compactness and yield per plant (*p*-value≤0.01) , with a significantly greater effect in both shade treatments (Table 5.1 and Fig. 5.3). The two shade treatments resulted in an average of 98.7% flower drop, whereas GAc-35ppm a lower percentage of 83.0% was observed. In shade treatments, bunch weight and yield per plant were reduced to only 10% of those measured in control vines. In GAc-35 ppm treatment bunch weight, compactness, number of berries and yield were reduced in average to 54.5% of the control (Fig. 5.3).

GAc treatment resulted in increased berry quality (*p*-value≤0.01) regarding berry weight, diameters, TA and firmness which were all higher than control (Table 5.2). SSC and colour were not statistically affected.

In trial 2 four thinning methods were compared: hand-thinning, GAc-35 ppm, SH50B-98% and SH50B-100%. Berry number was not statistically significantly different between treatments when analysed by ANOVA, due to a high heterogeneity of berries between bunches (Table 5.1). Nonetheless, bunch weight and compactness, as well as yield per plant were affected by thinning treatments (*p*-value≤0.01). Both shade treatments produced lighter bunches and lower yield per plant than hand-thinned vines (41.1% of the hand-thinned value for both characteristics). Bunches were less compact in SH50B-100%, with a calculated value of 2.6 berries per cm of rachis, when compared to the 5.0 and 4.9 berries per cm of rachis observed on hand-thinned and GAc-35 ppm treated vines, respectively.

Berries were lighter and smaller in longitudinal diameter in response to shade treatments, when compared to grapes developing in GAc-treated and hand-thinned vines (Table 5.2). Regarding berry SSC and firmness, the SH50B-98% treatment produced grapes with significantly higher values than those from the hand-thinning treatment. GAc-35ppm resulted in berries with similar characteristics to those hand-thinned, with exception of berry firmness values that were the highest obtained.

Table 5.1. Effect of shade and GAc treatments on percentage of flower drop, bunch weight, number of berries per bunch, rachis length, bunch compactness and yield per plant in 'Sugraone', 'Crimson Seedless' and 'Thompson Seedless' (mean values). *, ** and ns mean that treatments are significantly different at *p*-value≤ 0.05, ≤ 0.01 or not significantly different (ANOVA). Different letters separate mean values according to Tukey's HSD test (*p*-value≤0.05).n.a., not analyzed.

Cultivar	Trial	Treatment	Flower drop (%)	Bunch weight (g)	Berry number per bunch	Bunch compactness	Yield per plant (Kg)
Experiment 1							
Sugraone	1	Control	85.3 b	776.7 a	144.3 ab	3.0 ab	21.0 a
		GAc-1ppm	78.6 b	747.4 a	167.1 a	3.7 a	20.3 a
		S50B-90%	90.6 a	587.3 b	93.0 b	2.2 b	12.7 b
		S100B-90%	79.4 b	482.8 b	146.4 ab	3.7 a	13.1 b
			**	**	*	*	**
	2	Control	71.5	723.7 ab	171.9	3.9	41.3 ab
		GAc-1ppm	74.4	789.9 a	158.3	4.2	45.0 a
		S50B-100%	77.9	480.9 c	141.2	4.8	27.4 c
		S100B-100%	70.6	500.8 bc	177.4	4.1	28.5 bc
			ns	**	ns	ns	**
Crimson Seedless	1	Control	78.3	1037.7 a	194.3	4.4	41.5 a
		GAc-1ppm	79.0	957.1 a	192.7	3.8	38.3 a
		S50B-90%	78.1	955.1 a	186.2	4.0	38.2 a
		S100B-90%	82.1	582.7 b	170.0	3.5	22.1 b
			ns	**	ns	ns	**
	2	Control	64.7	758.6	264.9 a	6.6 a	35.7
		GAc-1ppm	55.2	841.7	274.5 a	7.2 a	39.6
		S50B-100%	77.1	555.9	141.7 b	3.6 b	26.1
		S100B-100%	58.0	821.2	254.3 a	6.3 a	38.6
			ns	ns	**	**	ns
Experiment 2							
Thompson Seedless	1	Control	63.1 c	1479.6 a	324.2 a	6.7 a	44.4 a
		GAc-35ppm	83.0 b	821.8 b	168.0 b	3.7 b	24.7 b
		S50B-100%	99.0 a	97.0 c	14.8 c	0.7 c	2.9 c
		S100B-100%	98.3 a	196.7 c	43.8 c	1.1 c	5.9 c
			**	**	**	**	**
	2	Hand thinned	n.a.	1884.9 a	252.3	5.0 a	52.8 a
		GAc-35ppm	82.5	1404.7 ab	246.6	4.9 a	39.3 ab
		S50B-98%	82.6	948.8 bc	207.6	3.5 ab	26.6 bc
		S50B-100%	90.8	601.1 c	136.4	2.6 b	16.8 c
			ns	**	ns	**	**

Table 5.2. Effect of shade and GAc treatments on berry weight, longitudinal and transversal diameters, SSC (soluble solids content), TA (titratable acidity), colour hue angle and berry firmness in 'Sugraone', 'Crimson Seedless' and 'Thompson Seedless' (mean values). *, **and ns mean that treatments are significantly different at *p*-value≤ 0.05, ≤ 0.01 or not significantly different (ANOVA). Different letters separate mean values according to Tukey's HSD test (*p*-value≤0.05). n.a., not analyzed.

Cultivar	**Trial**	**Treatment**	**Berry weight (g)**	**Berry longitudinal diameter (mm)**	**Berry transversal diameter (mm)**	**SSC (%)**	**TA (g L^{-1})**	**Colour (hue angle)**	**Firmness (N)**
Experiment 1									
Sugraone	1	Control	6.1 a	23.3 a	20.0 a	16.8 b	4.8 a	116.3 ab	n.a.
		GAc-1ppm	5.4 b	23.0 a	19.0 b	16.9 b	5.1 a	115.5 ab	n.a.
		S50B-90%	5.1 b	22.3 a	18.7 b	16.2 c	4.7 ab	116.9 a	n.a.
		S100B-90%	4.1 c	20.2 b	17.4 c	18.5 a	4.3 b	114.8 b	n.a.
			**	**	**	**	**	**	
	2	Control	6.5 b	24.6 b	19.2 a	17.3	4.8	114.0 b	15.5 b
		GAc-1ppm	7.1 a	26.7 a	19.7 a	16.4	4.7	116.5 a	19.1 a
		S50B-100%	4.2 c	21.0 c	17.5 b	17.9	4.8	117.5 a	18.9 a
		S100B-100%	4.1 c	20.5 c	16.7 c	17.9	4.9	117.0 a	17.6 ab
			**	**	**	ns	ns	**	**
Crimson Seedless	1	Control	5.7 a	26.2 a	17.8 a	17.1 b	5.5	54.7 a	14.8 a
		GAc-1ppm	5.5 a	26.6 a	17.6 a	17.9 a	5.4	45.7 b	15.8 a
		S50B-90%	4.7 b	24.7 b	16.5 b	17.8 a	5.5	46.1 b	13.8 a
		S100B-90%	3.6 c	20.8 c	15.8 c	17.8 a	5.6	47.6 b	11.1 b
			**	**	**	*	ns	**	**
	2	Control	4.9 a	23.0 ab	16.8 a	20.5 a	4.4 bc	14.8 c	14.2 b
		GAc-1ppm	4.2 b	22.4 b	16.2 b	17.6 b	5.4 a	54.4 a	17.8 a
		S50B-100%	4.8 a	23.2 a	16.8 a	20.1 a	3.9 c	13.9 c	15.3 ab
		S100B-100%	4.2 b	20.8 c	16.5 ab	18.3 b	4.6 b	31.6 b	14.7 b
			**	**	**	**	**	**	**
Experiment 2									
Thompson Seedless	1	Control	5.7 b	24.6 b	17.6 b	16.2	5.5 b	123.4	11.4 b
		GAc-35ppm	6.9 a	29.5 a	18.1 a	17.4	6.8 a	122.9	17.5 a
		S50B-100% †	n.a.	n.a.	n.a.	n.a.	n.a.	n.a.	n.a.
		S100B-100% †	n.a.	n.a.	-	n.a.	n.a.	n.a.	n.a.
			**	**	**		**	ns	**
	2	Hand thinned	8.1 a	29.9 a	19.7 a	18.1 b	6.6	122.7	10.8 c
		GAc-35ppm	7.5 a	29.9 a	19.0 ab	19.7 ab	6.6	121.9	14.5 a
		S50B-98%	4.3 b	24.1 b	18.3 b	20.3 a	5.5	121.8	12.6 b
		S50B-100%	4.9 b	23.9 b	17.3 c	19.4 ab	6.6	122.8	11.8 bc
			**	**	**	*	ns	ns	**

† Due to the reduced number of berries per bunch harvested in vines submitted to shade treatments (23.9 berries in average), berry quality characteristics could not be determined.

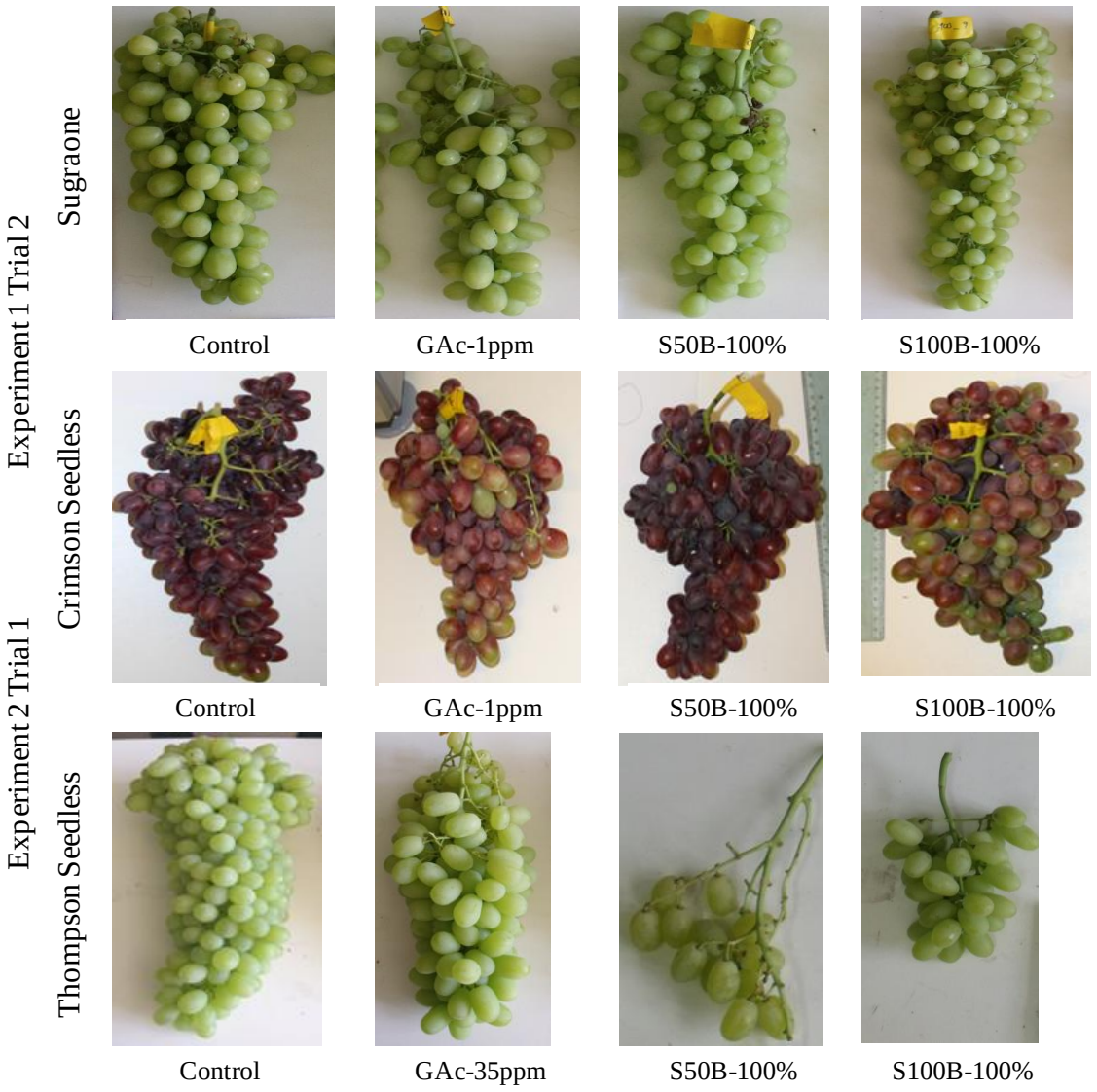

Figure 5.3. Visual illustrative aspect of representative bunches of Sugraone, Crimson Seedless and Thompson Seedless cultivars harvested from vines submitted to different thinning treatments (gibberellic acid spraying and shade imposition at flowering) and non-treated vines (control).

5.3.2.4 Berry skin polyphenols content

No significant differences were found between treatments concerning total polyphenols, *trans*-resveratrol and (+)-catechin skin contents, neither in 'Crimson Seedless' nor in 'Thompson Seedless' (Table 5.3). Quantified polyphenols, *trans*-resveratrol and (+)-catechin were in average 1043 and 548, 0.5 and 2.2, 10.3 and 88.6 mg kg^{-1} FW in 'Crimson Seedless' and 'Thompson Seedless', respectively. In 'Crimson Seedless' GAc thinning treatments induced a significant effect (p-value≤0.01) on malvidin-3-O-glucoside content, promoting a significant decrease than in controls and shade treatment (Table 5.3).

Table 5.3. Effect of shade and GAc treatment on total polyphenols, malvidin, *trans*-resveratrol and catechin berry skin content in 'Crimson Seedless' and 'Thompson Seedless' (mean values). ** and ns mean that treatments are significantly different at p-value≤ 0.01 or not significantly different (ANOVA). Different letters separate mean values according to Tukey's HSD test (p-value≤0.05). GA, galic acid; n.d., not detected.

Cultivar	Trial	Treatment	Total polyphenols (mg GA kg^{-1}FW)	*Trans*-resveratrol (mg kg^{-1}FW)	(+)-Catechin (mg kg^{-1}FW)	Malvidin-3-O-glucoside (mg kg^{-1}FW)
Experiment 1						
Crimson Seedless	2	Control	1184	0.64	7.43	195 a
		GAc-1ppm	988	0.66	11.13	40 b
		S50B-100%	959	0.29	12.30	281 a
			ns	ns	ns	**
Experiment 2						
Thompson Seedless	2	Hand thinned	567	2.08	76.19	n.d.
		GAc-35ppm	390	2.38	98.99	n.d.
		S50B-98%	579	2.84	94.92	n.d.
		S50B-100%	657	1.42	84.44	n.d.
			ns	ns	ns	

5.4 Discussion

GAc application at bloom is a practice commonly used in table grape production to induce cluster loosening. However, treatment doses and application timings are highly specific for each cultivar and vary according to the environment conditions. Therefore, treatment guidelines have been developed for each individual cultivar and region (Dokoozlian, 1998). The observed results disclosed that GAc application, on the south Portugal conditions, only increased the percentage of flower drop and changed bunch characteristics in the Thompson Seedless cultivar when compared with untreated vines (experiment 2, trial 1; Table 5.1) whereas, regarding to berry characteristics, differences were found in the three cultivars and trials (Table 5.2). The somewhat inconsistent results obtained in the two consecutive years trials for 'Crimson Seedless' and 'Sugraone' (e.g., increased berry weight in trial 1 and decreased in trial 2 in 'Sugraone',

increased SSC in trial 1 and decreased in trial 2 in Crimson Seedless), suggest a major effect of year-specific episodes on GAc response. The environment is known to play a key role in the response to growth regulator treatments, therefore the same cultivar can show different results over the years, as observed for 'Sovereign Coronation' after a three-years trial (Reynolds et al., 2006).

As mentioned previously, fruit set and sensitivity to exogenously applied GAc during bloom are cultivar dependent. In fact, it was observed that cultivars which endogenously produce less gibberellin 8 (GA_8) are more sensitive to external GAc applications, therefore responding with a higher degree of cluster loosening (Boll et al., 2009). Furthermore, recent results suggested that differential organ responses to exogenous GAc depend on the levels of endogenous bioactive gibberellins (Acheampong et al., 2015). On the other hand, the observed effect of GAc on cluster loosening, due to increased flower drop and decreased bunch compactness, exclusively in 'Thompson Seedless' was not a consequence from the higher GAc application rate (35 instead of 1 ppm in the other two cvs.), since our studies conducted in the same cultivars with doses of applied GAc higher than the recommended for each variety didn't induce increased flower drop (data not shown) Furthermore, according to Dokoozlian and Peacock (2001), in 'Crimson Seedless', GAc spray at 1 ppm resulted in a fruit set reduction, while higher doses resulted in unaccepted level of shot berries (parthenocarpic small berries that remain green at harvest) per bunch.

Nevertheless, the GAc treatment improved berry quality in 'Thompson Seedless' in both trials, resulting in similar berries dimensions and maturation level in the two consecutive year's trial. The alterations in the colour, firmness, SSC and TA observed in 'Crimson Seedless' GAc-treated berries from trial 2, agree with results in 'Italia' table grapes sprayed with this growth regulator for berry sizing at later stages (Ferrara et al., 2014) and appear to be associated to maturation delay (Table 5.2 and Fig. 5.3). This result further agrees with the lowest levels of malvidin-3-O-glucoside (Table 5.3) quantified in GAc treated berries, indicating a lower accumulation of anthocyanins, which are responsible for the colour of grape fruits and are the most abundant group of phenolic compounds in red cultivars (Crupi et al., 2012).

Total polyphenols, *trans*-resveratrol and (+)-catechin contents were unaffected by the imposed treatments. Although, according to Cantos et al. (2002), 'Crimson Seedless' presented approximately the same amount of total phenolic compounds as white varieties, our results showed higher content compared to 'Thompson Seedless'. On the other hand, 'Thompson Seedless' showed to be richer in trans-resveratrol and (+)-catechin levels. Grapes and related products are considered one of the most important dietary sources of trans-resveratrol (Burns et al., 2002), which content in the skin range from 0.05 to 2.5 mg kg^{-1} skin FW (Iacopini et al.,

2008) depending on cultivar. Regarding (+)-catechin, an abundant flavonoid in grape skin, our results agreed with the values obtained by Lutz et al. (2011) for 'Crimson Seedless'. For 'Thompson Seedless' only values of whole berry (skin and flesh) were previously reported, ranging from 4 to 15 mg kg^{-1} FW (Breksa et al., 2010; Meng et al., 2011), and a higher level of (+)-catechin is expected only in skin compared to whole berry determination (Cantos et al., 2002; Sun et al., 2001; Topalovic et al., 2010).

Regarding shade treatments, in 'Thompson Seedless' both moments of shade imposition increased percentage of flower drop and reduced bunch compactness at harvest, compared to untreated vines. In Sugraone and Crimson Seedless cultivars, the observation that only shade imposed at 50% cap fall showed to be effective on reducing bunch compactness agree with the hypothesis that C-starvation during the stage at bloom, when the reserves are lower, is a major factor in berries abscission induction (Lebon et al., 2008; Zapata et al., 2004). Our findings are in agreement with the previous authors regarding the simultaneous P_n decrease (Fig. 5.1) and associated decreased photoassimilate content in the petiole sap phloem, and flower drop enhancement (Table 5.1). As shown by other researchers, for example in 'Thompson Seedless' (Cortázar et al., 2005) and in Syrah (Prieto et al., 2010), low light intensities result in lower photosynthetic response of leaves corresponding to the logarithmic part of the photosynthetic light-response curve. This net photosynthetic rate reduction promotes an increase of competition for C-resources between the vegetative and reproductive sinks, with the reproductive growth at a disadvantage at this early stage of development (Byers et al., 1985; Corelli et al., 1990; Vasconcelos et al., 2009). Since both shade treatments reduced bunch weight and yield in 'Sugraone' and 'Thompson Seedless', while only S100B-90% had the same effect on 'Crimson Seedless', we hypothesize that C-starvation effect due to shade imposition at an earlier stage during bloom (50% cap fall) induced a berry number reduction, comparing with later shade imposition (100% cap fall) which is not as efficient reducing berry number but leads to reduction of berry dimensions. In fact, as shown in Table 5.2, shade imposed at 100% cap fall had a more pronounced effect on berry weight and diameters reduction compared with shade imposition at 50% cap fall. The reversible effects on leaf gas exchange after shade removal (Fig. 5.1) and, particularly the g_s increased disclosed in 'Crimson Seedless' vines after the shaded period can indicate adaptability to low light intensity (Cartechini and Palliotti, 1995).

Only in ‘Thompson Seedless’ both treatments were successful in significantly reduce fruit set. This cultivar was characterized by a higher rate of daily shoot and leaves growth (vegetative sink strength) during bloom, when compared to ‘Crimson Seedless’ (Fig. 5.2). The high vegetative vigour observed can indicate a greater competition between shoots and berries for photosynthetic resources, making this cultivar more sensitive to thinning treatments. As

previous observed in apple (*Malus* x *domestica* B.), fruitlet abscission can be induced by strengthening the sink activity of the vegetative part of the plant (Dal Cin et al., 2007).

5.5 Conclusion

The effects of shade imposition and GAc application at bloom were dependent on the year and cultivar. Moreover, even the time of shade imposition had influence on grapes final quality and vine productivity. 'Thompson Seedless' showed to be sensitive for both thinning methods. In this cultivar, GAc spraying successfully caused reduced fruit set and improved berry size and firmness, showing to be an effective thinning method also for south Portugal conditions. Total light reduction drastically increased grape loosening in 'Thompson Seedless' while a less percentage of light reduction (98%) resulted in similar bunch compactness to that observed in GAc treated vines. Furthermore, for 'Sugraone' and 'Crimson Seedless', only shade treatments imposed at 50% cap fall, with 90% and 100% of light reduction, respectively, were effective as thinning methods, as revealed by less compact bunches at harvest. This study provides the first report of the effect of light reduction on fruit set on field-grown seedless grapevines and shows that light management *via* shade nets can be used as an alternative thinning method. Optimization is however required to overcome the resulting effects of lower yield and formation of smaller berries.

5.6 References

Acheampong AK, Hu J, Rotman A, Zheng C, Halaly T, Takebayashi Y, *et al.* 2015. Functional characterization and developmental expression profiling of gibberellin signalling components in *Vitis vinifera*. *J. Exp. Bot*. 66: 1463-1476.

Boll S, Lang T, Hofmann H, Schwappac P. 2009. Correspondence between gibberellin-sensitivity and pollen tube abundance in different seeded vine varieties. *Mitteilungen Klosterneubg.* 59: 129-133.

Breksa AP, Takeoka GR, Hidalgo MB, Vilches A, Vasse J, Ramming DW. 2010. Antioxidant activity and phenolic content of 16 raisin grape (*Vitis vinifera* L.) cultivars and selections. *Food Chem*. 121: 740-745.

Burns J, Yokota T, Ashihara H, Lean MEJ, Crozier A. 2002. Plant foods and herbal sources of resveratrol. *J. Agric. Food Chem*. 50: 3337-3340.

Byers RE. 2003. Flower and fruit thinning and vegetative fruit balance. In Ferrere DC, Warington IJ (Eds.). *Apples: botany, production and uses.* Cabi publishing. Cambridge, U.K. 437-458.

Byers R E, Lyons J, Yoder K. 1985. Peach and apple thining by shading and photosynthetic inhibition. *J. Hort. Sci. Biotechnol*. 60: 465-472.

Byers RE, Carabaugh DH, Presley CN, Wolf TK. 1991. The influence of low light on apple fruit abscission. *J. Hort. Sc*. 66: 7-17.

Cantos E, Espín JC, Tomás-Barberán FA. 2002. Varietal differences among the polyphenol profiles of seven table grape cultivars studied by LC−DAD−MS−MS. *J. Agric. Food Chem. Amer. Chem. Soc*. 50: 5691-5696.

Cartechini A, Palliotti A. 1995. Effect of shading on vine morphology and productivity and leaf gas exchange characteristics in grapevines in the field. *Am. J. Enol. Vitic*. 46: 227-234.

Corelli L, Sansavini S and Ravaglia GF. 1990. Effects of shade and sorbitol on fruit growth andabscission in apple. *Proc. XXIII Int. Congr.*, Florence. 620.

Cortázar VG, Córdova C, Pinto M. 2005. Canopy structure and photosynthesis modelling of grapevines (*Vitis vinifera* L. cv. Sultana) grown on an overhead (parronal) trellis system in Chile. *Aust. J. Grape Wine Res*. 11: 328-338.

Crupi P, Coletta A, Milella RA, Perniola R, Gasparro M, Genghi R, *et al.* 2012. HPLC-DAD-ESI-MS analysis of flavonoid compounds in 5 seedless table grapes grown in Apulian region. *J. Food Sci*. 77: 174-181.

Dal Cin V, Boschetti A, Dorigoni A, Ramina A. 2007. Benzylaminopurine application on two different apple cultivars (*Malus domestica*) displays new and unexpected fruitlet abscission features. *Ann. Bot*. 99: 1195-1202

Devaux M, Ghashghaie J, Bert D, Lambrot C, Gessler A, Bathellier C, *et al.* 2009. Carbon stable isotope ratio of phloem sugars in mature pine trees throughout the growing season: comparison of two extraction methods. *Rapid Commun. Mass Spectrom*. 23: 2511–2518.

Di Stefano R, Cravero M.C. 1991. Metodi per lo studio dei polifenoli dell'uva. *Riv. Vitic. Enol*. 44: 37-45.

Di Stefano R, Cravero M.C, Gentilini N. 1989. Methods for the study of wine polyphenols. *L'enotecnico* 25: 83-89.

Dokoozlian NK. 1998.Use of plant growth regulators in table grape production in California. *Proc.Univ. Calif. Table Grape Prod. Course,* Visalia. 200–210.

Dokoozlian NK and Peacock WL. 2001. Gibberellic acid applied at bloom reduces fruit set and improves size of 'crimson seedless' table grapes. *HortScience*. 36: 706-709.

Domingos S, Scafidi P, Cardoso V, Leitao AE, Di Lorenzo R, Oliveira CM and Goulao LF. 2015. Flower abscission in *Vitis vinifera* L. triggered by gibberellic acid and shade discloses differences in the underlying metabolic pathways. *Front. Plant Sci*. 6: 457.

DuBois M, Gilles KA, Hamilton JK, Rebers PA, Smith F. 1956. Colorimetric method for determination of sugars and related substances. *Anal. Chem*. 28: 350–356.

Ferrara G, Mazzeo A, Netti G, Pacucci C, Matarrese AMS, Cafagna I, *et al.* 2014. Girdling, gibberellic acid, and forchlorfenuron: effects on yield, quality, and metabolic profile of table grape cv. Italia. *Am. J. Enol. Vitic*. 65: 381-387.

Ferree DC, Mcartney SJ, Scurlock DM. 2001. Influence of irradiance and period of exposure on fruit set of french-american hybrid grapes. *J. Am. Soc. Hort. Sci.* 126: 283-290.

Intrigliolo DS, Llacer E, Revert J, Esteve MD, Climent, MD, Palau D, *et al.* 2014. Early defoliation reduces cluster compactness and improves grape composition in Mandó, an autochthonous cultivar of *Vitis vinifera* from southeastern Spain. *Sci. Hortic.* 167: 71-75.

Lacopini P, Baldi M, Storchi P, Sebastiani L. 2008. Catechin, epicatechin, quercetin, rutin and resveratrol in red grape: Content, in vitro antioxidant activity and interactions. *J. Food Compos. Anal.* 21: 589-598.

Lebon G, Wojnarowiez G, Holzapfel B, Fontaine F, Vaillant-Gaveau N, Clément C. 2008. Sugars and flowering in the grapevine (*Vitis vinif*era L.). *J. Exp. Botany* 59: 2565-2578.

Lohitnavy N, Bastina S, Collins C. 2010. Early leaf removal increases flower abscission in *Vitis vinifera* 'Semillon'. *Vitis*. 49: 51-53.

Lopes C, Pinto PA. 2005. Easy and accurate estimation of grapevine leaf area with simple mathematical models. *Vitis*. 44: 55-61.

Lorenz D, Eichhorn K, Bleiholder H, Klose R, Meier U, and Weber E. 1994. Phänologische entwicklungsstadien der rebe (*Vitis vinifera* L. ssp. vinifera) – codierung und beschreibung nach der erweiterten bbch-skala. *Vitic. Enol. Sci.* 49: 66–70.

Lutz M, Jorquera K, Cancino B, Ruby R, Henriquez C. 2011. Phenolics and antioxidant capacity of table grape (*Vitis vinifera* L.) cultivars grown in Chile. *J Food Sci.* 76: 1088-1093.

Mcguire RG. 1992. Reporting of objective color measurements. *HortScience*. 27: 1254-1255.

Meng J, Fang Y, Zhang A, Chen S, Xu T, Ren Z, Han, *et al.* 2011. Phenolic content and antioxidant capacity of Chinese raisins produced in Xinjiang province. *Food Res. Int*. 44: 2830-2836.

Prieto JA, Giorgi EG, Peña JP. 2010. Modelling photosynthetic-light response on Syrah leaves with different exposure. *Vitis*. 49: 145-146.

Reynolds AG, Roller JN, Forgione A, De Savigny C. 2006. Gibberellic acid and basal leaf removal: Implications for fruit maturity, vestigial seed development, and sensory attributes of Sovereign Coronation table grapes. *Am. J. Enol. Vitic*. 57: 41-53.

Ristic R, Downey MO, Iland PG, Bindon K, Francis IL, Herderich, M, *et al.* 2007. Exclusion of sunlight from Shiraz grapes alters wine colour, tannin and sensory properties. *Aust. J. Grape Wine Res*. 13: 53-65.

Roubelakis KA, Kliewer WM. 1976. Influence of light intensity and growth regulators on fruit-set and ovule fertilization in grape cultivars under low temperature conditions. *Amer. J. Enol.Vitic.* 27: 163-167.

Schneider G. 1975. C-sucrose translocation in apple. *J. Amer. Soc. Hort. Sci*. 100: 22-24.

Sun B, Ricardo-da-Silva JM, Spranger MI. 2001. Quantification of catechins and proanthocyanidins in several Portuguese grapevine varieties and red wines. *Ciência Téc. Vitiv.* 16: 23-34.

Topalovic A, Milukovic-Petkovsek M. 2010. Changes in sugars, organic acids and phenolics of grape berries of cultivar Cardinal during ripening. *J. Food Agric. Environ*. 8: 223-227.

Vasconcelos MC, Greven M, Winefield CS, Trought MCT, Raw V. 2009. The flowering process of *Vitis vinifera*: A Review. *Am. J. Enol. Vitic*. 60: 411-434.

Weaver RJ, Pool RM. 1971. Berry response of 'Thompson Seedless' and 'Perlette' grapes to application of gibberellic acid. *J. Amer. Soc. Hort. Sci*. 96: 162-166.

Widmer A, Kockerols K, Schwan S, Stadler W, Bertshinger L. 2008. Towards grower-friendly apple crop thinning by tree shading. http://orgprints.org/13738/, 314-317.

Xia E-Q, Deng G-F, Guo Y-J, Li H-B. 2010. Biological activities of polyphenols from grapes. *Int. J. Mol. Sci.* 11: 622-646.

Zapata C, Deleens E, Chaillou S, Magne C. 2004. Partitioning and mobilization of starch and N reserves in grapevine (*Vitis vinifera* L.). *J. Plant Physiol*. 161, 1031-1040.

Zhang X-Y, Wang X-L, Wang X-F, Xia G-H, Pan Q-H, Fan R-C, *et al.*, 2006. A shift of phloem unloading from symplasmic to apoplasmic pathway is involved in developmental onset of ripening in grape berry. *Plant Physiol*. 142: 220–232.

Zhou C, Lakso A.N, Robinson T.L, Gan S. 2008. Isolation and characterization of genes associated with shade-induced apple abscission. *Mol. Genet. Genomics.* 280: 83-92.

Zhu H, Dardick C, Beers E, Callanhan A, Xia R, Yuan R. 2011. Transcriptomics of shading-induced and NAA-induced abscission in apple (*Malus domestica*) reveals a shared pathway involving reduced photosynthesis, alterations in carbohydrate transport and signaling and hormone crosstalk. *BMC Plant Biol*. 11: 138.

Zibordi M, Domingos S, Corelli Grappadelli L. 2009. Thinning apples *via* shading: an appraisal under field conditions. *J. Hort. Sci. Biotechnol*. 84: 138-144.

Zoffoli, J.P, Latorre, B.A, Naranjo, P. 2009. Preharvest applications of growth regulators and their effect on postharvest quality of table grapes during cold storage. *Postharvest Biol. Technol.* 51: 183-192.

Chapter 6

Final considerations

6. Final considerations

6.1 General Discussion

During the first two to three weeks after full bloom, an abrupt increase on fertilized ovary size and cell multiplication and embryo development occurs (Ojeda et al., 1999), triggering the process of converting carpels into developing berries, that is, the fruit set process. Also during this stage flower abscission occurs (Bessis et al., 2000; Intrigliolo and Lakso, 2009). Therefore it is a critical period when the number of berries, the final size of the berries and yield are defined.

Our data confirmed that the activation of the fruit set developmental program requires cell division stimulation, inhibition of senescence related genes and a dynamic interplay between carbon metabolism and transport regulation, sugar signaling and hormone balance (Table 2.4 and Fig. 2.8) agreeing with the previous the works (Giacomelli et al., 2013; Ojeda et al., 1999; Vriezen et al., 2008; Wang et al., 2009). The trend inversion in expression pattern of genes from carbohydrate metabolism, becoming predominantly up-regulated from 5 days after 100% cap fall, suggest lack of continuum in ovary development during fruit set stage, which is in accordance with the expression dynamics observed during fruit set in tomato (Table 2.4) (Wang et al., 2009). On the other hand, the globally down-regulation of genes related to sugar, amino acid and peptide transporters indicated that nutrient transport is a constrain during fruit set (Ruan et al., 2012). Our results also suggest that the accumulation of sugar signaling molecules and enzymes may be an important event coupled with hormonal signaling pathways during onset of berry development (Ramon et al., 2008). Regarding hormonal regulation during onset of berry development, the down-regulation of a gene involved in IAA inactivation and auxin associated MADS-box transcription factors, and the up-regulation of GA20ox2 indicated that the levels of auxin and GA increased during initial steps of fruit set, as previously proposed (Giacomelli et al., 2013; Mariotti et al., 2011; Serrani et al., 2007) (Fig. 6.1). In addition, ethylene signaling pathway seemed to be activated by up-regulation of a gene putatively member of AP2/ERF superfamily of transcription factors involved fruit set and activation of defense mechanism under stress conditions (Kühn et al., 2014; Vriezen et al., 2008). Our results also suggested that CK degradation was induced from 3 to 5 days after 100% cap fall, although the previously reported up-regulation of CK biosynthetic enzymes in grapevine about 13 days after pollination (Dauelsberg et al., 2011).

In table grapes fruit set is often excessive and the natural drop, which enables the plant to self-regulate its fruit load, is not sufficient to satisfy fresh market quality standards (Di Lorenzo et al., 2011). An alternative thinning method to GAc spray at bloom was tested, consisting in imposing a light reduction stress which lead to C-starvation conditions (Table 3.3). Different

varieties were tested in greenhouse and field conditions, showing that the natural flower drop and the efficacy of thinning methods depends on climatic conditions and cultivar (Table 3.1 and Table 5.1). Experiments conducted in controlled conditions with Black Magic seeded cultivar showed that GAc spray effectiveness depends in climatic conditions, acting as a flower abscission inducer only in the late production cycle, in agreement with previous studies (Reynolds et al., 2006). Whereas shade imposition increased flower drop rate and decreased bunch compactness in both cycles, and improved berry characteristics in the early cycle resulting in a successful thinning method (Table 3.2), showing that current assimilates are determinant to the developing cluster, despite the carbohydrate reserves (Caspari et al., 1998). In field experiments, with vines grown under multiple stress conditions, only Thompson Seedless cultivar showed to be sensitive to both abscission inducing treatments (Table 5.1), probably due to the comparable higher vegetative growth observed (Fig.5.2) like previously suggested (Duchêne et al., 2003; Iwanami et al., 2012). Also other characteristics derived from different genetic background can be implicated in sensitivity for abscission inducing, as the levels of endogenous bioactive gibberellins in flowers (Acheampong et al., 2015; Boll et al., 2009).

Our results, from analyses conducted in both experimental conditions, disclosed that GAc and shade induced flower abscission by different mechanisms. Unlike the observed in apple with auxin and CK spray which promoted nutritional stress within the tree (Botton et al., 2011; Zhu et al., 2011), GAc act as grapevine flower abscission inducer by up-regulating genes and accumulating metabolites related to photosynthesis, energy production processes and stimulation of cell metabolism (Table 4.4, Fig. 4.5 and Fig. 4.6). Shading induced a higher number of changes on transcriptomic and metabolomic profiles (Table 3.3, Fig.4.2 and Fig.6.1) than GAc spray, activating flower abscission by reducing drastically photosynthesis and carbohydrates metabolism and transport, causing energy deprivation and carbon/nitrogen imbalance which result in repression of cell division and induction of senescence (Supplementary Table S4.2). Also hormone metabolism and signaling pathways and sugar signaling were implicated in flower abscission competence acquisition induced by shade, as previously reported (Li et al., 2013; Zhu et al., 2011) (Fig. 4.4, Table 4.7, Table 4.8 and Fig. 6.1). Both treatments seemed to induce abscission by common pathways regarding hormone mediation, inducing auxin biosynthesis and repressing GA biosynthesis pathway. While GAc treatment seemed to induce a negative-feedback regulation of bioactive GA biosynthesis, the effect of shade on GA metabolism was also extended to a repression of GA signaling pathway with the up-regulation of DELLA (Acheampong et al., 2015; Davière and Achard, 2013). Signals derived from hormone related pathways may interplay with polyamines metabolism in the abscission activation pathway. Although putrescine content increased in GAc treated

inflorescences and decreased in shade, N-acetylputrescine resulting from putrescine catabolism, decreased in both treatments, and an accumulation of MTA was observed in GAc and shade, as a result of downstream polyamines biosynthesis from putrescine which has an inhibitory action on this pathway. Therefore, the increasing in the abscission rate is related with changes on free polyamines, as previously demonstrated in several species (Aziz, 2003; De Dios et al., 2006; Gomez-Jimenez et al., 2010) and may be implicated in modulation of genes involved in ethylene biosynthesis and signalling pathways (Parra-Lobato and Gomez-Jimenez, 2011).

The results described along this thesis suggest that auxin and GA metabolism has to be fine-tuned in order to induce fruit set or cessation of flower development and abscission (Sundberg and Østergaard, 2009; Vriezen et al., 2008). Also MYB transcription factors which are involved in several processes as controlling stress tolerance, embryogenesis, hormone response (GA signaling) and regulation of secondary metabolism (Ambawat et al., 2013), showed a specific expression pattern in onset or cessation of berry development (Table 2.4 and Table 4.11). In particular, WER and MYB113 families were induced during fruit set and repressed by shade, indicating that regulation of flavonoid biosynthetic pathway (Deluc et al., 2008; Gonzalez et al., 2008) in addition to protection role is implicated on ascertain floweret destiny ‘to abscise or not to abscise' within 'Thompson Seedless' inflorescences.

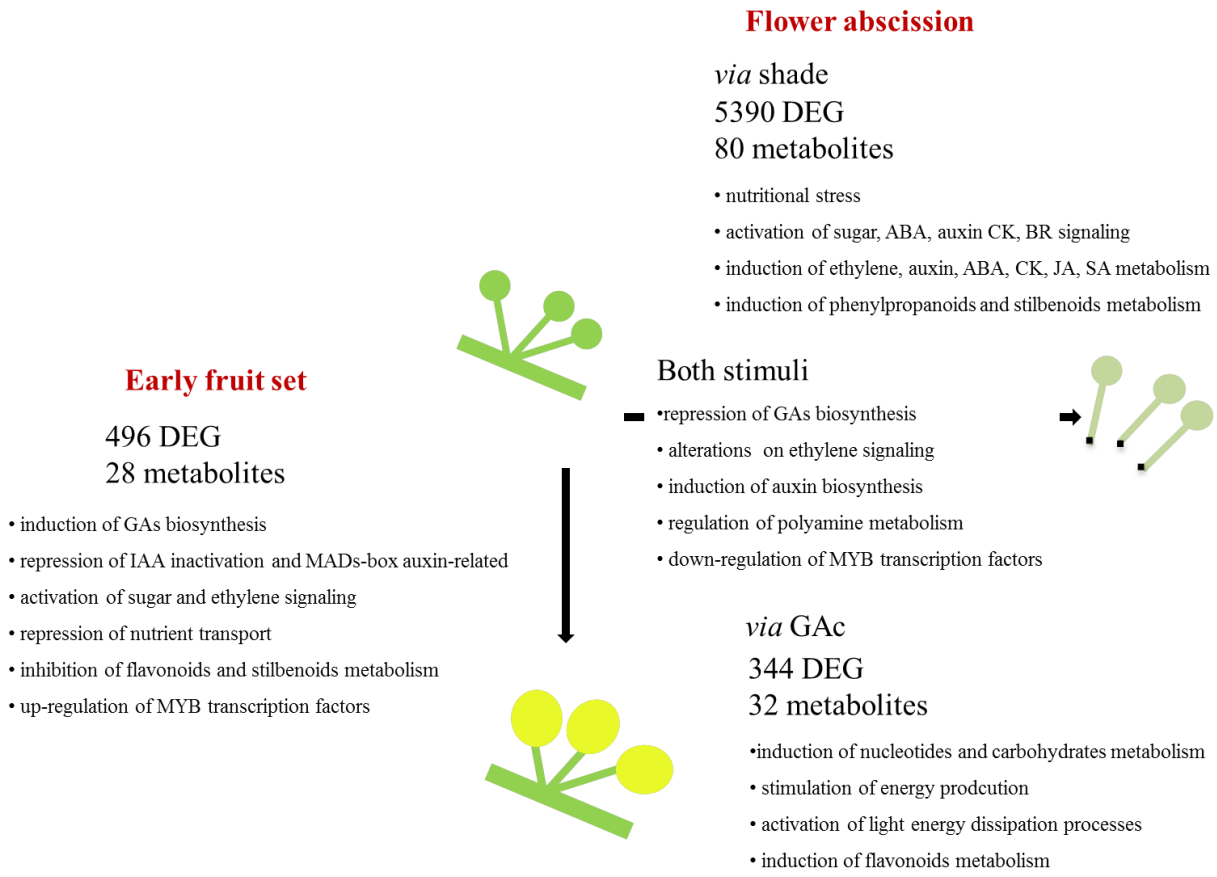

Figure 6.1 Proposed model of regulatory events during fruit set and flower abscission in stenospermocarpic grapevine (cv. Thompson seedless).

6.2 Conclusions and future perspectives

A conceptual model is proposed providing new insights on fruit set and flower abscission regulation in grapevines (Fig. 6.1). In summary, the data presented in this study indicates that early hormonal mediation, mainly through regulation of GA and auxin biosynthesis and ethylene signaling, sustains the ability of flowers to persist in the inflorescence and develop into berries during fruit set stage. The induction of flower drop triggered by GAc and light interception suggested two distinct mechanisms leading to abscission based on energy production stimulation and nutritional stress, respectively. The disclosed alternative pathways leading to abscission can be applied in the development and optimization of strategies for abscission control in fruit crop species.

According to our results, shading was considered an efficient thinning method in Black Magic cultivar growing in late cycle on greenhouse conditions, resulting in a reduced fruit set and improving bunch and berry quality in late production cycle, whereas in seedless cultivars tested in field conditions, reduction of bunch compactness was achieved, but optimization is required to overcome the formation of smaller berries.

The explanation for the observed secondary metabolism differences between 'Black Magic' and 'Thompson Seedless', in response do shading, may be the different types of embryo development (seeded versus stenospermocarpic cultivar), the programming for skin pigmentation (black versus white) that will take place later in the berry development, and/or the different growing conditions (greenhouse versus field). Knowing if and how these differences relate to, or can influence the abscission regulation is a future research topic.

This work can also serve as starting point for studies about fruit set and abscission regulation in specific organs as rachis, ovary and pedicel. Study of specific events occurring in AZ and non-AZ cells of grapevine flower pedicel during abscission are part of our ongoing work. RNA was extracted from AZ and pedicel (non-AZ) tissues, its quality and amount evaluated and all transcriptome is currently being sequenced. Using RNA-Seq data coupled with immunolocalization assays and other biochemical analysis, will allow us to determine key processes regulating the activation and progress of the cell separation leading to abscission (Supplementary Figure S6.1).

In addition, the cause of differences on cultivar response, besides differences on vegetative vigor and endogenous levels of GAs, can be due to aspects of the AZ differentiation process specific of each cultivar, including morphological alterations as number of cells layers within AZ located at the boundary of pedicel, which can be also elucidated in future studies.

6.3 References

Acheampong AK, Hu J, Rotman A, Zheng C, Halaly T, Takebayashi Y, Jikumaru Y, et al. 2015. Functional characterization and developmental expression profiling of gibberellin signalling components in *Vitis vinifera*. *J. Exp. Bot.* 66: 1463–1476.

Ambawat S, Sharma P, Yadav NR and Yadav RC. 2013. MYB transcription factor genes as regulators for plant responses: an overview. *Physiol. Mol. Biol. Plants*. 19: 307–321.

Aziz A. 2003. Spermidine and related metabolic inhibitors modulate sugar and amino acid levels in *Vitis vinifera* L.: possible relationships with initial fruitlet abscission. *J. Exp. Bot.* 54: 355–363.

Bessis R, Charpentier N, Hilt C and Fournioux J-C. 2000. Grapevine fruit set: Physiology of the abscission zone. *Aust. J. Grape Wine Res.* 6: 125–130.

Boll S, Lang T, Hofmann H and Schwappac P. 2009. Correspondence between gibberellin-sensitivity and pollen tube abundance in different seeded vine varieties. *Mitteilungen Klosterneubg.* 59: 129–133.

Botton A, Eccher G, Forcato C, Ferrarini A, Begheldo M, Zermiani M, Moscatello S, et al. 2011. Signaling pathways mediating the induction of apple fruitlet abscission. *Plant Physiol.* 155: 185–208.

Caspari HW, Lang A and Alspach P. 1998. Effects of Girdling and Leaf Removal on Fruit Set and Vegetative Growth in Grape. *Am. J. Enol. Vitic.* 49: 359–366.

Dauelsberg P, Matus JT, Poupin MJ, Leiva-Ampuero A, Godoy F, Vega A and Arce-Johnson P. 2011. Effect of pollination and fertilization on the expression of genes related to floral transition, hormone synthesis and berry development in grapevine. *J. Plant Physiol.* 168: 1667–1674.

Davière J-M and Achard P. 2013. Gibberellin signaling in plants. *Development*. 140: 1147–1151.

Deluc L, Bogs J, Walker AR, Ferrier T, Decendit A, Merillon J-M, Robinson SP, et al. 2008. The transcription factor VvMYB5b contributes to the regulation of anthocyanin and proanthocyanidin biosynthesis in developing grape berries. *Plant Physiol.* 147: 2041–2053.

De Dios P, Matilla AJ and Gallardo M. 2006. Flower fertilization and fruit development prompt changes in free polyamines and ethylene in damson plum (*Prunus insititia* L.). *J. Plant Physiol.* 163: 86–97.

Giacomelli L, Rota-Stabelli O, Masuero D, Acheampong AK, Moretto M, Caputi L, Vrhovsek U, et al. 2013. Gibberellin metabolism in *Vitis vinifera* L. during bloom and fruit-set: functional characterization and evolution of grapevine gibberellin oxidases. *J. Exp. Bot.* 64: 4403–4419.

Gomez-Jimenez MC, Paredes MA, Gallardo M and Sanchez-Calle IM. 2010. Mature fruit abscission is associated with up-regulation of polyamine metabolism in the olive abscission zone. *J. Plant Physiol.* 167: 1432–1441.

Gonzalez A, Zhao M, Leavitt JM and Lloyd AM. 2008. Regulation of the anthocyanin biosynthetic pathway by the TTG1/bHLH/Myb transcriptional complex in Arabidopsis seedlings. *Plant J.* 53: 814–827.

Intrigliolo DS and Lakso AN. 2009. Berry abscission is related to berry growth in Vitis labruscana 'Concord' and Vitis vinifera 'Riesling'. Vitis. 48: 53–54.

Iwanami H, Moriya-Tanaka Y, Honda C, Wada M, Moriya S, Okada K, Haji T, et al. 2012. Relationships among apple fruit abscission, source strength, and cultivar. *Sci. Hortic.* 146: 39–44.

Kühn N, Abello C, Godoy F, Delrot S and Arce-Johnson P. 2014. Differential behavior within a grapevine cluster: decreased ethylene-related gene expression dependent on auxin transport is correlated with low abscission of first developed berries. *PLoS One*. 9: e111258.

Li C, Wang Y, Huang X, Li J, Wang H and Li J. 2013. De novo assembly and characterization of fruit transcriptome in *Litchi chinensis Sonn* and analysis of differentially regulated genes in fruit in response to shading. *BMC Genomics*. 14: 552.

Mariotti L, Picciarelli P, Lombardi L and Ceccarelli N. 2011. Fruit-set and early fruit growth in tomato are associated with increases in indoleacetic acid, cytokinin, and bioactive gibberellin contents. *J. Plant Growth Regul.* 30: 405–415.

Ojeda H, Deloire A, Carbonneau A, Ageorges A and Romieu C. 1990. Berry development of grapevines: Relations between the growth of berries and their DNA content indicate cell multiplication and enlargement. *Vitis.* 38: 145-150.

Parra-Lobato MC and Gomez-Jimenez MC. 2011. Polyamine-induced modulation of genes involved in ethylene biosynthesis and signalling pathways and nitric oxide production during olive mature fruit abscission. *J. Exp. Bot.* 62: 4447–4465.

Ramon M, Rolland F and Sheen J. 2008. Sugar sensing and signaling. *Arabidopsis Book*. 6: e0117.

Reynolds AG, Roller JN, Forgione A and De Savigny C. 2006. Gibberellic Acid and Basal Leaf Removal: Implications for Fruit Maturity, Vestigial Seed Development, and Sensory Attributes of Sovereign Coronation Table Grapes. *Am. J. Enol. Vitic.* 57: 41–53.

Ruan Y-L, Patrick JW, Bouzayen M, Osorio S and Fernie AR. 2012. Molecular regulation of seed and fruit set. *Trends Plant Sci.* 17: 656–665.

Di Lorenzo R, Gambino C and Scafidi P. 2011. Summer Pruning in Table Grape. *Adv. Hortic. Sci.* 25: 143–150.

Serrani JC, Sanjuán R, Ruiz-Rivero O, Fos M and García-Martínez JL. 2007. Gibberellin regulation of fruit set and growth in tomato. *Plant Physiol.* 145: 246–257.

Sundberg E and Østergaard L. 2009. Distinct and dynamic auxin activities during reproductive development. *Cold Spring Harb. Perspect. Biol.* 1: a001628.

Vriezen WH, Feron R, Maretto F, Keijman J and Mariani C. 2008. Changes in tomato ovary transcriptome demonstrate complex hormonal regulation of fruit set. *New Phytol.* 177: 60–76.

Wang H, Schauer N, Usadel B, Frasse P, Zouine M, Hernould M, Latché A, et al. 2009. Regulatory features underlying pollination-dependent and -independent tomato fruit set revealed by transcript and primary metabolite profiling. *Plant Cell*. 21: 1428–1452.

Zhu H, Dardick C, Beers E, Callanhan A, Xia R and Yuan R. 2011. Transcriptomics of shading-induced and NAA-induced abscission in apple (*Malus domestica*) reveals a shared pathway involving reduced photosynthesis, alterations in carbohydrate transport and signaling and hormone crosstalk. *BMC Plant Biol.* 11: 138.

Supplementary Material

Supplementary Material

Chapter 2

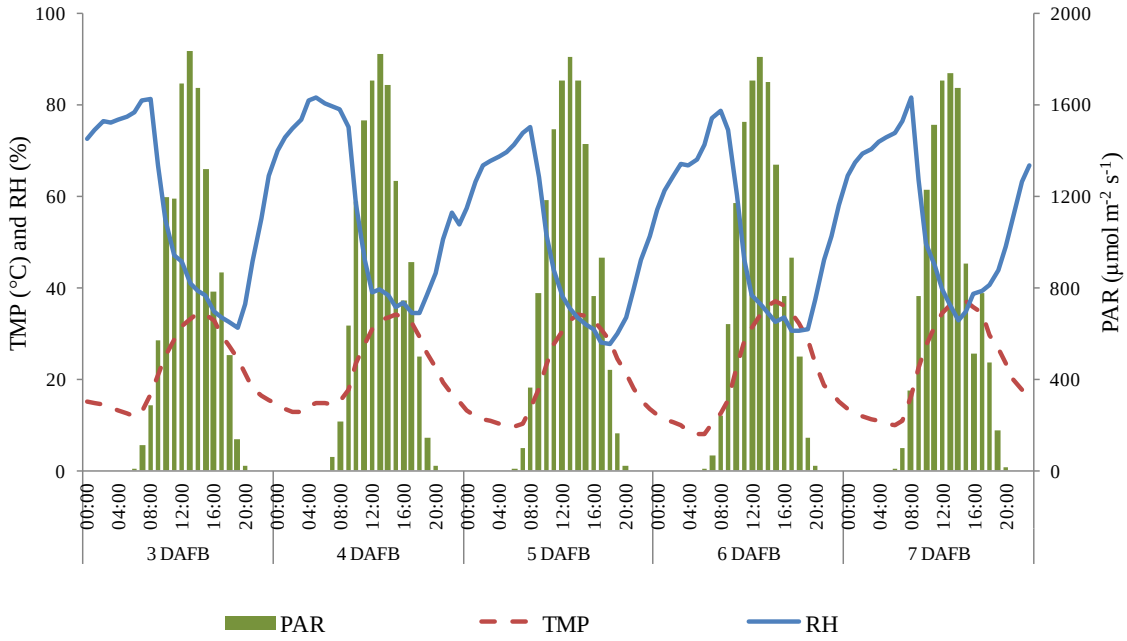

Supplementary Figure S2.1. Microclimate conditions registered during early fruit set stage monitored above the vines canopy. Vines were grown under an overhead trellis system covered with plastic. Photosynthetically active radiation (PAR), temperature (TMP) and relative humidity (RH) were registered every 15 min.

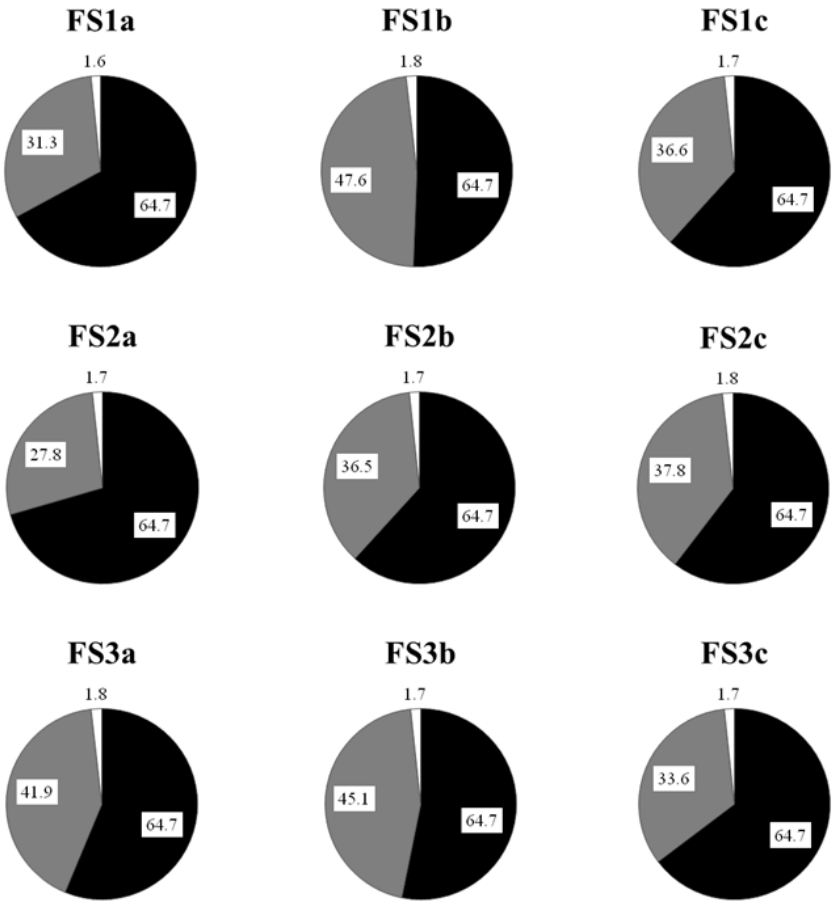

Supplementary Figure S2.2. Pie charts summarizing the results of alignment of the samples against the *Vitis vinifera* L. genome. Percentage of reads by sample, mapped uniquely (black), unmapped (grey) or mapped in multiple locations (white).

A

KOG functional categories
General function prediction only
Signal transduction mechanisms
Posttranslational modification, protein turnover, chaperones
Transcription
Function unknown
Translation, ribosomal structure and biogenesis
Secondary metabolites biosynthesis, transport and catabolism
Intracellular trafficking, secretion, and vesicular transport
Carbohydrate transport and metabolism
RNA processing and modification

B

KEGG functional categories
Purine metabolism
Starch and sucrose metabolism
Thiamine metabolism
Phenylalanine metabolism
Pentose and glucuronate interconversions
Phenylpropanoid biosynthesis
Pyrimidine metabolism
Glycerolipid metabolism
Amino sugar and nucleotide sugar metabolism
Cysteine and methionine metabolism

C

GO biological process		GO molecular function		GO celular component	
GO:0044699	single-organism process	GO:0016740	transferase activity	GO:0043231	intracellular membrane-bounded organelle
GO:0006807	nitrogen compound metabolic process	GO:0043168	anion binding	GO:0005737	cytoplasm
GO:0044260	cellular macromolecule metabolic process	GO:0000166	nucleotide binding	GO:0043227	membrane-bounded organelle
GO:0044710	single-organism metabolic process	GO:1901265	nucleoside phosphate binding	GO:0016020	membrane
GO:0043170	macromolecule metabolic process	GO:0036094	small molecule binding	GO:0043229	intracellular organelle
GO:0044237	cellular metabolic process	GO:0043167	ion binding	GO:0043226	organelle
GO:0044238	primary metabolic process	GO:1901363	heterocyclic compound binding	GO:0044424	intracellular part
GO:0071704	organic substance metabolic process	GO:0097159	organic cyclic compound binding	GO:0005622	intracellular
GO:0009987	cellular process	GO:0003824	catalytic activity	GO:0044464	cell part
GO:0008152	metabolic process	GO:0005488	binding	GO:0005623	cell

Supplementary Figure S2.3. List of the ten most representative KOG (A) and KEGG categories (B) and GO terms (C) in the grapevine (*Vitis vinifera* L.) genome.

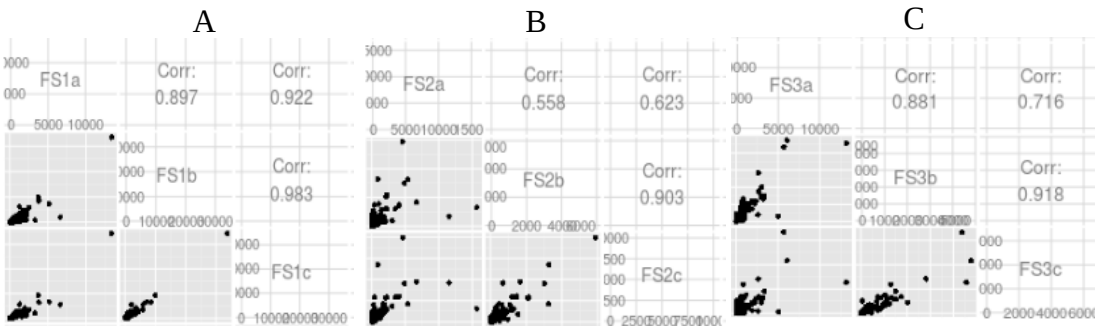

Supplementary Figure S2.4. Pearson correlation plots of RNA-Seq reads between individual biological replicates in each time-point, FS1 (A), FS2 (B), FS3 (C). Analyses were performed with R software using ln-transformed read counts for the DEG as input. All correlation values are significant at p-value≤0.001.

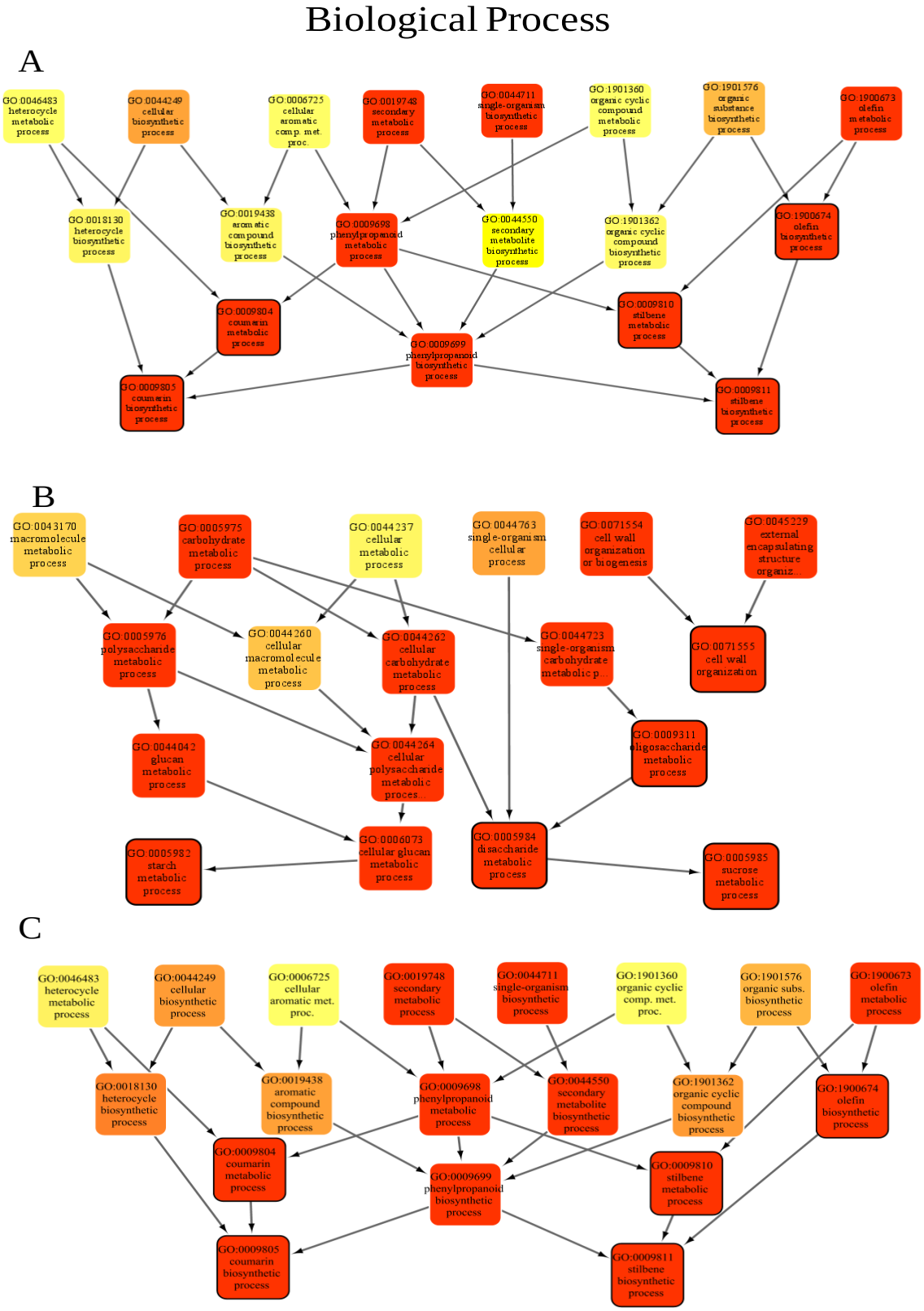

Supplementary Figure S2.5. Acyclic graphs with the mostly enriched GO categories in differentially expressed genes. The top 5 and top 5-related biological processes in the transition from FS1 to FS2 (A), FS2 to FS3 (B) and FS1 to FS3 (C) are shown. The color scale presented is related with the *p*-value, where the redder the node, lower the *p*-value. The nodes with black outline are the top 5 enriched categories.

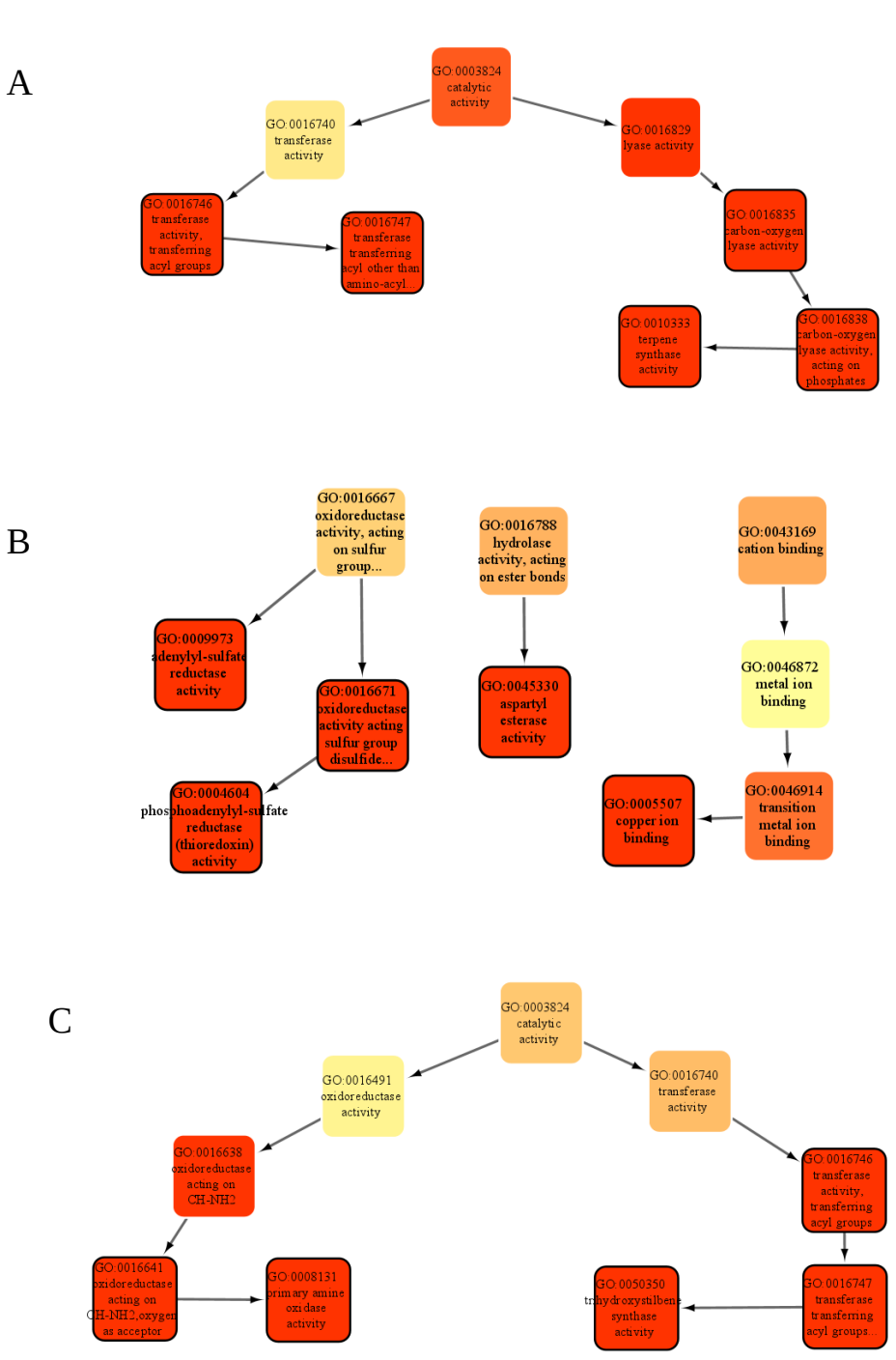

Supplementary Figure S2.5 (continued). Acyclic graphs with the mostly enriched GO categories in differentially expressed genes. The top 5 and top 5-related molecular function in the transition from FS1 to FS2 (A), FS2 to FS3 (B) and FS1 to FS3 (C) are shown. The color scale presented is related with the *p*-value, where the redder the node, lower the *p*-value. The nodes with black outline are the top 5 enriched categories.

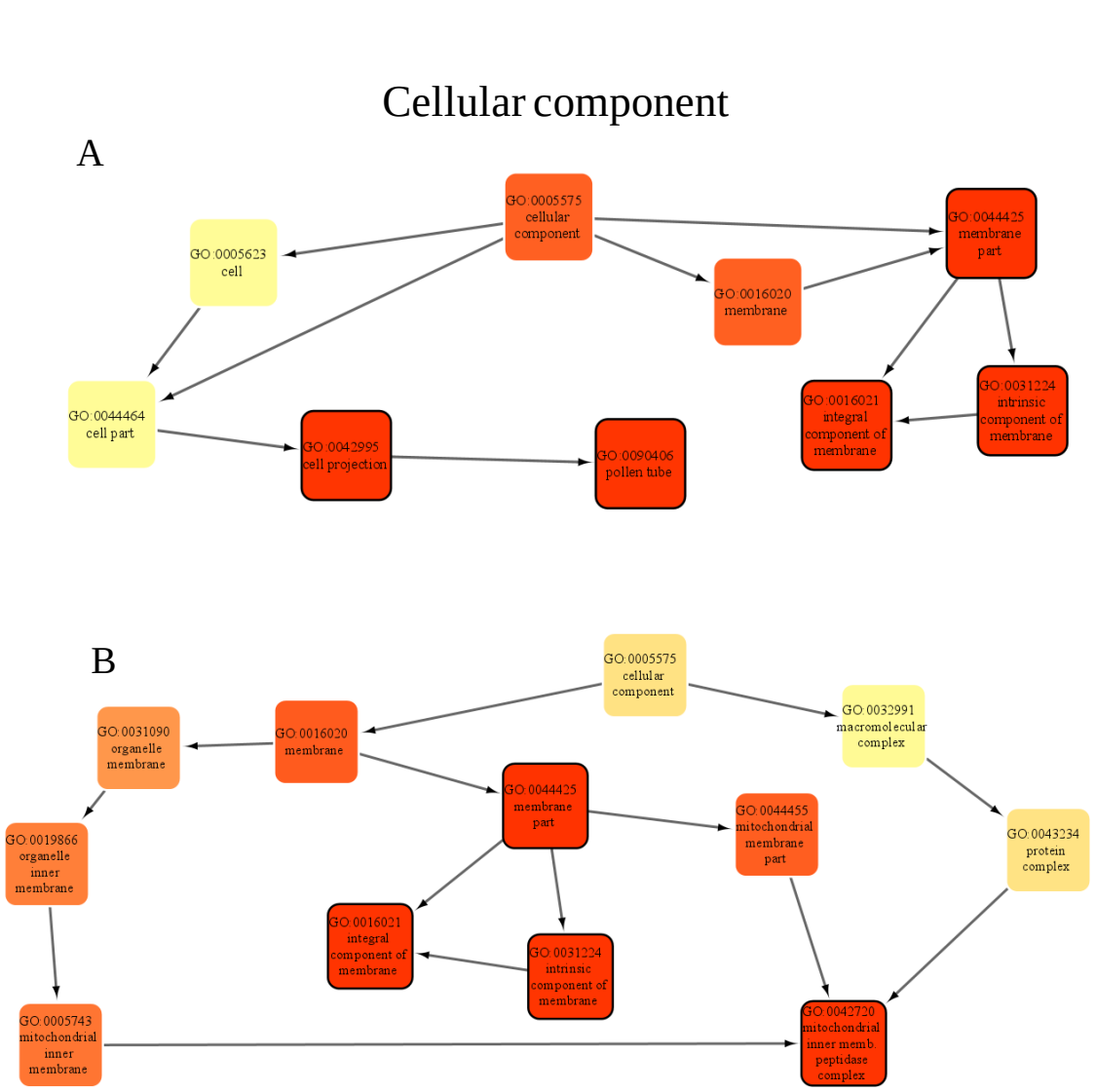

Supplementary Figure S2.5 (continued). Acyclic graphs with the mostly enriched GO categories in differentially expressed genes. The top 5 and top 5-related cellular component in the transition from FS1 to FS2 (A) and FS2 to FS3 (B) are shown. The color scale presented is related with the *p*-value, where the redder the node, lower the *p*-value. The nodes with black outline are the top 5 enriched categories.

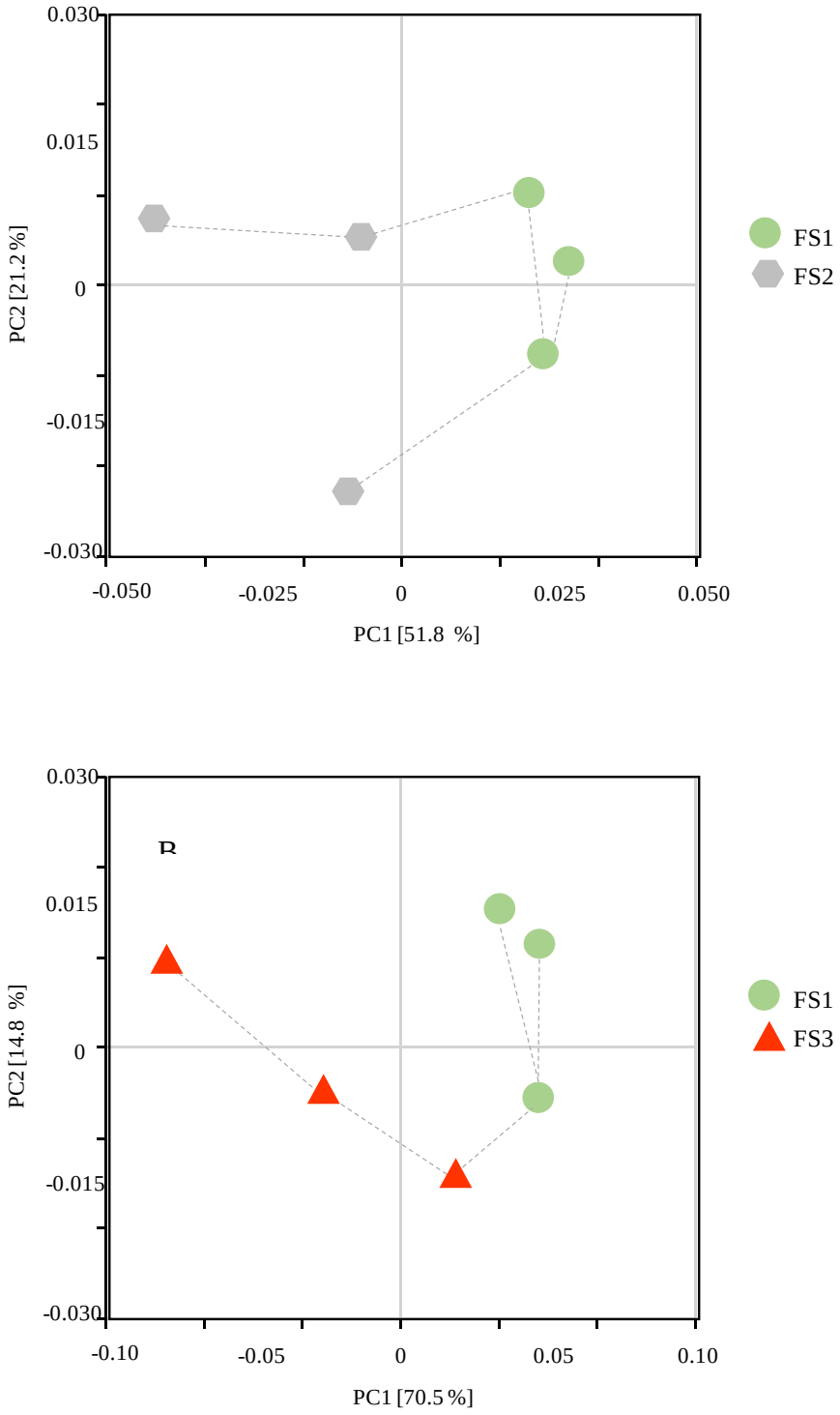

Supplementary Figure S2.6. Principal Coordinate Analysis of metabolites relative content at fruit set stage 1 and 2 (A) and 1 and 3 (B). Data were ln-transformed and analysis was conducted based on the pair-wise correlation matrix using the NTsys-PC software package. Green, grey and red indicate the three different time-points – FS1, FS2, FS3 – and their respective replicates. Samples are connected by minimum-spanning tree. A) PC1 explains 51.84% and PC2 21.19%. B) PC1 explains 70.50% and PC2 14.82%.

The following tables are provided in digital format, due to their dimensions:

Supplementary Table S2.1. Identification of new splicing events between the reference genome (cv.Pinot Noir) and our data set using using Cufflinks software.

Supplementary Table S2.2. List of genes significantly affected during fruit set and their annotation regarding functional categories and gene code identification, pattern-related gene cluster and respective fold-change. Red and green shaded cells indicate down and up -regulated genes, respectively. Yellow and blue shaded cells with a and b letters, respectively, represents the separation of the mean relative expression in each fruit set stage.

Supplementary Table S2.3. List of GO enriched categories in each pair-wise comparison between fruit set stages. Enrichment analysis was performed using R bioconductor topGO package with Fisher's exact test and p-value$\leq$0.01.

Supplementary Table S2.4. Heat map illustrating metabolite changes in grapevine inflorescences during fruit set. Red and green shaded cells indicate p-value$\leq$0.05 (red indicates that the mean values are significantly lower for that comparison; green values significantly higher). Light red and light green shaded cells indicate 0.05<p-value$\leq$0.10 (light red indicates that the mean values trend lower for that comparison; light green values trend higher).

Supplementary Table S2.5. Enzymatic classification of differentially expressed genes, performed withBlast2GO software, respective gene code identification, description and fold-change for each pair-wise comparison of fruit set stages.

Supplementary Material

Chapter 3

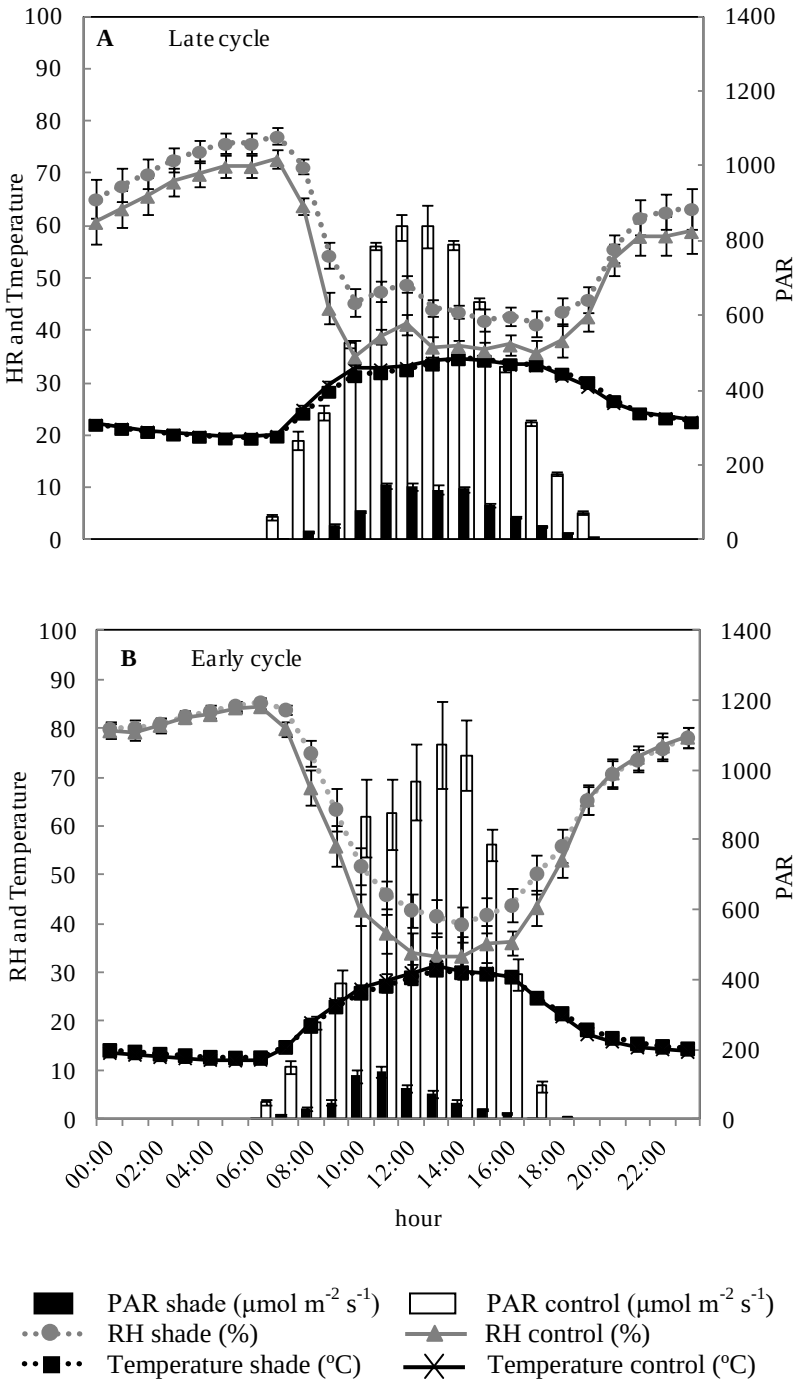

C

DAB	Maximum temperature (ºC)
1	37.5
2	36.6
3	37.1
4	35.8
5	35.8
6	33.2
7	33.2
8	32.4
9	34.5
10	35.3
11	36.2
12	35.3

D

DAB	Maximum temperature (ºC)
1	32.4
2	31.6
3	32.0
4	34.1
5	32.0
6	34.5
7	29.6
8	26.8
9	28.7
10	30.3
11	37.9
12	29.2

Supplementary Figure S3.1. Microclimate conditions recorded during bloom period (twelve days) under shaded and unshaded conditions in late (A) and early (B) production cycles. Mean values per hour of relative humidity (RH), temperature and photosynthetic active radiation (PAR) (mean±se). Maximum temperatures registered in late (C) and early (D) cycle.

The following table is provided in digital format:

Supplementary Table S3.1. Heat map illustrating metabolite changes in grapevine inflorescences in response to GAc and shade treatments. Red and green shaded cells indicate *p*-value<0.05 (red indicates that the mean values are significantly lower for that comparison; green values significantly higher). Light red and light green shaded cells indicate 0.05≤*p*-value≤0.10 (light red indicates that the mean values trend lower for that comparison; light green values trend higher).

Supplementary Material

Chapter 4

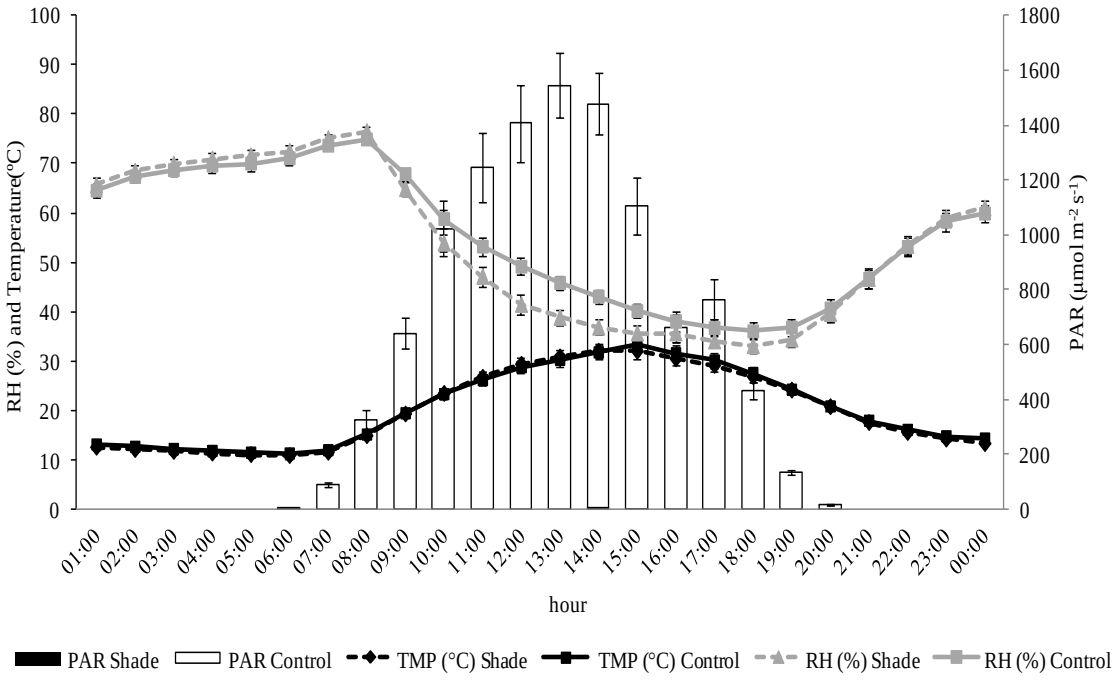

Figure S4.1. Microclimate conditions recorded during bloom period (twelve days) under shaded and unshaded conditions. Mean values per hour of relative humidity (RH), temperature and photosynthetic active radiation (PAR) (mean±se).

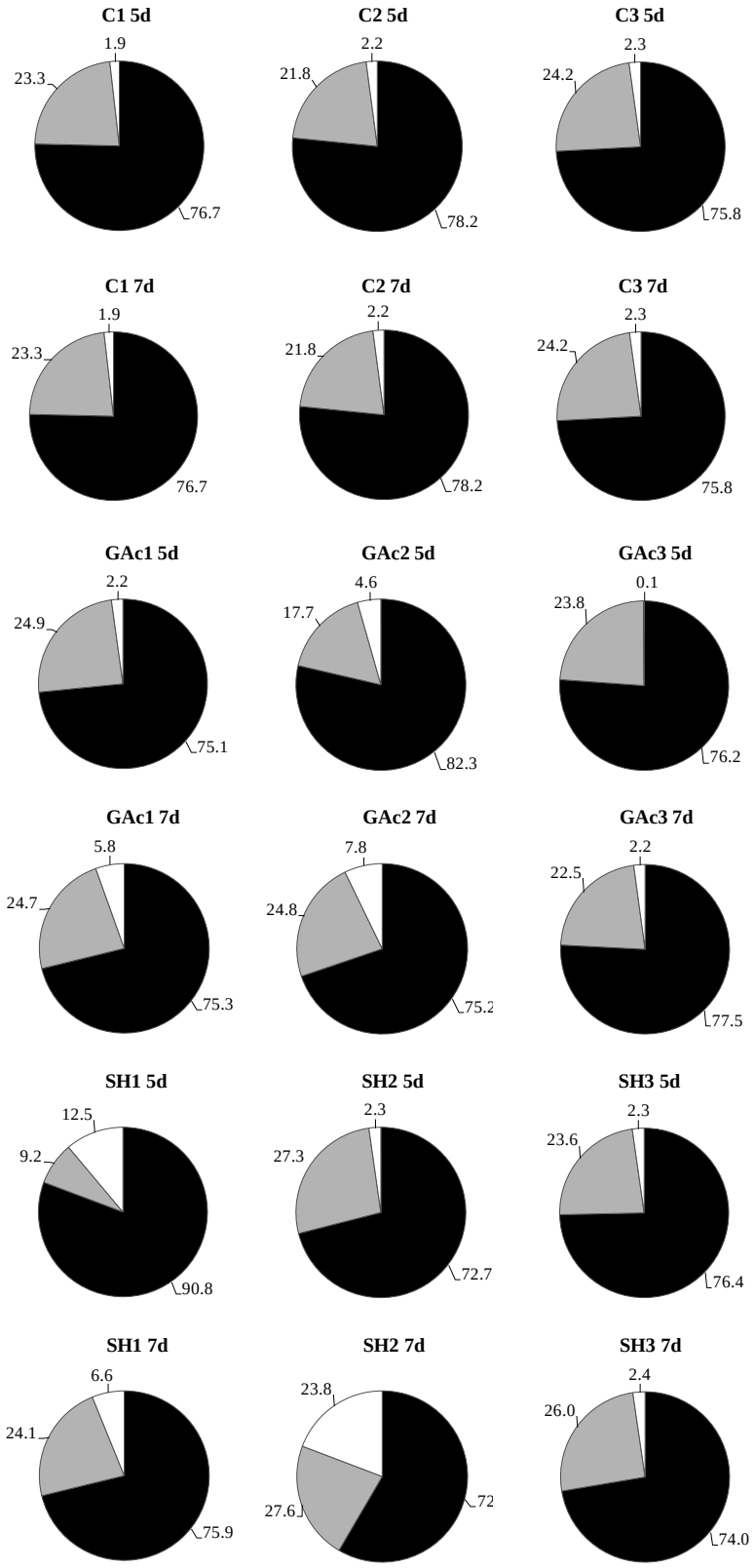

Supplementary Figure S4.2. Pie charts summarizing the results of alignment of each sample against the *Vitis vinifera* L. genome. Percentage of reads by sample, mapped uniquely (black), unmapped (grey) or mapped in multiple locations (white).

A

NCBI	GID	description	Fold-change (q-rtPCR)				Fold-change (RNAseq)				primer forward (5'-3')	primer reverse (5'-3')	bp
			GAc5d	GAc7d	SH5d	SH7d	GAc5d	GAc7d	SH5d	SH7d			
XM_002276122.1	VIT_04s0023g02420	mitogen-activated protein kinase 4	0.36	0.41	**1.60**	**2.68**	0.65	0.25	0.97	**1.51**	TATTATCAAGTCCCCGCAGCC	GAGGTTCCCAGGCTTCAAGTC	127
XM_002273277.2	VIT_05s0020g02910	mitogen-activated protein kinase kinase 5	-0.10	-0.34	-0.47	**-2.09**	0.00	0.11	-0.43	**-3.10**	AGGAGGTTGCTGCTCTCTTCC	GCAGGCCTCAAGTTTGGTTCC	127
XM_002284983.2	VIT_06s0004g03130	auxin response factor 4	0.21	-0.12	-0.37	**-2.39**	-0.56	-0.19	-0.60	**-2.52**	GCCAAGGCGACATCTGCTTAC	AGCTCTCCACCTTCACCTCTC	103
XM_002284771.1	VIT_06s0004g03540	mitogen-activated protein kinase 3	-0.50	0.07	**1.60**	**2.29**	-0.24	0.21	1.32	**2.10**	CAGAAGGCCTTTATTTGCGGG	TCCGAACAAACCCAAGATCAG	99
XM_002283455.2	VIT_11s0016g02970	mitogen-activated protein kinase kinase 6	0.73	-0.11	-0.01	-0.17	-0.34	0.44	-0.62	**-2.24**	GACCTCGTGAGTCACCCTTTC	AGGAGGTTCCAAGCTGCCTAC	84
XM_002266023.1	VIT_11s0052g00440	auxin efflux carrier component 2	0.55	-1.44	**-2.14**	-1.48	0.55	-0.20	-0.55	**-1.92**	ATCGATCAGGACTCAGGCAGC	GTCATGACGCTTGTTGGAGGC	99
XM_002276344.1	VIT_13s0047g00250	ethylene insensitive 3-like	0.41	0.22	1.43	**2.31**	-0.15	-0.11	0.71	**1.66**	GACTGCCAAAGAGAGTGCCAC	AAAGATCCACTCCCACCAGCC	117
XM_003634159.1	VIT_17s0000g02420	auxin efflux carrier component 1	-0.22	-0.29	0.16	-0.96	-0.34	-0.36	-0.55	**-1.67**	TTGTCGTCTACCACTCCACGG	CCACCCGCTACCATTGAGTAG	131

B

NCBI	description	primer forward (5'-3')	primer reverse (5'-3')	bp
XM_002282480.3	actin 1	CTTCCAGCCATCTCTCATTGG	TGTTGCCATAGAGGTCCTTCC	107
XM_002263109.2	glyceraldehyde-3-phosphate dehydrogenase	GGAATAGCACTCAACGAGAAG	TGCCATGTGGACAATCAAGTC	99
M_002282083.2	polyubiquitin	TGGGTCTCAGCCATTTGAAAG	GCCTCACTAACGACCACTTAG	111

C

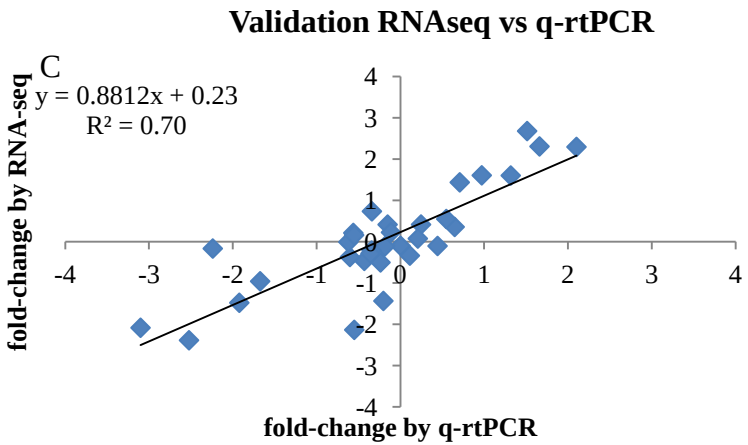

Supplementary Figure S4.3. Quantitative rtPCR validation of the RNA-seq. NCBI reference, gene identification (GID), fold-change quantification by q-rtPCR and RNA seq, primers and amplicon length (bp) for abscission related-genes (A). NCBI reference, primers and amplicon length are also given for reference genes (B) . Data are means of 3 replicates. The pearson correlation coefficient between q-rtPCR and RNA-Seq obtained fold-changes (R= 0.84) is significant at *p*-value≤0.001 (C).

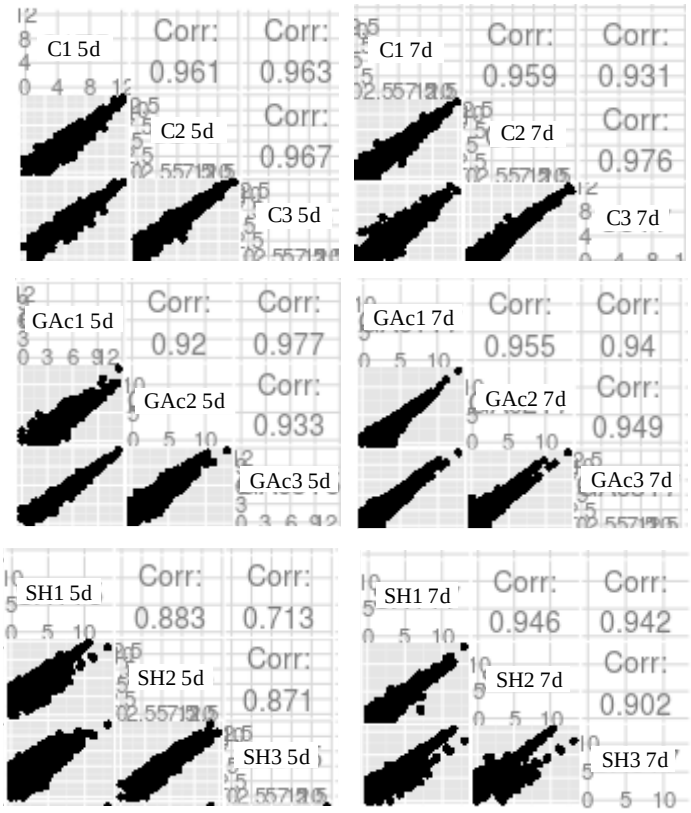

Supplementary Figure S4.4. Pearson correlation plots of RNA-Seq reads between individual biological replicates in each time-point (5 and 7d) and treatment (control, GAc and shade). Analyses were performed with R software using ln-transformed read counts for the DEG as input. All correlation values are significant at p-value≤0.001.

A

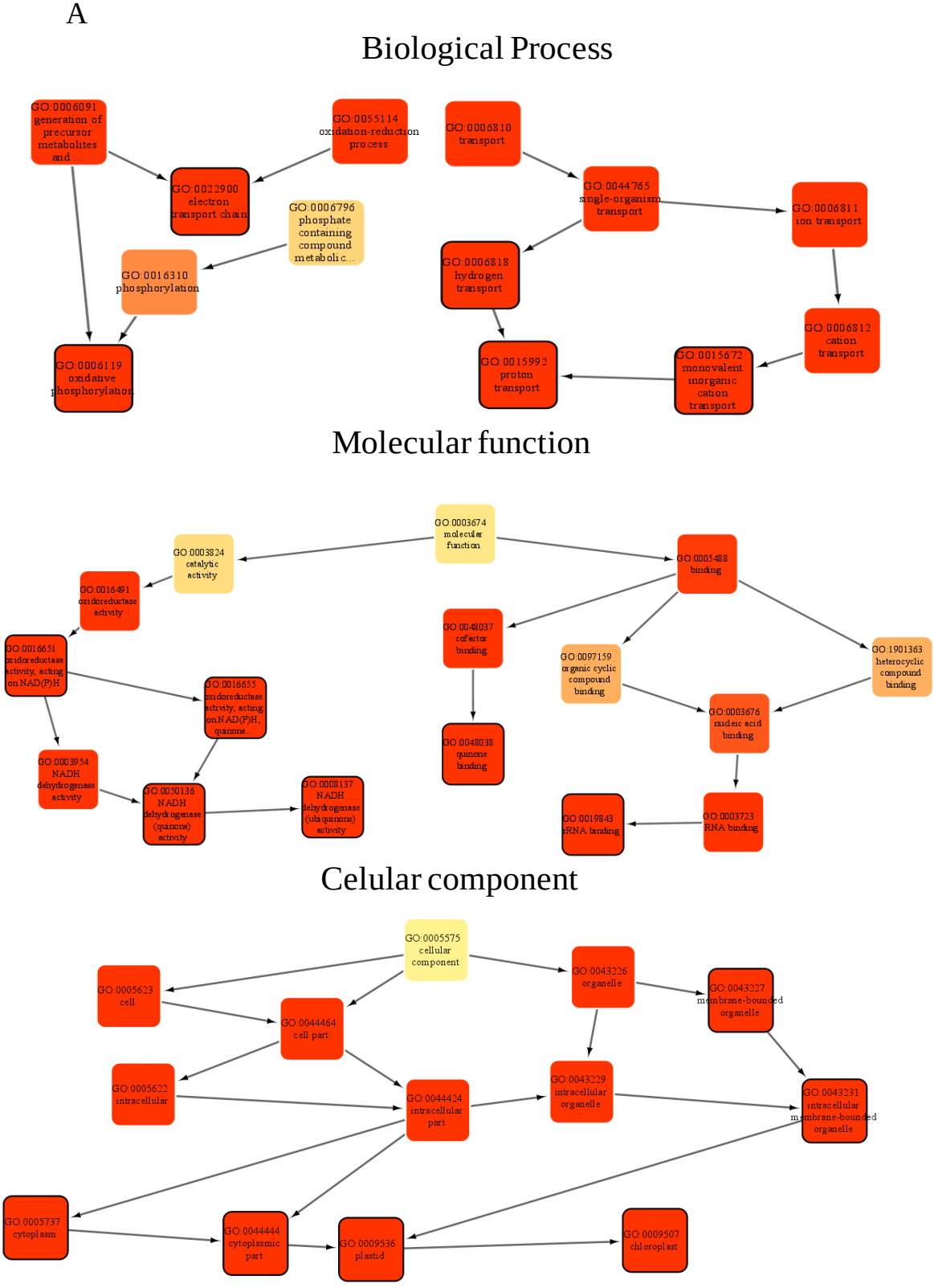

Supplementary Figure S4.5. A) Acyclic graphs with the mostly enriched GO categories in differentially expressed genes at GAc 7d. The top 5 and top 5-related biological processes, molecular function and cellular component are shown. The color scale presented is related with the *p*-value, where the redder the node, lower the *p*-value. The nodes with black outline are the top 5 enriched categories.

B

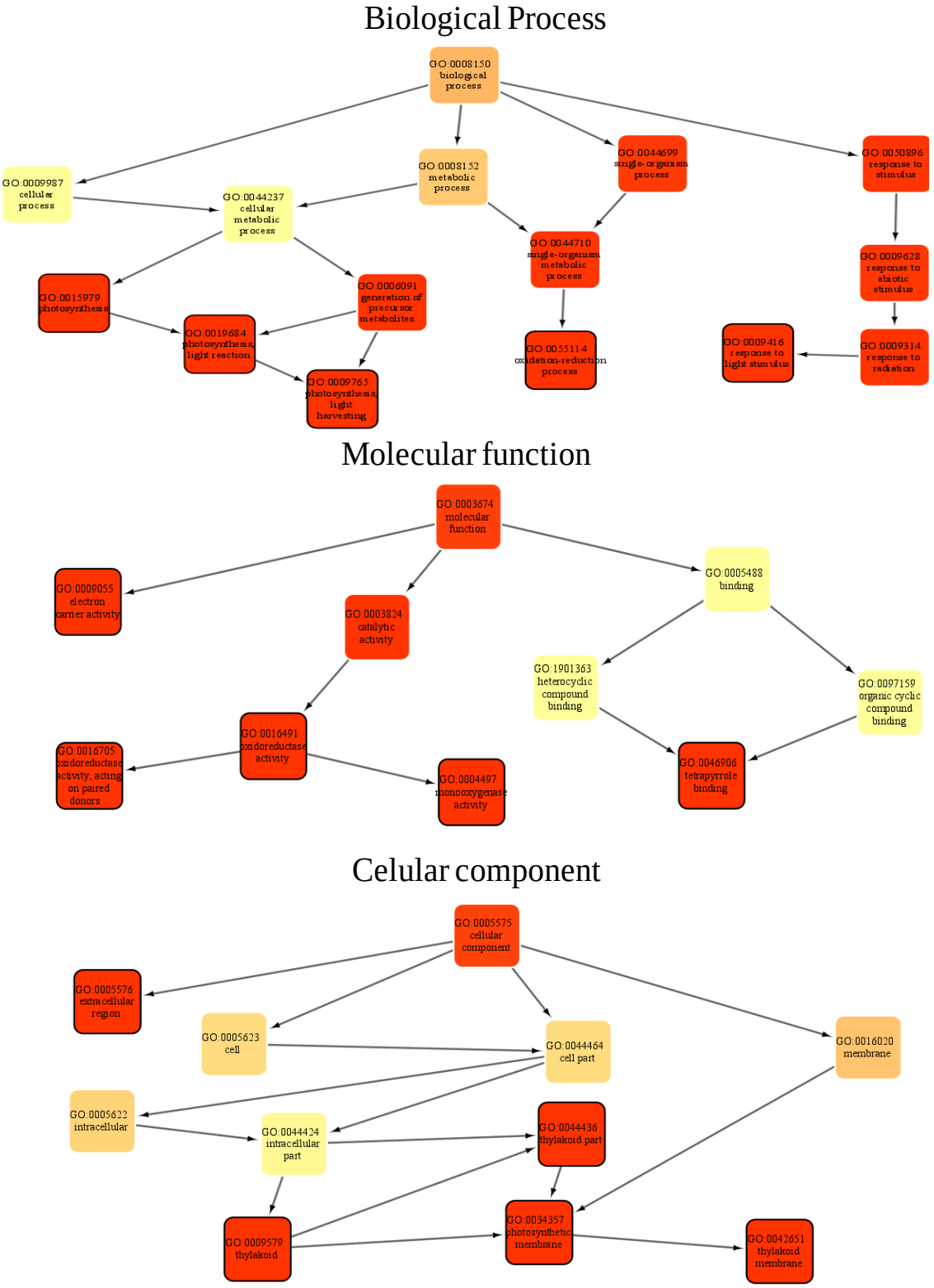

Supplementary Figure S4.5 (continued). B) Acyclic graphs with the mostly enriched GO categories in differentially expressed genes at Shade 5d. The top 5 and top 5-related biological processes, molecular function and cellular component are shown. The color scale presented is related with the *p*-value, where the redder the node, lower the *p*-value. The nodes with black outline are the top 5 enriched categories.

C

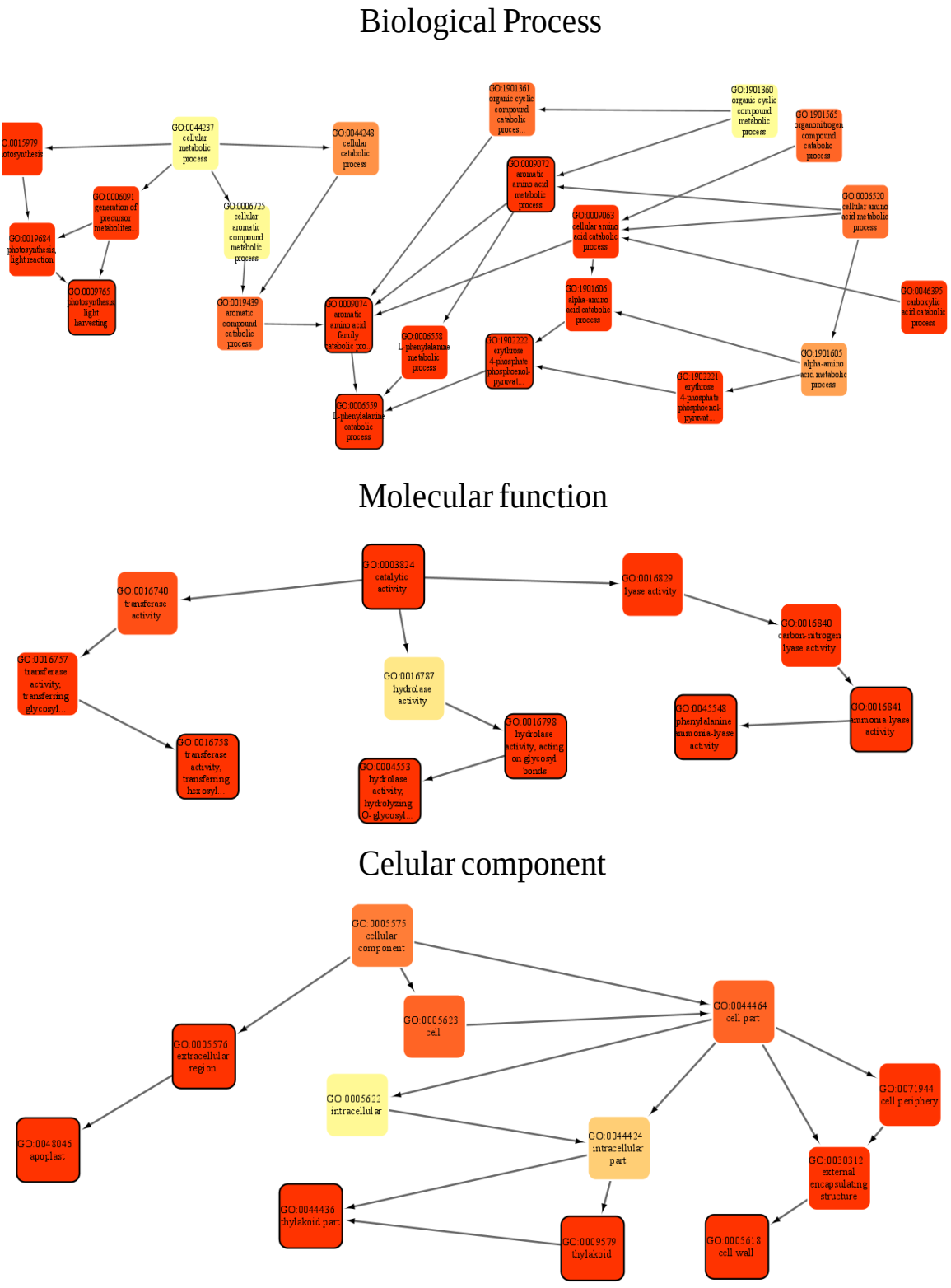

Supplementary Figure S4.5. (continued) C) Acyclic graphs with the mostly enriched GO categories in differentially expressed genes at Shade 7d. The top 5 and top 5-related biological processes, molecular function and cellular component are shown. The color scale presented is related with the *p*-value, where the redder the node, lower the *p*-value. The nodes with black outline are the top 5 enriched categories.

Supplementary Table S4.1. Parameters for hormone identification in Mass Spectrometry. Cone voltage potential, collision energy (CE) and other performance characteristics.

	RT (min)	**Dection Limit (µg/L)**	**Ion mode**	**Cone Voltage (V)**	**Quantifying trace CE (eV)**	**1° qualifying trace CE (eV)**	**2° qualifying trace CE (eV)**
GA1	4.01	5	ESI-	40	347>229; (30)	347>259; (20)	347>273; (30)
GA3	3.95	5	ESI-	36	345>143; (38)	345>221; (24)	345>239; (14)
GA4	6.18	5	ESI-	44	331>289; (24)	331>213; (32)	331>243; (22)
GA8	3.03	5	ESI-	35	363>257; (20)	363>275; (20)	315>271; (20)
GA9	6.62	5	ESI-	40	315>227; (20)	315>253; (25)	315>271; (20)
GA12	7.37	5	ESI-	50	331>201; (35)	331>269; (30)	331>287; (25)
GA20	5.24	5	ESI-	40	331>147; (32)	331>173; (34)	331>243; (18)
GA34	5.74	5	ESI-	34	347>199; (30)	347>241; (20)	347>259; (20)
GA53	6.30	5	ESI-	55	347>121; (40)	347>189; (36)	347>233; (32)
ABA	5.00	5	ESI-	24	263>153; (10)	263>201; (16)	263>204; (18)
IAA	4.30	5	ESI+	22	176>77; (34)	176>103; (28)	176>130; (15)

Multiple reaction monitoring mode in negative ion mode (capillary voltage, 1.08 kV) and with argon (0.20 mL/min; gas) and nitrogen (1000 L/h) as collision and desolvation gas, respectively.

The following tables are provided in digital format, due to their dimensions:

Supplementary Table S4.2. List of genes significantly affected by GAc and shade treatments and their annotation regarding functional categories and gene annotation, pattern-related gene cluster and respective fold-change.

Supplementary Table S4.3. Heat map illustrating metabolite changes in grapevine inflorescences in response to GAc and shade treatments at 5 and 7d. Red and green shaded cells indicate p-value$\leq$ 0.05 (red indicates that the mean values are significantly lower for that comparison; green values significantly higher). Light red and light green shaded cells indicate 0.05 <p-values$\leq$ 0.10 (light red indicates that the mean values trend lower for that comparison; light green values trend higher).

Supplementary Table S4.4. Enzymatic classification of differentially expressed genes, performed withBlast2GO software, respective gene code identification, description and fold change for each treatment at 5d and 7d.

Supplementary Table S4.5. List of GO enriched categories in each pair-wise comparison. Enrichment analysis was performed using R bioconductor topGO package with Fisher's exact test and p-value$\leq$0.01.

Supplementary Material

Chapter 5

Supplementary Figure 5.1. Aspects of the thinning method *via* reduction of intercepted light in seedless cultivars grown on an overhead trellis system covered with plastic, which provides the required structure to support and fix the shading nets, in Herdade Vale da Rosa, Ferreira do Alentejo.

Supplementary Material

Chapter 6

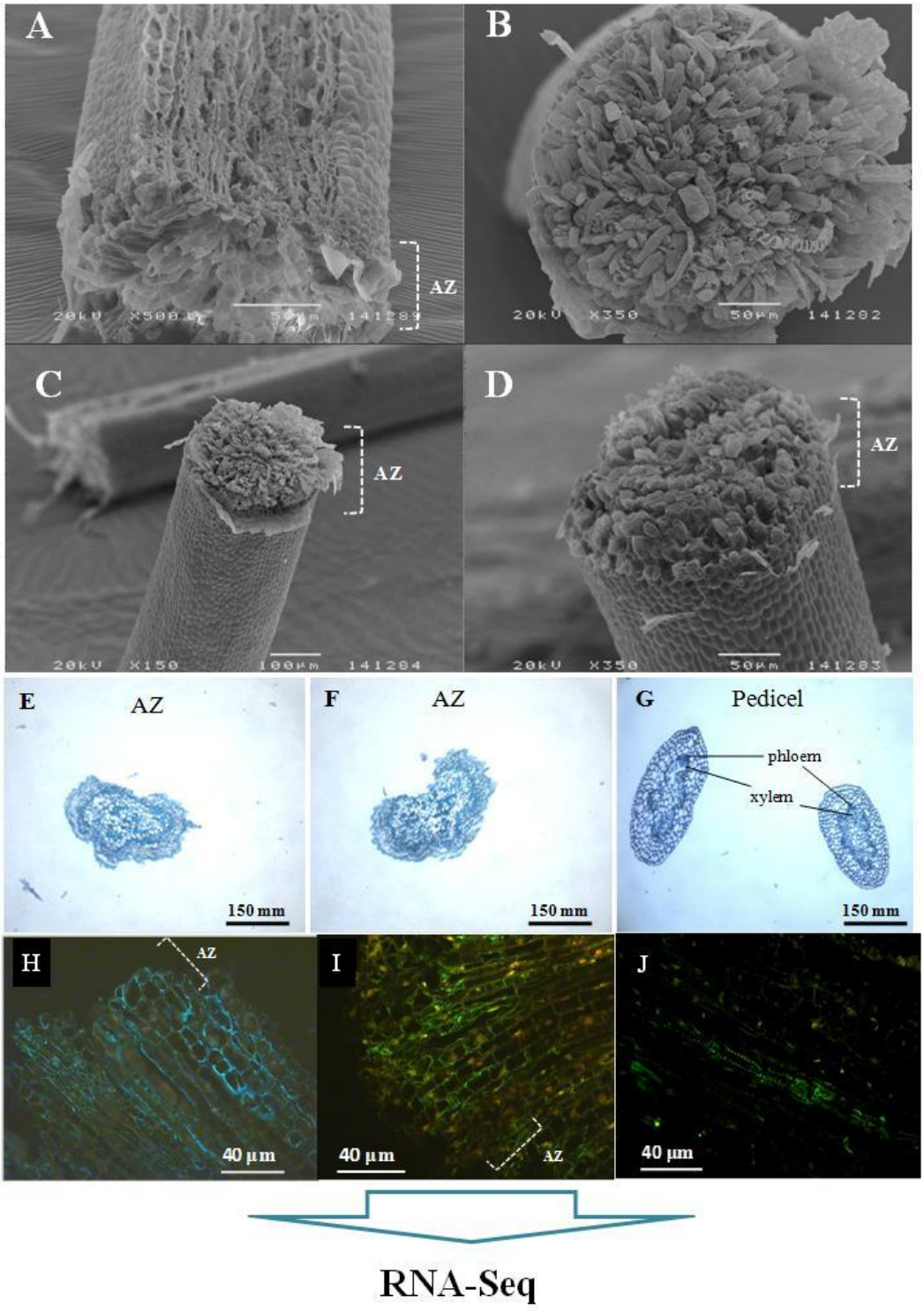

Supplementary Figure 6.1. Micrographs of morphological characteristics (by scanning electron (A, B, C, D) and light microscopy (E, F, G)) showing differences on cells conformation and organization between abscission zone (AZ) and adjacent pedicel. Micrographs of immunofluorescence detection of (1-4)-β-D-galactan with LM5 (H), (1-5)-α-L-arabinan with LM6 (I) and unsubstituted and low-substituted xylan and arabinoxylan with LM11 (J) antibodies showing no major differences in this specific cell wall polysaccharides between AZ and non-AZ adjacent cells.